Molecular basis of TAPBPR-mediated peptide editing on MHC class I molecules

Florin Tudor Ilca

Department of Pathology

University of Cambridge

Tennis Court Road

Cambridge

CB2 1QP

Corpus Christi College

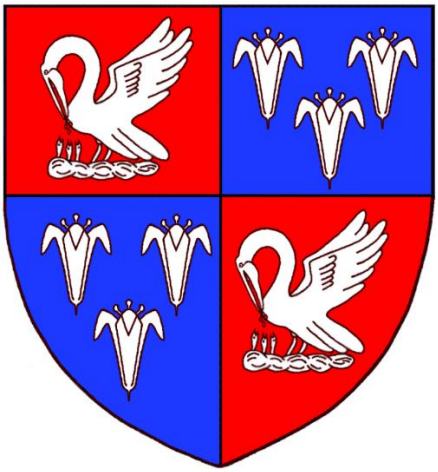

This dissertation is submitted for the degree of Doctor of Philosophy

September 2019

Declaration

This thesis is strictly the result of my own work and does not include any work performed in collaboration, except where specifically mentioned in the text.

It is not substantially the same as any that I have submitted, or, is being concurrently submitted for a degree or diploma or other qualification at the University of Cambridge or any other University or similar institution except as declared in the Preface and specified in the text. I further state that no substantial part of my dissertation has already been submitted, or, is being concurrently submitted for any such degree, diploma or other qualification at the University of Cambridge or any other University or similar institution except as declared in the Preface and specified in the text.

This thesis is in compliance with the word limit imposed by the Degree Committee of the Department of Pathology, comprising fewer than 60,000 words excluding tables, figure legends and bibliography.

Florin Tudor Ilca

Cambridge

September 2019

Abstract

Major histocompatibility complex (MHC) class I molecules present fragments of the cellular proteome, in the form of short peptides, to the cell surface for the inspection by cytotoxic T cells. This process is a crucial immunosurveillance mechanism used to induce appropriate immune responses against intracellular pathogens and cancer. In order to generate optimal T cell-mediated immune responses, prior to their export to the cell surface, MHC class I molecules undergo a process known as peptide selection. Optimal peptide selection is facilitated by two intracellular peptide editors, tapasin and TAPBPR. TAPBPR was shown to shape the peptide repertoire presented on MHC class I at the cell surface, either by directly catalysing peptide exchange on MHC class I molecules or by associating with the quality control enzyme UDP-glycoprotein glucosyltransferase 1 (UGT1), which selects optimally-loaded MHC class I molecules for export to the cell surface.

Given that unlike tapasin, TAPBPR could catalyse peptide editing on MHC class I on its own in solution, I sought to test whether TAPBPR could also function as a peptide exchange catalyst on MHC class I molecules present on the surface of cells. By examining the artefactual expression of TAPBPR at the cell surface upon over-expression, I developed two novel cellular assays which allowed me to explore the function of TAPBPR as a peptide exchange catalyst on plasma membrane-expressed MHC class I molecules. I showed that, when given access the cell surface, TAPBPR can promote efficient peptide exchange on surface expressed MHC class I molecules. These assays allowed me to demonstrate that the 22-35 loop of TAPBPR was essential for its peptide exchange function. Moreover, I revealed that residue L30 within the loop was both necessary and sufficient for the efficient ability of TAPBPR to dissociate peptides from MHC class I molecules that typically accommodate hydrophobic anchor residues in their F pocket. This enabled me to propose a new mechanistic model for TAPBPR-mediated peptide editing. I further addressed the molecular basis governing the compatibility between TAPBPR and MHC class I molecules, by screening a wide panel of human leukocyte antigen (HLA) class I allotypes for their relative propensities to undergo peptide editing by TAPBPR. TAPBPR displayed a clear functional preference for HLA-A molecules, particularly for members of the A2 and A24 supertypes, over HLA-B and -C molecules. This preference appears to be driven by specific molecular features of the MHC class I F pocket, in particular residues H114 and Y116.

Finally, I explored the potential translational applications of using TAPBPR as a peptide exchange catalyst on surface-expressed MHC class I molecules. I demonstrated that recombinant TAPBPR can be utilised to load immunogenic peptides of choice directly onto plasma-membrane expression MHC class I, thus overriding the internal antigen presentation pathway. Subsequently, I revealed that, TAPBPR can be used to induce T cell-mediated killing of tumour cells. These findings highlight a potential therapeutic application of TAPBPR in increasing the immune recognition of tumours.

Acknowledgements

The completion of the research presented in this thesis would not have been possible without the help and support of many people. First and foremost, I would like to thank my supervisor, Dr. Louise Boyle, first of all, for offering me the opportunity to be part of her group and second, for her continuous guidance and inspiration throughout the course of my projects. I am particularly grateful to her for allowing me to implement my own ideas and for constantly pushing me to reach beyond my comfort zone. Second, Dr. Andreas Neerincx was absolutely vital for the progress of my research, equipping me with a variety of methods and techniques as well as with practical and diligent work ethic.

I am extremely grateful for the privilege of working with Dr. Janet Deane, who provided assistance and guidance with protein expression and purification experiments, as well as valuable insight into the structural biology aspect of the project. Moreover, I would like to thank Dr. Mark Wills and Dr. Maike the la Roche, who taught and assisted me in performing various primary T cell assays. Many thanks also to Dr. Gemma Brewin and Dr. Sarah Peacock, who provided us access to the facilities at the Tissue Typing Labs, as well as supervision during my experiments there. Finally, I had the pleasure of supervising Linnea Drexhage, a very talented master student, who helped me characterise the impact of polymorphisms in MHC class I molecules on their interactions with TAPBPR.

A few key results presented in this thesis were only possible with the help of our external collaborators, Prof. Stefan Stefanovic and Ana Marcu, from the University of Tübingen, as well as Dr. Clemmens Hermann, from the University of Cape Town, who performed the peptide elution and analysis work presented here. In addition, I would like to thank Prof. Paul MacAry, from the University of Singapore, and Prof. Peter Cresswell, from Yale University, for providing reagents essential for this work.

In the Department of Pathology, I am particularly grateful to Prof. John Trowsdale for his constant support, useful discussions and feedback sessions throughout my PhD programme. I am also grateful to the members of the Trowsdale and Kaufman groups for useful conversations and for providing regents. I would particularly like to thank to Dr. Stephen Graham for being my mentor and providing guidance and support with my academic progress as well as with career prospects in science.

Finally, I am extremely grateful to Wellcome and to the University of Cambridge, for the funding provided and for offering me the opportunity to undertake my PhD.

Table of Contents

List of Figures

List of Tables

Abbreviations

ABC	ATP-binding cassette
AIDS	Acquired immune deficiency syndrome
APC	Professional antigen presenting cell
β_2m	Beta-2-microglobulin
BSA	Bovine serum albumine
CD	Cluster of differentiation
CLIP	Class II-associated invariant chain peptide
cryo-EM	Cryogenic electron microscopy
CTL	Cytotoxic T lymphocyte
DC	Dendritic cell
DMSO	Dimethyl sulfoxide
EBV	Epstein-Barr virus
EDTA	Ethylenediaminetetraacetic acid
ER	Endoplasmic reticulum
ERAD	Endoplasmic reticulum-associated protein degradation
ERAP	Endoplasmic reticulum aminopeptidase
ERAAP	Endoplasmic reticulum aminopeptidases associated with antigen processing
ERp57	Endoplasmic reticulum protein 57
FACS	Fluorescence-activated cell sorting
FCS	Foetal calf serum
GFP	Green fluorescent protein
HCMV	Human cytomegalovirus
HCV	Hepatitis C virus
HEK	Human embryonic kidney
HIV	Human immunodeficiency virus
HLA	Human leukocyte antigen
HRP	Horseradish peroxidase
IFN	Interferon
Ig	Immunoglobulin
Ii	Invariant chain

kDa	Kilodalton
KIR	Killer cell immunoglobulin-like receptor
LILR	Leukocyte immunoglobulin-like receptors
LMP	Low molecular mass poylpeptides
mAb	Monoclonal antibody
MACS	Magnetic-activated cell sorting
Mbps	Megabase pairs
MECL-1	Multicatalytic endopeptidase complex-like 1
MHC	Major histocompatibility complex
MIIC	MHC class II compartment
NEM	N-ethylmaleimide
Ni-NTA	Nickel-nitrilotriacetic acid
NK	Natural killer
NMR	Nuclear magnetic resonance
PAGE	Polyacrylamide gel electrophoresis
PBMC	Peripheral blood mononuclear cell
PBS	Phosphate-buffered saline
PCR	Polymerase chain reaction
PE	Phycoerythrin
PLC	Peptide loading complex
pMHC	Peptide-MHC complex
PMSF	phenylmethylsulfonyl fluoride
SDS	Sodium dodecyl sulfate
TAMRA	5-carboxytetramethylrhodamine
TAP	Transporter associated with antigen processing
TAPBP	TAP-binding protein
TAPBPR	TAPBP-related
TBS	Tris-buffered saline
TCR	T cell receptor
TNF-α	Tumour necrosis factor α
UGT1	UDP-glucose:glycoprotein glucosyltransferase 1
WT	Wild type

1. Introduction

1.1. Role of MHC molecules in the immune system

1.1.1. Antigen presentation

The process of antigen presentation is crucial for T cell-mediated immune recognition of both extracellular and intracellular pathogens, as well as other cellular abnormalities. Antigen presentation is the process by which cells display small fragments of the cellular proteome at their surface, for inspection by T cells. The peptides presented at the cell surface are loaded onto major histocompatibility (MHC) molecules. By sampling the peptide pool presented on MHC molecules, T cells will recognise peptides derived from foreign or abnormal proteins and target these cells for destruction. Thus, the process of antigen presentation enables T cell immunosurveillance of infections and cancer and thus lies at the core of adaptive immunity.

T cell receptors (TCRs), expressed on the surface of T cells, can recognize peptides presented on two different classes of MHC molecules, class I and class II (Katz et al., 1973a, Katz et al., 1973b, Rosenthal and Shevach, 1973, Shevach and Rosenthal, 1973, Zinkernagel and Doherty, 1974). MHC class I molecules are present in all nucleated cells in the body and present peptides to T cells that express the co-receptor CD8 ($CD8^+$ T cells) (Swain, 1983, Emmrich et al., 1986, Gao et al., 1997). $CD8^+$ T cells, also known as cytotoxic T lymphocytes (CTLs), are effector T cells that kill target cells upon recognition of foreign peptides bound to MHC class I molecules. MHC class I molecules present peptides mainly derived from intracellular sources and thus confer protection against intracellular pathogens, such as viruses, or against tumour development. In contrast, MHC class II molecules are only expressed in professional antigen presenting cells (APCs) and present peptides to T cells expressing the surface co-receptor CD4 ($CD4^+$ T cells) (Janeway et al., 1988, Swain, 1983). $CD4^+$ T cells are referred to as “helper” T cells, as they modulate the activation of other immune cells, such as B cells or macrophages. The peptides presented on MHC class II molecules are derived mainly from extracellular sources. Thus, MHC class II molecules protect against either extracellular or intravesicular pathogens, such as bacteria or parasites.

1.1.2. Function in innate immunity

In addition to their role in presenting antigenic peptides to T cells for the generation of adaptive immune responses, MHC class I molecules play a key role in the immunosurveillance mechanisms of natural killer (NK) cells. Killer cell immunoglobulin-like receptors (KIRs), found on the surface of NK cells, detect expression levels of MHC class I at the cell surface. In case a cell downregulates its MHC class I expression, for instance due to viral infection or tumorigenesis, it will fail to send inhibitory signals to the NK cells via KIR-mediated recognition and will hence be susceptible to killing by NK cells (Karre et al., 1986, Ljunggren and Karre, 1990). Although the majority of KIRs serve inhibitory functions, there are a few KIRs that transmit activating signals upon recognition of specific MHC class I targets (Moretta et al., 1995, Stewart et al., 2005). Apart from KIRs, MHC class I molecules are also recognized by leukocyte immunoglobulin-like receptors (LILRs), found predominantly on the surface of myeloid lineages (Colonna et al., 1997, Cosman et al., 1997, Cella et al., 1997). LILRs expressed on professional APCs such as macrophages or dendritic cells (DCs) modulate cytokine release and expression of costimulatory molecules, thus influencing the signalling of these cells to the adaptive immune system. In contrast to the interactions of MHC class I molecules with T cell receptors (TCRs), which occur strictly in a peptide-dependent manner, the recognition of MHC class I by KIRs and LILRs are considerably less sensitive to the bound peptides (Natarajan et al., 2002).

1.2. MHC in health and disease

As its name suggests, the MHC was historically discovered in the field of transplantation. More than a century ago, the existence of a genetic basis of compatibility in tissue transplants was first proven by Little and Tizzier (Little and Tyzzer, 1916). Upon performing tumour transplantations in mice, they discovered that hybrid mice from two inbred strains allowed for the growth of tumour transplanted from either parental strain donor, however tumours transplanted between two unrelated mouse strains were rejected. Later, Gorer demonstrated that the observed transplant rejection was a result of an immune reaction from the donor (Gorer and Schutze, 1938). Following allogeneic and xenogeneic transplantations in rabbits, formation of antibodies specific for the donor tissues was observed in the serum of the recipient (Gorer and Schutze, 1938). Gorer attributed histocompatibility to a set of antigenic molecules, later discovered to be encoded in a specific genomic region, at the time termed the

"strong H" locus and currently known as the H-2 locus (Snell, 1948), which is the equivalent of the MHC locus in mice. Intense efforts towards unravelling the genetic and immunological complexity of the MHC were made in the following decades, until Zinkernagel and Doherty demonstrated that T cells induced by viral infection recognize infected cells in an antigen-specific, MHC-restricted manner (Zinkernagel and Doherty, 1974). It was later understood that in addition to their roles in viral infections and transplantation, MHC are crucial for conferring protection against other pathogens (e.g. bacteria or parasites), as well as cancer, and are generally responsible for the induction of autoimmune reactions (Bodmer, 1987, Trowsdale and Knight, 2013).

Pathogens are considered to be the main drive for the extraordinary polymorphism in the MHC genes (Zinkernagel and Doherty, 1979, Lederberg, 1999). Studies in chickens, which, in contrast to mammals, possess only one dominantly expressed MHC class I allele, "the minimal essential" (Kaufman et al., 1999, Kaufman et al., 1995), have revealed a striking correlation between the dominant MHC class I allele expressed and their susceptibility to either Rous sarcoma virus and Marek's disease virus (Kaufman and Wallny, 1996). The explanation for the observed association of a particular MHC allele with disease outcome was based on the distinct peptide repertoire presented on each MHC class I molecule, enabling highly allele-specific T cell responses.

In humans, polymorphism in MHC molecules has been mainly associated with different progression levels of viral diseases, such as acquired immune deficiency syndrome (AIDS), and susceptibility to autoinflammatory conditions (ankylosing spondylitis, rheumatoid arthritis, type 1 diabetes, systemic lupus erythematosus), drug hypersensitivity (e.g. abacavir) and cancer (Illing et al., 2012, Trowsdale and Knight, 2013, Naranbhai and Carrington, 2017). However, given that humans express a multigene family of MHC class I and class II molecules and are thus more capable of controlling pathogens, the majority of human MHC-associated diseases are autoimmune (Trowsdale and Knight, 2013).

1.3. The MHC region

Located on chromosome 6, the human MHC region, also known as the human leukocyte antigen (HLA), encompasses approximately 3.6 Mbps and comprises a high number of genes

involved in immune response generation (Campbell and Trowsdale, 1993, Forbes and Trowsdale, 1999). The MHC gene family is divided into three subgroups, based on their distribution along the chromosome: class I, class II and class III. The class I region encodes the heavy chains of three classical HLA class I genes (HLA-Ia), namely HLA-A, -B and -C, and three non-classical HLA class I genes (HLA-Ib), namely HLA-E, -F and -G. The class II region includes the α- and β- chains of each of the three HLA class II molecules, HLA-DR, -DQ and DP, as well as various components of the cellular machinery responsible for the processing and loading of HLA class I molecules with peptide fragments. Finally, the class III region, which sits in between the class I and class II regions, does not contain any elements of the antigen presentation pathway, comprising mostly genes encoding for cytokines and elements of the complement system (Campbell and Trowsdale, 1993, Forbes and Trowsdale, 1999).

1.4. The structure of MHC class I molecules

MHC class I molecules consist of a transmembrane heavy α chain, which is highly polymorphic, and a non-covalently attached, conserved soluble light chain, beta-2-microglobulin (β_2m) (**Figure 1a**) (Bjorkman et al., 1987). The α chain has a molecular weight of 45 kDa and consists of three domains: α1, α2 and α3. The α1 and α2 domains form the peptide binding groove, a membrane-distal superdomain which includes two antiparallel α helices on top of 8 β strands. The α3 is an immunoglobulin-like domain, which, together with β_2m, forms the membrane-proximal region of MHC class I molecules (Bjorkman et al., 1987). The peptide binding groove of MHC class I molecules is restrictive with respect to the peptide length, which is typically between 8 and 11 amino acids (**Figure 1b**) (Fremont et al., 1992, Madden et al., 1991). Specific amino acids of the groove typically compose six binding pockets (A-F) (**Figure 1c**) (Garrett et al., 1989), which accommodate the corresponding side chains of the bound peptide, known as anchor residues. Therefore, the peptide specificity of a particular MHC class I molecule, also known as its peptide binding motif, is determined by the shape, depth and charge of its peptide binding groove and of its individual binding pockets. The affinity of a peptide for a particular MHC class I molecule is partly determined by the interactions between the anchor residues of the peptide and the pockets of the MHC class I groove (Falk et al., 1991, Madden et al., 1991, Matsumura et al., 1992, Guo et al., 1992). In addition, peptide affinity is also determined by the hydrogen bonds between its N- and C- termini with specific tyrosine residues at the two ends of

the groove (Madden et al., 1992). Consequently, both the shape/sequence and the length of the peptide are crucial for its ability to stably bind to an MHC class I molecule.

In addition to determining the peptide's ability to get stably anchored into the MHC class I binding groove, the sequence of the peptide is also crucial for the recognition of peptide-MHC (pMHC) class I complexes by the TCR (Madden et al., 1992, Zhang et al., 1992). Since each TCR recognizes a distinct pMHC conformation, both the overall shape of the peptide as well as its impact on the overall conformation of the class I binding groove is critical for the interaction with the TCR. Specifically, the peptide residues that generally play the highest impact on TCR recognition are either the anchor residues, usually found at positions 2 and 9 of the peptide, that drive the affinity of the peptide for MHC class I, or, typically the ones on positions 4-6, via their direct interactions with the TCR.

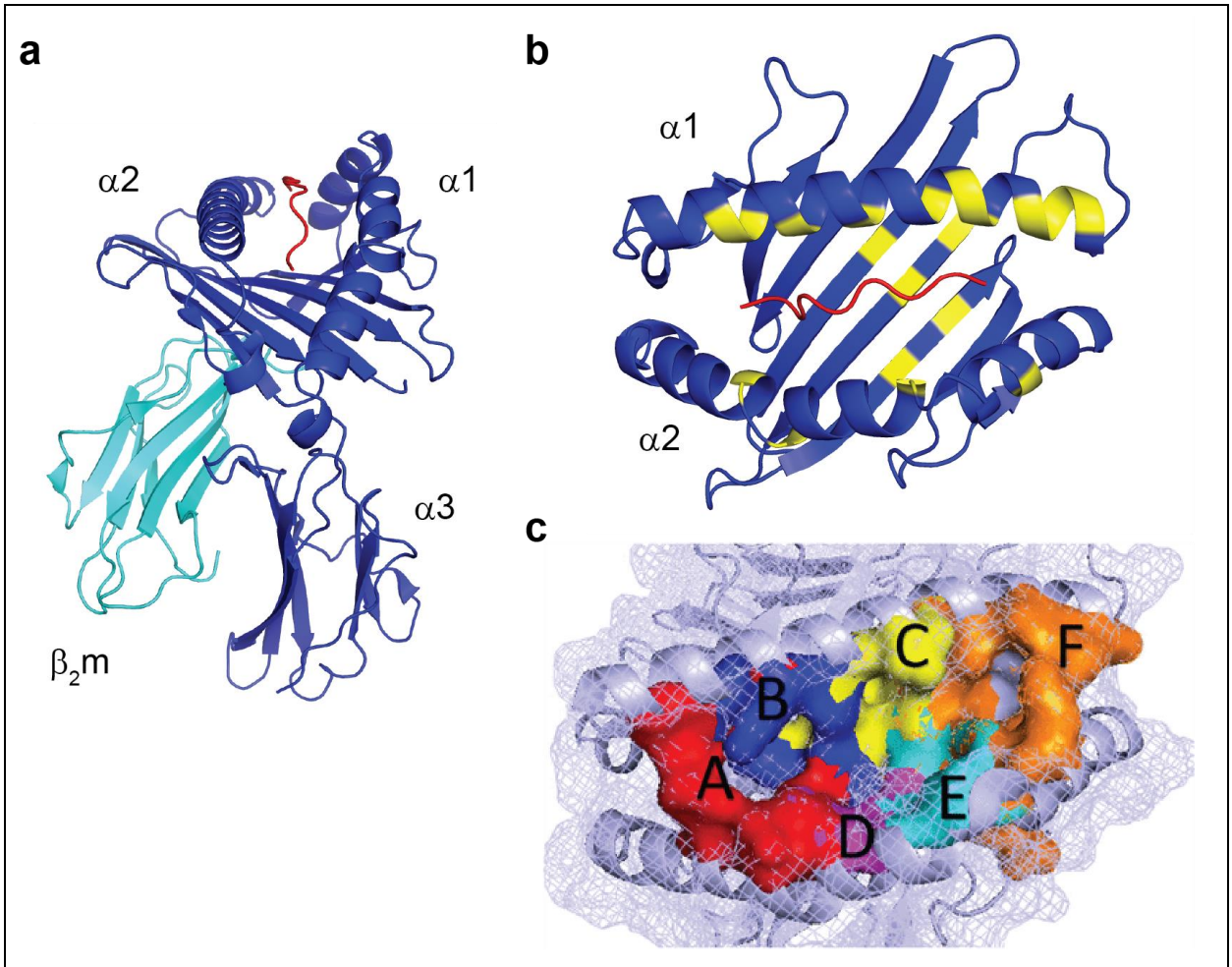

Figure 1: Structure of the MHC class I molecule. Pymol image of the crystal structure of HLA-B27 (PDB ID 1HSA) shown as (**a**) a side view of the entire MHC class I HC-β_2m-peptide complex or (**b**) as a top view of the peptide binding groove. In **b**) highly polymorphic amino acid residues across different alleles are highlighted in yellow. (**c**) Representation of the specificity pockets A-F within the peptide binding groove, as described by Ramsbottom et al. (Ramsbottom et al., 2018).

1.5. Polymorphisms in MHC class I molecules and relevance in immune responses

The MHC class I locus contains the most polymorphic genes in humans, comprising over 10,000 alleles. The vast majority of polymorphisms found in HLA class I molecules, reside at the sites of the peptide binding groove that determine the peptide specificity of individual HLA class I molecules (**Figure 1b**). Consequently, although many different HLA class I allotypes are structurally similar, each individual allotype can bind and present a distinct set of peptides, thus eliciting highly specific $CD8^+$ T cell responses. The peptide repertoire presented by a particular HLA class I molecule profoundly influences the susceptibility of an individual to infectious diseases or autoinflammatory conditions. For instance, specific pairs of HLA class I allotypes that differ in only one amino acid respectively, such as HLA-B*57:03 and HLA-B*57:02, HLA-B*35:01 and -B*35:03 or HLA-B*42:01 and -B*42:02, are associated with significantly different progression rates of the human immunodeficiency virus (HIV), mainly via their different peptide sets presented for immune recognition (Gao et al., 2001, Kloverpris et al., 2012a, Kloverpris et al., 2012b). Similarly, single amino acid differences across different HLA class I pairs, at positions key for determining peptide specificity, have also been shown to strongly influence predisposition to specific autoinflammatory diseases. For instance, ankylosing spondylitis is associated with the presence of HLA-B*27:05, but not HLA-B*27:06 or B*27:09 (Fiorillo et al., 1998), while birdshot chorioretinopathy shows a strong association with HLA-A*29:02, but not with HLA-A*29:01 (LeHoang et al., 1992).

1.6. The canonical MHC class I antigen processing and presentation pathway

1.6.1. Generation of antigenic peptides

Antigenic peptides that bind in the peptide binding groove of MHC class I molecules are generated in the cytosol, as a result of proteasomal degradation (**Figure 2**). It is currently understood that these peptides originate from the turnover of self-proteins, defective ribosomal products and proteins of foreign origin, such as viral or from other intracellular parasites (Eisenlohr et al., 2007, Yewdell et al., 1996, Rock et al., 2014, Rock and Goldberg, 1999). The constitutively-expressed 26S proteasome degrades cellular proteins into peptides of

appropriate length for translocation into the endoplasmic reticulum (ER) lumen. Upon exposure to inflammatory stimuli, such as IFNs or TNF-α, three constitutively expressed subunits of the proteasome are replaced by two specialized subunits encoded in the MHC region, namely the low molecular mass poylpeptides (LMP) 2 and 7 (Brown et al., 1991, Glynne et al., 1991, Kelly et al., 1991a, Ortiz-Navarrete et al., 1991), and by the multicatalytic endopeptidase complex-like 1 MECL-1, which is not encoded in the MHC region (Groettrup et al., 1996, Nandi et al., 1996). This version of the proteasome is known as the immunoproteasome. The immunoproteasome displays a different cleavage profile compared to the constitutive proteasome, showing enhanced cleavage after hydrophobic amino acid residues (Driscoll et al., 1993, Gaczynska et al., 1994). Thus, the immunoproteasome is more efficient at degrading proteins of foreign origin (i.e. viral proteins) and at generating antigenic peptides. It is thus highly abundant in antigen presenting cells and plays a vital role during infection.

1.6.2. Transport of peptides into the ER

Following proteasomal degradation, peptides of appropriate length and sequence are transported from the cytoplasm into the ER lumen by the transporter associated with antigen processing (TAP) protein complex (Deverson et al., 1990, Spies et al., 1990, Trowsdale et al., 1990). The TAP belongs to the ATP-binding cassette (ABC) transporter family and consists of two subunits, TAP1 and TAP2, encoded in the MHC region. TAP1 and TAP2 generally form heterodimers that are imbedded in the ER membrane.

It has been shown that in TAP1-deficient cells, the surface expression of MHC class I molecules is drastically reduced and that the rate of degradation of MHC class I molecules is enhanced (Salter and Cresswell, 1986, Spies et al., 1992, Spies and DeMars, 1991). Moreover, $TAP1^{-/-}$ mice are deficient of peripheral $CD8^{+}$ T cells specifically, due to the severely impaired MHC class I expression at the surface of thymocytes (Van Kaer et al., 1992).

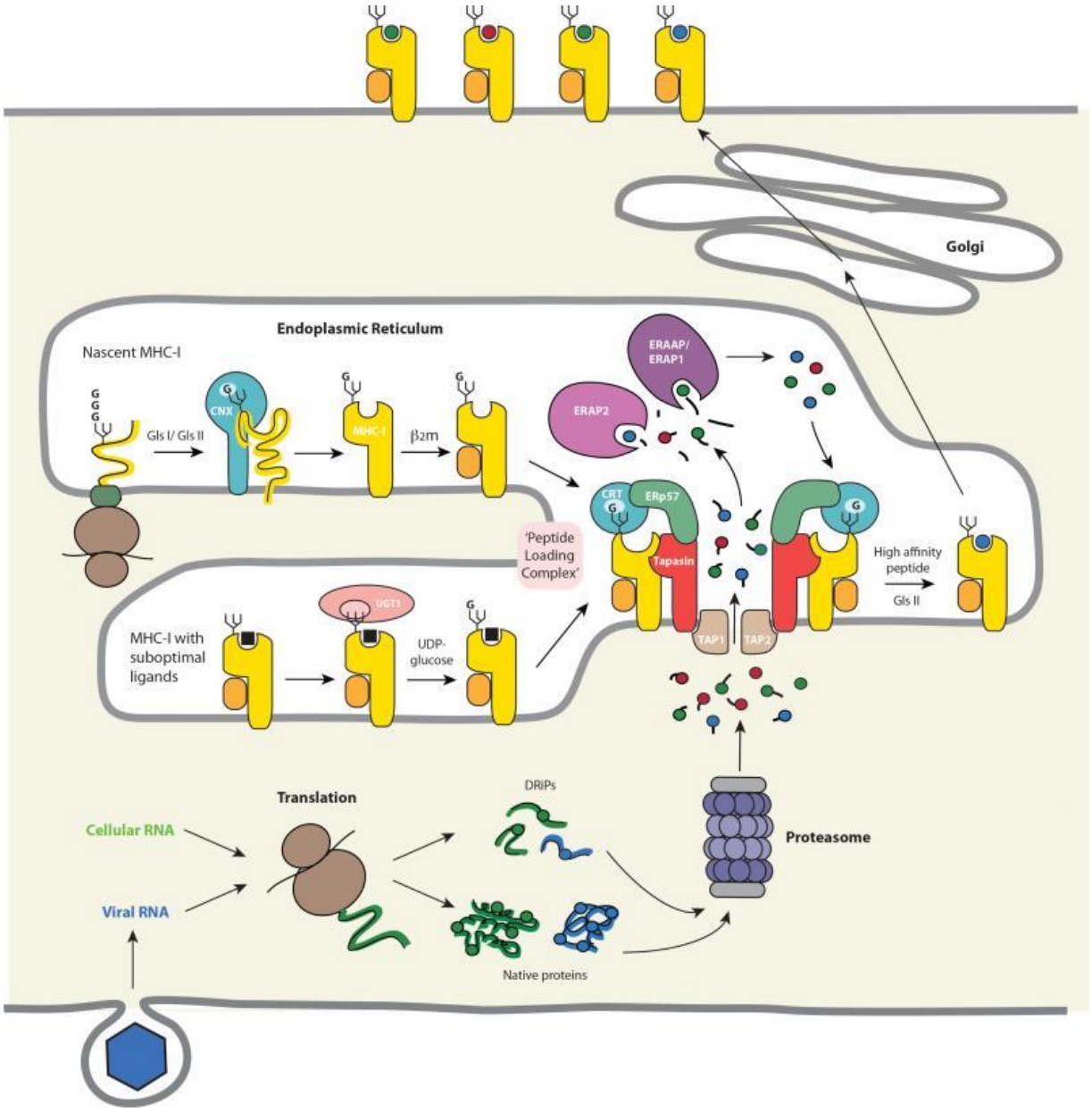

Figure 2: Classical MHC class I antigen processing and presentation pathway, adapted from Blum et al. (Blum et al., 2013). Following their import into the ER lumen, nascent MHC class I heavy chain acquire N-linked glycan, which are subsequently trimmed to a single glucose residue (G) by glucosidases 1 and 2 (Gls I/GLS II). Calnexin (CNX) binds to the N-linked glucose residue of the MHC class I heavy chain and modulates its folding and subsequent assembly with β_2m. Once assembled, the peptide-receptive MHC class I heterodimers associate with the PLC, composed of calreticulin (CRT), ERp57, TAP and tapasin, which ensures their proximity to the influx of peptide into the ER and loading with high-affinity peptides. MHC class I molecules loaded with high-affinity peptides are exported from the ER and trafficked to the cell surface. Sub-optimally loaded MHC class I molecules are recruited by UGT1, which reglucosylates them and recycles them to the PLC for a subsequent round of peptide editing. Peptides are generated from the proteasomal degradation of either DRiPs or native protein that are generated by the translation of mRNA of either self or foreign (e.g. viral) origin. These peptides are translocated into the ER by TAP and further trimmed by ER aminopeptidases (ERAAP/ERAP1 and ERAP2).

1.6.3. Peptide trimming in the ER

Once translocated in the ER lumen, peptides undergo further processing by the endoplasmic reticulum aminopeptidases associated with antigen processing (ERAP1/2 in humans and ERAAP in mice) (Saric et al., 2002, Serwold et al., 2002) (**Figure 2**). ERAP1, either free or in complex with ERAP2 (ERAP1/2), was proposed to trim precursor peptides from their N-terminus to their correct length, allowing them to efficiently bind into the MHC class I peptide binding groove. Although some studies have proposed that ERAP works in synergy with the MHC class I molecule in trimming peptides to the correct length for binding, the crystal structures of both ERAP1 and ERAP2 suggest that these enzymes are more suited for processing free peptides rather than MHC class I-associated peptides (Nguyen et al., 2011). Based on these findings, it has been suggested that ERAP uses an "intrinsic ruler" to trim peptides to the proper length, point at which the peptides dissociate from ERAP and are ready for loading onto MHC class I molecules (Chang et al., 2005, Nguyen et al., 2011). Regarding the role of ERAP in the generation of immune responses, previous work has shown that in the absence of ERAP1 in mice, the $CD8^+$ T cell-mediated immune responses to certain viral epitopes, of either vaccinia or lymphocytic choriomeningitis virus (LCMV) origin, are enhanced, however to others these responses are either reduced or unchanged (York et al., 2006). Thus, ERAP1 has only been shown to play a critical role in the hierarchy of immunodominance in viral infections, however it has not been proven so far to significantly affect the overall ability of the immune responses to combat viral infections. ERAAP however was demonstrated to confer protection against non-viral infections, such as *Toxoplasma gondii*. $ERAAP^{-/-}$ mice were no longer able to present an immunodominant and protective epitope derived from *Toxoplasma gondii* and thus enabled the uncontrolled replication of the pathogen (Blanchard et al., 2008). Interestingly, apart from its role in infections, multiple studies have also proven the importance of ERAP1 in certain autoimmune diseases in humans, associated with specific MHC class I alleles (Evans et al., 2011, Pazar et al., 2010, Wellcome Trust Case Control et al., 2007). Namely, specific alleles of the highly polymorphic ERAP1, with increased catalytic activity, showed a high-association rate to ankylosing spondylitis in HLA-B27-positive patients (Evans et al., 2011, Pazar et al., 2010). Moreover, ERAP1 was revealed to influence psoriasis susceptibility across individuals carrying HLA-C*06:02 (Genetic Analysis of Psoriasis et al., 2010, Sun et al., 2010). These studies together highlight the extreme consequences of aberrant peptide trimming on MHC class I antigen presentation in human health and disease.

1.6.4. Early folding and assembly of MHC class I dimers

Upon translocation in the ER lumen, the MHC class I heavy chain undergoes N-linked glycoslylation at residue Asn-86 (Bjorkman et al., 1987, Parham et al., 1977). The glycosylated heavy chain then recruits the lectin chaperone calnexin, which facilitates its correct folding. Calnexin is a transmembrane protein and together with its soluble homologue, calreticulin, is involved in the chaperoning and quality control of glycoproteins in the ER (Hammond et al., 1994, Hebert et al., 1995, Peterson et al., 1995). Calnexin also recruits ER protein 57 (ERp57), an ER-resident protein disulphide isomerase (PDI), which ensures the proper disulphide bond formation in the α3 domain of the MHC class I heavy chain, further stabilising the molecule (Zhang et al., 2006). The calnexin-ERp57 complex protects the folded MHC class I heavy chain from degradation and subsequently enables its association with the soluble subunit β_2m (Vassilakos et al., 1996). Assembly of the MHC class I heavy chain with β_2m was shown to be significantly reduced in the absence of calnexin (Vassilakos et al., 1996). A more recent study demonstrated the importance of the N-linked glycosylation for the chaperone-mediated folding and assembly of the MHC class I heavy chain-β_2m dimer, as mutation of the N-linked glycosylation site on the MHC class I heavy chain (N86Q) abolished chaperone binding and hence severely impaired the dimer formation (Rizvi et al., 2011). Following assembly, the resulting highly unstable peptide-receptive MHC class I heterodimer recruits the peptide loading complex.

1.6.5. The peptide loading complex

As its name implies, the peptide loading complex (PLC) is responsible for the loading of empty MHC class I molecules with optimal peptides prior to their export from the ER (**Figure 2**). The PLC consists of the TAP transporter, the lectin chaperone calreticulin, ERp57 and tapasin. Within the PLC, calreticulin is associated to the monoglucosylated glycan of MHC class I molecules, tapasin is bound to the MHC class I heavy chain (Sadasivan et al., 1996, Ortmann et al., 1997), while ERp57 associates to both tapasin and calreticulin, acting as a bridge between the two chaperones (Frickel et al., 2002). TAP is linked to the MHC class I molecule by tapasin (Ortmann et al., 1997, Sadasivan et al., 1996). In contrast to calnexin, which was associated with early folding events of MHC class I molecules, calreticulin was suggested to participate in the later stages of MHC class I assembly. Studies using calreticulin-deficient cell lines revealed a

critical role of calreticulin in the peptide loading of MHC class I molecules rather than in the early assembly of MHC class I and β_2m (Gao et al., 2002).

Regarding the sequence of events leading to the assembly of the PLC, the current view is that calreticulin associates first to the MHC class I heavy chain, as it replaces calnexin following the association of β_2m onto the heavy chain (Gao et al., 2002, Chapman and Williams, 2010, Hulpke and Tampe, 2013). Subsequently, the MHC class I-calreticulin complex recruits the preassembled ERp57-tapasin-TAP complex (Ortmann et al., 1997, Sadasivan et al., 1996, Hulpke and Tampe, 2013). The recently identified structure of the PLC, achieved using cryo-EM, enabled the direct visualisation of the different stages of PLC assembly onto MHC class I molecules (Blees et al., 2017). This study confirmed the previously proposed model of assembly of the PLC components onto peptide-receptive MHC class I molecules.

Upon acquiring high-affinity peptides, MHC class I molecules are released from the PLC (Spiliotis et al., 2000, Chapman and Williams, 2010) and are then subjected to further quality control checkpoints in the pathway. One such checkpoint is represented by the UDP-glycoprotein glucosyltransferase 1 (UGT1), which is responsible for reglucosylating MHC class I molecules loaded with sub-optimal peptides and for their subsequent recycling back to the PLC (**Figure 2**), for a subsequent round of peptide loading (Zhang et al., 2011, Wearsch et al., 2011). Despite UGT1 fulfilling a general role in the quality control machinery of glycoproteins (Sousa et al., 1992, Trombetta et al., 1989), this enzyme has been demonstrated to play a function role in the selection of optimally-loaded MHC class I molecules for export to the cell surface (Zhang et al., 2011, Wearsch et al., 2011).

1.7. Function of tapasin on MHC class I molecules

The TAP-binding protein (TAPBP), also known as tapasin, was the first-discovered molecular chaperone strictly dedicated to the MHC class I antigen presentation pathway. The gene encoding for tapasin is located in the MHC locus, more specifically within the MHC class II region, similarly to TAP1/2 and two of the immunoproteasome subunits. Tapasin plays a crucial role in the optimal loading of MHC class I molecules with high-affinity peptides and consequently on their efficient expression at the cell surface. Therefore, tapasin is crucial for the generation of optimal $CD8^+$ T cell-mediated immune responses. Tapasin fulfils several molecular functions which are described in-depth below.

1.7.1. Assembly of the PLC and binding to MHC class I

The entire assembly of the PLC revolves around the presence of tapasin and its ability to interact with MHC class I molecules (Figure 2). Tapasin is a type I transmembrane glycoprotein that forms a direct interaction with each of the other components of the peptide loading complex, as well as with MHC class I (Frickel et al., 2002, Gao et al., 2002, Ortmann et al., 1997, Sadasivan et al., 1996, Blees et al., 2017), bringing all these molecules together for the loading process. Despite the ability of tapasin to form a direct interaction with the MHC class I heavy chain, it requires the presence of the entire PLC in order to stably associate with MHC class I molecules. Moreover, once tapasin can no longer access the MHC class I molecule, upon loading it with a high-affinity peptide, the entire PLC disassembles (Spiliotis et al., 2000).

Despite the lack of a high-resolution structure of tapasin in complex with MHC class I, the interaction sites between the two proteins has been heavily investigated. On the MHC class I side, the affinity for tapasin has been attributed to the amino acid residues on positions 222-229, found in the α3 domain (Suh et al., 1999, Yu et al., 1999). Upon mutation of these residues, MHC class I loses its ability to interact with tapasin and subsequently with TAP. Interestingly, the same residues of MHC class I were previously shown to be essential for the interaction with CD8 (Gao et al., 1997, Salter et al., 1990). In a more recent study, it was suggested that the residues 333-335 of the tapasin IgC domain are key for the interaction with the 222-229 loop of MHC class I (Turnquist et al., 2001, Turnquist et al., 2002).

The second interaction site between the two proteins appears to be involving residues 122-134 of MHC class I, spanning the two beta sheets and the loop connecting them, found underneath the α2-1 region (Beissbarth et al., 2000, Lewis et al., 1996, Paquet and Williams, 2002, Peace-Brewer et al., 1996, Yu et al., 1999). Mutation of specific amino acids in this region has been shown to abolish tapasin binding as well as to severely impair surface expression of MHC class I molecules. Based on the solved crystal structure of tapasin in complex with ERp57 (Dong et al., 2009), the 122-134 region of MHC class I has been suggested to interact with set of positively-charged amino acid residue found in the IgV domain of tapasin, at the TN6 and TN7 sites.

1.7.2. Bridging TAP and MHC class I

Tapasin is able to bind simultaneously to the TAP transporter and to MHC class I, thus physically bridging the two main participants in the peptide loading process, namely the source of peptide and the peptide acceptor (Sadasivan et al., 1996, Blees et al., 2017). This ensures the proximity of the peptide-receptive MHC class I molecules to the site of peptide-influx into the ER lumen, providing the availability of a peptide-rich environment during the loading process. Moreover, by physically associating with TAP, tapasin was shown to be important for the stabilization and function of TAP in the cell. In the absence of tapasin, TAP was shown to undergo increased ER-associated degradation (ERAD) (Lehner et al., 1998). These findings were further backed up by the observation that tapasin transfections into tapasin-deficient 721.220 cells, which are defective in MHC class I peptide presentation (Greenwood et al., 1994), rescued surface expression of MHC class I molecules, as well as their recognition by $CD8^+$ T cells (Ortmann et al., 1997, Lehner et al., 1998).

1.7.3. Peptide editing on MHC class I molecules

1.7.3.1. Optimisation of peptide presentation on MHC class I

In addition to stabilizing peptide-receptive MHC class I molecules to facilitate their loading with peptide, tapasin is also responsible for ensuring that only high-affinity peptides bound to MHC class I molecules are exported for presentation (Howarth et al., 2004, Purcell et al., 2001, Williams et al., 2002). In doing so, tapasin catalyses the process referred to as “peptide editing”, actively exchanging sub-optimally loaded peptides of lower affinity for ones of higher affinity, until MHC class I molecules acquire optimal peptides. Tapasin-mediated peptide editing is thus crucial for the presentation of stably-bound antigens on MHC class I molecules at the cell surface and for generating the appropriate immune responses. In tapasin-deficient cells, a wide panel of MHC class I molecules suffer a significant decrease in their ability to load and present cargo at the cell surface. Moreover, tapasin-deficient mice display a severe impairment in the $CD8^+$ T cell and NK cell-mediated immune responses, associated with reduced level of MHC class I surface expression and with an altered peptide repertoire towards less stably bound peptides (Garbi et al., 2000, Grandea et al., 2000).

1.7.3.2. Proposed mechanisms of peptide editing

To enable efficient loading of MHC class I molecules with peptides of high affinity, tapasin is thought to catalyse the dissociation of low-affinity peptides loaded onto MHC class I, allowing their replacement with peptides of higher affinity. Two assays were developed to directly assess the ability of tapasin to edit peptides on MHC class I molecules. First, Chen and Bouvier have shown, by tethering recombinant versions of tapasin and MHC class I refolds via a leucine zipper, that tapasin directly facilitates dissociation of low-affinity peptides from class I molecules (Chen and Bouvier, 2007). Second, Wearsch and Cresswell showed that recombinant tapasin-ERp57 conjugates promote peptide binding to MHC class I molecules found intracellularly and also edited peptides on these molecules to maximize their affinity (Wearsch and Cresswell, 2007).

In trying to characterize the mechanisms of tapasin-mediated peptide exchange, based on the proposed interaction site between tapasin with the α2-1 region of the MHC class I groove (Dong et al., 2009), multiple studies speculated that tapasin actively decreases the binding energy between the C-terminus of the sub-optimally loaded peptides and the MHC class I binding groove (Van Hateren et al., 2010). Moreover, tapasin was proposed to stabilize the empty F pocket of the MHC class I binding groove to facilitate a subsequent round of peptide loading (Sieker et al., 2007, Zacharias and Springer, 2004). Since tapasin was suggested to bind exclusively to peptide-receptive conformations of MHC class I molecules, it is believed that tapasin traps the open conformation of MHC class I molecules loaded with low-affinity peptides, conformations which are highly unstable and occur transiently during sporadic partial dissociation of the peptide (Elliott, 1997, Elliott and Williams, 2005, Yu et al., 1999, Wright et al., 2004). In doing so, tapasin shifts the equilibrium between the two conformations of the peptide-loaded MHC class I molecule towards the open/receptive state, promoting the dissociation of the bound low-affinity peptide and its subsequent exchange by high-affinity ones (Praveen et al., 2010, Wright et al., 2004).

In accordance with these predictions, a more recent study relying on molecular dynamics simulation suggested that tapasin mediates peptide dissociation from MHC class I in a “tug-of-war” manner, by actively pulling the α2-1 helix region of the binding groove away from the peptide (Fisette et al., 2016). This in turn would disrupt hydrogen bonds between the peptide binding groove and the C-terminus of the peptide, thus decreasing their binding energy. In

addition, this model predicted that tapasin additionally stabilizes the F pocket of the class I binding groove, facilitating the access of the incoming peptide (Fisette et al., 2016).

1.7.4. Allelic dependence of HLA class I on tapasin

Despite the suggestive role of tapasin in the optimal loading of MHC class I molecules and hence in the expression of stable pMHC class I complexes at the cell surface, previous studies have shown that HLA class I molecules exhibit a wide spectrum of dependencies on tapasin for optimal surface expression and peptide presentation. In other words, some HLA class I allotypes seemed considerably more dependent on tapasin for efficient peptide presentation at the cell surface than others (Rizvi et al., 2014, Williams et al., 2002, Wright et al., 2004). These studies have addressed tapasin-dependency mainly as a read-out of surface expression levels or thermostability of MHC class I molecules, in the presence or absence of tapasin. Interestingly, while most HLA class I allotypes show a clear reduction in surface expression levels in the absence of tapasin, there are a few, such as HLA-B*44:05, -A*02:01 or -B*27:05, that remain largely unaffected (Park et al., 2003, Peh et al., 1998, Rizvi et al., 2014, Williams et al., 2002).

Several studies have suggested that residue 116 in particular, which is highly polymorphic in MHC class I molecules, influences tapasin-dependence by affecting the overall plasticity of the MHC class I F pocket and hence the availability of open MHC class I conformations, accessible to tapasin (Sieker et al., 2007, Wright et al., 2004, van Hateren et al., 2015, Van Hateren et al., 2010, Garstka et al., 2011). Interestingly however, residue 116 was also suggested to influence the specificity of the F pocket for peptide residues (Garrett et al., 1989), however the extent to which the MHC class I F pocket specificity influences tapasin-dependency remains largely unclear, given the lack of any clear correlation between the two.

These studies, having mainly assessed tapasin-dependency across HLA-B molecules, have concluded that, generally, molecules belonging to the Bw4 group are more dependent on tapasin, in terms of efficient folding and peptide loading, as well as regarding their successful expression at the cell surface. However, there were multiple exceptions to this trend, with Bw6 molecules, such as HLA-B*08:01 or HLA-B*15:03, displaying higher tapasin-dependence than many Bw4 allotypes (Rizvi et al., 2014). Moreover, Bw4 molecules such as B*44:05 displayed low dependency on tapasin for stable surface expression levels compared to most HLA-B

molecules belonging to the Bw6 group. Based on this work and the work of other groups interrogating allelic-dependence of HLA class I on tapasin (Park et al., 2003), there are currently no precise criteria on which tapasin-dependence of HLA class I molecules is based.

1.8. Non-canonical MHC class I antigen presentation pathways

1.8.1. TAP-independent peptide loading of MHC class I molecules

While the canonical pathway is the main source of pMHC class I complexes expressed at the cell surface, the acquisition of antigenic pathways MHC class I molecules is possible via alternative pathways, all of which occur independently of TAP-mediated translocation of peptides into the ER lumen. This phenomenon was first observed in the human T2 cell line (a T cell X B cell line expressing HLA-A2, however lacking both TAP1 and TAP2) (Salter and Cresswell, 1986, Salter et al., 1985). Despite the low surface expression levels of HLA-A2 in these cells, analysis of the immunopeptidome revealed that the most abundant peptides presented on HLA-A2 were derived from the signal sequences of both membrane and secreted proteins, sequences required for the translocation of these proteins into the ER lumen and which are then cleaved by the signal peptidase (Henderson et al., 1992, Wei and Cresswell, 1992). It was later shown that such peptides derived from protein signal sequences bound to HLA-A2 in T2 cells can even induce $CD8^+$ T cell-mediated recognition (Henderson et al., 1993). Moreover, presentation of signal sequence-derived peptides was also discovered in TAP-expressing cells, however, naturally, at much lower abundance (Huczko et al., 1993). The presentation of these peptides however was restricted to HLA class I molecules that typically accommodate hydrophobic amino acid residues present at the C-terminus of the peptide, such as HLA-A2 and HLA-B7, given the preferred cleavage site of the signal peptidase (Huczko et al., 1993, Wei and Cresswell, 1992).

The importance of these alternative antigen presentation pathways has also been highlighted *in vivo*, as patients with the TAP-deficiency syndrome (Gadola et al., 2000), characterised by mutations in TAP1 or TAP2 (de la Salle et al., 2002), displayed $CD8^+$ T cell-mediated immune responses against Epstein-Barr virus (EBV) infection (de la Salle et al., 2002, Lautscham et al., 2001). These responses were found to be exclusively against viral epitopes predicted to get

loaded onto MHC class I molecules independently of TAP. Strikingly, these TAP-deficient patients appear to control such viral infections rather efficiently.

Having highlighted the importance of TAP-independent pathways in the generation of immune responses against intracellular pathogens, the exact mechanisms by which MHC class I molecules acquire peptides without the involvement of the PLC remain poorly understood. There have been numerous reports addressing the various pathways used to generate and load peptide epitopes onto MHC class I molecules, mainly focusing on the endovacuolar and endosomal compartments as cellular sites for this process (Oliveira and van Hall, 2013, Vyas et al., 2008).

1.8.2. Cross-presentation

One alternative MHC class I presentation pathway, specific to phagocytic immune cells, is known as cross-presentation. In order to alert the adaptive immune system of infections or tumours occurring in peripheral tissues, dendritic cells (DCs) need to sample the affected cells and migrate to the lymph nodes, where they present the foreign or abnormal peptides to T cells in order to generate appropriate adaptive immune responses. This means that DCs must first acquire the antigenic peptides either from intracellular sources of the infected cells or, in a vaccination setting, from extracellular sources. The process by which phagocytic antigen-presenting cells (APCs) capture antigens from exogenous sources, load and present them on their own MHC class I molecules is known as cross-presentation. “Cross-priming” is another term used to describe this process, given that these cross-presented antigens are displayed by the DCs for the priming of T cells against specific peptides of foreign origin (Bevan, 1976b, Bevan, 1976a).

Intense efforts have been made in the pursuit of unravelling the mechanisms and pathways governing cross-presentation. The fact that MHC class I molecules have been shown to be able to passively exchange peptides at pH values between 4.5 and 5.5 indicate that MHC class I molecules could acquire exogenous antigens in the endocytic compartments (Gromme et al., 1999, Stryhn et al., 1996). Three main endocytic pathways for cross-presentations have been presented thus far, namely a cytosolic pathway, a vacuolar pathway and a phagosome-to-ER pathway. The cytosolic pathway (Kovacsovics-Bankowski and Rock, 1995) involves the phagocytosed antigens being translocated into the cytosol from the phagosome (potentially via

the Sec61 transporter), point where they undertake the canonical antigen presentation pathway on MHC class I molecules. In the vacuolar pathway (Pfeifer et al., 1993, Schirmbeck et al., 1995, Song and Harding, 1996), exogenous antigens are directly processed in the early phagosome by resident cathepsins (Shen et al., 2004). The resulting antigenic peptides are then loaded onto MHC class I molecules (presumably by passively exchanging loaded self-peptides) which are recycled from the cell surface into the early phagosome via recycling endosomes. Following their loading with the pathogen-derived peptides, the mechanisms by which recycled MHC class I molecules are trafficked from the phagosome back to the plasma membrane remain poorly understood. Finally, in the phagosome-to-ER pathway, the phagosome fuses with the ER, enabling the transfer of both components of the canonical antigen presentation pathway and, potentially, components of the endoplasmic reticulum-associated protein degradation (ERAD) pathway from the ER to the phagosome (Guermonprez et al., 2003, Houde et al., 2003). Thus, misfolded soluble proteins internalized through the phagosome could get degraded in the phagosome, exported into the cytosol and then reacquired by the phagosome as peptides and loaded onto MHC class I molecules via the PLC. This pathway however is the most controversial among the three, having been subjected to consistent criticism (Gros and Amigorena, 2019, Rock and Shen, 2005, Touret et al., 2005).

Despite the progress concerning the broad understanding of the potential routes of cross-presentation, as well as of the cellular and molecular participants to this process, there is still a clear lack of understanding of the detailed molecular mechanisms by which exogenous antigens internalized by phagocytic cells gain access to and are loaded onto MHC class I molecules. The most interesting question in my opinion is regarding the means by which antigenic peptides resulted from the exogenous sources get physically loaded onto MHC class I molecules. It seems rather unlikely that exogenous antigens would simply replace self-peptides bound to MHC class I molecules, even in slightly acidic environments such as endocytic compartments, without a dedicated molecular chaperone to catalyse this exchange process. I base this speculation on the comparison with MHC class II molecules, which cannot exchange CLIP for antigenic peptides found in endosomes, even during prolonged time periods, in the absence of the corresponding peptide exchange catalyst HLA-DM or while the negative regulator of HLA-DM, namely HLA-DO, is switched on (**see section 1.10**).

1.9. Discovery of TAPBPR, a novel MHC class I-dedicated chaperone

For over two decades, tapasin was considered to be the sole MHC class I-dedicated chaperone. However, several years ago, the Boyle lab has discovered another chaperone on this pathway, namely the tapasin-related protein TAPBPR (Boyle et al., 2013). Despite sharing 22% sequence identity and 33% domain homology with tapasin, the gene encoding for TAPBPR (*tapbpl*) is not located on the MHC locus, together with the other components of the pathway, but at chromosome position 12p13.3 (Teng et al., 2002), near a paralogous region of the MHC (Du Pasquier, 2000). However, similarly to the genes encoded in the MHC region, expression of TAPBPR is also IFN-γ-inducible (Landis et al., 2006).

1.9.1. Binding to MHC class I molecules

Similarly to tapasin, TAPBPR was also shown to form a direct interaction with MHC class I molecules (Boyle et al., 2013). Moreover, the two chaperones were suggested to bind in a similar orientation to the MHC class I molecules, given the same residues of the MHC class I molecule were essential for its interactions with both tapasin and TAPBPR (Hermann et al., 2013). Namely, interaction studies upon performing site-directed mutagenesis revealed that essential for the interaction with MHC class I is a patch stretching over residues between positions 205 and 272 on neighbouring β-sheets of TAPBPR, residues completely conserved in tapasin (Hermann et al., 2013). Additionally, residues 331-337 on the IgC domain of TAPBPR, partially conserved in tapasin, however present at homologous positions within the protein structures, were shown to drive association with either the α3 domain of the MHC class I heavy chain, or with β_2m. Consequently, TAPBPR and tapasin were shown to bind to MHC class I in a mutually exclusive manner (Hermann et al., 2013).

Two recently discovered crystal structures of the TAPBPR-MHC class I complex confirmed the previously described interaction sites between MHC class I and TAPBPR, as well as the resulting orientation of TAPBPR onto MHC class I (Jiang et al., 2017, Thomas and Tampe, 2017). Moreover, these crystal structures, together with the one obtained for the PLC by cryogenic electron microscopy (cryo-EM), confirmed the similar orientations of tapasin and TAPBPR when bound to MHC class I (Hermann et al., 2013).

However, in contrast to tapasin, which binds to MHC class I within the confines of the PLC, TAPBPR is capable of stably interacting with MHC class I independently of TAP, tapasin or other

components of the PLC (Boyle et al., 2013). In fact, TAPBPR is not part of the PLC, nor does it bind to any component of the PLC (Boyle et al., 2013). Furthermore, TAPBPR also seems to have a higher intrinsic affinity for MHC class I compared to tapasin, given that TAPBPR on its own can form a stable interaction with MHC class I (Boyle et al., 2013, Hermann et al., 2015b), whereas tapasin requires either artificial tethering or the presence of the entire PLC for stably associating with MHC class I (Chen and Bouvier, 2007, Wearsch and Cresswell, 2007). Based on recent studies, it seems that the ability of TAPBPR to form stronger interactions with MHC class I than tapasin could be partially attributed to particular residues in its IgC domain, such as Q334 or S335, which are not conserved in tapasin (Hermann et al., 2013) and were suggested to be involved in polar interactions with the α3 domain of MHC class I heavy chain (Jiang et al., 2017, Thomas and Tampe, 2017). Additionally, TAPBPR seems to have a higher degree of conformational plasticity than tapasin, which appears to be more rigid by comparison, allowing it to better mould onto the MHC class I molecule at individual interaction sites (Thomas and Tampe, 2017).

Another difference in the binding to MHC class I between tapasin and TAPBPR is represented by their relative dependencies on the N-linked glycan on the MHC class I heavy chain. Given its dependence on the PLC for efficient association with MHC class I, tapasin relies on the prior recruitment of calreticulin on the MHC class I heavy chain. Therefore, mutation of the N-linked glycosylation motif on MHC class I was shown to impair tapasin binding (Neerincx and Boyle, 2018, Rizvi et al., 2011). However, these non-glycosylated MHC class I molecules displayed an increased level of binding to TAPBPR (Neerincx and Boyle, 2018). These results are consistent with previous work from the Boyle lab, according to which MHC class I molecules show a higher accessibility to TAPBPR in the absence of tapasin (Hermann et al., 2013), suggesting that TAPBPR could potentially sever overlapping functions.

1.9.2. Cellular trafficking

Despite its high abundance in the ER, TAPBPR was shown to also traffic through the medial Golgi compartment (**Figure 3**)(Boyle et al., 2013). In constrast to tapasin, whose cellular localization is restricted to the ER, based on its ER-retrieval motif KKXX (Jackson et al., 1990, Lehner et al., 1998, Nilsson et al., 1989), the tail of TAPBPR does not contain any obvious motif associated with retention in the ER. Moreover, tapasin and TAPBPR were suggested to reside in

different sub-compartments of the ER (Neerincx and Boyle, 2017, Boyle et al., 2013). Tapasin is associated with the TAP transporter, being present in the peptide-rich regions. Since TAPBPR does not bind TAP and can be exported through the medial Golgi, it was suggested to reside mainly in the peptide poor, outer layers of the ER (Neerincx and Boyle, 2017, Hermann et al., 2015a, Kamhi-Nesher et al., 2001).

1.9.3. Peptide editing

Similarly to tapasin, TAPBPR was shown to directly mediate peptide editing on MHC class I molecules (Hermann et al., 2015b). More specifically, in a similar assay to the one used by Chen and Bouvier for tapasin (Chen and Bouvier, 2007), recombinant TAPBPR was shown to enhance the dissociation rate of fluorescently-labelled peptides from recombinant MHC class I refolds (Hermann et al., 2015b, Morozov et al., 2016). However, as opposed to tapasin, which requires artificial tethering to MHC class I to mediate peptide dissociation (Chen and Bouvier, 2007), TAPBPR was capable of catalysing this process without the need of any artificial modifications, partly due to its seemingly higher affinity for MHC class I compared to tapasin. This further suggested that TAPBPR alone is capable of editing peptides on MHC class I molecules.

Regarding the molecular mechanisms used by TAPBPR in mediating peptide dissociation from MHC class I molecules, the two recently characterised crystal structures of TAPBPR in complex with MHC class I both revealed that, somehow similar to the tug-of-war model proposed for tapasin (Fisette et al., 2016), TAPBPR appears to pull the α2-1 region of the MHC class I peptide binding groove away from the C-terminus of the peptide, presumably to promote peptide dissociation (Jiang et al., 2017, Thomas and Tampe, 2017). In support of this idea is the finding described by both structures, namely that TAPBPR binding to MHC class I molecules induces a twist of the Y84 residue of MHC class I, involved in hydrogen bond formation with the C-terminus carboxyl group of the bound peptide, towards the outside of the groove. This proposed mechanism of TAPBPR-mediated peptide dissociation was further confirmed by a recent study relying on nuclear magnetic resonance (NMR) analysis of the interactions between soluble TAPBPR and MHC class I refolds (McShan et al., 2018).

In addition to the interactions with the α2-1 region of the MHC class I, Thomas and Tampe claim to have captured a floppy loop region of TAPBPR in the proximity of the MHC class I binding groove and suggest that this loop might be involved in facilitating the dissociation of

the C-terminus of bound peptides (Thomas and Tampe, 2017). However, this loop was poorly resolved based on the raw diffraction data, with several side chains of the resolved structure and even part of the peptide backbone falling outside of the electron density map. Moreover, this loop was not resolved on the crystal structure by Jiang and colleagues (Jiang et al., 2017). Therefore, alternative conformations of this loop regions are likely to occur and, moreover, the impact of this region on the catalytic function of TAPBPR remains to be determined.

1.9.4. Interaction with UGT1

A study conducted in the Boyle lab revealed that TAPBPR recruits UGT1 (**Figure 3**)(Neerincx et al., 2017), an enzyme previously shown to play a key role in the quality control machinery involved in MHC class I peptide presentation (Zhang et al., 2011, Wearsch et al., 2011). TAPBPR appears to associate with UGT1, involving the only free cysteine residue of TAPBPR, at position 94. UGT1 was suggested to identify sub-optimally loaded peptide to send them back to the peptide loading complex for a subsequent round of peptide editing. Thus, the identification of TAPBPR interaction with UGT1 raised the question of whether TAPBPR, apart from directly dissociating sub-optimally loaded peptides from MHC class I, acts as an additional checkpoint on the pathway, by selecting peptides for presentation on MHC class I molecules. In support of the hypothesis that TAPBPR works in complex with UGT1 on selecting pMHC class I molecules for presentation is the finding that mutation of the C94 residue of TAPBPR, which abolished interaction with UGT1, triggers a significant change in the MHC class I-associated immunopeptidome (Neerincx et al., 2017).

1.9.5. Shaping the peptide repertoire presented on MHC class I

Naturally, given its ability to directly catalyse peptide dissociation from MHC class I molecules (Hermann et al., 2015b, Morozov et al., 2016) and to recruit UGT1 for recycling sub-optimally loaded MHC class I molecules back to the PLC (**Figure 3**)(Neerincx et al., 2017), TAPBPR was shown to significantly influence the repertoire of peptides presented at the cell surface (Hermann et al., 2015b). However, despite the similar peptide editing functions of tapasin and TAPBPR, their effects on peptide presentation on MHC class I differ considerably. In contrast to tapasin, which is crucial for the presentation of peptides stably bound to MHC class I molecules, the effect of TAPBPR on the immunopeptidome was shown to be considerably subtler.

Whereas the absence of tapasin leads to a severe impairment in the stability of pMHC class I complexes and consequently of the surface expression levels of MHC class I molecules (Howarth et al., 2004, Williams et al., 2002), in the absence of TAPBPR, the overall levels of MHC class I molecules at steady state are not significantly affected (Boyle et al., 2013, Hermann et al., 2015b). In fact, only a relatively small pool of normally retained pMHC class I complexes escape to the cell surface in TAPBPR-deficient cells. Moreover, the stability of individual pMHC class I complexes appears to be only marginally decreased in the absence of TAPBPR (Boyle et al., 2013, Hermann et al., 2015b). Based on these findings, it is currently unclear based on which criteria TAPBPR selects pMHC class I complexes for export to the cell surface.

Our current understanding of the function of TAPBPR in antigen presentation is that TAPBPR acts as an additional quality control checkpoint on the MHC class I pathway, by selecting peptides for presentation on MHC class I molecules. TAPBPR appears to fulfil this role by directly dissociating sub-optimally loaded peptides from MHC class I molecules which have gone through tapasin-mediated peptide editing or/and by recruiting UGT1 to reglucosylate the resulting peptide-receptive MHC class I molecules back to the PLC for a subsequent round of editing. Upon facilitating the dissociation of bound peptides from MHC class I molecules, it is possible that TAPBPR subsequently enables the loading of incoming peptides, however this is rather unlikely given the suggested localization of TAPBPR away from the peptide-rich environment within the ER (Neerincx and Boyle, 2017, Neerincx et al., 2017).

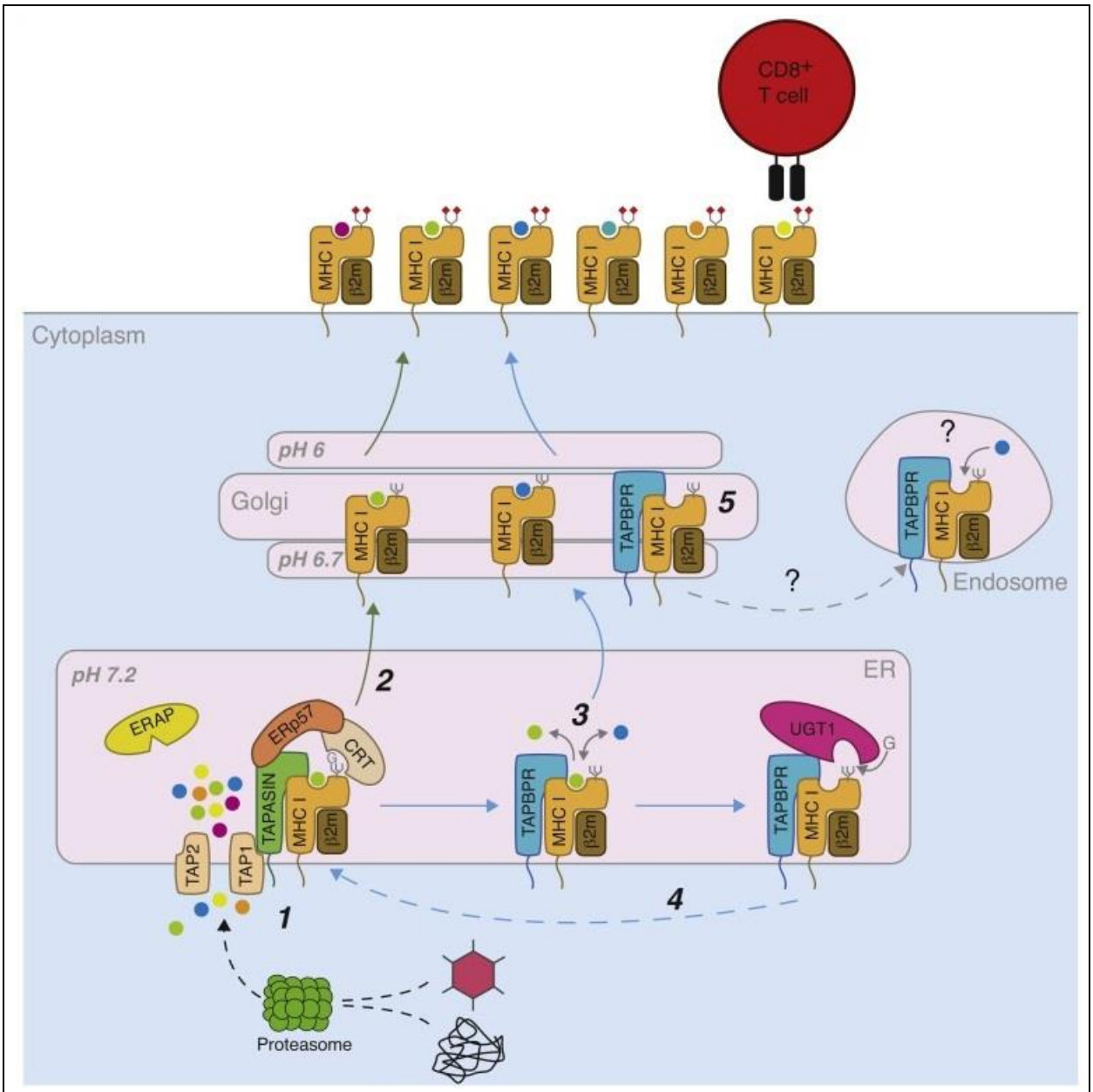

Figure 3: Proposed model of TAPBPR function in the MHC class I antigen presentation pathway, taken from Neerincx and Boyle (Neerincx and Boyle, 2017). TAPBPR is thought to bind sub-optimally loaded MHC class I molecules by the PLC and catalyse the dissociation of the bound peptide. Subsequently, TAPBPR either enables the association of high-affinity peptides or recruits UGT1, which reglucosylates the resulting peptide-receptive MHC class I molecules and recycles them to the PLC for a subsequent round of peptide editing. In contrast to tapasin, which solely localizes in the ER lumen, TAPBPR traffics through the medial Golgi and potentially through the endosomal compartment, in complex with MHC class I molecules.

1.10. Similarities between MHC class I and class II pathways

In contrast to MHC class I molecules, which get loaded with peptides in the ER lumen, MHC class II molecules acquire their antigens in late endocytic compartments. Upon their folding and assembly in the ER lumen, MHC class II molecules recruit a transmembrane protein that associates with the peptide binding groove of MHC class II, known as MHC class II-associated invariant chain (Ii), in a similar fashion to antigenic peptides (**Figure 4**) (Kvist et al., 1982, Machamer and Cresswell, 1982, Sung and Jones, 1981). This chaperone guides the trafficking of MHC class II molecules from the ER lumen into late endosomes (Bakke and Dobberstein, 1990, Lotteau et al., 1990), while preventing their loading with peptide in the ER (Newcomb and Cresswell, 1993, Roche and Cresswell, 1990). The invariant chain is cleaved in a particular late endosomal compartment, referred to as the MHC class II compartment (MIIC), leaving only the short peptide associated with the MHC class II groove, known as CLIP (class II-associated invariant chain peptide) (Cresswell et al., 1987, Reyes et al., 1991, Roche and Cresswell, 1991).

Similarly to MHC class I molecules, loading of antigenic peptides on MHC class II molecules is catalysed by a dedicated chaperone, HLA-DM, an MHC class II homologue (Cho et al., 1991, Denzin and Cresswell, 1995, Kelly et al., 1991b, Morris et al., 1994, Sloan et al., 1995). HLA-DM directly mediates the dissociation of CLIP from MHC class II, consequently facilitating the association of antigenic peptides (**Figure 4**) (Denzin and Cresswell, 1995, Sloan et al., 1995, Kropshofer et al., 1996, Vogt et al., 1996). Moreover, based on the discovery of the crystal structure of HLA-DM in complex with HLA-DR1 (Pos et al., 2012), HLA-DM was suggested to use a similar molecular mechanism as tapasin in promoting peptide dissociation, with the mention that, in contrast to tapasin, HLA-DM destabilizes the interactions between the MHC class II groove at the N-terminus of the peptide, instead of at the C-terminus. Unlike the MHC class I pathway, in addition to a peptide editor, the MHC class II pathway comprises another chaperone, namely the MHC class II homologue HLA-DO, which functions as negative regulator of HLA-DM (Denzin et al., 1997, Kropshofer et al., 1998, Liljedahl et al., 1996). HLA-DO inhibits the HLA-DM-mediated release of CLIP and loading of antigenic peptides onto MHC class II molecules (**Figure 4**). Based on its ability to regulate the peptide editor in the pathway, HLA-DO has been proposed to shape the peptide repertoire presented on MHC class II for optimal effectiveness, acting as an additional checkpoint in the pathway. In terms of its overall effect on peptide selection, TAPBPR might be fulfilling a similar role on the MHC class I pathway.

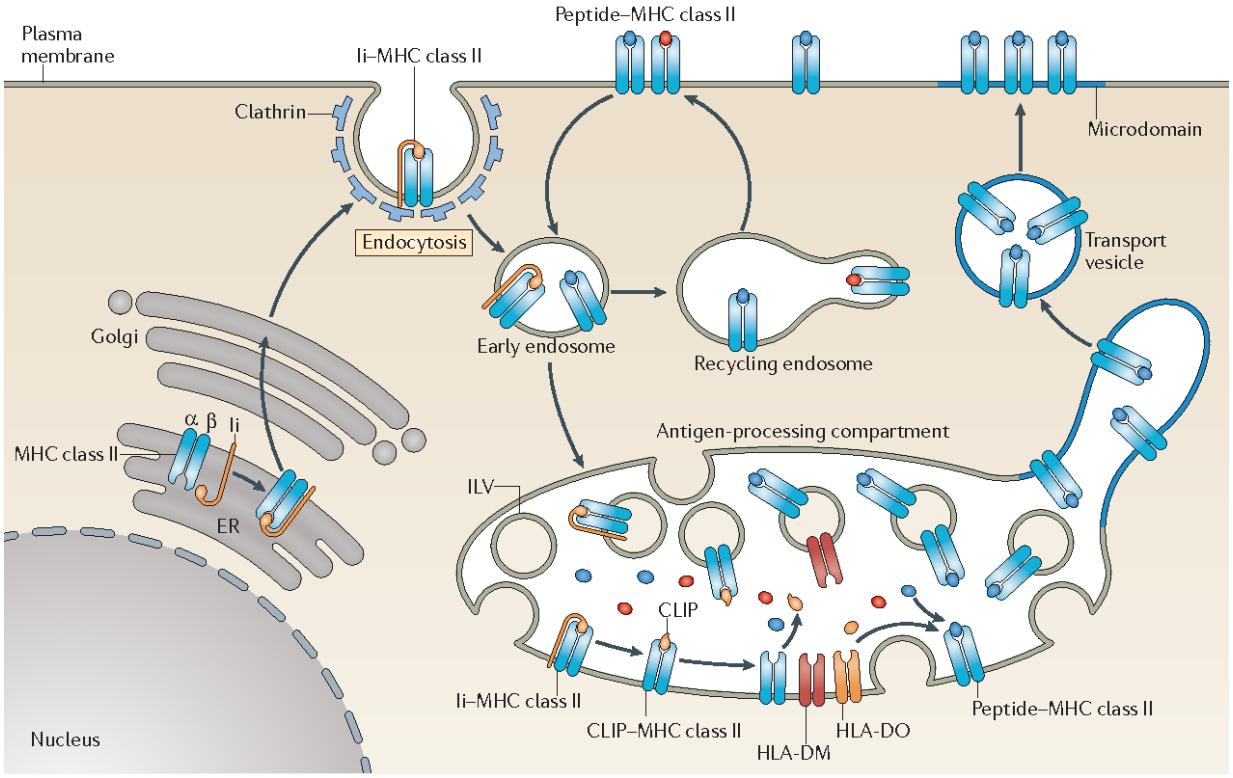

Figure 4: MHC class II presentation pathway, taken from Roche and Furuta (Roche and Furuta, 2015). Upon their folding and assembly in the ER lumen, MHC class II dimers, consisting of the transmembrane chains α and β bind to the invariant chain (Ii), which directs their trafficking from the ER through the Golgi and into early endosomes, via the cell surface. These endosomes are then fused with the antigen processing compartment, where the Ii bound to MHC class II molecules is cleaved, leaving only a small peptide (CLIP) attached to the peptide binding groove of MHC class II. In the same compartment, HLA-DM, whose activity is regulated by HLA-DO, catalyses the exchange of CLIP with exogenous peptide antigens internalized by pinocytosis. Once loaded with exogenous peptides, MHC class II molecules are transported to the cell surface.

1.11. Aims

Structural predictions generated in the lab, based on the previously characterised interaction sites between TAPBPR and MHC class I and based on domain homology between TAPBPR and tapasin, have identified a loop region of TAPBPR, comprising residues 22-35, at the interface with the peptide binding groove of MHC class I. These predictions were made prior to the discovery of the crystal structures of TAPBPR in complex with MHC class I (Jiang et al., 2017, Thomas and Tampe, 2017), only one of which claimed to capture the same TAPBPR loop in the proximity of the MHC class I groove (Thomas and Tampe, 2017). Based on our structural predictions, it was hypothesized that the 22-35 loop of TAPBPR could be a functional region involved in peptide editing on MHC class I (**Figure 21**). Moreover, based on the amino acid sequence of the loop, I speculated that TAPBPR potentially uses the loop to dissociate bound peptides from MHC class I molecules by competing with part of the peptide for binding to the groove of MHC class I.

Therefore, the main objective of my PhD was to experimentally characterise the involvement of the loop in the peptide editing function of TAPBPR. In order to address this question, my first aim was to develop a high throughput cell-based assay which would allow me to directly measure the ability of TAPBPR to mediate peptide exchange on MHC class I molecules on a cellular membrane. Subsequently, I sought to use this high throughput system to screen various TAPBPR loop mutants for their ability to bind MHC class I molecules and to mediate peptide exchange. Finally, I aimed to assess how polymorphisms in MHC class I molecules influence their ability to interact with TAPBPR and their propensity to undergo TAPBPR-mediated peptide editing.

2. Materials and Methods

2.1. Constructs

The cloning of full-length TAPBPR^{WT} and TAPBPR^{TN5} in the lentiviral vector pHRSIN-C56W-UbEM, which expresses the protein of interest under the control of the spleen focus-forming virus (SFFV) promoter and EGFP under the control of an ubiquitin promoter was previously described (Boyle et al., 2013). Tapasin was amplified from cDNA isolated from human foreskin fibroblasts using primers tapasin^{WT}-BamHI-for and tapasin^{WT}-NotI-rev (See **Table 1** for primer sequences) and was then cloned into the pHRSIN-C56W-UbEM vector. The chimeric constructs TAPBPR^{PM} and tapasin^{PM} were generated using a two-step PCR procedure, where the ectodomain and transmembrane domains of either TAPBPR (amplified using primers TAPBPR^{WT}-BamHI-for and TAPBPR^{PM}-rev) or tapasin (amplified using primers tapasin^{WT}-BamHI-for and tapasin^{PM}-rev) were fused to the cytoplasmic tail of CD8 (amplified with primers TAPBPR^{PM}-for and CD8 tail-NotI-rev, or tapasin^{PM}-for and CD8 tail-NotI-rev, respectively). TAPBPR^{ER} was produced using a similar procedure, in which the ectodomain of TAPBPR (amplified with primers TAPBPR^{WT}-BamHI-for and TAPBPR^{ER}-rev) was fused to the transmembrane and cytoplasmic domains of tapasin (amplified using primers TAPBPR^{ER}-for and tapasin^{WT}-NotI-rev). All TAPBPR constructs described in this study were variants of the α TAPBPR isoform, as this has been described as the only TAPBPR isoform present in a wide range of tissues and cell lines (Boyle et al., 2013).

Table 1: Panel of primers used to generate the TAPBPR chimeric constructs

Primer name	Primer sequence (5'-3')
TAPBPR^{WT}– EcoRV-for	GCGCGATATCAGCAGCCTCCATGGGCA
TAPBPR^{WT}– NotI-rev	GCGCGCGGCCGCTCAGCTGGGCTGGCTTACA
TAPBPR^{PM} – for	GATGTTCCTGGGGCTTCAGAGACGAAGACGTGTTTGCAAATGTCC
TAPBPR^{PM} – rev	GGACATTTGCAAACACGTCTTCGTCTCTGAAGCCCCAGGAACATC
tapasin^{WT}– BamHI-for	GCGCGGATCCCGCAGCGCCATGAAGTCCCTGTCTCTGCTCC
tapasin^{WT}– NotI-rev	GCGCGCGGCCGCTCACTCTGCTTTCTTCTTTGAATCCTTG
tapasin^{PM}– for	CTTCAAGGCACTGGGCTGGCGAAGACGTGTTTGCAAATGTCC
tapasin^{PM}– rev	GGACATTTGCAAACACGTCTTCGCCAGCCCAGTGCCTTGAAG
TAPBPR^{ER}– for	CCTGGAGGTAGCAGGTCTTTCAGCCTTGGGAGTCATCTTTGC
TAPBPR^{ER}– rev	GTTCTCAAGGGAGGGCCCTGTTCTCCGCTCTGGTGGG
CD8 tail – NotI-rev	GCGCGCGGCCGCTTAGACGTATCTCGCCGAAAGGC
TAPBPR soluble – for	GCGCGCTAGCCACCATGGGCACACAGGAGGGC
TAPBPR soluble – rev	GCGCGCGGCCGCTCATCAGTGATGGTGATGGTGGTGTCTCCGCTCTGGTGGGACA

TAPBPR^{Øloop}, in which amino acids 22–35 were replaced with glycine, alanine and serine residues, was generated based on the TAPBPR^{WT} template, using the following procedure: first, amino acids 22–28 were mutated by quick-change PCR using primers M22-for and M22-rev (**Table 2**). Subsequently, amino acids 29–35 were mutated using a two-step PCR procedure. In the first step, the TAPBPR insert was amplified in two separate pieces, starting from each side of the mutation site (primers TAPBPR^{WT}-BamHI-for and M29-rev for the N-terminus-containing side and primers M29-for and TAPBPR^{WT}-NotI-rev for the C-terminus-containing side). In the second step, the two pieces bearing complementary regions over the mutated site were used in a second PCR reaction to amplify the entire TAPBPR mutated insert using primers TAPBPR^{WT}-BamHI-for and TAPBPR^{WT}-NotI-rev. TAPBPR^{L30G} and TAPBPR^{ØG30L} were generated from TAPBPR^{WT} and from TAPBPR^{Øloop} respectively, using primers L30G-for and L30G-rev or ØG30L-for and ØG30L-rev respectively (**Table 2**), by quick change PCR. All TAPBPR and tapasin mutants were cloned into the lentiviral vector pHRSIN-C56W-UbEM.

Table 2: Panel of primers used to generate the TAPBPR loop mutants

Construct	**Primer sequence (5'-3')**
M22-for	GTCCTAGACTGTTTCCTGGTGGCGGCCGGTGGGAGCGGTGGAGCTCTCGCCAGCAGTG
M22-rev	CACTGCTGGCGAGAGCTCCACCGCTCCCACCGGCCGCCACCAGGAAACAGTCTAGGAC
M29-for	GCGGCCGGTGGGAGCGGTGGAGGTGGCAGCGGCGGTG
M29-rev	TCCACCGCTCCCACCGGCCGCCACCAGGAAACAGTCTAGGAC
L30G-for	GTGGAGCTGGCGCCAGCAGT
L30G-rev	ACTGCTGGCGCCAGCTCCAC
ØG30L-for	GGTGGAGGTCTGGGCGGCGGTGC
ØG30L-rev	GCACCGCCGCCCAGACCTCCACC

The luminal domains of TAPBPR^{WT}, TAPBPR^{TN5} and of all TAPBPR loop mutants were also cloned in a PiggyBac transposon vector, using primer TAPBPR-soluble-for and TAPBPR-soluble-rev (**Table 1**), to produce secreted versions of these proteins, containing a polyHis tag at the C-terminus, in a mammalian expression system.

cDNA templates for the panel of HLA class I alleles used in this study were obtained from Peter Parham (Stanford University), Elisabeth Chalmeau, (University Nantes, France), Jane Goodall (University of Cambridge, UK), Ashley Moffet (University of Cambridge, UK), Sebastian Springer (Jacobs University, Bremen, Germany), Rajiv Khanna (Queensland Institute of Medical Research, Australia), and Jim McCluskey (University of Melbourne, Australia). These were amplified and cloned into the lentiviral vector pHRSINcPPT-SGW, as previously described (Boyle

et al., 2013). The HLA-A*68:02^{WT} construct was cloned by consecutive rounds of quick-change site-directed mutagenesis, using the HLA-A*68:01^{WT} construct as a template (see **Table 3** for primer sequences). Since residue 116 was mutated last in this process, the HLA-A*68:02^{Y116D} mutant was the final intermediate in this cloning process. The HLA-A*68:01^{D116Y}, A*02:01^{Y116D}, A*02:01^{V12M}, A*02:01^{S105P}, A*68:02^{M12V}, A*68:02^{P105S}, B*27:05^{D116Y}, B*44:05^{D114H} and C*01:02^{D114H} were generated by quick-change PCR, using primers listed in **Table 3**. All HLA class I mutants were cloned into the pHRSINcPPT-SGW vector. Human cytomegalovirus (HCMV) pp65 was cloned into the lentiviral vector pHRSIN-C56W-UbEM.

All the constructs used and generated in this work, namely each full-length TAPBPR, soluble TAPBPR and HLA construct, were sequence verified.

Table 3: Panel of HLA class I mutants

Primer name	Sequence 5'-3'
A6801_V12M_Fwd	CTACACTTCCATGTCCCGGC
A6801_V12M_Rev	GCCGGGACATGGAAGTGTAG
A6801_M97R_Fwd	CACCATCCAGAGGATGTATGGC
A6801_M97R_Rev	GCCATACATCCTCTGGATGGTG
A6801_S105P_Fwd	CGTGGGGCCGGACGGGC
A6801_S105P_Rev	GCCCGTCCGGCCCCACG
A6801_R114H_Fwd	GCGGGTACCACCAGGACGCC
A6801_R114H_Rev	GGCGTCCTGGTGGTACCCGC
A6801_D116Y_Fwd	GTACCACCAGTACGCCTACG
A6801_D116Y_Rev	CGTAGGCGTACTGGTGGTAC
A6801_D116Yonly_Fwd	GTACCGGCAGTACGCCTAC
A6801_D116Yonly_Rev	GTAGGCGTACTGCCGGTAC
A2_Y116D_Fwd	GTACCACCAGGACGCCTACG
A2_Y116D_Rev	CGTAGGCGTCCTGGTGGTAC
B2705_D116Y_Fwd	GTACCACCAGTACGCCTACG
B2705_D116Y_Rev	CGTAGGCGTACTGGTGGTAC
B4405_D114H_Fwd	CGCGGGTATCATCAGTACGC
B4405_D114H_Rev	GCGTACTGATGATACCCGCG
C0102_D114H_Fwd	GCGGGTATCACCAGTACGC
C0102_D114H_Rev	GCGTACTGGTGATACCCGC
A0201_V12M_Fwd	CACATCCATGTCCCGGCC
A0201_V12M_Rev	GGCCGGGACATGGATGTG
A0201_S105P_Fwd	GACGTGGGGCCGGACTGG
A0201_S105P_Rev	CCAGTCCGGCCCCACGTC
A6802_M12V_Fwd	CTACACTTCCGTGTCCCGGC
A6802_M12V_Rev	GCCGGGACACGGAAGTGTAG
A6802_P105S_Fwd	CGTGGGGTCGGACGGG
A6802_P105S_Rev	CCCGTCCGACCCCACG

2.2. Cell lines

HeLaM, a variant of the HeLa cell line which is more responsive to IFNγ (a gift from Paul Lehner, University of Cambridge, UK), HEK 293T (from Paul Lehner, University of Cambridge, UK), MCF-7 (human breast carcinoma), EL4 (mouse T cell lymphoma) cells and all derived cell lines were maintained in Dulbecco's Modified Eagle's medium (DMEM; Sigma-Aldrich, UK) supplemented with 10% fetal bovine serum (FBS) (Gibco, Thermo Fisher Scientific), 100 U/ml penicillin and 100 µg/ml streptomycin (Gibco, Thermo Fisher Scientific), at 37°C with 5% CO_2. To induce expression of endogenously-expressed TAPBPR and up-regulate the surface expression of MHC class I molecules, cells were treated with 200 U/ml IFNγ (Peprotech, UK), of either human or mouse origin, depending on the cell line, for 48–72 h. All cells were confirmed to be mycoplasma negative (MycoAlert, Lonza, UK).

2.3. Lentiviral transduction and transfections

Lentivirus was produced in HEK-293T cells, by transfecting the cells with either the pHRSIN-C56W-UbEM or pHRSINcPPT-SGW lentiviral vector, containing the insert of interest, along with the packaging vector pCMVΔR8.91 and the envelope vector pMD.G, in the presence of FuGENE (Promega, UK). Transductions were performed by collecting virus-containing supernatant at 48 h and again at 72 h and adding it onto target cells, through a syringe filter, in the presence of 8 µg/mL polybrene (Sigma-Aldrich, UK).

HeLaM-TAPBPR^{KO} cells (HeLaM^{KO}) were transduced with each TAPBPR and tapasin full-length variant described in this study. HeLaM cell line deficient of the HLA-A, -B and -C (HeLaM-HLA-ABC^{KO}) was transduced with each specified HLA class I constructs to generate a panel of HeLaM cells expressing single individual HLA class I allotypes.

2.4. Antibodies

TAPBPR was detected using either PeTe-4, a mouse monoclonal antibody (mAb) specific for the native conformation of TAPBPR, raised against amino acids 22–406 of human TAPBPR (Boyle et al., 2013) that does not cross-react with tapasin (Hermann et al., 2013), or ab57411, a mouse mAb raised against amino acids 23–122 of TAPBPR that recognizes denatured TAPBPR (Abcam, UK). Tapasin was detected using Pasta-1, a mouse mAb specific for the native conformation of

tapasin (Dick et al., 2002), or with R.gp48N, a rabbit polyclonal antibody specific for the denatured form of tapasin (Sadasivan et al., 1996)(kind gifts from Peter Cresswell, Yale University School of Medicine). MHC class I heavy chains were detected using the mouse mAb HC10 (Stam et al., 1986) and mAb HCA2 (Stam et al., 1990). β_2m was detected using a rabbit polyclonal antibody (Dako, UK). Folded MHC class I molecules present either at the cell surface or coupled to SABs were detected using W6/32, a pan-MHC class I mouse mAb that recognizes a conformational epitope of the α2 domain of MHC class I, only in the presence of β_2m and peptide (Barnstable et al., 1978). $OVA_{257-264}$ [SIINFEKL] peptide on H-2K^b was detected using the mAb 25D-1.16 (Thermofisher). The Epstein-Barr Virus derived peptide Latent Membrane Protein $1_{125–133}$ [YLLEMLWRL] in association with HLA-A*02:01 was detected using the TCR-like mAb L1 (Sim et al., 2013) (a king gift from Paul MacAry, University of Singapore). Calnexin was detected via western blot analysis using the rabbit polyclonal antibody ADI-SPA-860 (Enzo Life Sciences, UK). A mouse IgG2a isotype control was also used as a control (Sigma-Aldrich).

2.5. MHC class I-binding peptides

Fluorescently-labelled peptides specific to individual HLA class I allotypes or to the mouse MHC class I molecule H-2K^b were derived from epitopes selected using SYFPEITHI database (Rammensee et al., 1999), the Immune Epitope Database and Analysis Resource or the HIV molecular immunology epitope database(www.hiv.lanl.gov)(**Table 4**). All peptides were purchased from Peptide Synthetics, UK, at over 95% purity, verified by HPLC.

Table 4: Fluorescently-labelled MHC class I-binding peptides used in this study

Peptide sequence	Original epitope	Origin	MHC class I allotype(s) specificity
NLVPK*VATV	NLVPMVATV	HCMV	HLA-A*02:01
YLLEK*LWRL	YLLEMLWRL	EBV	HLA-A*02:01
IMDQK*PFSV	IMDQVPFSV	EBV	HLA-A*02:01
CLGGK*LTMV	CLGGLLTMV	EBV	HLA-A*02:01
LLGRK*SFEV	LLGRNSFEV	tumour-associated	HLA-A*02:01
ELAGK*GILTV	ELAGIGILTV	tumour-associated	HLA-A*02:01
RLLQK*TELV	RLLQETELV	tumour-associated	HLA-A*02:01
YVVPFVAK*V	YVVPFVAKV	self	HLA-A*02:01; -A*68:02; -C*02:02
ETVSK*QSNV	ETVSEQSNV	neoantigen	HLA-A*68:02
EGVSK*QSNG	ETVSEQSNV	neoantigen	HLA-A*68:02
KTGGPIYK*R	KTGGPIYKR	influenza virus	HLA-A*68:01
PYLFK*LAAI	PYLFWLAAI	EBV	HLA-A*23:01
RVLDK*VEKW	N/A	artificial	HLA-A*32:01
SRYWK*IRTR	SRYWAIRTR	influenza virus	HLA-B*27:05; -B*27:09
SPAIK*QSSM	SPAIFQSSM	HIV	HLA-B*07:02; -B35; -A30
SHETK*IIEL	SHETVIIEL	neoantigen	HLA-B*38:01
EEFGK*AFSF	EEFGRAFSF	self	HLA-B*44:05
LNPSK*AATL	LNPSVAATL	HCV	HLA-C*01:02
SIINFEK*L	SIINFEKL	mouse ovalbumin	H-2K^{b}

- K* = lysine labelled with 5-carboxytetramethylrhodamine [TAMRA]

2.6. Expression and purification of TAPBPR protein

In order to produce secreted soluble forms of either the TAPBPR loop variants or the TN5 mutant of TAPBPR, the lumenal domains of these proteins were cloned into a modified version of the PB-T-PAF vector where the N-terminal Protein A fusion was removed and a C-terminal His_6 tag introduced. These soluble TAPBPR proteins were stably expressed in 293T cells using the PiggyBac expression system. 48 hr after transfection, cells were transferred for at least 5 days into selection media (DMEM supplemented with 10% FBS, 1% pen/strep, 3 µg/mL puromycin (Invivogen, San Diego, CA) and 700 µg/mL geneticin (Thermo Fisher Scientific, UK). To induce protein expression, cells were harvested and transferred into DMEM supplemented with 5% FBS, 1% pen/strep and 2 µg/mL doxycycline (Sigma-Aldrich, UK). After 5–7 days, the media was collected and TAPBPR was purified using nickel-nitrilotriacetic acid (Ni-NTA) affinity chromatography. The purity of the elution fractions assessed by SDS-PAGE, followed by Coomassie staining.

2.7. Differential scanning fluorimetry (DSF)

Thermofluor analysis was performed in 96-well low-profile clear PCR plates for Viia7 cyclers (Axygen). Reactions of 20 µl consisted of 5 µg protein, 1x protein Thermal Shift Dye (Life Technologies) in PBS at pH 7.4. The melting curve was performed using a Viia7 thermocycler between 20°C and 95°C in 1°C steps with 20 s equilibration time per step and fluorescence monitored on the ROX channel.

2.8. Flow cytometry

For analysis by flow cytometry, cells were first detached from the flasks by trypsinisation and then washed in 1% bovine serum albumin (BSA) dissolved in 1x phosphate-buffered saline (PBS) at 4°C. Cells were then stained for 30 min at 4°C in 1% BSA containing one of the following antibodies: W6/32, PeTe4, Pasta-1, TCR-like mAb L1, 25-D1.16 or an isotype control antibody. After washing the cells to remove excess unbound antibody, the primary antibodies bound to the cells were detected by incubation at 4°C for 25 min with goat anti-mouse Alexa-Fluor 647 IgG (Invitrogen Molecular Probes, Thermo Fisher Scientific). Following three subsequent rounds of washing, the fluorescence levels were detected using a BD FACScan analyser with Cytek modifications and analysed using FlowJo (FlowJo, LLC, Ashland, OR).

2.9. Single antigen bead screen

3 µL of the LABScreen® single antigen HLA bead suspension (One Lambda, Inc., CA, USA) were added per well of a 96-well plate and incubated with either 100 nM or 1 µM soluble TAPBPR^{WT} or TAPBPR^{TN5} at 22°C, with rotation, for 60 min. The beads were washed three times in wash buffer (One Lambda, Inc., CA, USA) to remove any excess of soluble TAPBPR. Subsequently, the beads were first incubated with PeTe4 antibody for 30 min, washed and then incubated with a PE-conjugated goat anti-mouse IgG (Abcam, UK) for another 30 min at 22°C. After a subsequent round of washing, cells were re-suspended in 1x PBS and the TAPBPR levels bound to the beads were measured by a using the Luminex Fluoroanalyser system (One Lambda, Inc., CA, USA) and analysed using the HLA Fusion^{TM} software (One Lambda, Inc., CA, USA).

2.10. BFA decay assays

IFN-γ-stimulated HeLa-HLA-ABC^{KO} cells, reconstituted with individual HLA class I allotypes were treated with 10 µg/mL BFA (Sigma-Aldrich), diluted in regular media, for different time periods. Cells were then harvested and the levels of MHC class I molecules present at the surface of each cell line, at each time point, were measured by flow cytometry, by staining with the W6/32 antibody.

2.11. Immunoprecipitation, gel electrophoresis and western blotting

For immuno-precipitation from the whole cell lysates, IFNγ-stimulated cells were harvested, washed in PBS and then snap-frozen in dry ice for >5 min. Cells were then lysed in 1% triton X-100 (VWR, Radnor, PN), Tris-buffered saline (TBS) (20 mM Tris-HCl, 150 mM NaCl, 2.5 mM $CaCl_2$), whenever TAPBPR was pulled down, or in 1% digitonin-TBS, whenever tapasin was pulled down, supplemented with 10 mM N-ethylmaleimide (NEM), 1 mM phenylmethylsulfonyl fluoride (PMSF) (Sigma-Aldrich), and protease inhibitor cocktail (Roche, UK) for 30 min at 4°C. Nuclei and cell debris were pelleted by centrifugation at 13,000 × g for 15 min and supernatants were collected. TAPBPR was then pulled down from the whole cell lysate using protein A sepharose beads conjugated to the PeTe4 antibody, at 4°C, over 90 min, with rotation. Following immunoprecipitation, beads were washed thoroughly in 0.1% detergent-TBS to remove unbound protein. For separation by gel electrophoresis, the samples were heated at 94°C for 10 min in sample buffer (125 mM Tris-HCl pH 6.8, 4% SDS, 20% glycerol, 0.04% bromophenol blue), supplemented with 100 mM β-mercaptoethanol. In order to detect the samples by western blotting, proteins were transferred onto an Immobilon transfer membrane (Merck Millipore). Membranes were blocked using 5% (w/v) dried milk and 0.05% (v/v) Tween 20 in PBS for 30 min and subsequently incubated with the indicated primary antibody for 1–16 h. After washing, membranes were incubated with species-specific HRP-conjugated secondary antibodies for 1-2 h at room temperature, washed and detected by enhanced chemiluminescence using Western Lightning (Perkin Elmer, UK) and Super RX film (Fujifilm, UK). Films were scanned on a CanoScan8800F using MX Navigator Software (Canon, UK).

For immunoprecipitation of the TAPBPR fraction present at the plasma membrane, prior to lysis, harvested cells were incubated with 2 µg PeTe4 antibody in 1% BSA in 1x PBS for 1 h with

rotation at 4°C. Excess antibody was removed by washing the cells 5 times in 1x PBS at 4°C. Subsequently, cells were lysed and the TAPBPR fraction originally present the plasma membrane, bound to the PeTe4 antibody, was then precipitated using protein A sepharose beads alone (GE Healthcare) for 2 h at 4°C with rotation. The intracellular fraction of TAPBPR was pulled-down from the resulting flow through using the same procedure as the one used to pull down TAPBPR from the whole cell lysate.

For pulldown experiments using soluble TAPBPR proteins, protein A sepharose precleared lysates from IFNγ-stimulated HeLaM-TAPBPR^{KO} cells were incubated with 2 µg of the soluble TAPBPR variant for 90 min at 4°C. Immunoprecipitation of soluble TAPBPR was performed using PeTe4 as above. Soluble TAPBPR variants were detected on western blots with the anti-poly His primary antibody.

2.12. Peptide binding

Target cell lines were seeded at 25,000-30,000 cells/well in 12-well plates and stimulated with IFNγ. Following the stimulation period, the cells were washed 3 times with 1x PBS and incubated with 300 µL opti-MEM at 37°C (Thermo Fisher Scientific, UK). In case the peptide binding was done in the presence of recombinant TAPBPR, the cells were treated with or without recombinant TAPBPR. After 15 min, the desired TAMRA-labelled peptide was added to the cells, at concentration dependent on the MHC class I molecule tested, and incubated at 37°C for different time periods, dependent on the MHC class I molecule tested. In case the peptide binding was facilitated by over-expressed TAPBPR, the labelled peptide was directly added to the cells, without using recombinant TAPBPR. Following the peptide treatment, the cells were washed three times in 1x PBS and harvested. The level of bound peptide/cell was determined by flow cytometry, using the YelFL1 channel (Cytek).

2.13. Peptide exchange

HeLaM-TAPBPR^{KO} cells, reconstituted with TAPBPR, were seeded at 25,000 cells/well and stimulated with IFNγ. The cells were then washed and treated with 10 nM TAMRA-labelled peptide of interest diluted in opti-MEM for 15 min at 37°C, as described above. Following the

binding step, the peptide-containing media was removed, the cells were washed and then treated with media alone or with different concentrations of non-labelled peptide for another 15 min at 37°C. The cells were then washed and harvested and the level of bound peptide per cell was determined by flow cytometry, using the YelFL1 channel (Cytek).

2.14. FluoroSpot T cell assay

2.14.1. Expansion of HCMV-specific $CD8^+$ T cells

$CD8^+$ T cells were isolated from peripheral blood mononuclear cells (PBMC) by magnetic-activated cell sorting (MACS), using anti-CD8 direct beads (Miltenyi Biotec, Bisley, United Kingdom) for magnetic separation and then resuspended in supplemented RPMI + 10% Fetal Bovine Serum (FBS) (Invitrogen) + 10% heat inactivated autologous donor serum. Cells were stimulated with peptide-pulsed irradiated autologous PBMC in the presence of 2.5 IU/ml human recombinant IL-2 (National Institute for Biological Standards and Control, Potters Bar, United Kingdom) in round bottom 96 well plates at 37°C and 5 % CO_2 for 10 – 14 days. Fresh media was replenished every five days. The specificity of expanded $CD8^+$ T cell cultures was tested using IFNγ FluoroSpot assays, upon stimulation with HeLaM cells over-expressing both HLA-A2 and pp65. The HLA-A2-restricted peptide from HCMV pp65 used in this study was NLVPMVATV ($pp65_{495\text{-}504}$).

Ethical approval for this study was obtained from the Addenbrookes National Health Service Hospital Trust institutional review board (Cambridge Research Ethics Committee). Informed written consent was obtained from all recipients in accordance with the Declaration of Helsinki (LREC 97/092).

2.14.2. Experimental set up

Target cells (MCF-7 or HeLaM-HLA-ABC^{KO} reconstituted with HLA-A*02:01 heavy chain) were seeded at 80,000 cells/well of a 6-well plate and stimulated with IFNγ for 72 h. Cells were then washed 3 times with 1x PBS and incubated with 600 µL pre-warmed opti-MEM, containing either soluble $TAPBPR^{WT}$, $TAPBPR^{TN5}$, or without TAPBPR. After 15 min, 100 pM NLVPMVATV peptide was added to the desired samples and incubated for another 60 min. Following peptide

treatment, cells were washed 3 times in 1x PBS and harvested. Each sample was then washed again twice in 1x PBS and resuspended in X-VIVO 15 media (Lonza, Slough, UK) at $1x10^6$ cells/mL. Target cells were then irradiated for 20 min, in order to cease proliferation throughout the experiment. Triplicate wells of NLVPMVATV-specific $CD8^+$ T cells in X-VIVO 15 media were incubated in coated Fluorospot plates (Human IFNγ FLUOROSPOT (Mabtech AB, Nacka Strand, Sweden)), either at 8,000 or at 4,000 cells/well, with target cells, at 50,000 cells/well, at 37°C in a humidified CO_2 atmosphere for 20 hours. The cells and medium were decanted from the plate and the assay was developed following the manufacturer's instructions. Developed plates were read using an AID iSpot reader (Autoimmun Diagnostika (AID) GmbH, Strassberg, Germany) and counted using EliSpot v7 software (Autoimmun Diagnostika).

2.15. Mice

OT-I $RAG2^{-/-}$ mice were a generous gift from Suzanne Turner (Dept. of Pathology, University of Cambridge) and were bred and housed in accordance with UK Home Office regulations.

2.16. Cytotoxicity assay

To generate OT-I cytotoxic T lymphocytes (CTL), spleens were extracted from OT-I $RAG2^{-/-}$ mice and single cell suspensions of splenocytes were obtained using a 70 µm cell strainer (Greiner Bio-one). Splenocytes were stimulated with 10 nM $OVA_{257-264}$ (SIINFEKL) peptide (Peprotech, UK). After 3 days of culture, cells were washed, transferred into fresh T cell media on a daily basis and used 3-4 days later. T cells were cultured in RPMI 1640 medium with L-glutamine (Gibco, Thermo Fisher Scientific), 10% heat–inactivated FCS (Biosera), 50 µM of β-mercaptoethanol, 1 mM sodium pyruvate (Gibco, Thermo Fisher Scientific), 10 mM Hepes (Sigma-Aldrich), 50 IU/ml recombinant murine IL-2 (Peprotech, UK) and 50 U/ml penicillin and streptomycin (Gibco, Thermo Fisher Scientific) (T cell media).

The CytoTox96 Non-Radioactive Cytotoxicity Assay (Promega) was used to measure EL4 target cell death. Target $H\text{-}2^b$ EL4 cells were washed the day prior to the experiment and resuspended in fresh DMEM at $3x10^5$ - $4x10^5$ cells/ml. The following morning, the EL4 cells were washed once and resuspended in warm opti-MEM at $5x10^5$ cells/ml. The cells were treated initially with

1 µM soluble TAPBPR alone or with carrier alone for 10 min, after which either 1 nM $OVA_{257-264}$ (SIINFEKL) peptide or carrier alone was added to the cells for another 30 min. Cells were then washed 1x in Opti-MEM and 2x in killing assay media (RPMI medium minus phenol red, 2% FCS) and subsequently resuspended in killing assay media at $1x10^5$ cells/ml in a round-bottom 96-well plate. Effector OT-I T cells were washed in killing assay media once and then added to the plate at titrated effector to target cell (E:T) ratios. Plates were incubated at 37°C and after 6-7 hours. EL4 killing was assessed by release of lactate dehydrogenase in the supernatant.

2.17. Isolation of HLA peptides

HLA class I molecules were isolated from HeLaM-$TAPBPR^{KO}$ cells transduced with either $TAPBPR^{WT}$, $TAPBPR^{Øloop}$ or $TAPBPR^{ØG30L}$ using standard immunoaffinity chromatography, using the pan-HLA class I-specific antibody W6/32 (produced in-house), as described previously (Kowalewski and Stevanovic, 2013). Tissue typing confirmed the HeLaM cells express HLA-A*68:02, -B*15:03 and -C*12:03. These experiments were performed by Ana Marcu, from the lab of Prof. Stefan Stefanović (University of Tübingen, Germany).

2.18. Analysis of HLA ligands by LC-MS/MS

Peptides isolated from pulled-down MHC class I molecules were analysed in five technical replicates. Peptide samples were separated by nanoflow high-performance liquid chromatography (RSLCnano, Thermo Fisher Scientific, Waltham, MA) using a 50 µm × 25 cm PepMap rapid separation liquid chromatography column (Thermo Fisher Scientific) and a gradient ranging from 2.4% to 32.0% acetonitrile over the course of 90 min. The eluted peptides were analysed in an online-coupled LTQ Orbitrap XL mass spectrometer (Thermo Fisher Scientific) using a top five CID (collision-induced dissociation) fragmentation method. These experiments were performed by Ana Marcu, from the lab of Prof. Stefan Stefanović (University of Tübingen, Germany).

2.19. Database search and HLA annotation

Spectra were annotated to corresponding peptide sequences by database search across the human proteome as included in the Swiss-Prot database (20,279 reviewed protein sequences, September 27th 2013), by using the SEQUEST HT search engine (Eng et al., 1994) integrated into ProteomeDiscoverer 1.4 (Thermo Fisher Scientific). Data processing was performed without enzyme specificity, with peptide length restricted to 8–12 amino acids, and methionine oxidation set as dynamic modification. The false discovery rate was computed using the Percolator algorithm (Kall et al., 2007) and set to 5%. HLA class I allotype annotation was performed using NetMHCpan-4.0, with a percentile rank threshold of 2%. These experiments were performed by Ana Marcu, from the lab of Prof. Stefan Stefanović (University of Tübingen, Germany) and by Dr. Clemens Hermann (University of Cape Town, RSA).

2.20. Label-free quantitation

Label-free quantitation (LFQ) was used as previously described (Nelde et al., 2018) to assess the relative peptide abundances between TAPBPR^{WT}, TAPBPR^{Øloop} or TAPBPR^{ØG30L}-expressing cells. Relative quantitation of HLA peptides was performed by calculating the area under the curve of the respective precursor extracted ion chromatogram (XIC), using ProteomeDiscoverer 1.4 (Thermo Fisher Scientific). For LFQ analysis, the total injected peptide amount of all samples was normalised prior to LC-MS/MS analysis. Volcano plots were generated using an in-house R script (v3.2) and display pairwise comparisons of the ratios of the mean areas for each individual ligand in the five LFQ-MS runs. Significant modulation was defined by an adjusted p-value of < 0.01 and a fold change of $\geq \log_2$ 2-fold change, as calculated by two-tailed t-tests implementing Benjamini-Hochberg correction. These experiments were performed by Ana Marcu, from the lab of Prof. Stefan Stefanović (University of Tübingen, Germany).

2.21. Statistics

Throughout the study, statistics were performed as unpaired t tests using GraphPad Prism. Data was summarised mainly as mean ± SD, unless otherwise specified. Significance was determined based on p values. No tests for assessment of normality were performed.

3. Chapter 3: Designing an assay to identify functional regions of TAPBPR involved in peptide editing

3.1. Background

In order to explore the molecular mechanisms of TAPBPR-mediated peptide exchange on MHC class I and to identify key functional regions of TAPBPR essential for this process, I first needed to establish an appropriate peptide exchange assay for TAPBPR. Prior to this work, the only known assay to test the ability of TAPBPR to mediate peptide exchange on MHC class I molecules was the one established by the Elliott lab (University of Southampton, UK) in collaboration with the Boyle group (Hermann et al., 2015b), based on the pre-existing assay designed by Chen and Bouvier for tapasin (Chen and Bouvier, 2007). This assay, which was later reproduced by another group (Morozov et al., 2016), relies on assessing the effect of the luminal domain of TAPBPR alone on the dissociation of fluorescently-labelled peptides from recombinant MHC class I refolds, in solution, by fluorescence polarization (FP) measurements.

However, this assay exhibited a number of important limitations which I believed would not allow for efficient screening of TAPBPR mutants for their ability to edit peptides. The two most concerning limitations of this assay were its low sensitivity and its extremely low throughput nature. Regarding its sensitivity, addition of TAPBPR in the range of 0.1 – 1.0 μM to recombinant MHC class I molecules, refolded with high-affinity fluorescently-labelled peptides in solution, induced an extremely low dissociation rate of the peptide (Hermann et al., 2015b). This would leave little space for any intermediate peptide exchange phenotypes, potentially corresponding to partially dysfunctional TAPBPR mutants. This could have been a result of refolding the HLA-A2 molecules only with individual high-affinity peptides of choice, instead of using a pool of peptides with different affinities for A2, which is what TAPBPR naturally encounters inside the cell. Regarding the throughput of the experimental procedure, each experiment requires manual generation of individual MHC class I refolds, with individual peptides of choice, process which generally takes between five and seven days. Moreover, once generating the refolds, the peptide exchange experiment spans over 4 – 6 hours.

I thus decided to establish an alternative system that would allow for a higher sensitivity of the peptide exchange read-out and one that would additionally enable measuring TAPBPR-

mediated peptide exchange in a high-throughput manner. Such an assay would subsequently allow me to explore the molecular mechanisms of TAPBPR-mediated peptide editing on MHC class I molecules.

3.2. Results

3.2.1. TAPBPR is present at the cell surface when over-expressed in HeLaM cells

One interesting property of TAPBPR, previously described by the Boyle lab, is its ability to traffic to the cell surface upon over-expression (Boyle et al., 2013), property which was not observed for tapasin. It is important to mention that endogenously-expressed TAPBPR has only been detected intracellularly and that, only when over-expressed, gets trafficked to the cell surface. Since TAPBPR was shown to mediate peptide exchange on MHC class I alone, without the need of additional cellular factors or mutation of the protein (Hermann et al., 2015b, Morozov et al., 2016), its observed presence at the cell surface upon over-expression raised the interesting question of whether TAPBPR retains its ability to function as a peptide exchange catalyst on MHC class I at this atypical location. If so, the presence of TAPBPR at the cell surface upon over-expression could allow me to measure TAPBPR-mediated peptide exchange on MHC class I molecules on a cellular membrane. The plasma membrane is arguably the only cellular location where this process could be measured directly, as the luminal domains of the proteins are exposed to the extracellular space, enabling direct access of surface expressed MHC class I molecules to exogenously-added peptides (e.g. quantifiable by flow-cytometry).

A HeLaM cell line over-expressing TAPBPR^{WT} was created by reconstituting the TAPBPR knock-out HeLaM cells (HeLaM^{KO})(generated by Dr. Andreas Neerincx, University of Cambridge)(Hermann et al., 2015b) with TAPBPR^{WT} (HeLaM^{KO}TAPBPR^{WT}). TAPBPR^{WT} was cloned in lentiviral vector, upstream of an eGFP reporter gene (Boyle et al., 2013), for assessing transduction efficiency (**Figure 5a**). I first tested HeLaM^{KO}TAPBPR^{WT} cells for surface expression levels of both TAPBPR and MHC class I, by flow cytometry (**Figure 5b and 5c**). Whereas endogenously expressed TAPBPR was undetectable at the cell surface in IFNγ-treated HeLaM cells, the cells over-expressing TAPBPR^{WT} showed a clear presence of TAPBPR at the surface (**Figure 5b**). Second, TAPBPR over-expression led to a considerable down-regulation in MHC class I surface expression, while the presence or absence of endogenous TAPBPR did not

significantly alter the steady state level of MHC class I at the cell surface (**Figure 5c**), as previously described (Boyle et al., 2013). To understand whether HLA-A and HLA-B molecules were downregulated to a similar extent by over-expression of TAPBPR, I measured the levels of HLA-A (**Figure 5d**) and HLA-B molecules (**Figure 5c**) respectively, on cells over-expressing TAPBPR, and compared these levels to the ones detected on HeLaM and HeLaM^{KO} cells. Interestingly, while HeLaM^{KO}TAPBPR^{WT} cells showed a clear reduction, of almost 90%, in the surface expression of HLA-A compared to HeLaM cells (**Figure 5b**), the levels of HLA-B were very similar between these two cell lines (**Figure 5c**). This suggests that TAPBPR preferentially decreases expression of HLA-A molecules at the cell surface in HeLaM cells. However, this phenomenon seems to be applicable solely for over-expressed TAPBPR, as knocking out endogenous TAPBPR did not trigger any difference in MHC class I surface expression (**Figure 5c-e**).

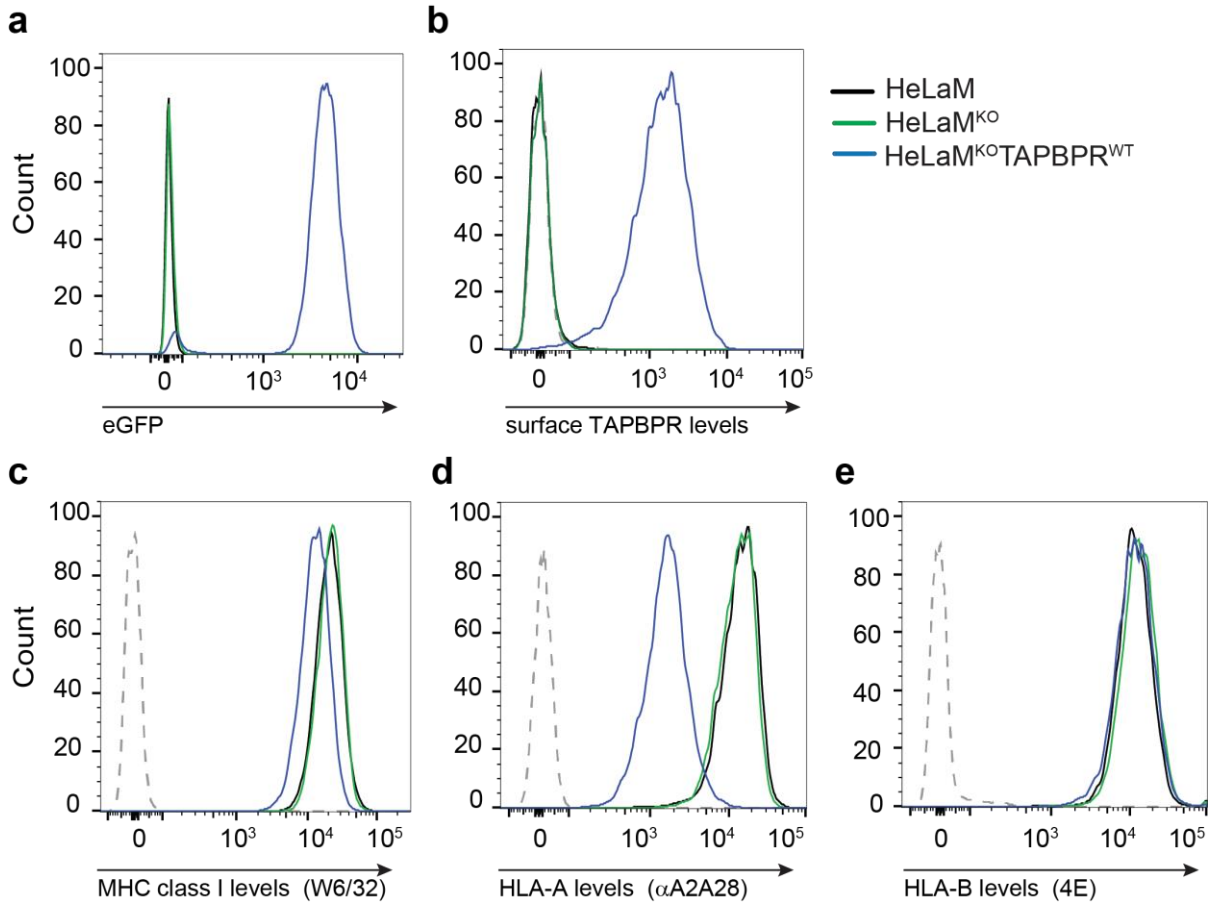

Figure 5: Over-expressed TAPBPR is trafficked to the cell surface and down-regulates MHC class I surface expression. TAPBPR was cloned upstream of an eGFP reporter gene in a lentiviral vector and transduced into HeLaM^{KO} cells for stable over-expression (HeLaM^{KO}TAPBPR^{WT}). Histograms show the levels of (**a**) eGFP expression or of (**b**) TAPBPR, (**c**) MHC class I molecules, recognized by the W6/32 mAb, (**d**) HLA-A molecules, recognized by the αA2A28 mAb and (**e**) HLA-B molecules, recognized by the 4E mAb, at the surface of HeLaM, HeLaM^{KO} and HeLaM^{KO}TAPBPR^{WT} cells. For each measurement, a sample stained with an isotype control antibody was chosen as a negative control (dashed grey line). All histograms are representative of three independent experiments.

To assess the effect of TAPBPR on peptide exchange on MHC class I, I tested whether TAPBPR over-expression could facilitate the binding of exogenously-added peptides to the surface of HeLaM^{KO}TAPBPR^{WT} cells. To this end, I decided to use fluorescently-labelled peptides with high affinity for MHC class I, which would permit quantifying the level of bound peptide per cell using flow cytometry. The first peptide I used was ETVSK$_{TAMRA}$QSNV (ETVSK*QSNV), a fluorescently-labelled derivative of ETVSEQSNV, which was reported to be a carcinoma-specific peptide, presented on HLA-A*68:02, which is an allele expressed in HeLaM cells (Hogan et al., 1998). I thus tested the binding of ETVSK*QSNV to HeLaM^{KO}TAPBPR^{WT} cells and compared it to the binding of the labelled peptide to HeLaM and HeLaM^{KO} cells.

3.2.2. TAPBPR over-expression significantly promotes peptide binding to cells

In my initial experiment, I tested the binding of 10 µM ETVSK*QSNV (ETV*) to cells stimulated with IFNγ for 48 h at 37^{o}C in opti-MEM (**Figure 6**). I used the peptide at 10 µM, as the peptide concentrations used for previously-reported peptide-pulsing experiments in human cells have varied between 10 and 50 µM (e.g. references (Wills et al., 1996, Zehn et al., 2006)). Also, I chose opti-MEM over regular DMEM due to the lack of protein that could potentially interfere with the peptide binding to cells. IFNγ stimulation was necessary in order to boost the MHC class I levels on HeLaM^{KO}TAPBPR^{WT} cells, since TAPBPR over-expression severely downregulates MHC class I surface expression in HeLaM cells in the absence of IFNγ (**Figure 5**)(Boyle et al., 2013). Upon performing this experiment however, I observed a progressive increase in the fluorescence of the cells, which continued even after 3 hours (**Figure 6a**). Since even HeLaM and HeLaM^{KO} cells showed a rapid and progressive increase in fluorescence, I concluded that at 37^{o}C, the fluorescence of these cells may reflect constant endocytosis of the exogenously added peptide, due to active trafficking at the plasma membrane, which may occur both by pinocytosis or via binding to MHC class I molecules at the cell surface. The rapid accumulation of peptide was also likely a result of using a high peptide concentration in the experiment.

Nevertheless, the fluorescence signal observed for HeLaM^{KO}TAPBPR^{WT} cells was considerably higher than the one recorded for both HeLaM^{KO} and HeLa cells (**Figure 6b**), despite the lower HLA-A*68:02 levels on the surface of HeLaM^{KO}TAPBPR^{WT} cells (**Figure 5d**). On the other hand, presence or absence of endogenously-expressed TAPBPR did not appear to influence the level of peptide binding to the cell surface (**Figure 6b**). This result was encouraging, as it showed that

over-expressed TAPBPR appeared to trigger an enhancement either in the binding of MHC class I-specific peptides to cells or in their internalisation.

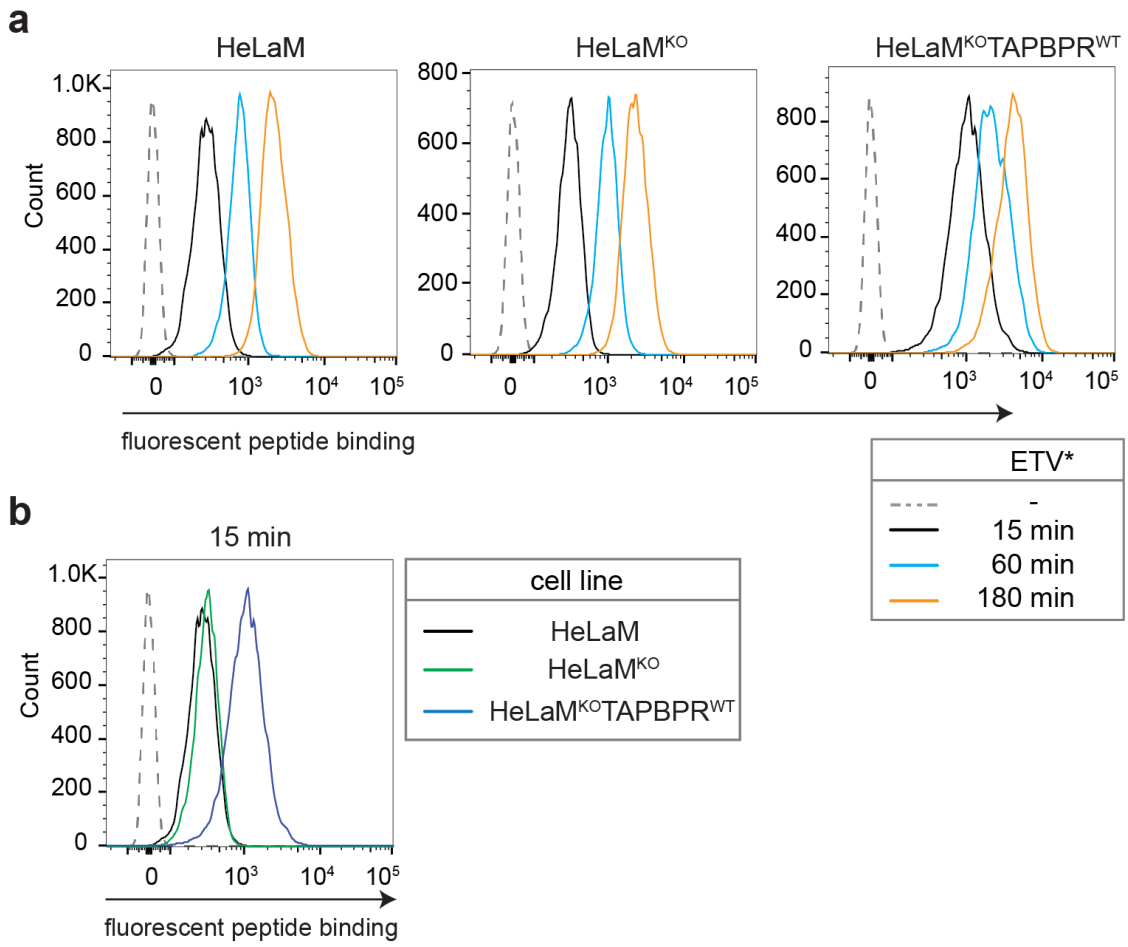

Figure 6: Progressive internalisation of peptides into cells at 37°C. (**a**) Following stimulation with IFNγ for 48 h, HeLaM cells (right), HeLaM^{KO} cells (left) and HeLaM^{KO}TAPBPR^{WT} cells (right) were treated without peptide (dashed grey line) or with 10 µM ETV* for different time periods (black = 15 min, teal = 60 min, orange = 180 min). (**b**) Comparison of the amount of peptide bound to each of the cell lines in panel **a**), upon incubation of the cells with ETV* for 15 min. Samples treated without peptide were chosen as negative controls (dashed grey line). The amount of peptide bound to/accumulated in the cells was measured by flow cytometry. These histograms are representative examples of three independent experiments.

To overcome the high amount of peptide internalization, I progressively decreased both the peptide concentration and the exposure time of the cells to the fluorescent peptide. In addition, to understand how much of the observed fluorescence level was due to MHC class I-independent peptide internalisation, I performed this analysis on HeLaM cells in which the heavy chains of HLA-A, -B and -C molecules had been knocked out (HeLaM-HLA-ABC^{KO})(cell line generated by Dr. Andreas Neerincx, University of Cambridge)(Neerincx and Boyle, 2018) and compared the bound levels of fluorescent peptide to the ones observed on HeLaM cells and HeLaM^{KO}TAPBPR^{WT} cells (**Figure 7**).

When exploring the kinetics of the peptide binding to cells, in the presence or absence of TAPBPR at the cell surface, I observed that, even at extremely low peptide concentrations, of 1 - 10 nM, HeLaM^{KO}TAPBPR^{WT} cells exhibited a high level of peptide binding, whereas HeLaM cells did not show a significant level of peptide binding until the peptide concentration was raised above 100 nM (**Figure 7a**). Moreover, HeLaM^{KO}TAPBPR^{WT} cells required ~100-fold less peptide than HeLaM cells to achieve an equivalent fluorescence level, suggesting a clear enhancement by TAPBPR in peptide binding to cells. Since MHC class I-deficient HeLaM-HLA-ABC^{KO} cells appeared to begin fluorescing only when the peptide concentration was increased to 10 µM, I concluded that the observed peptide binding to the MHC class I-positive cell lines at lower peptide concentrations was occurring strictly in an MHC class I-dependent manner.

To understand how rapidly TAPBPR facilitates peptide binding to MHC class I molecules, I treated the cell lines with 10 nM peptide and measured the level of bound peptide after different treatment periods. Strikingly, presence of TAPBPR at the cell surface triggered a strong enhancement in peptide binding at the cell surface within only a few minutes (**Figure 7b**). In fact, the level of peptide bound to HeLaM^{KO}TAPBPR^{WT} cells after 5 minutes was twice higher compared to the level observed onto HeLaM cells after 180 min. At such low peptide concentration, there did not appear to be any peptide binding occurring to HeLaM-HLA-ABC^{KO} cells, even after 180 min of peptide treatment, indicating the lack of passive peptide internalization.

These results demonstrate that TAPBPR mediates peptide loading onto cells extremely rapidly and at very low peptide concentrations, in an MHC-class I dependent manner. Based on these findings, I decided to use 10 nM fluorescent peptide and a treatment period of 15 min as a standard for interrogating TAPBPR-mediated peptide binding to MHC class I molecules.

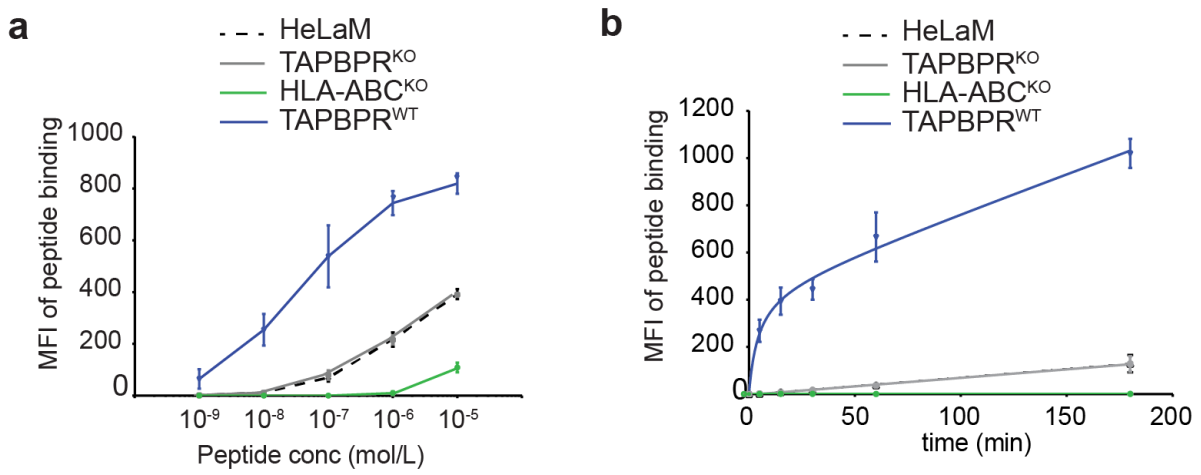

Figure 7: Over-expressed TAPBPR facilitates peptide binding onto cell surface MHC class I molecules rapidly and at low peptide concentrations. (**a**) Dose-response and (**b**) time course curves showing the level of exogenously-added ETVSK*QSNV bound to IFNγ–stimulated HeLaM, HeLaM^{KO}, HeLaM^{KO}TAPBPR^{WT} or HeLaM-HLA-ABC^{KO} cells, treated with (**a**) increasing concentration of ETVSK*QSNV for 15 min or with (**b**) 10 nM ETVSK*QSNV from 0 to 180 min at 37 °C. Line graphs show MFI ± SD from three independent experiments. Taken from Ilca et al. (Ilca et al., 2018a).

3.2.3. Over-expressed TAPBPR mediates peptide loading onto MHC class I molecules present at the cell surface

I was next interested in confirming that over-expressed TAPBPR was facilitating peptide loading onto the cell surface pool of MHC class I molecules instead of enabling this process in intracellular compartments (i.e. recycling endosomes). To this end, I performed a similar peptide binding experiment upon blocking cellular trafficking. In order to block both export and import from the cell surface, I decided to perform the peptide treatment at 4°C, a temperature at which all cellular trafficking ceases (Breuer et al., 1995, Klausner et al., 1983, Schmid and Carter, 1990).

Consistent with the results from the experiment performed at 37°C with low peptide exposure, I observed a clear increase in the binding of ETVSK*QSNV to the HeLaM^{KO}TAPBPR^{WT} cells compared to HeLaM^{KO} cells (**Figure 8**). Moreover, I found that peptide binding to HeLaM^{KO}TAPBPR^{WT} cells saturated after only 15 min (**Figure 8a**) and at very low concentrations (**Figure 8b**), suggesting that there was no progressive accumulation of the peptide into the cells and that the fluorescence level detected reflected exclusively the amount of peptide bound at the cell surface. However, the level of peptide binding to HeLaM^{KO} cells considerably increased from the 15 min time point to the 60 min one (**Figure 8a**), as well as with increasing peptide concentration (**Figure 8b**), indicating that the binding rate of the peptide is significantly

enhanced by TAPBPR over-expression. I excluded the possibility that the observed increase in peptide binding to cells over-expressing TAPBPR could be due to a higher binding capacity at the cell surface, since cells over-expressing TAPBPR display a considerably lower amount of surface expressed HLA-A*68:02 molecules compared to HeLaM^{KO} cells (**Figure 5d**).

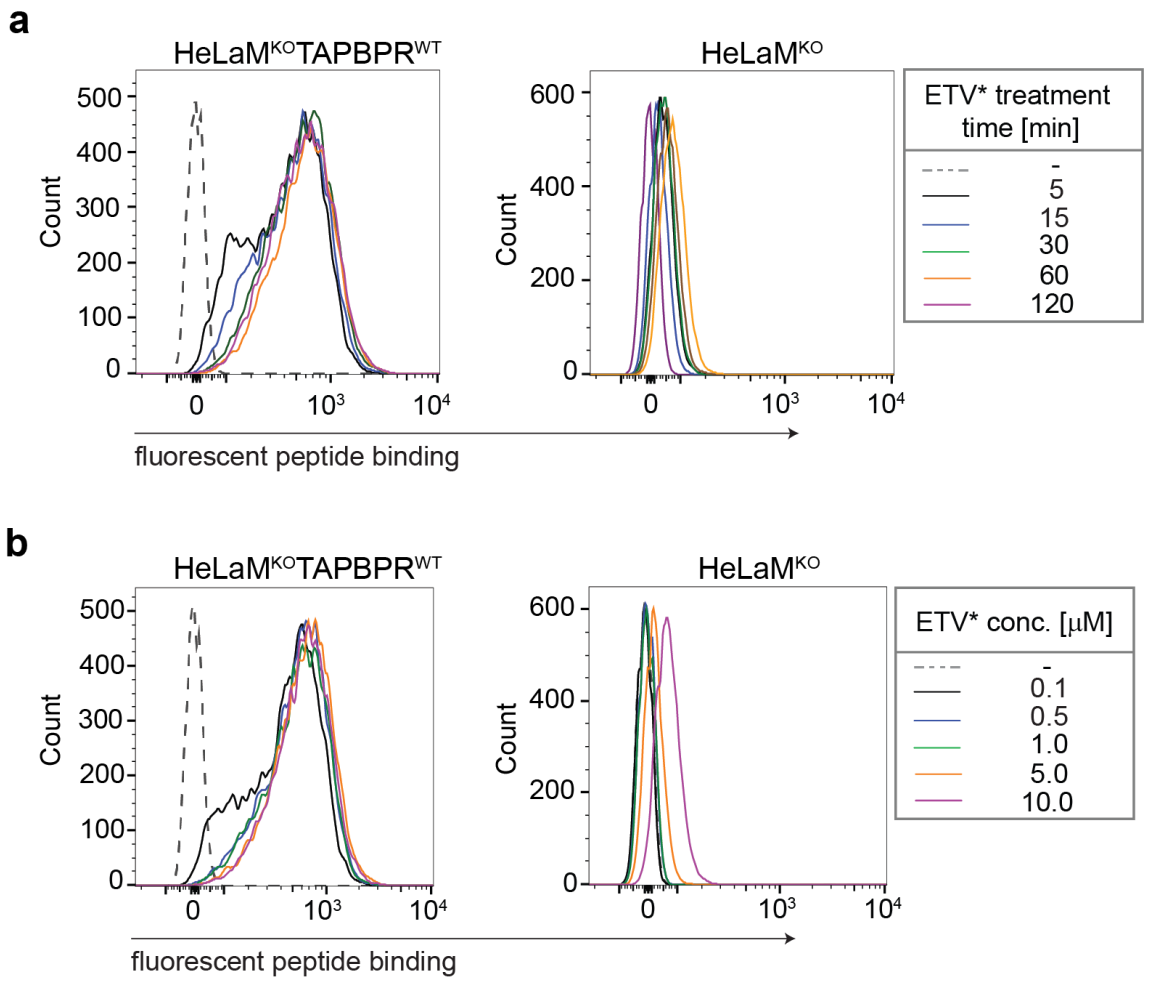

Figure 8: Over-expressed TAPBPR promotes rapid peptide loading onto cell surface MHC class I molecules at 4°C. (**a**) Time course and (**b**) dose-response histograms showing the level of ETVSK*QSNV bound to the surface of IFNγ-stimulated HeLaM^{KO}TAPBPR^{WT} (left panels) or HeLaM^{KO} cells (right panels) treated with either (**a**) 1 µM ETVSK*QSNV for 5 – 120 min or with (**b**) 0.1 – 10 µM ETVSK*QSNV for 60 min at 4°C. These histograms are representative examples of three independent experiments. Adapted from Ilca et al. (Ilca et al., 2018b).

Finally, to confirm that the observed TAPBPR-mediated peptide binding onto MHC class I molecules was occurring based on the affinity of the peptide for MHC class I, I tested whether TAPBPR was able to load peptides of low affinity for MHC class I molecules onto the cell surface. For this purpose, I designed a fluorescently-labelled peptide with low affinity for HLA-A*68:02, namely EGVSK*QSNG (ETVΔ2/9*), obtained by replacing the anchor residues on positions 2 and 9 of the high-affinity peptide ETVSK*QSNV with glycine residues. In contrast to the ETV*, ETVΔ2/9* did not show any binding to HeLaM^{KO}TAPBPR^{WT} cells (**Figure 9**), suggesting

that TAPBPR mediates peptide binding to MHC class I molecules present at the cell surface in a peptide affinity-dependent manner.

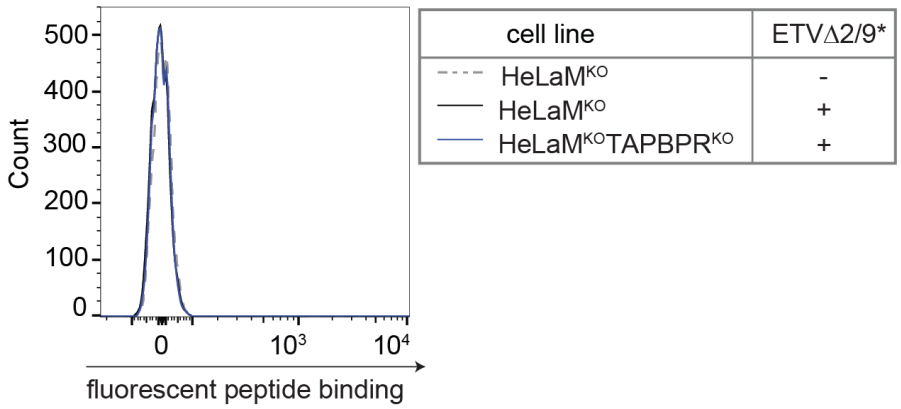

Figure 9: Over-expressed TAPBPR does not mediate loading of low-affinity peptides onto cell surface MHC class I molecules. Histograms depicting level of bound EGVSK*QSNG (ETVΔ2/9*) to IFNγ-stimulated HeLaM^{KO}TAPBPR^{WT} (blue) or HeLaM^{KO} (black line) cells, upon treatment with 10 nM ETVΔ2/9* for 15 min at 37°. HeLaM^{KO} cells treated without peptide were chosen as a negative control (dashed grey line). This is a representative example of three independent experiments. Taken from Ilca et al. (Ilca et al., 2018b).

3.2.4. TAPBPR present at the cell surface facilitates peptide loading onto MHC class I molecules

To provide evidence that the pool of TAPBPR present at the cell surface, rather than its over-expression, is responsible for loading the surface MHC class I molecules with exogenously-added peptide, we generated two chimeric TAPBPR constructs that deliver TAPBPR to different subcellular compartments. Plasma membrane-targeted TAPBPR (TAPBPR^{PM}) was achieved by fusing the luminal and transmembrane domains of TAPBPR with the cytosolic tail of CD8 (Nilsson et al., 1989) (construct generated by Dr. Andreas Neerincx, University of Cambridge), while an ER-retained TAPBPR variant (TAPBPR^{ER}) (Li et al., 1997, Ortmann et al., 1997) was achieved by fusing the luminal domain of TAPBPR with the transmembrane and cytosolic domains of tapasin. Whereas TAPBPR^{ER} was not detected at the cell surface upon over-expression, TAPBPR^{PM} showed a high surface expression level (**Figure 10a and 10b**).

When testing the ability of these TAPBPR chimeric proteins to promote peptide binding onto MHC class I molecules present at the cell surface, only cells expressing TAPBPR^{PM} showed enhanced binding of the HLA-A*68:02-specific high-affinity peptides ETVSK*QSNV and YVVPFVAK*V (YVV*). Moreover, the level of peptide binding facilitated by TAPBPR^{PM} compared to TAPBPR^{WT} was proportional to the relative surface expression levels of the two TAPBPR

variants (**Figure 10c, 10d and 10e**). Consistent with previous observations (**Figure 9**), there was no binding of the low-affinity peptide EGVSK*QSNG to any of the cell lines tested (**Figure 10e**). Together, these findings confirm that TAPBPR present at the cell surface, rather than its overexpression, promotes exogenous peptide loading onto cell surface MHC class I molecules, in a peptide affinity-based manner.

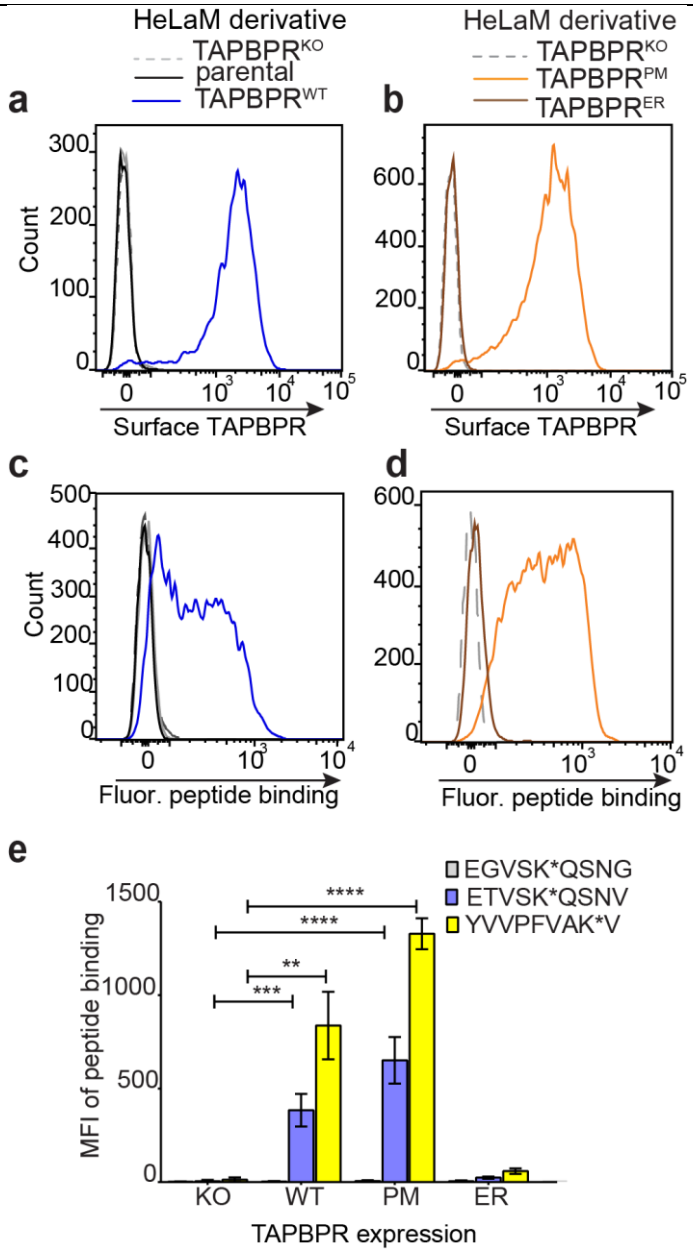

Figure 10: TAPBPR present at the cell surface enhances exogenous peptide binding onto surface expressed MHC class I molecules. (**a** and **b**) Surface expression profiles of TAPBPR on IFNγ–treated (**a**) HeLaM cells, HeLaM^{KO} or HeLaM^{KO}TAPBPR^{WT} cells or on (**b**) HeLaM^{KO}, HeLaM^{KO}TAPBPR^{PM} or HeLaM^{KO}TAPBPR^{ER} cells. (**c** and **d**) Histograms show the typical peptide binding level detected when the cell lines depicted in either panel **a**) or **b**) respectively were incubated with ETVSK*QSNV at 10 nM, for 15 min at 37 °C. (**e**) Bar charts summarizing the level of fluorescent peptide bound when cells were incubated with 10 nM of EGVSK*QSNG (grey), ETVSK*QSNV (blue), or YVVPFVAK*V (yellow) for 15 min at 37 °C. Bars show mean fluorescence intensity (MFI) ± SD from three independent experiments. n/s not significant, $^{**}P \leq 0.01$, $^{***}P \leq 0.001$, $^{****}P \leq 0.0001$ using unpaired two-tailed *t* test. Taken from Ilca et al. (Ilca et al., 2018b).

For general reference, throughout this thesis, peptides were classified as high-affinity for a specific MHC class I molecule simply based on their previously reported ability to stably bind to the MHC class I molecule and based the compatibility between their anchor residues and the MHC class I binding motif. Peptides were classified as low-affinity for a specific MHC class I molecule, based on the obvious lack of compatibility between their anchor residues and the MHC class I binding motif. No precise kinetic parameters were measured in this work for any peptide-MHC class I interactions.

3.2.5. TAPBPR present on the plasma membrane associates with MHC class I molecules at the cell surface

Given that TAPBPR promotes peptide loading of MHC class I molecules at the cell surface, I wanted to confirm the physical association between TAPBPR and MHC class I at this subcellular location. For this purpose, I performed an immuno-precipitation experiment in which I sequentially pulled down the fraction of TAPBPR present at the cell surface and then the intracellular pool of TAPBPR. The levels of MHC class I bound to the each individual TAPBPR fraction were measured by western blot (**Figure 11**).

As expected, $TAPBPR^{PM}$ and $TAPBPR^{WT}$ were present in high amounts in the cell surface pull-down fraction, while $TAPBPR^{ER}$ showed negligible levels at the cell surface despite its high abundance in the intracellular fraction. The cell surface TAPBPR pools from both $TAPBPR^{PM}$- and $TAPBPR^{WT}$-expressing cells confirmed the association of TAPBPR with MHC class I at the plasma membrane (**Figure 11**). However, as opposed to the intracellular fraction of $TAPBPR^{WT}$, the extracellular fraction of $TAPBPR^{WT}$ showed no association with its known binding partner UGT1 (Neerincx et al., 2017), which is an ER-resident enzyme, further verifying the lack of cross-contamination between the cell surface and the intracellular pull-down fractions (**Figure 11**). Intracellularly, each of the three TAPBPR variants showed significant levels of MHC class I bound. However, only $TAPBPR^{WT}$ and $TAPBPR^{ER}$ showed binding to UGT1, confirming the predicted sub-cellular localization of the $TAPBRP^{WT}$ and $TAPBPR^{ER}$, mainly in the ER, while $TAPBPR^{PM}$ was expected to be present primarily through the secretory pathway.

Taken together, all these findings indicate the active involvement of TAPBPR in facilitating the loading of exogenous peptides onto cell surface MHC class I molecules.

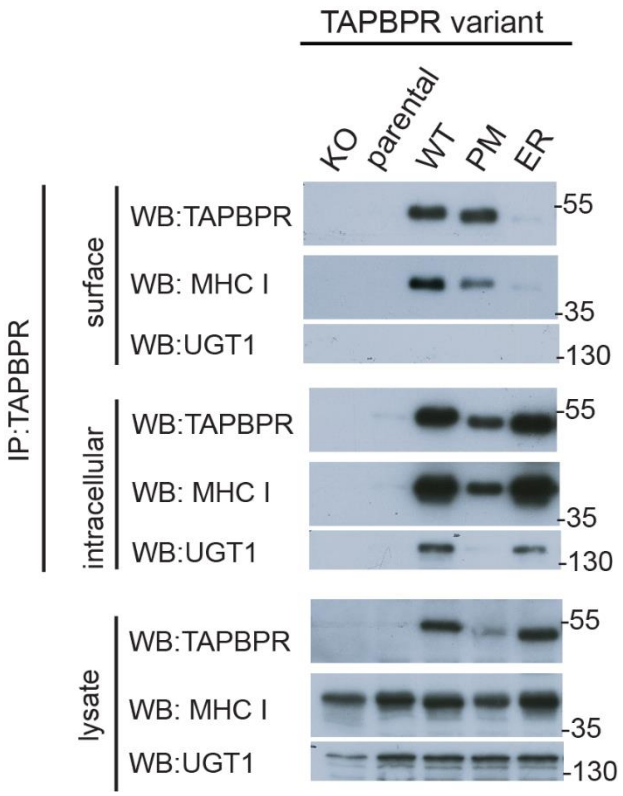

Figure 11: Surface-expressed TAPBPR interacts with MHC class I molecules at the cell surface. Western blot analysis of immunoprecipitation experiments, where either the surface or the intracellular pool of TAPBPR was pulled down from IFNγ-stimulated HeLaM^{KO} cells over-expressing TAPBPR^{WT}, TAPBPR^{PM} or TAPBPR^{ER}. Membranes were stained for TAPBPR, MHC class I (using HC10), or UGT1 on pull-down samples and lysate fractions as indicated. The data shown here is representative of three independent experiments. Taken from Ilca et al. (Ilca et al., 2018b).

3.2.6. Surface-expressed tapasin does not promote substantial peptide loading of MHC class I molecules

Since tapasin is also a peptide editor on MHC class I molecules, I next tested whether tapasin is also capable of retaining its peptide editing function on MHC class I molecules, when delivered to the cell surface. To target tapasin to the cell surface, we generated another chimeric construct, fusing the luminal and transmembrane domains of tapasin to the cytosolic tail of CD8 (tapasin^{PM}) (construct generated by Dr. Andreas Neerincx, University of Cambridge). As expected, upon over-expression, I only detected tapasin^{PM} at the cell surface, whereas tapasin^{WT} was not (**Figure 12a**).

When I measured the ability of the two tapasin variants to modulate exogenous peptide binding to cell surface MHC class I molecules, while tapasin^{WT} did not show a significant enhancement in the loading of YVVPFVAK*V, cells expressing tapasin^{PM} did show a slightly

higher level of bound peptide compared to the parental HeLaM cell line (**Figure 12b and 12c**). However, this difference was >10-fold lower than the one recorded for TAPBPR^{PM} (**Figure 10d and 10e**), indicating that TAPBPR is a much more efficient peptide loading catalyst than tapasin at the cell surface. In fact, we speculate that the slight increase in peptide loading observed upon over-expression of tapasin^{PM} is more likely due to the export of peptide-receptive MHC class I molecules together with tapasin^{PM} to the cell surface, or to the disruption of the peptide loading complex by this abundant plasma membrane-targeted tapasin variant, rather than tapasin directly catalysing peptide exchange.

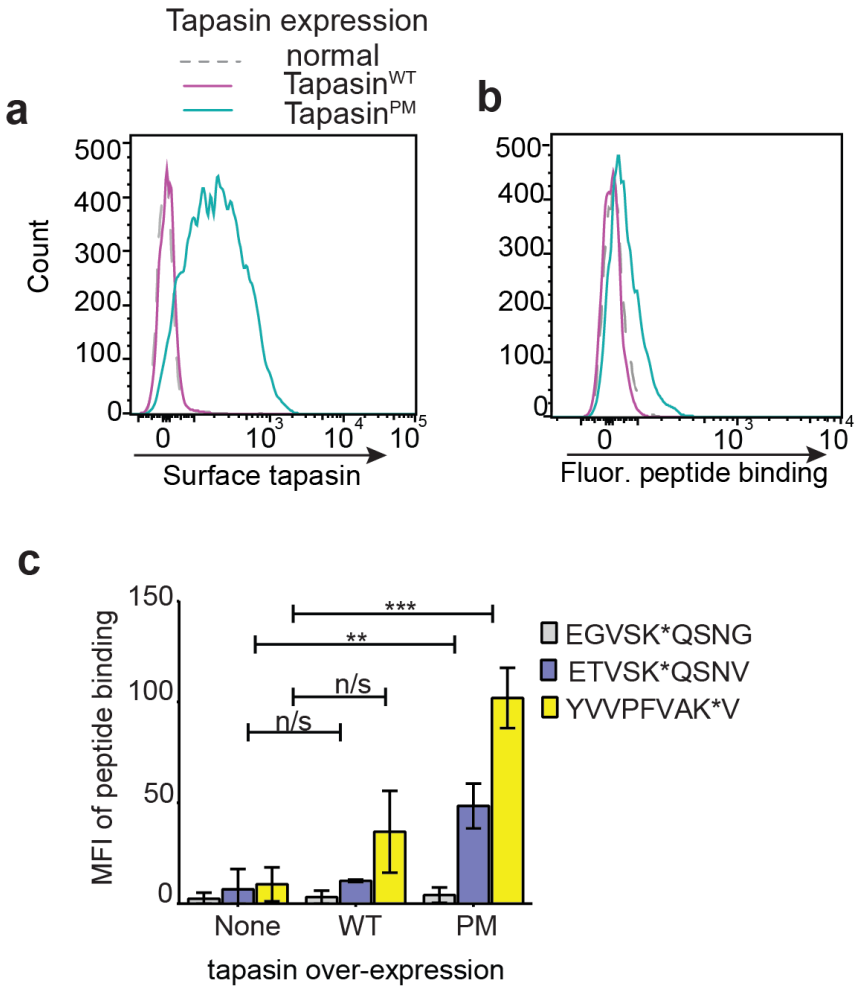

Figure 12: Over-expressed tapasin present at the cell surface does not mediate efficient peptide loading onto surface expressed MHC class I molecules. (**a**) Surface expression profiles of tapasin, detected using the mAb Pasta1, on IFNγ–treated (**a**) HeLaM cells or on HeLaM cells transduced with either tapasin^{WT} or with tapasin^{PM}. (**b**) Histograms showing the typical peptide binding level detected when the cell lines depicted in panel **a**) were incubated with 10 nM ETVSK*QSNV for 15 min at 37 °C. (**c**) Bar charts summarizing the level of fluorescent peptide bound when cells were incubated with 10 nM of the low-affinity peptide EGVSK*QSNG (grey) or with either of the high-affinity peptides ETVSK*QSNV (blue) or YVVPFVAK*V (yellow) for 15 min at 37 °C. Bars show mean fluorescence intensity (MFI) ± SD from three independent experiments. n/s not significant, $^{**}P \leq 0.01$, $^{***}P \leq 0.001$, using unpaired two-tailed *t* test. Taken from Ilca et al. (Ilca et al., 2018b).

My results are consistent with the previous differences reported between TAPBPR and tapasin in modulating peptide exchange on recombinant MHC class I refolds, in which TAPBPR alone efficiently mediates peptide dissociation (Hermann et al., 2015b, Morozov et al., 2016). In contrast, tapasin requires artificial tethering to MHC class I or other co-factors in order to promote peptide exchange (Chen and Bouvier, 2007, Wearsch and Cresswell, 2007).

3.2.7. TAPBPR functions as a peptide exchange catalyst on MHC class I molecules at the cell surface

There are two conceivable mechanisms by which TAPBPR mediates peptide loading on cell surface MHC class I molecules: it could either drag peptide-receptive MHC class I molecules along with it through the secretory pathway to the cell surface or it could actively exchange the endogenous peptides presented on MHC class I for the exogenously-added ones.

To address this question, I designed an assay to directly test whether TAPBPR was capable of actively mediating peptide dissociation from cell surface-expressed MHC class I molecules. First, cells were treated with 10 nM of fluorescently labelled peptide to prime the peptide-receptive MHC class I molecules present at the cell surface. Subsequently, the cells were washed thoroughly to remove any excess of unbound fluorescent peptide. Finally, I tested the ability of cells over-expressing TAPBPR to dissociate the bound fluorescent peptide in the presence of an excess of unlabelled competitor peptides with different affinities for HLA-A*68:02 (**Figure 13a**). The level of peptide dissociation was measured by the decrease in fluorescence levels of the cells, upon applying the unlabelled competitor. The treatment periods with both the fluorescent peptide and the non-fluorescent competitor were 15 min, in order to diminish peptide internalisation and to quantify binding and dissociation of the peptides strictly to cell surface MHC class I molecules. Using this technique, I observed a high dissociation of both ETVSK*QSNV (**Figure 13c and 13e**) and YVVPFVAK*V (**Figure 13b and 13d**), in the presence of high-affinity competitor peptides (either ETVSEQSNV or YVVPFVAKV), but not in the presence of the low-affinity peptide EGVSEQSNG.

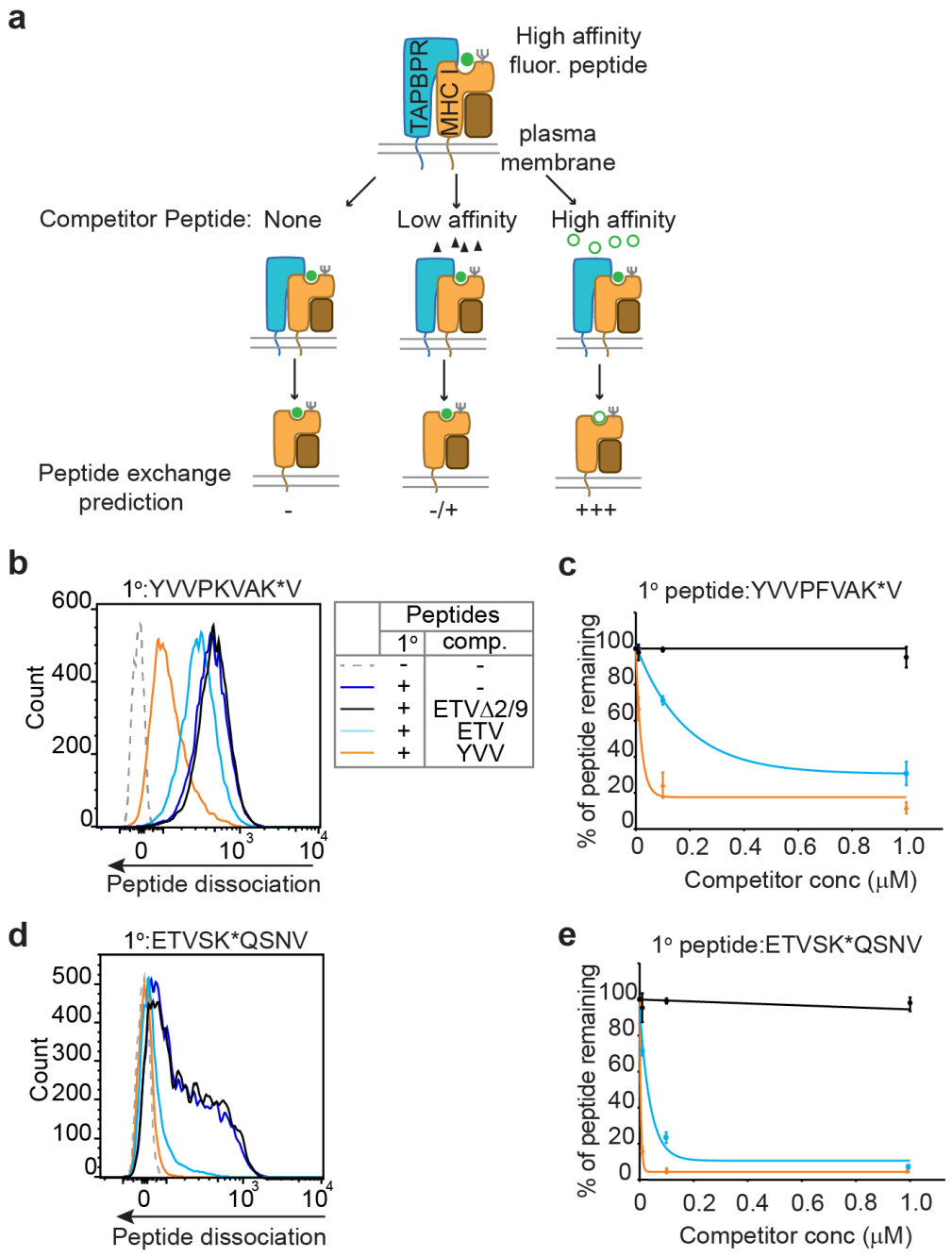

Figure 13: TAPBPR present at the cell surface actively mediates peptide exchange on surface-expressed MHC class I molecules. (**a**) Schematic depiction of the experimental set-up used to measure peptide dissociation by plasma membrane-bound TAPBPR. (**b**-**e**) IFNγ–stimulated HeLaM^{KO}TAPBPR^{WT} cells were incubated with 10 nM of either (**b** and **c**) YVVPKVAK*V or (**d** and **e**) ETVSK*QSNV for 15 min at 37 °C, then washed thoroughly to remove unbound peptide. The dissociation level of the fluorescent peptides was subsequently measured in the presence or absence of increasing concentrations of the non-labelled competitor peptides YVVPFVAKV (YVV), ETVSEQSNV (ETV), or EGVSEQSNG (ETVΔ2/9), which were added to cells for 15 min at 37 °C. (**b** and **d**) Histograms showing the typical dissociation levels of the bound fluorescent peptide observed following incubation with 100 nM competitor peptide. (**c** and **e**) Line graphs showing the percentage of fluorescent peptide remaining on the cell surface ±SD following treatment with increasing concentrations of the non-labelled peptides from three independent experiments. Adapted from Ilca et al. (Ilca et al., 2018b).

These results suggest that plasma membrane-expressed TAPBPR directly promotes peptide exchange on MHC class I molecules based on the affinity of the incoming peptide. Remarkably, within only 15 min of exposure to the non-labelled competitor, roughly 80% of both ETVSK*QSNV (**Figure 13c and 13e**) and YVVPFVAK*V (**Figure 13b and 13d**) dissociated from MHC class I in the presence of their respective non-labelled equivalents. This again highlights the high efficiency of TAPBPR-mediated peptide dissociation from cell surface-expressed MHC class I, especially given the relatively high-affinity of the dissociated fluorescent peptides.

It is important to point out that although the binding of YVVPFVAK*V (**Figure 13b**) to cells over-expressing TAPBPR appeared as a single sharp fluorescence peak, the binding of ETVSK*QSNV appeared bimodal in comparison (**Figure 10b and 13d**). We believed that this is due to the higher affinity of YVVPFVAK*V compared to ETVSK*QSNV, which allows it to reach saturation in its binding to the surface pool of MHC class I molecules even at such low concentrations and short exposure times as the one used in the experiment. To test this hypothesis, I assessed the binding patter of ETVSK*QSNV across the entire cell population over-expressing TAPBPR, when peptide was added for different time periods (**Figure 14a**) and at different concentrations (**Figure 14b**). As expected, once the peptide exposure was either increased over 60 min (**Figure 14a**) or added at concentrations ≥100 nM (**Figure 14b**), the binding of ETVSK*QSNV was brought up to comparable levels and distribution as the binding of YVVPFVAK*V, added to cells at 10 nM for 15 min (**Figure 13b**). The higher affinity of YVVPFVAK*V compared to ETVSK*QSNV is also backed up by the higher dissociation rates of both fluorescent peptides used in the peptide exchange assays, in the presence of YVVPFVAKV than in the presence of ETVSEQSNV (**Figure 13b-e**).

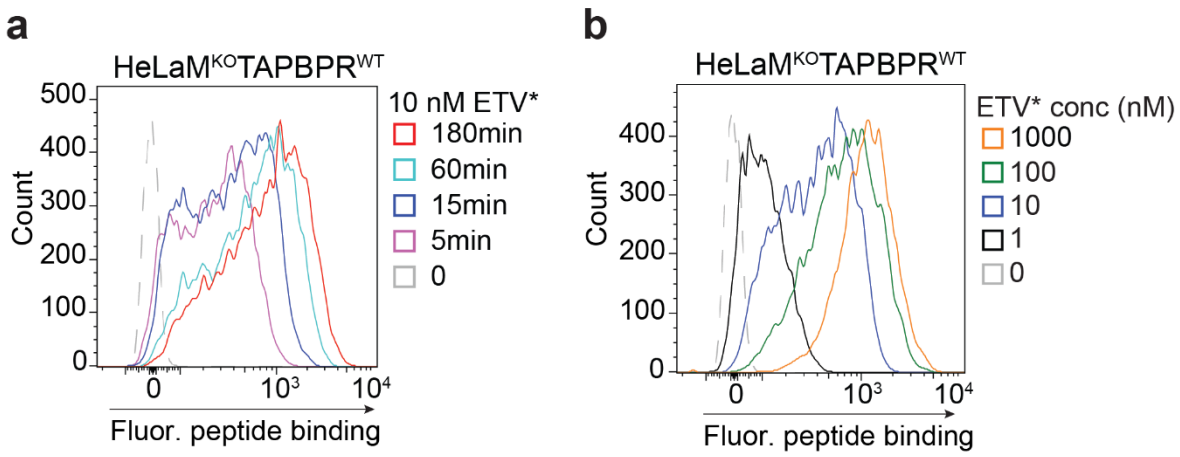

Figure 14: Peptide loading by over-expressed TAPBPR with varying peptide exposure. IFNγ–stimulated HeLaM^{KO}TAPBPR^{WT} cells were treated with ETV* at 37°C, (**a**) at 10 nM for different time periods or (**b**) at different peptide concentrations for 15 min. Histograms are representative examples of three independent experiments. A cell sample treated without fluorescent peptide was included as a negative control (grey dashed line). Taken from Ilca et al. (Ilca et al., 2018b).

To further confirm that the peptide exchange observed on cell surface MHC class I in the assay performed at physiological temperature occurs exclusively at the cell surface and that the fluorescent peptide is not exchange in endosomal compartments, I again performed the peptide exchange assay at 4°C, to block cellular trafficking (Breuer et al., 1995, Klausner et al., 1983, Schmid and Carter, 1990) (**Figure 15**). Surprisingly, TAPBPR retains its ability to mediate peptide dissociation (**Figure 15a and 15b**) from MHC class I molecules at low temperatures, albeit at a significantly slower rate (**Figure 15b**).

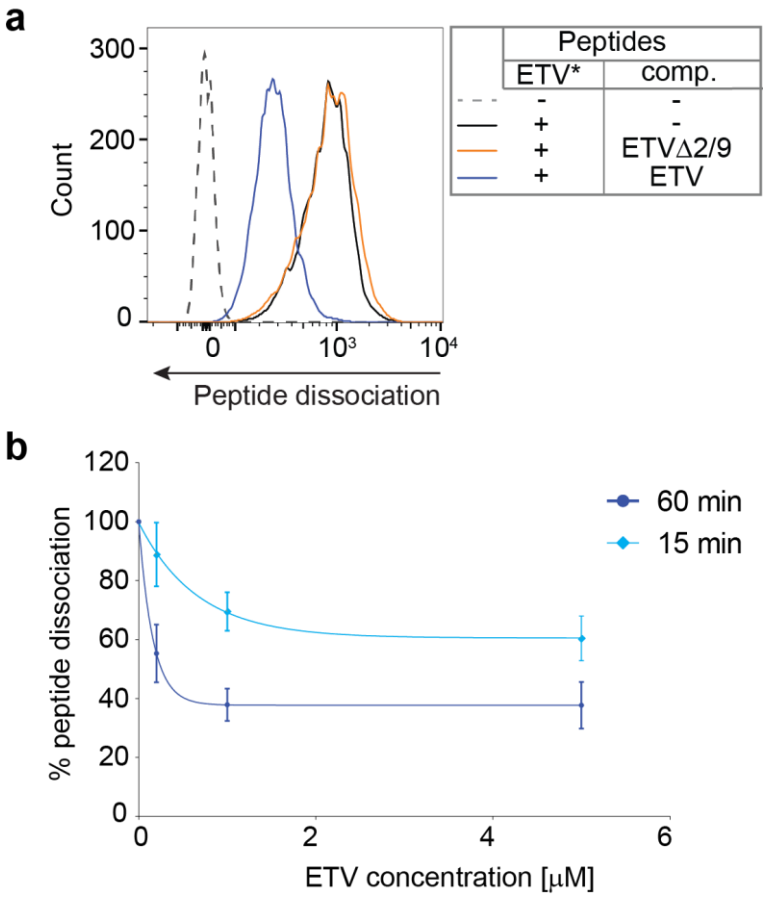

Figure 15: Cell surface TAPBPR mediates peptide exchange on surface-expressed MHC class I molecules even at 4°. (**a** and **b**) IFNγ–stimulated HeLaM^{KO}TAPBPR^{WT} cells were incubated with 1 µM ETVSK*QSNV for 60 min at 4°C, then washed thoroughly to remove unbound peptide. The dissociation of ETVSK*QSNV was subsequently measured in the presence of the non-labelled competitor peptides ETVSEQSNV (ETV) or EGVSEQSNG (ETVΔ2/9). (**a**) Histograms showing the typical dissociation levels of ETVSK*QSNV observed following incubation with 1 µM competitor peptides. (**b**) Line graphs showing the percentage of ETVSK*QSNV remaining on the cell surface ±SD following treatment with increasing concentrations of the non-labelled peptide ETVSEQSNV, added for either 15 min (light blue) or 60 min (dark blue), from three independent experiments. Taken from Ilca et al. (Ilca et al., 2018b).

When comparing the efficiencies of TAPBPR-mediated peptide dissociation between my cellular system here and the already established soluble system (Hermann et al., 2015b), where the luminal domain of TAPBPR alone was shown to enhance peptide dissociation from HLA-A*02:01 refolds, the difference is striking; in the soluble system, the dissociation reaction does not reach equilibrium even after 6 h (Hermann et al., 2015b), whereas in my cellular system, more than 80% of the peptide is dissociated after only 15 min of applying an excess of unlabelled peptide. This suggest that TAPBPR-mediated peptide dissociation is occurring at a much higher rate on a cellular membrane compared to in solution. Moreover, it is important to consider that, in contrast to the soluble system, in the cellular assay, the proteins are under their naturally-

occurring conformations, namely membrane-bound and comprising their corresponding post-translational modifications.

3.2.8. Soluble TAPBPR binds to cell surface HLA-A*68:02 class I molecules

Given that I have shown that full-length TAPBPR delivered to the cell surface is capable of actively promoting peptide dissociation from MHC class I molecules, I asked whether the luminal domain of TAPBPR alone (soluble TAPBPR), added exogenously to cells, could also function as a peptide exchange catalyst on MHC class I molecules. This assay would thus serve as an additional system to test TAPBPR-mediated peptide exchange on MHC class I molecules. Unlike over-expressing full-length TAPBPR, which clearly altered the surface pool of MHC class I molecules (**Figure 5d** and **Figure 7**), adding soluble TAPBPR exogenously onto the cell surface allowed me to assess the peptide exchange ability of TAPBPR onto a pool of MHC class I molecules present at steady state, presenting a naturally-occurring peptide repertoire.

I thus expressed soluble TAPBPR^{WT} containing a C-terminal polyHis tag in 293T cells, using the Piggy-Bac inducible expression system set up in the lab by Dr. Andreas Neerincx (University of Cambridge), and purified it by Ni-NTA affinity chromatography. Using this system, soluble TAPBPR protein was obtained in high yields (7-10 mg/L of media) and at relatively high purity, which was assessed by SDS-PAGE followed by coomassie staining (**Figure 16a**).

Upon incubating HeLaM cells with 100 nM soluble TAPBPR^{WT} for only 15 min, I detected high levels of TAPBPR^{WT} bound to the cell surface. This binding was dependent on the ability of TAPBPR to associate with MHC class I molecules present at the cell surface, as the TN5 TAPBPR mutant (TAPBPR^{TN5}), which cannot bind to MHC class I (Hermann et al., 2013), was not detected bound to HeLaM cells (**Figure 16b**). Moreover, TAPBPR did not show any binding to HeLaM-HLA-ABC^{KO} cells (**Figure 16b**), which are deficient of MHC class I, however the binding was restored once HeLaM-HLA-ABC^{KO} cells were reconstituted with HLA-A*68:02 (**Figure 16c**). These findings confirmed that soluble TAPBPR was exclusively binding to MHC class I molecules present at the cell surface.

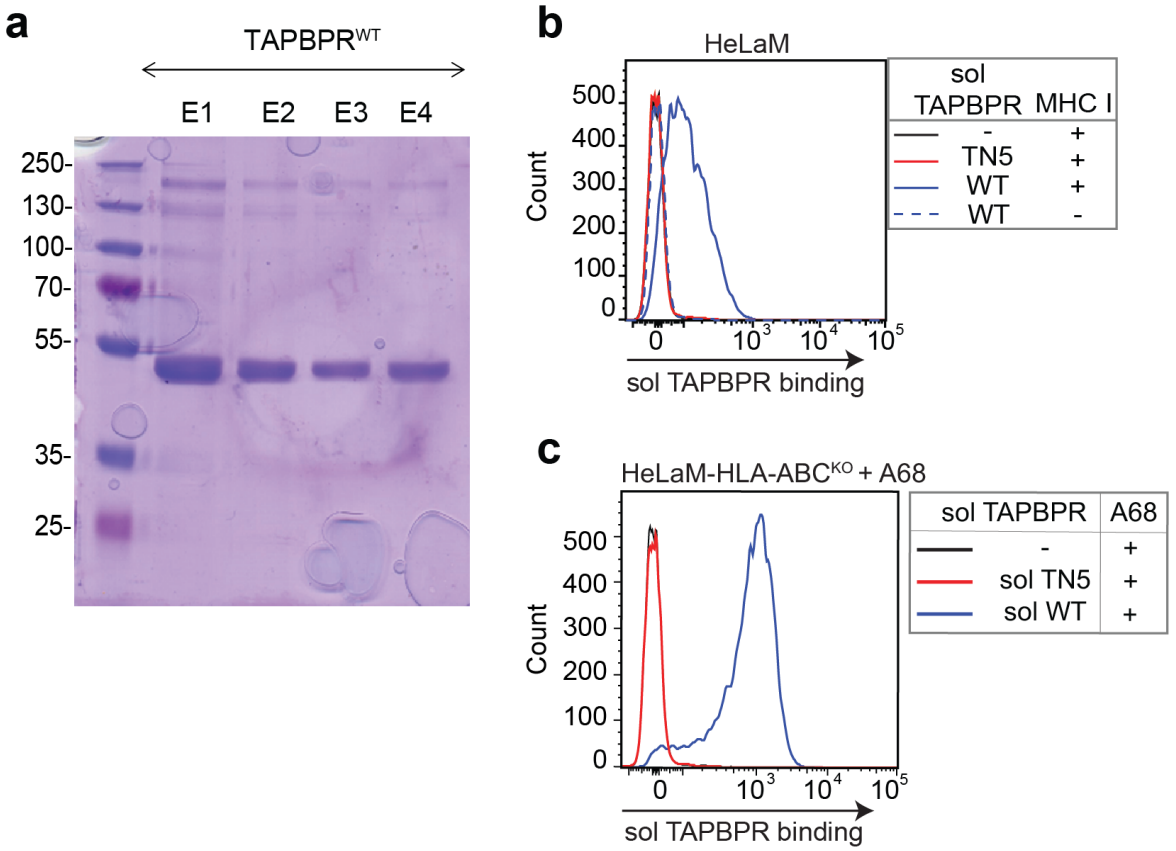

Figure 16: Soluble TAPBPR associates with MHC class I molecules present at the cell surface. (**a**) Expression and purity of the luminal domain of TAPBPR^{WT} (soluble TAPBPR), assessed by coomassie staining of an SDS/PAGE, after the protein was purified from the culture supernatant using Ni-NTA affinity chromatography. E1-E4 represent the elution fractions collected. (**b**) Histograms showing the binding of the soluble versions of either TAPBPR^{WT} to either HeLaM (blue line) or HeLa-HLA-ABC^{KO} (dashed blue line) cells or of TAPBPR^{TN5} to HeLaM cells (red line), when TAPBPR was added at 100 nM for 30 min at 37°. (**c**) Histograms showing the binding of either soluble TAPBPR^{WT} (blue) or soluble TAPBPR^{TN5} (red) to HeLa-HLA-ABC^{KO} cells reconstituted with HLA-A*68:02. Cells treated with no TAPBPR were chosen as a negative control (black line). These are representative examples of three independent experiments. Taken from Ilca et al. (Ilca et al., 2018b).

3.2.9. Soluble TAPBPR facilitates peptide exchange onto surface-expressed HLA-A*68:02

I next explored the capacity of soluble TAPBPR to facilitate peptide exchange on cell surface MHC class I molecules, by testing its ability to replace endogenously-presented peptides on MHC class I molecules with exogenously-added fluorescently labelled peptides (**Figure 17**). To this end, cells were first incubated with 100 nM TAPBPR alone for 15 min, followed by incubation with varying concentrations of fluorescent peptides with different affinities for another 15 min. The amount of bound fluorescent peptide was measured by flow cytometry, in a similar manner to the assays performed with over-expressed TAPBPR (**Figure 17a**). I observed

that soluble TAPBPR promoted the loading of both high-affinity peptides ETVSK*QSNV and YVVPFVAK*V, but not of the low-affinity peptide EGVSK*QSNG to both HeLaM cells (**Figure 17b and 17c**) and to HeLaM-HLA-ABC^{KO} cells reconstituted with HLA-A*68:02 (**Figure 17d**). Negligible peptide binding was observed to HeLaM-HLA-ABC^{KO} cells in the presence of TAPBPR^{WT} (**Figure 17e**) or to HeLaM cells in the presence of TAPBPR^{TN5} (**Figure 17b, 17c and 17e**), indicating that the peptide binding was occurring in an MHC class I-dependent manner. Remarkably, presence of soluble TAPBPR allowed for a high level of exogenous peptide binding at extremely low peptide concentrations, requiring ~1000-fold less peptide than in the absence of TAPBPR to achieve similar levels of loaded peptide (**Figure 17e**). These results demonstrate that the luminal domain of TAPBPR alone is capable of catalysing peptide exchange on HLA-A*68:02 molecules present at the cell surface with extremely high efficiency.

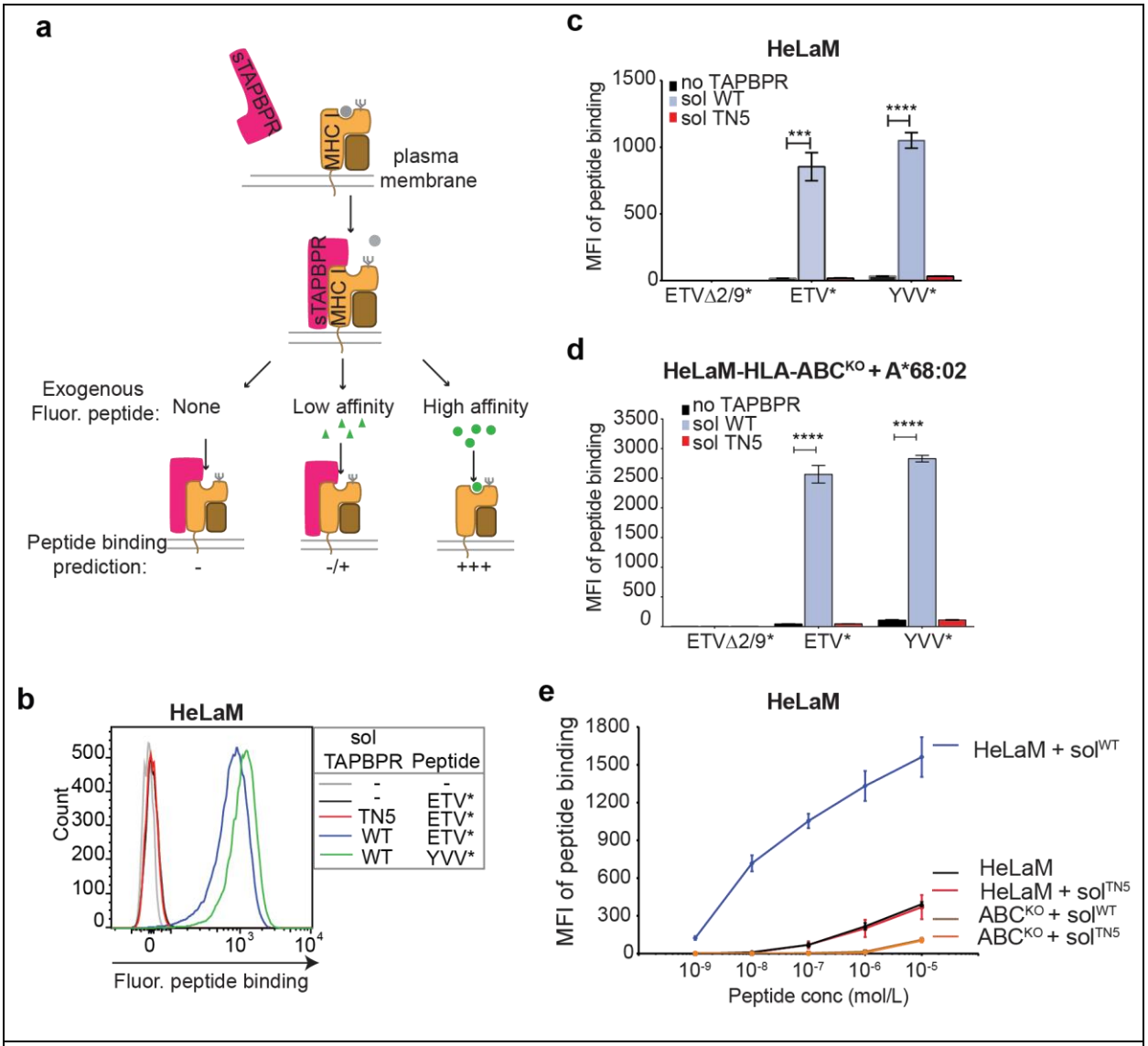

Figure 17: Soluble TAPBPR added exogenously enhances exogenous peptide association onto surface-expressed MHC class I molecules. (**a**) Schematic representation of the experimental set-up used to assess peptide exchange on surface-expressed MHC class I by soluble TAPBPR. IFNγ–treated (**b** and **c**) HeLaM or (**d**) HeLaM-HLA-ABC^{KO} cells reconstituted with HLA-A*68:02 were incubated with or without 100 nM soluble TAPBPR^{WT} or TAPBPR^{TN5} for 15 min at 37 °C, followed by incubation with or without 10 nM of ETVSK*QSNV (ETV*), YVVPFVAK*V (YVV*), or EGVSK*QSNG (ETVΔ2/9) for 15 min at 37°C. (**b**) Histograms showing the typical binding levels of ETVSK*QSNV or YVVPFVAK*V to the cell surface. (**c**) Bars graphs showing the MFI of fluorescent peptide binding ±SD from three independent experiments. (**e**) Dose–response curves exhibiting ETVSK*QSNV binding to IFNγ-treated HeLaM and HeLaM-HLA-ABC^{KO} cells, treated with or without 100 nM of either soluble TAPBPR^{WT} or soluble TAPBPR^{TN5} and with increasing concentrations of peptide, for 15 min at 37 °C ±SD, from three independent experiments. Taken from Ilca et al. (Ilca et al., 2018b).

3.2.10. Soluble TAPBPR dissociates from HLA-A*68:02 upon loading high-affinity peptides

Binding of TAPBPR and peptides to recombinant MHC class I refolds was shown to occur in a competitive manner, as loading of high-affinity peptides onto MHC class I molecules was shown to lead to the dissociation of soluble TAPBPR (Hermann et al., 2015b, Morozov et al., 2016). I was thus interested to test whether upon facilitating the loading of exogenously-added high-affinity peptides onto cell surface MHC class I molecules, TAPBPR would dissociate from MHC class I. To this end, I measured the level of soluble TAPBPR bound to the surface of HeLaM cells, upon treatment with or without peptide. The results showed that, indeed, binding of ETVSK*QSNV and YVVPFVAK*V, but not of the low-affinity peptide EGVSK*QSNG, triggered significant dissociation of soluble TAPBPR from cell surface MHC class I molecules on HeLaM cells (**Figure 18a**). The same results were obtained when running these experiments on HeLaM-HLA-ABC^{KO} cells reconstituted with HLA-A*68:02 (**Figure 18a**). Treatment with YVVPFVAK*V triggered a higher dissociation level of soluble TAPBPR from cell surface MHC class I than treatment with ETVSK*QSNV, which was consistent with the relative abilities of the two peptides to bind to HLA-A*68:02 (**Figure 18a**). Moreover, increasing concentrations of the high affinity peptides ETVSK*QSNV and YVVPFVAK*V, but not of the low-affinity peptide EGVSK*QSNG, led to an increasing level of TAPBPR dissociation from the cell surface (**Figure 18b and 18c**). Together, this data clearly supports the competitive binding model between TAPBPR and peptide to MHC class I. In other words, soluble TAPBPR dissociates endogenously-presented peptides from cell surface MHC class I molecules, consequently attaching to MHC class I, however it detaches from MHC class I once the bound MHC class I molecule acquires a high-affinity peptide.

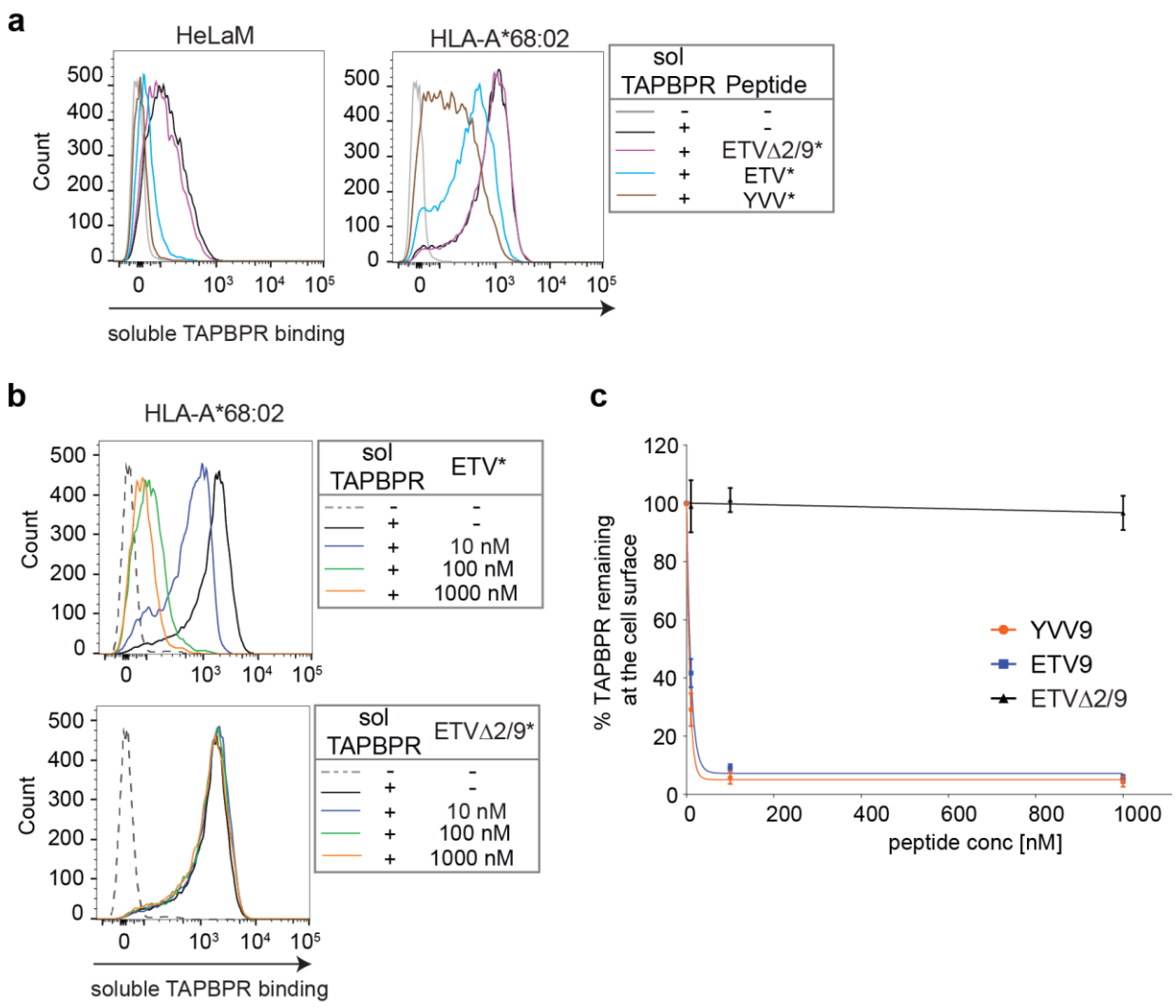

Figure 18: Soluble TAPBPR dissociates from surface-expressed MHC class I molecules upon binding of high-affinity peptides. IFNγ-stimulated HeLaM cells and HeLaM-HLA-ABC^{KO} cells reconstituted with HLA-A*68:02 (HeLa-A*68:02) were incubated with or without 100 nM soluble TAPBPR^{WT} for 15 min at 37°C, followed by incubation with or without different concentrations of EGVSK*QSNG, ETVSK*QSNV or YVVPFVAK*V for 15 min at 37°C. Subsequently, the amount of TAPBPR remaining on the cell surface was detected by staining with the TAPBPR specific mAb PeTe4. (**a**) Histograms showing TAPBPR binding to either HeLaM cells (left) or HeLa-A*68:02 cells (right), in the presence or absence of 10 nM EGVSK*QSNG, ETVSK*QSNV or YVVPFVAK*V. (**b**) Histograms showing TAPBPR binding to HeLa-A*68:02 cells in the presence of increasing concentrations of either ETVSK*QSNV (top) or EGVSK*QSNG (bottom). (**c**) Line graphs showing the remaining percentage of TAPBPR bound to the cell surface in the presence of increasing concentrations of EGVSK*QSNG, ETVSK*QSNV or YVVPFVAK*V, ±SD from three independent experiments. Taken from Ilca et al. (Ilca et al., 2018b).

3.2.11. Soluble TAPBPR mediates peptide exchange on MHC class I molecules in a peptide affinity-based manner

To assess whether the observed enhancement in peptide loading by TAPBPR was restricted to HLA-A*68:02 or whether TAPBPR can function as a peptide exchange catalyst on other human MHC class I molecules, I extended my analysis by exploring the ability of TAPBPR to load various peptides onto HLA-A*02:01 (**Figure 19**). To this end, I reconstituted HeLaM-HLA-ABC^{KO} cells with HLA-A*02:01 and performed a similar peptide binding experiment as the one described above, this time however using HLA-A*02:01-specific peptides. Satisfyingly, TAPBPR was capable of efficiently loading peptides on HLA-A*02:01 as well (**Figure 19a and 19b**). However, it proved to function considerably less efficiently on HLA-A*02:01 compared to HLA-A*68:02, requiring a 10-fold higher TAPBPR concentration in order to provide a comparable level of peptide loading. As expected, TAPBPR only facilitated the loading of peptide reported to bind to HLA-A*02:01 onto HeLaM-HLA-ABC^{KO} cells over-expressing HLA-A*02:01, namely NLVPK*VATV (HCMV-derived), YVVPFVAK*V (self-peptide) and YLLEK*LWRL (EBV-derived) (**Figure 19a and 19b**). Correspondingly, TAPBPR was not able to load peptides specific for other HLA class I allotypes, namely for HLA-A*68:02 (ETVSK*QSNV) or HLA-B*27:05 (SRYWK*IRTR), onto HLA-A*02:01. Surprisingly however, the loading of the other EBV-derived peptide tested, CLGGK*LTMV, specific for HLA-A*02:01, was not significantly enhanced in the presence of soluble TAPBPR (**Figure 19a and 19b**). This could be a result of the potentially lower affinity of this peptide for HLA-A*02:01, compared to the other peptide tested, which would not allow it to outcompete the bound soluble TAPBPR from the resulted peptide-receptive HLA-A*02:01 molecules. Taken together, these results show that TAPBPR can function as a peptide exchange catalyst on different MHC class I molecules at the cell surface, based on the affinity of the incoming peptide.

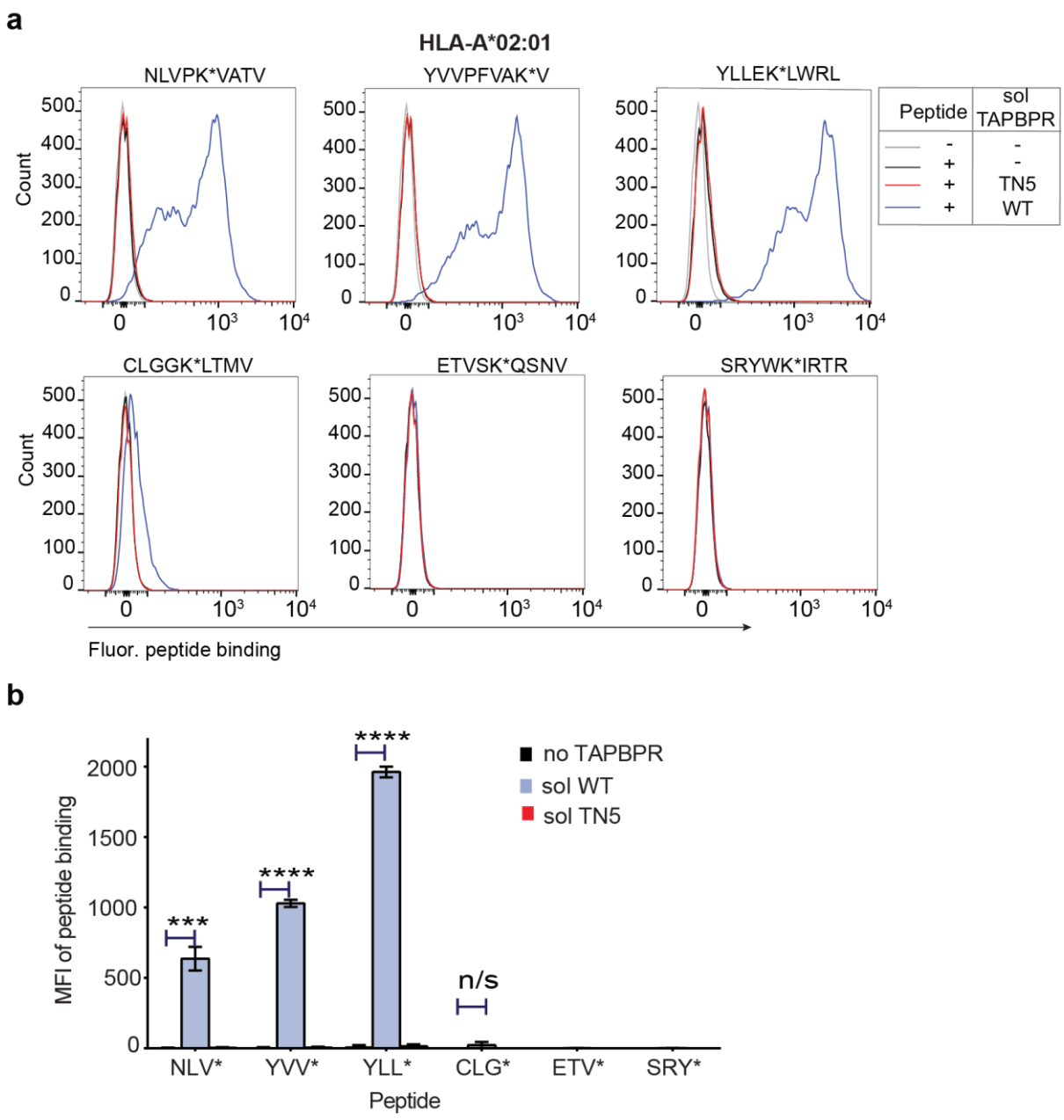

Figure 19: Soluble TAPBPR facilitates efficient peptide loading onto surface-expressed HLA-A*02:01 molecules, in an affinity-based manner. (**a**) Histograms showing the binding levels of different fluorescent peptides to IFNγ–treated HeLaM-HLA-ABC^{KO} cells reconstituted with HLA-A*02:01 (HeLa-A2), in the presence or absence of either soluble TAPBPR^{WT} or TAPBPR^{TN5}. Cells were incubated with or without 1 µM soluble TAPBPR^{WT} or TAPBPR^{TN5} for 15 min, followed by treatment with 10 nM of NLVPK*VATV (NLV*), YVVPFVAK*V (YVV*), YLLEK*LWRL (YLL*), CLGGK*LTMV (CLG*), ETVSK*QSNV (ETV*) or SRYWK*IRTR (SRY*) for 60 min. (**b**) Bar graphs show the MFI of fluorescent peptide binding to HeLaM-A2 cells from two independent experiments with duplicates. ***$P \leq 0.001$, ****$P \leq 0.0001$, n/s not significant, using unpaired two-tailed *t* test. Taken from Ilca et al. (Ilca et al., 2018b).

3.3. Discussion

Although TAPBPR naturally functions as an intracellular peptide exchange catalyst on MHC class I molecules, I have demonstrated that, when artificially given access to the MHC class I molecules present strictly at the cell surface, TAPBPR retains its ability to mediate peptide exchange. Moreover, both the soluble and the full-length versions of TAPBPR were capable of efficiently catalysing peptide exchange on surface-expressed MHC class I molecules. I have therefore developed two novel assays to assess TAPBPR-mediated peptide exchange on MHC class I molecules in a cellular system, which complements the previously established technique using soluble MHC class I refolds (Hermann et al., 2015b, Morozov et al., 2016). I show that human TAPBPR promotes peptide exchange on different MHC class I molecule and that the efficiency of TAPBPR-mediated peptide exchange is dependent on the MHC class I allotype and on the affinity of the incoming peptide for the corresponding MHC class I molecule.

However, there were a few challenges encountered throughout the development of these assays, mostly due to active trafficking at the plasma membrane. Most notably, the continuous export of new pMHC class I molecules made it difficult to perform kinetic measurements of TAPBPR-mediated peptide dissociation at physiological temperature. Moreover, due to the significant level of peptide internalization, either via MHC class I or by pinocytosis (**Figure 7**), low peptide exposures were used to best highlight the level of TAPBPR-mediated peptide exchange on MHC class I molecules occurring strictly at the cell surface (**Figures 10, 17 and 19**). To cease cellular trafficking, I performed the same assays on cells incubated at 4°C and still observed a high enhancement in peptide binding on cell surface MHC class I by TAPBPR (**Figure 8**). However, the magnitude of the effect of TAPBPR on peptide editing at 4°C was significantly reduced compared to the one recorded at physiological temperatures, most likely due to the reduced protein dynamics at lower temperatures. To inhibit cellular trafficking at physiological temperatures, one would need to treat the cells with a mixture of inhibitors, to block both cellular export (e.g. brefeldin A)(Fujiwara et al., 1988) and import (e.g. dynasore)(Macia et al., 2006), which I have not attempted in my peptide exchange assays due to the high likelihood of this causing high toxicity levels to the cells.

Nonetheless, despite these mild shortcomings, these novel cell-based peptide exchange assays, specific for TAPBPR, offer a number of advantages over the previously established cell-free assay used to measure TAPBPR-mediated peptide exchange on bacterial MHC class I refolds

(Hermann et al., 2015b, Morozov et al., 2016). First, in contrast to the cell-free system, my assays test the interactions between TAPBPR and MHC class I molecules in their naturally-occurring transmembrane conformations, either for both TAPBPR and MHC class I, or for MHC class I alone, thus taking into account the restrictions imposed on the proteins by a cellular membrane. Second, in contrast to the bacterial MHC class I refolds, which are refolded using individual peptides of choice, MHC class I molecules present at the cell surface are loaded with a pool of different peptides, spanning a relatively wide affinity spectrum, creating less bias and broader range of ligands for TAPBPR. I believe that this is the main reason why the cellular assays show a much higher efficiency of TAPBPR-mediated peptide exchange compared to the cell-free assay, with the exchange reaction saturating within minutes at the cell surface, which is many-fold quicker than the one observed in solution.

Given the higher sensitivity of the cellular system over the cell-free one for assessing TAPBPR-mediated peptide exchange on MHC class I molecules, as well as its consistent results across different MHC class I molecules, I decided to use these assays as functional read-out for investigating the catalytic mechanism of peptide exchange by TAPBPR.

4. Chapter 4: Characterising the involvement of the K22-D35 loop of TAPBPR in its peptide editing function

4.1. Background

Prior to the recent publications of the crystal structure of TAPBPR in complex with MHC class I, previous members of the Boyle lab, in collaboration with Dr. Janet Deane (CIMR, University of Cambridge), docked the structure of TAPBPR, obtained via homology modelling based on the known tapasin structure (PDB ID 3F8U)(Dong et al., 2009) and on mutagenesis data which revealed critical regions for the TAPBPR-MHC class I interaction (Hermann et al., 2013), onto the structure of HLA-A*02:01 (PDB ID 3HLA) (**Figure 20a**). This docking model revealed a region of TAPBPR, stretching from residues 22 to 35, to be in close vicinity to the peptide binding groove of MHC class I, more specifically near the F pocket of the groove (**Figure 20b**). This region contains a loop, which appears to be different from the homologous loop of tapasin. The tapasin loop is significantly shorter and was not captured in the crystal structure (**Figure 20b**)(Dong et al., 2009).

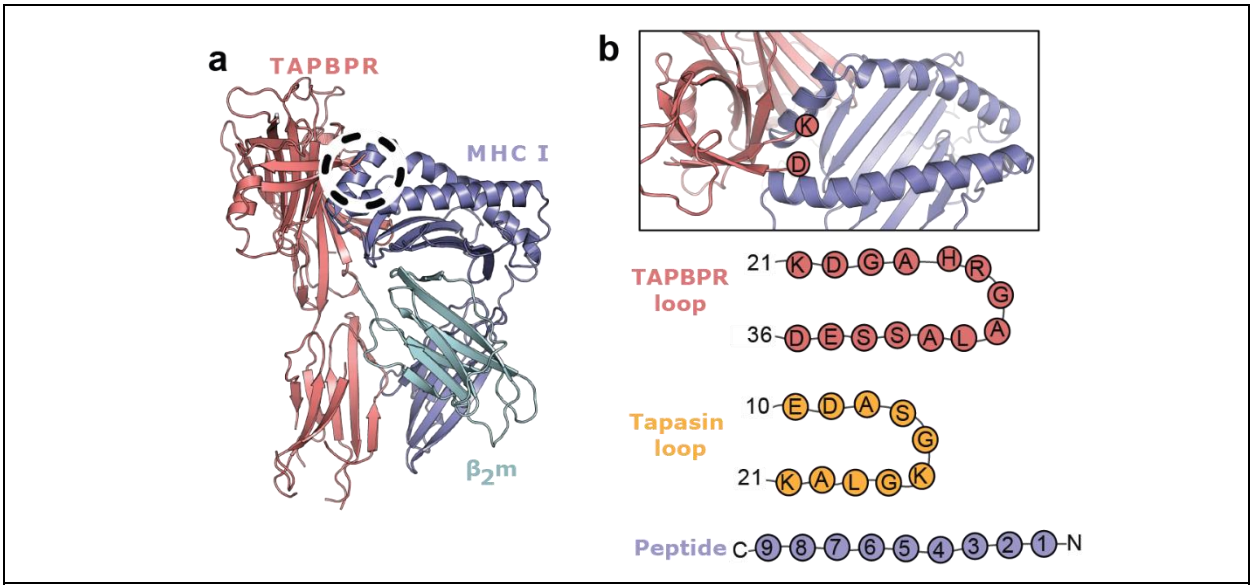

Figure 20: Predicted interaction of the TAPBPR loop with the peptide binding groove of MHC class I. (**a**) Docking model of TAPBPR (pink) onto HLA-A*02:01 (heavy chain in blue and β_2m in cyan) (PDB ID 3HLA), based on interaction studies. (**b**) Top panel, depiction of the predicted proximity of the K22-D35 loop of TAPBPR to the peptide binding groove, based on the positions of residues K22 and D35 (viewed from the top of complex shown in panel **a**); lower panel, schematic representations of the amino acid sequences of the TAPBPR loop and of the homologous loop of tapasin (PDB ID 3F8U), compared to the length and orientation of a 9-mer peptide. Taken from Ilca et al. (Ilca et al., 2018a).

The two recently published crystal structures of TAPBPR in complex with MHC class I molecules (Jiang et al., 2017, Thomas and Tampe, 2017) support our model, showing a similar orientation of TAPBPR onto MHC class I (**Figure 21a**). Moreover, the structure from Thomas and Tampe confirms the localization of the TAPBPR loop in the proximity of the MHC class I F pocket (Thomas and Tampe, 2017). However, the positioning and orientation of the loop in the two structures is poorly described. In the structure by Jiang et al, the loop was not sufficiently well ordered and is thus missing from the resolved crystal structure. The loop does appear in the structure by Thomas and Tampe, however it was poorly modelled, with multiple atoms, not only of the side chains but also belonging to the backbone of the loop, falling outside of the electron density of the structure (**Figure 21b**). This indicates that multiple conformations of the loop are possible and casts doubt on the presence of the unconventional short helix in the middle of the loop, as described in the structure.

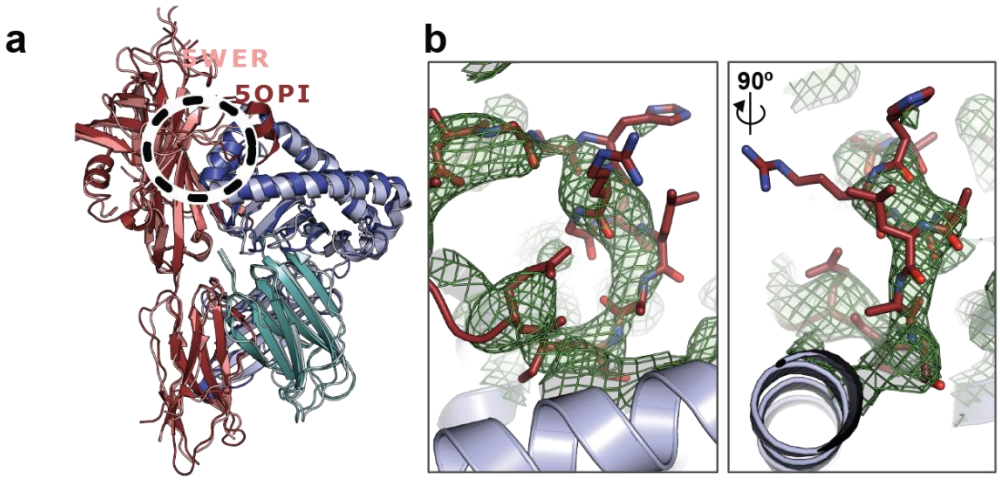

Figure 21: The loop of TAPBPR was poorly modelled in the crystal structure of TAPBPR:MHC class I complex. (**a**) Overlay of two recent X-ray structures of TAPBPR in complex with MHC class I (PDB ID 5WER and 5OPI) coloured similarity to our TAPBPR:MHC class I docking model (**Figure 20,** panel **a**). The position of the TAPBPR loop is circled (black dashed line). (**b**) The electron density map ($2F_o$-F_c, green mesh) and the resolved model (brown sticks, residues D23-E34) of the TAPBPR loop (PDB ID 5OPI). The two views of the loop and electron density shown are rotated by 90 degrees. Taken from Ilca et al. (Ilca et al., 2018a).

Although the two crystal structures clearly highlight the conformational changes undergone by MHC class I molecules, upon binding to TAPBPR, which offer insight into how TAPBPR could potentially mediate the dissociation of peptides from MHC class I, they only show the starting point and the end point of this process. It is therefore crucial to understand the mechanism

behind TAPBPR-mediated peptide dissociation from MHC class I and whether this loop of TAPBPR indeed serves a catalytic function.

Using my novel cellular peptide exchange assays specific for TAPBPR (**Chapter 3**), I could now attempt to design and screen TAPBPR loop mutants for their ability to edit peptides on cell surface-expressed MHC class I molecules in a high-throughput manner.

4.2. Results

4.2.1. Designing and expressing TAPBPR loop mutants

First, to test whether the presence of the loop was important for the peptide exchange function of TAPBPR, I designed a mutant in which I replaced all 14 residues of the loop with either glycine, alanine and serine residues, in order to generate a potentially functionless loop mutant (Øloop) (**Table 5**). Second, based on the work by Springer and colleagues, who showed that dipeptides, specifically carrying long hydrophobic residues on position 2, are able to bind into the F pocket of the MHC class I peptide binding groove (Saini et al., 2013, Saini et al., 2015), I decided to target the leucine residue on position 30 of TAPBPR, the only long hydrophobic residue of the loop. I thus generated two additional TAPBPR mutants, one by replacing the L30 residue alone with a glycine (L30G) and the other by reconstituting the L30 residue alone onto the empty loop mentioned above (ØG30L) (**Table 5**). This would inform on whether L30 is either necessary and/or sufficient for the ability of TAPBPR to mediate peptide dissociation from MHC class I.

Table 5: Panel of TAPBPR loop mutants generated on both full-length and soluble TAPBPR

TAPBPR variant	Loop sequence
WT	KDGAHRGALASSED
Øloop	AAGGSGGGGSGGAA
L30G	KDGAHRGAGASSED
ØG30L	AAGGSGGGLGGGAA

I first tested whether the changes made to the loop affected the overall stability or conformation of TAPBPR. Upon over-expression in HeLaM^{KO} cells, all three full-length TAPBPR mutants showed similar expression levels as TAPBPR^{WT} (**Figure 22**). Moreover, the levels of MHC class I and UGT1 pulled down on each TAPBPR variant via immunoprecipitation were very similar to one another, suggesting that mutating the loop did not alter the stability of TAPBPR or its ability to interact with its known binding partners (**Figure 22**).

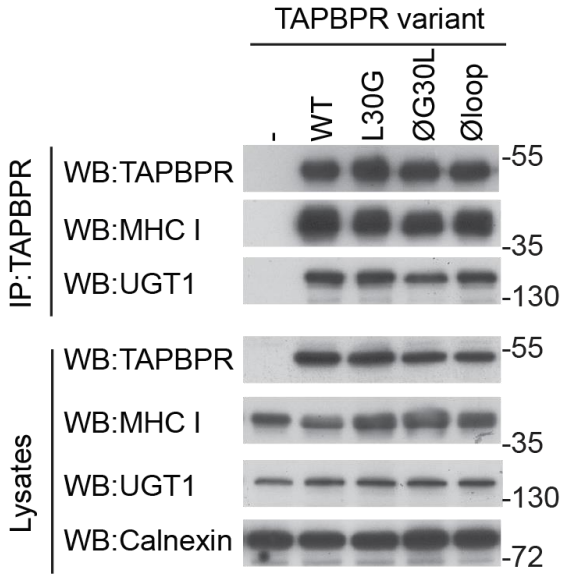

Figure 22: Mutation of the loop does not alter expression levels of TAPBPR, nor its ability to interact with MHC class I and UGT1. TAPBPR loop variants listed in **Table 5**, over-expressed in HeLaM^{KO} cells, were immunoprecipitated, using the TAPBPR-specific mAb PeTe-4, from the corresponding whole cell lysates. Western blot analysis was done on the pull-down samples to measure relative levels of MHC class I and UGT1 bound. The lysates were also stained for TAPBPR to highlight the relative expression levels of the loop mutants. The lysates were blotted for calnexin, as a loading control. This is a representative example of three independent experiments. Taken from Ilca et al. (Ilca et al., 2018a).

4.2.2. The K22-D35 loop of TAPBPR is an essential region for mediating peptide dissociation from HLA-A*68:02

I next tested the ability of the TAPBPR loop mutants to mediate peptide exchange on MHC class I molecules, using the novel cellular peptide exchange assays which I developed. First, I assessed whether the over-expressed loop mutants, present at the cell surface, facilitate peptide dissociation from MHC class I molecules, using an identical experimental set-up as the one previously described in **Figure 15**.

Upon treating the cell lines over-expressing each TAPBPR variant with the fluorescent peptide YVVPFVAK*V that has high affinity for HLA-A*68:02, surprisingly, all TAPBPR variants showed a similar increase in peptide loading onto the cell surface (**Figure 23a**). As previously mentioned, this could have been a result of the high number of peptide-receptive MHC class I molecules brought along to the cell surface by TAPBPR through the secretory pathway. However, when I then tested the ability of the TAPBPR loop variants to actively dissociate the fluorescent peptide from HLA-A*68:02 in the presence of an excess of the equivalent non-labelled competitor peptide YVVPFVAKV (**Figure 23b**), in contrast to the efficient peptide dissociation (associated with the decrease in fluorescence of the cells) observed with $TAPBPR^{WT}$, $TAPBPR^{Øloop}$-expressing cells showed very little dissociation of the fluorescent peptide (**Figure 23c, 23d and 23e**). These results indicate that the K22-D35 loop is indeed essential for the ability of TAPBPR to dissociate peptides from MHC class I molecules.

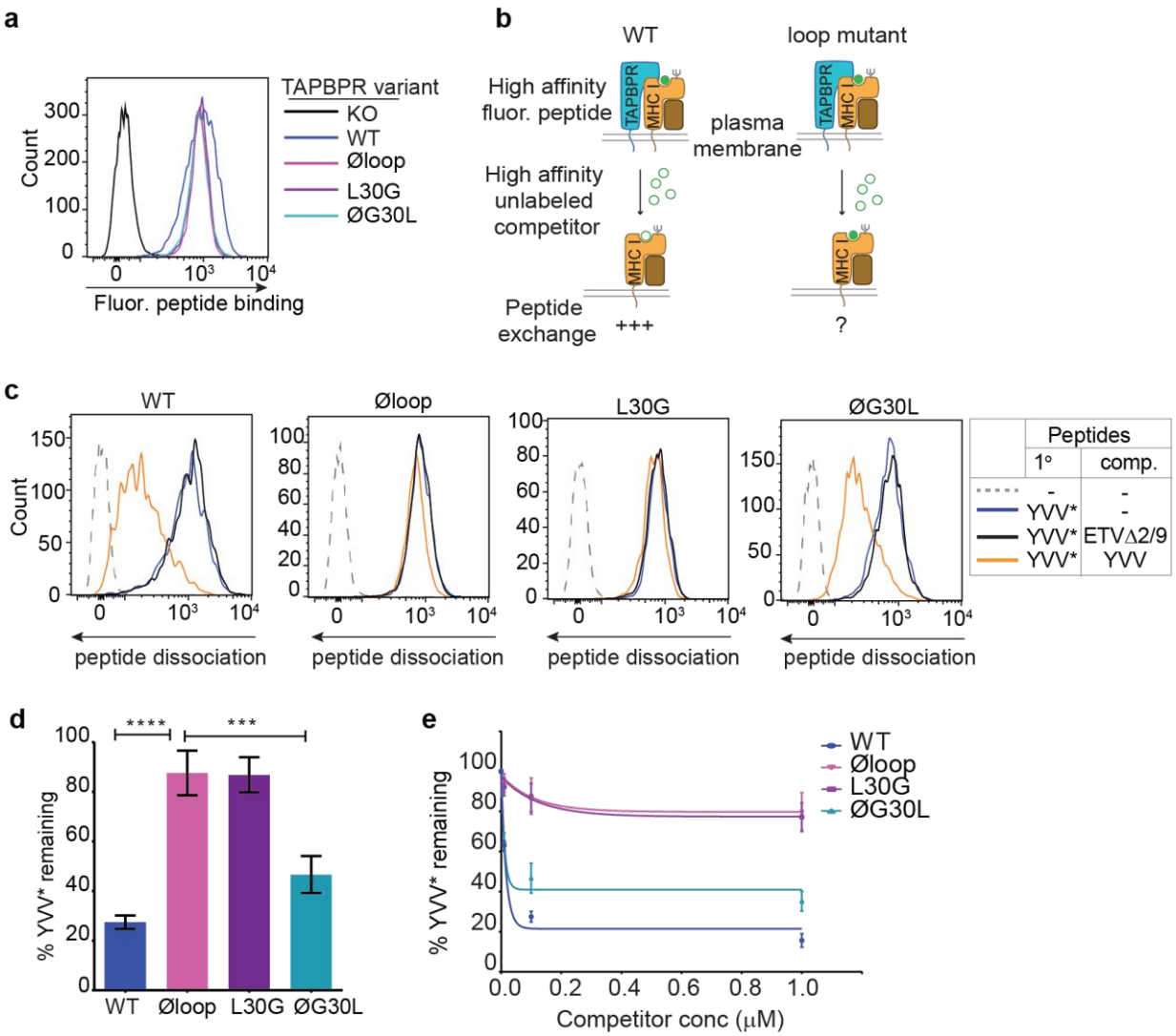

Figure 23: The K22-D35 loop of TAPBPR is essential for mediating peptide dissociation.
(**a**) Histograms showing typical peptide binding to the surface of IFNγ-treated cells over-expressing each of the TAPBPR loop variants, after cells were incubated with 10 nM YVVPFVAK*V peptide for 15 min at 37°C. (**b**) Schematic depiction of the experimental set-up used to compare the efficiency of peptide dissociation activity by plasma membrane-bound TAPBPR^{WT} with the plasma membrane-bound TAPBPR loop mutants. (**c**) Histograms depicting the level of dissociation of YVVPFVAK*V (YVV*) in the absence (blue line) and presence of 100 nM non-labelled competitor peptide YVVPFVAKV (YVV)(orange line) or EGVSKQSNG (ETVΔ2/9) (black line). (**d-e**) Graphs show the percentage of fluorescent peptide YVVPFVAK*V (YVV*) remaining, after the addition of (**d**) 100 nM or (**e**) increasing concentrations of the non-labelled competitor peptide YVVPFVAKV, as a percentage of the bound level of YVVPFVAK*V observed in the absence of a competitor peptide. Error bars show -/+SD.****p≤0.0001, ***p≤0.001 using unpaired two-tailed t-tests, based on four independent experiments. Taken from Ilca et al. (Ilca et al., 2018a).

4.2.3. L30 is a crucial residue for the peptide exchange function of TAPBPR on HLA-A*68:02

Next, to assess the involvement of the L30 residue of the loop in the peptide exchange function of TAPBPR, I used the same assay to test the ability of TAPBPR^{L30G} and TAPBPR^{ØG30L} to mediate peptide dissociation from surface-expressed HLA-A*68:02 molecules. As observed above with TAPBPR^{WT} and with TAPBPR^{Øloop}, both TAPBPR^{L30G} and TAPBPR^{ØG30L} were shown to facilitate loading of exogenously-added peptides onto cell surface HLA-A*68:02 (**Figure 23a**). However, TAPBPR^{L30G} was completely incapable of dissociating the bound fluorescent peptide, even in the presence of 1 µM unlabelled competitor peptide (**Figure 23c, 23d and 23e**). Strikingly, mutating L30 residue alone led to the same impairment in the ability of TAPBPR to dissociate peptide, as mutating the entire loop. Moreover, the crucial role of the L30 residue in peptide exchange was confirmed by the fact that TAPBPR^{ØG30L}, on which residue L30 alone was reconstituted on a fully dysfunctional loop, was restored to a functional peptide exchange catalyst on HLA-A*68:02, albeit with a reduced efficiency compared to TAPBPR^{WT} (**Figure 23c, 23d and 23e**). More exactly, the presence of TAPBPR^{WT} at the cell surface led to a dissociation level of about 75% of the fluorescent peptide form the cell surface, in the presence of 100 nM unlabelled competitor, while in the presence of TAPBPR^{ØG30L}, about 55% of the fluorescent peptide was dissociated. For the same concentration of unlabelled competitor used, the dysfunctional TAPBPR loop mutants, TAPBPR^{Øloop} and TAPBPR^{L30G}, both showed very slight dissociation levels of florescent peptide, which could be attributed to TAPBPR-independent exchange of the labelled peptide by the non-labelled peptide, which was added in high excess (**Figure 23d and 23e**). To further highlight the impact of the loop and of the L30 residue on the peptide exchange function of TAPBPR, while TAPBPR^{WT} and TAPBPR^{ØG30L} promoted rapid and highly efficient peptide dissociation even at competitor concentrations as low as 10 nM, TAPBPR^{Øloop} and TAPBPR^{L30G} were extremely inefficient at exchanging the fluorescent peptide for the non-labelled peptide, even when 1 µM of competitor peptide was used (**Figure 23e**). Taken together, these results clearly indicate that residue L30 of the TAPBPR loop is both necessary and sufficient for the peptide exchange function of TAPBPR.

4.2.4. Mutation of L30 residue severely impairs the peptide exchange ability of soluble TAPBPR on HLA-A*68:02

Having shown that soluble TAPBPR^{WT} is capable of promoting efficient peptide exchange on a cell surface MHC class I molecules (**Chapter 3**), I used soluble TAPBPR loop mutants as a second mean to assess the importance of the loop for peptide exchange. In contrast to over-expression of TAPBPR, which appears to be dragging peptide-receptive MHC class I molecules along with it to the cell surface through the secretory pathway, the use of soluble TAPBPR allows us to overcome this problem, by simply adding TAPBPR exogenously to non-modified cell lines. This way, TAPBPR will only have access to cell surface MHC class I molecules folded with peptides of relatively high affinities.

The soluble versions of the TAPBPR loop mutants were produced by cloning the luminal domains of TAPBPR mutants upstream of a polyHis tag, expressing the proteins in a HEK 293T cells and finally purifying them from tissue culture supernatant by Ni-NTA affinity chromatography. All mutants showed high purity levels, as assessed by coomassie staining (**Figure 24a**). Differential scanning fluorimetry revealed that all TAPBPR loop variants had a highly similar melting temperature, of approximately 55°C, suggesting that mutations made to the loop had not altered the overall stability of TAPBPR (**Figure 24b**).

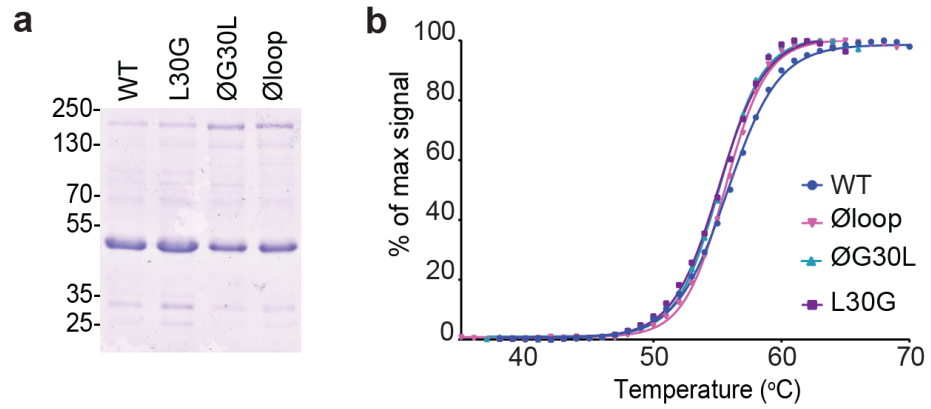

Figure 24: The soluble versions of the TAPBPR loop variants show equivalent thermostability to TAPBPR^{WT}. (**a**) Relative expression and purity levels of soluble variants of WT, L30G, ØG30L, and Øloop TAPBPR, after their purification from the culture supernatant using Ni-NTA affinity chromatography. (**b**) Differential scanning fluorimetry showing that the three TAPBPR loop mutants have equivalent melting points and thermal denaturation profiles as TAPBPR^{WT}. These graphs are representative examples of two independent experiments, ran with triplicate samples each. Taken from Ilca et al. (Ilca et al., 2018a).

Remarkably, when assessing the ability of the TAPBPR loop mutants to mediate peptide exchange on HLA-A*68:02 expressed on HeLaM cells, the results using the soluble proteins were highly consistent with the results obtained using the over-expressed the full-length TAPBPR mutants (**Figure 25**). Namely, when measuring the loading of ETVSK*QSNV onto the surface of HeLaM cells, TAPBPR^{WT} was the most efficient peptide exchange catalyst, followed by TAPBPR^{ØG30L}, which exhibited ~33% of the peptide exchange activity observed for TAPBPR^{WT} (**Figure 25a and 25b**). Again, both TAPBPR^{Øloop} and TAPBPR^{L30G} were highly inefficient at catalysing peptide exchange on HLA-A*68:02, both showing only ~3% of the catalytic activity of TAPBPR^{WT}. The same hierarchy in the peptide exchange ability across the TAPBPR loop variants (WT>ØG30L>L30G>TN5) was maintained over a wide range of TAPBPR concentrations (**Figure 25c**), as well as when using another HLA-A*68:02-specific peptide, YVVPFVAK*V (**Figure 25a & 25b**).

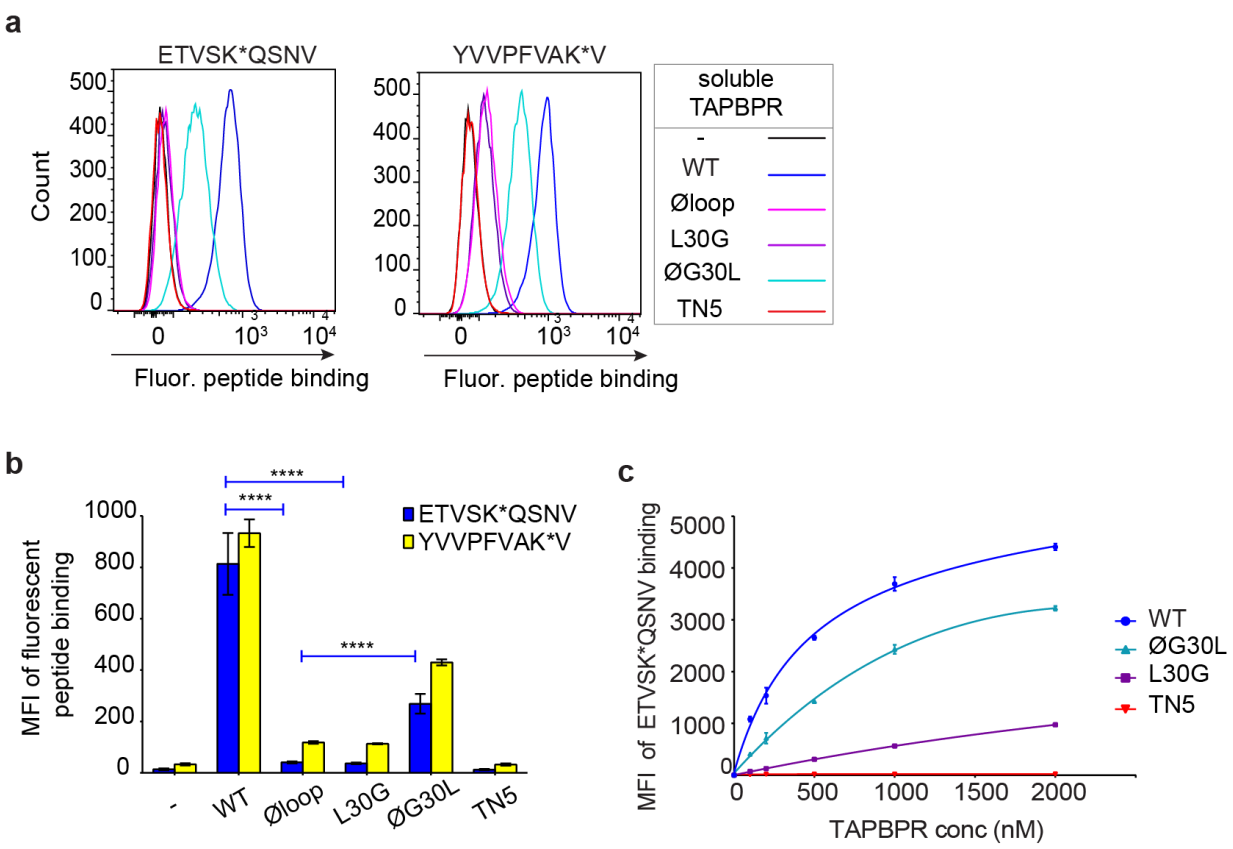

Figure 25: Soluble TAPBPR loop mutants exhibit severe impairment in their ability to mediate peptide exchange on surface-expressed HLA-A*68:02 molecules. (**a**) Histograms showing the typical fluorescent peptide binding levels to IFNγ-treated HeLaM cells incubated with or without 100 nM of each exogenously-added soluble TAPBPR variant for 15 min at 37°C, followed by treatment with 10 nM of either ETVSK*QSNV (left) or YVVPFVAK*V (right) for an additional 15 min. Soluble TAPBPR^{TN5}, a TAPBPR variant which cannot bind to MHC class I (Hermann et al., 2013), is included as a negative control. (**b**) Bar graphs summarising the results in panel **a**). (**c**) Dose-response curves of ETVSK*QSNV binding to IFNγ-treated HeLaM cells, upon incubation with increasing concentrations of each soluble TAPBPR variant prior to the addition of 10 nM ETVSK*QSNV. Error bars represent MFI -/+SD from four independent experiments. ****p≤0.0001 using unpaired two-tailed t-tests. Taken from Ilca et al. (Ilca et al., 2018a).

4.2.5. L30 residue is essential for the stable association of soluble TAPBPR with peptide-loaded MHC class I molecules

I have thus far shown that stable association of soluble TAPBPR with surface-expressed MHC class I molecules leads to a high level of peptide dissociation from MHC class I. In turn, TAPBPR dissociates from surface-expressed MHC class I molecules upon loading exogenously-added high-affinity peptides (**Figure 20**). These observations confirmed the previous studies which suggested that binding of TAPBPR and peptides to MHC class I occurs in a competitive manner (McShan et al., 2018, Morozov et al., 2016). Thus, I hypothesized that TAPBPR can only bind stably to cell surface MHC class I molecules if capable of first dissociating the endogenous

peptides presented on then. To test this hypothesis, I measured the ability of the loop mutants to bind to HeLaM-HLA-ABC^{KO} cells reconstituted with HLA-A*68:02 (**Figure 26**). Satisfyingly, upon incubating the cells with 100 nM of each TAPBPR loop variants, the TAPBPR binding hierarchy was the same as that observed for peptide exchange ability (WT>ØG30L>L30G/Øloop>TN5) (**Figure 26a**). This result suggests that, indeed, TAPBPR with an impaired ability to mediate peptide exchange cannot access MHC class I molecules loaded with peptides of relatively high affinity, such as the ones expressed on the surface of cells.
As I had previously shown that the full-length TAPBPR loop mutants were capable of associating with MHC class I molecules intracellularly upon over-expression (**Figure 22**), I tested the ability of the soluble versions of the loop mutants to associate with the total pool of MHC class I molecules from cell lysates, by immunoprecipitation experiments (**Figure 26b**). In contrast to their ability to bind to MHC class I molecules present exclusively at the cell surface, all soluble loop mutants were shown capable of binding to MHC class I from the whole-cell lysates of HeLaM^{KO} cells (**Figure 26b**). This confirmed that mutating the loop of soluble TAPBPR did not impair its intrinsic ability to associate with MHC class I, but only impacted its peptide editing function. Nonetheless, there were slightly lower amounts of MHC class I pulled down on TAPBPR^{Øloop} and TAPBPR^{L30G}, compared to TAPBPR^{WT}. A major difference between the cell surface pool and the total cellular pool of MHC class I is the intracellular availability of peptide-receptive conformations. Based on my results, I speculated that TAPBPR variants with an impaired ability to edit peptides are still capable of binding to peptide-receptive MHC class I molecules, however, in contrast to functional TAPBPR molecules, they cannot access peptide-loaded MHC class I, due to their inability to dissociate the peptide. This is consistent with previous findings according to which binding of TAPBPR and peptide to MHC class I occurs in a mutually exclusive manner (Hermann et al., 2015b, McShan et al., 2018, Morozov et al., 2016).

To further support this hypothesis, I tested the relative ability of the TAPBPR loop mutants to bind to cell surface MHC class I molecules, following pre-incubation of HeLaM cells at 26°C, a condition which increases the expression of peptide-receptive MHC class I molecules at the cell surface (Ljunggren and Karre, 1990, Schumacher et al., 1990). All TAPBPR loop mutants, but not TAPBPR^{WT}, showed a considerably increased binding to surface MHC class I at 26°C compared to at 37°C (**Figure 26c and 26d**). In fact, the defective TAPBPR mutants, TAPBPR^{Øloop} and TAPBPR^{L30G}, showed the highest increase in binding to surface MHC class I, of ~7-fold. TAPBPR^{ØG30L} exhibited an increased binding of ~2.5-fold, while the binding level of TAPBPR^{WT}

was not significantly changed (**Figure 26d**). Consistent with this result was the corresponding increase in ability of the loop mutants to promote loading of the high affinity peptide ETVSK*QSNV at 26°C compared to 37°C (**Figure 26e and 26f**).

Moreover, incubation of cells cultured at 26°C with YVVPFVAK*V, to prime the MHC class I molecules with high affinity peptide prior to testing TAPBPR binding (**Figure 27a**), resulted in a strong reduction in the binding of TAPBPR^{Øloop} to the cell surface, while the binding of TAPBPR^{WT} was unaffected (**Figure 27b and 27c**). This provides further confirmation that the observed association of TAPBPR with cell surface MHC class I molecules is dictated by the ability of TAPBPR to dissociate the endogenous peptide presented on MHC class I at steady state.

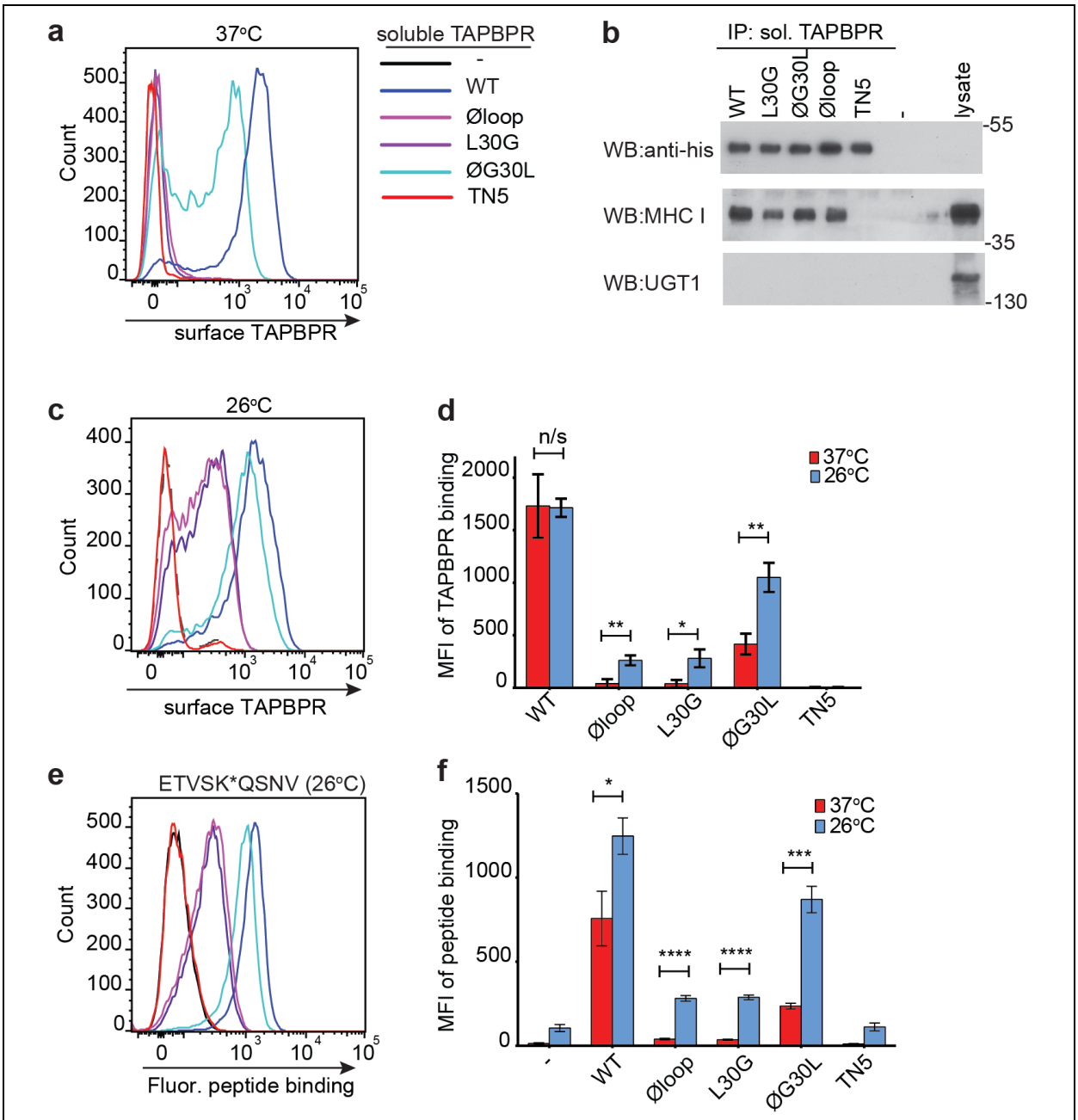

Figure 26: Residues K22-D35 are essential for the ability of soluble TAPBPR to associate with peptide-loaded MHC class I molecules. (**a** and **c**) Histograms showing the binding of each soluble TAPBPR loop variant to HeLaM-HLA-ABC^{KO} cells over-expressing HLA-A*68:02, upon incubation with 100 nM TAPBPR (**a**) at 37°C or (**c**) at 26°C for 30 min. TAPBPR^{TN5} is included as a negative control. (**b**) TAPBPR pull-downs on IFNγ-treated HeLaM^{KO} cells incubated with soluble TAPBPR loop mutants. TAPBPR^{TN5} is included as a non-MHC class I binding control. This data is representative of three independent experiments. Membranes were stained for TAPBPR, using an anti-polyHis mAb, for MHC class I heavy chain and for UGT1. (**d**) Bar graph summarising the TAPBPR binding to HeLaM-HLA-ABC^{KO}+A*68:02 cells at 37°C with 26°C from three independent experiments. Error bars represent -/+SD. (**e**) Histograms showing typical levels of bound fluorescent peptide to IFNγ-stimulated HeLaM cells treated with or without 100 nM soluble TAPBPR variants for 15 min at 26°C, followed by incubation with 10 nM ETVSK*QSNV for another 15 min at 26°C. (**f**) Bar graph comparing ETVSK*QSNV binding to HeLaM cells treated with or without soluble TAPBPR variants at 37°C with treatment at 26°C, based on three independent experiments. Error bars represent -/+SD. n/s = not significant, *p≤0.05, **p≤0.01, ***p≤0.001, ****p≤0.0001, using unpaired two-tailed t-tests. Taken from Ilca et al. (Ilca et al., 2018a).

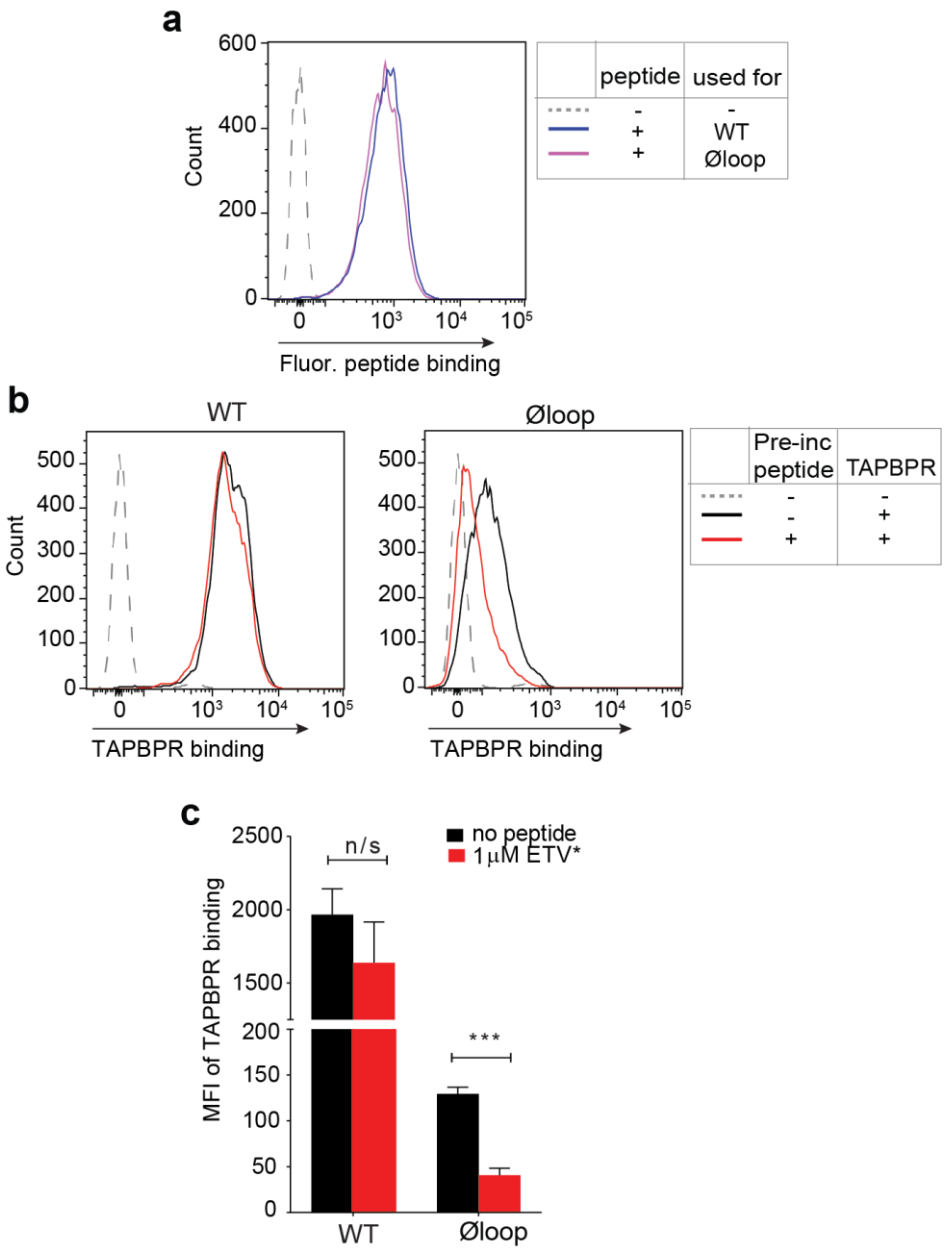

Figure 27: Peptide priming to cell surface MHC class I inhibits the binding of TAPBPR with a mutated loop. IFNγ-stimulated HeLaM-HLA-ABC^{KO} cells reconstituted with HLA-A*68:02 were treated with or without 10 nM YVVPFVAK*V for 15 min at 26°C. Excess peptide was then washed off and cells were incubated with 100 nM of either soluble TAPBPR^{WT} or TAPBPR^{Øloop}. (**a**) Histograms showing the level of YVVPFVAK*V peptide bound to HeLaM cells, prior to the addition of soluble TAPBPR. (**b**) Histograms showing the level of bound TAPBPR^{WT} (left) or TAPBPR^{Øloop} (right) on cell treated with or without peptide. (**c**) Bar graphs summarise the results in panel **b**). Error bars show -/+SD. n/s = not significant, ***p≤0.001 using unpaired two-tailed t-tests, based on four independent experiments. Taken from Ilca et al. (Ilca et al., 2018a).

4.2.6. Mutation of the K22-D35 loop of TAPBPR alters the peptide repertoire presented on MHC class I

Having shown that the K22-D25 loop of TAPBPR is essential for mediating efficient peptide dissociation from MHC class I molecules, we were interested in assessing whether mutation of the TAPBPR loop alters the peptide repertoire presented on MHC class I on cells. To this end, we thus compared the immunopeptidomes of IFNγ-stimulated HeLaM^{KO} cells reconstituted with either TAPBPR^{WT}, TAPBPR^{Øloop} or TAPBPR^{ØG30L}, in collaboration with Ana Marcu from Prof. Stefan Stefanovic's lab (University of Tubingen, Germany) and with Dr. Clemens Hermann (University of Cape Town, RSA) (**Figure 28**). We found considerable changes in the peptides presented on MHC class I between cells expressing TAPBPR^{WT} and TAPBPR^{Øloop}. Namely, while 1276 peptides were found in both cell lines, 461 peptides were only found in cells expressing TAPBPR^{WT} and 550 peptides were only present in cells expressing TAPBPR^{Øloop} (**Figure 28a**). Label-free quantitation by mass spectrometry revealed changes in the abundance of a high number of peptides between TAPBPR^{WT} and TAPBPR^{Øloop}; among the peptides found in both cell lines, 193 exhibited increased abundance in TAPBPR^{WT}-expressing cells, while 222 exhibited increased abundance in TAPBPR^{Øloop}-expressing cells (**Figure 28b**). These results demonstrate that mutation of the K22-D35 loop of TAPBPR triggers significant changes in the peptide repertoire presented on MHC class I molecules. We then compared the peptides presented on MHC class I between cells expressing either or TAPBPR^{WT} and TAPBPR^{ØG30L}, to assess the impact of the L30 residue of TAPBPR on its ability to mediate peptide editing. Although there were still significant differences in the peptide repertoires between the two cell lines, reconstitution of L30 residue alone on the empty TAPBPR loop appeared to reduce some of the changes in peptide abundance observed upon mutating the entire TAPBPR loop (**Figure 28a and 28b**). Finally, upon assignment of the peptides presented on MHC class I molecules to the different MHC class I protein products found in HeLaM cells, namely HLA-A*68:02, HLA-B*15:03 and HLA-C*12:03, a very similar distribution was observed for all three TAPBPR loop variants (**Figure 28c and 28d**).

However, in the experiments presented above (**Figure 28a-d**), the peptides were eluted for analysis straight after harvesting the cells. In other words, we think that the cells may not have been allowed to recover their steady state surface levels of either MHC class I or TAPBPR following the use of trypsin, which could have potentially diminished the ability of TAPBPR to dissociate peptides from MHC class I. We thus performed the immuno-peptidomics analysis on

cells which were allowed to recover at 37°C following trypsinisation (**Figure 28e-h**). We anticipated that this additional recovery period would also enable over-expressed TAPBPR^{WT} and TAPBPR^{ØG30L}, but not TAPBPR^{Øloop}, to actively dissociate a fraction of the peptides presented on MHC class I and thus further highlight the effect of this catalytic region of TAPBPR on peptide editing. First, the results of this experimental set-up confirmed the changes in the peptide repertoire presented on MHC class I upon mutation of the TAPBPR loop (**Figure 28e and 28f**). However, this time, there was a significant difference in peptide distribution across the different HLA class I allotypes found in HeLaM cells between cells expressing TAPBPR^{WT} and TAPBPR^{Øloop} (**Figure 28g and 28h**). Namely, based on a presence/absence approach, only 29% of the peptides analysed were now assignable to HLA-A*68:02 in TAPBPR^{WT}-expressing cells, compared to 37% in cells expressing TAPBPR^{Øloop}. Interestingly, compared to when assigning the peptides immediately following cell harvesting, the percentage of HLA-A*68:02-assignable peptides remained the same in cells expressing TAPBPR^{Øloop}, but decreased considerably for TAPBPR^{WT} (**Figure 28g**). Consistent with this, when assigning only the upregulated peptides recorded for each cell line, remarkably, more than 80% of the peptides up-regulated in TAPBPR^{Øloop}-expressing cells were assignable to HLA-A*68:02, compared to only ~20% for TAPBPR^{WT} (**Figure 28h**). In keeping with these findings, we observed similar changes in the peptide repertoire assigned to HLA-A*68:02 upon reconstitution of L30 alone onto the dysfunctional loop, as the ones observed for TAPBPR^{WT} (**Figure 28g and 28h**). To highlight the reproducibility of these results, the comparison across the five technical replicates within this dataset are shown in **Figure 29**. These findings indicate that TAPBPR, containing a functional loop, dissociates a proportion of the peptides loaded onto HLA-A*68:02 in cells, but this effect is much less pronounced on HLA-B*15:03 and HLA-C*12:03. Moreover, it appears that mutation of the L30 residue of the TAPBPR loop leads to a less stringent peptide selection on this HLA class I allotype and thus further supports the involvement of this residue in the catalytic function of TAPBPR.

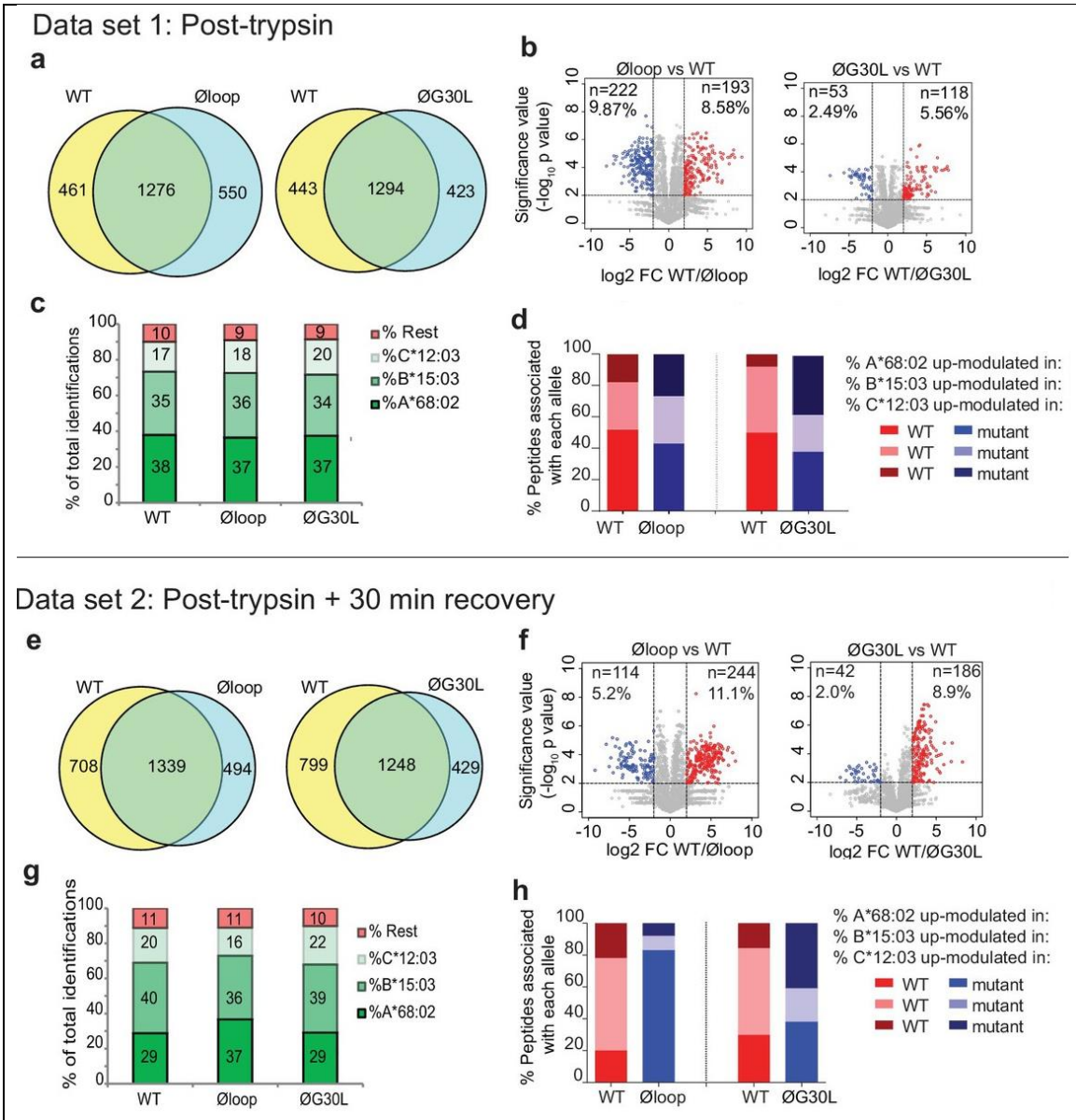

Figure 28: Mutation of the TAPBPR loop alters the peptide repertoire presented on MHC class I in cells. Peptide sets were eluted from MHC class I complexes isolated via immunoprecipitation on the W6/32 mAb from IFNγ-induced HeLaM^{KO} cells over-expressing TAPBPR^{WT}, TAPBPR^{Øloop} or TAPBPR^{ØG30L}. Peptides were then analysed using LC-MS/MS. (**a**–**d**) Cells were frozen immediately following harvest using trypsin, while in (**e**–**h**), cells were given a recovery period of 30 min at 37°C, in media, after harvesting and prior to freezing. The sequences of the identified peptides are available in the Dryad Digital Repository (DOI: https://doi.org/10.5061/dryad.p5k0156). (**a** and **e**) Venn diagrams comparing all the identified peptides between TAPBPR^{WT} and either TAPBPR^{Øloop} (left) or TAPBPR^{ØG30L} (right), by a presence/absence approach. (**b** and **f**) Volcano plots summarising label-free quantitation display the relative abundance of each shared peptide between two cells lines, paired similarly as in **a**) and **e**). Coloured dots indicate the peptides which are significantly either up- or down- modulated between two cell lines, after applying an adjusted p-value of <0.01. n = number of significantly up- or down-modulated peptides, % = the fraction of significantly modulated peptides in a specific cell line of the total pool of shared peptides. (**c** and **g**) Bar graphs depicting the assignment of the shared peptides identified in **a**) and **e**) to each individual MHC class I allotype found in HeLaM cells (HLA-A*68:02, -B*15:03 or -C*12:03); unassigned peptides appear in orange (rest). (**d** and **h**) Bar graphs depicting the significantly modulated peptides in **b**) and **f**) matched to each individual MHC class I allotype, using the NetMHCpan-4.0. Taken from Ilca et al. (Ilca et al., 2018a). This data was generated and analysed by Ana Marcu, from the lab of Prof. Stefan Stefanović (University of Tübingen, Germany).

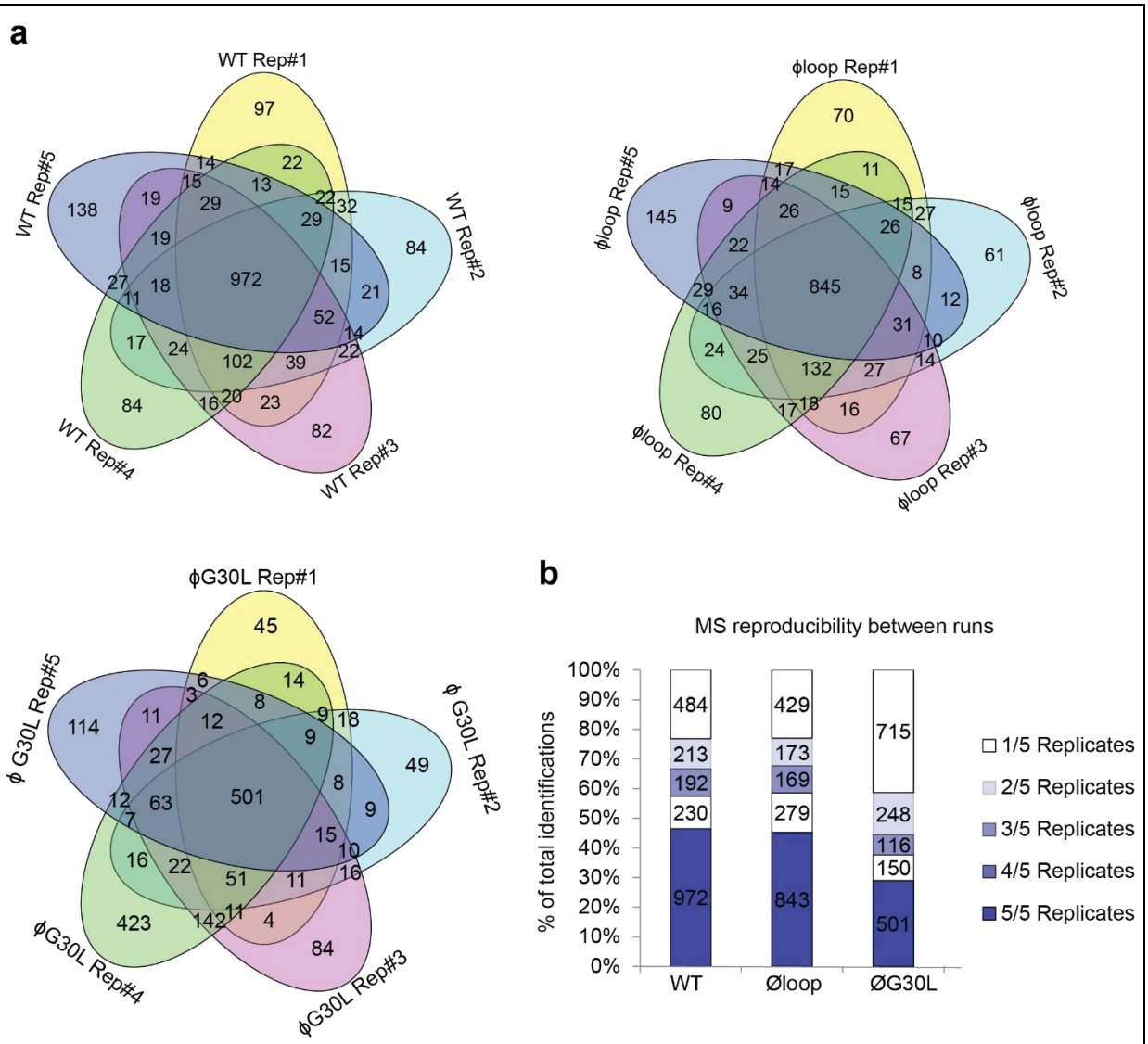

Figure 29: Technical reproducibility of the immunopeptidome analysis by LC-MS/MS. The peptide elution and immunopeptidome analysis were performed in 5 technical replicates for each dataset. (**a**) Venn diagrams showing the peptidome overlaps among the 5 replicates within one experiment. (**b**) Bar graphs display the percentage of peptides found in 1-5 out of the 5 replicates for each of the TAPBPR loop variant-expressing cell lines. The sequences of the identified peptides are available in the Dryad Digital Repository (DOI: https://doi.org/10.5061/dryad.p5k0156). Taken from Ilca et al. (Ilca et al., 2018a). These data were generated and analysed by Ana Marcu, from the lab of Prof. Stefan Stefanović (University of Tübingen, Germany).

To further explore this observed preference of TAPBPR for HLA-A*68:02 over HLA-B*15:03 and HLA-C*12:03, I assessed the ability of soluble TAPBPR to bind to each HLA class I allotype, chemically coupled to beads (**Table 6**). To this end, I incubated the beads with soluble TAPBPR at room temperature, washed the beads thoroughly and measured the level of TAPBPR on each bead set by flow cytometry. This binding experiment revealed a strong interaction between $TAPBPR^{WT}$ and HLA-A*68:02, but a lack of stable association with either HLA-B*15:03 and HLA-C*12:03 (**Table 6**). This clear preferential association of TAPBPR across the HLA class I allotypes

expressed in HeLaM cells likely explains the observed reduction only in the peptides assignable to HLA-A*68:02 by TAPBPR carrying a functional loop. Consistent with this hypothesis, soluble TAPBPR^{Øloop} showed considerably weaker binding to HLA-A*68:02, compared to TAPBPR^{WT}. Together, these findings demonstrate that the loop, and especially the L30 residue, is important for the ability of TAPBPR to shape the peptide repertoire presented on MHC class I molecules in cells, particularly on HLA-A*68:02 (**Table 6**).

Table 6: Binding of TAPBPR variants to each HLA class I allotype found in HeLaM cells

HLA class I allotype	TAPBPR^{WT}	no TAPBPR	TAPBPR^{Øloop}	W6/32
A*68:02	14461 ±(139)	418.3 (± 31.1)	2576.3 ±(19.6)	23344
B*15:03	21.7 ±(2.3)	6 (± 10.4)	17.3 ±(1.5)	23670
C*12:03	249 ±(12)	146 (±16.8)	175 ±(14.8)	23814

- values are displayed in normalized MFI units

4.2.7. L30 enables TAPBPR to mediate efficient peptide exchange on MHC class I molecules that accommodate hydrophobic residues in their F pocket

Given the proximity of the TAPBPR loop to the F pocket region of MHC class I (**Figure 5**) (Thomas and Tampe, 2017), as well as the crucial role played by the L30 residue the TAPBPR loop in the ability of TAPBPR to mediate peptide exchange (**Figures 23 and 25**), I hypothesized that the TAPBPR loop facilitates peptide dissociation from MHC class I, by inserting its L30 residue into the MHC class I F pocket, thus competing with the C-terminus of the peptide. If correct, this competitive binding would only be possible for MHC class I molecules that can accommodate a leucine or similar hydrophobic residues in their F pocket.

To test this hypothesis, I assessed the involvement of the TAPBPR loop in peptide exchange on two other MHC class I molecules, HLA-A*02:01 and H-2K^b, to which TAPBPR has been previously shown to bind (Boyle et al., 2013, Morozov et al., 2016) and which, similarly to HLA-A*68:02, have F pocket specificities for hydrophobic residues (Rammensee et al., 1999). Compared to HLA-A*68:02, HLA-A*02:01 binds similar residues in both B and F pocket, whereas H-2K^b has an entirely different peptide binding motif, the only similarity being that it also accommodates hydrophobic residues in its F pocket (**Figure 30a**). Given the ability of both HLA-A*02:01 and H-2K^b to accommodate a leucine residue in their F pocket, I predicted that the ability of TAPBPR to mediate peptide exchange on them would be heavily dependent on L30.

To this end, I designed fluorescently-labelled peptides of high affinity for both HLA-A*02:01 (NLVPK*VATV, used previously in **Chapter 3**) and H-2K^{b} (SIINFEK*L)(Saini et al., 2015) and tested their binding to the surface of either HeLaM-HLA-ABC^{KO} cells reconstituted with HLA-A*02:01, or to the mouse cell line EL4 which expresses H-2K^{b}, respectively, in the presence of the different TAPBPR loop mutants (**Figure 30b and 30c**). As expected, I observed a similar hierarchy in the ability of the TAPBPR loop variants to mediate peptide exchange as the one obtained for HLA-A*68:02 (**Figure 25**), with TAPBPR^{WT} being the most efficient, followed by TAPBPR^{ØG30L}, while TAPBPR^{Øloop} and TAPBPR^{L30G} were both highly inefficient (**Figure 30c**). For instance, when measuring the binding of NLVPK*VATV to HLA-A*02:01-expressing cells, TAPBPR^{ØG30L}, TAPBPR^{Øloop} and TAPBPR exhibited ~54%, ~23% and ~32% of the catalytic activity of TAPBPR^{WT}, respectively (**Figure 30b and 30c**).

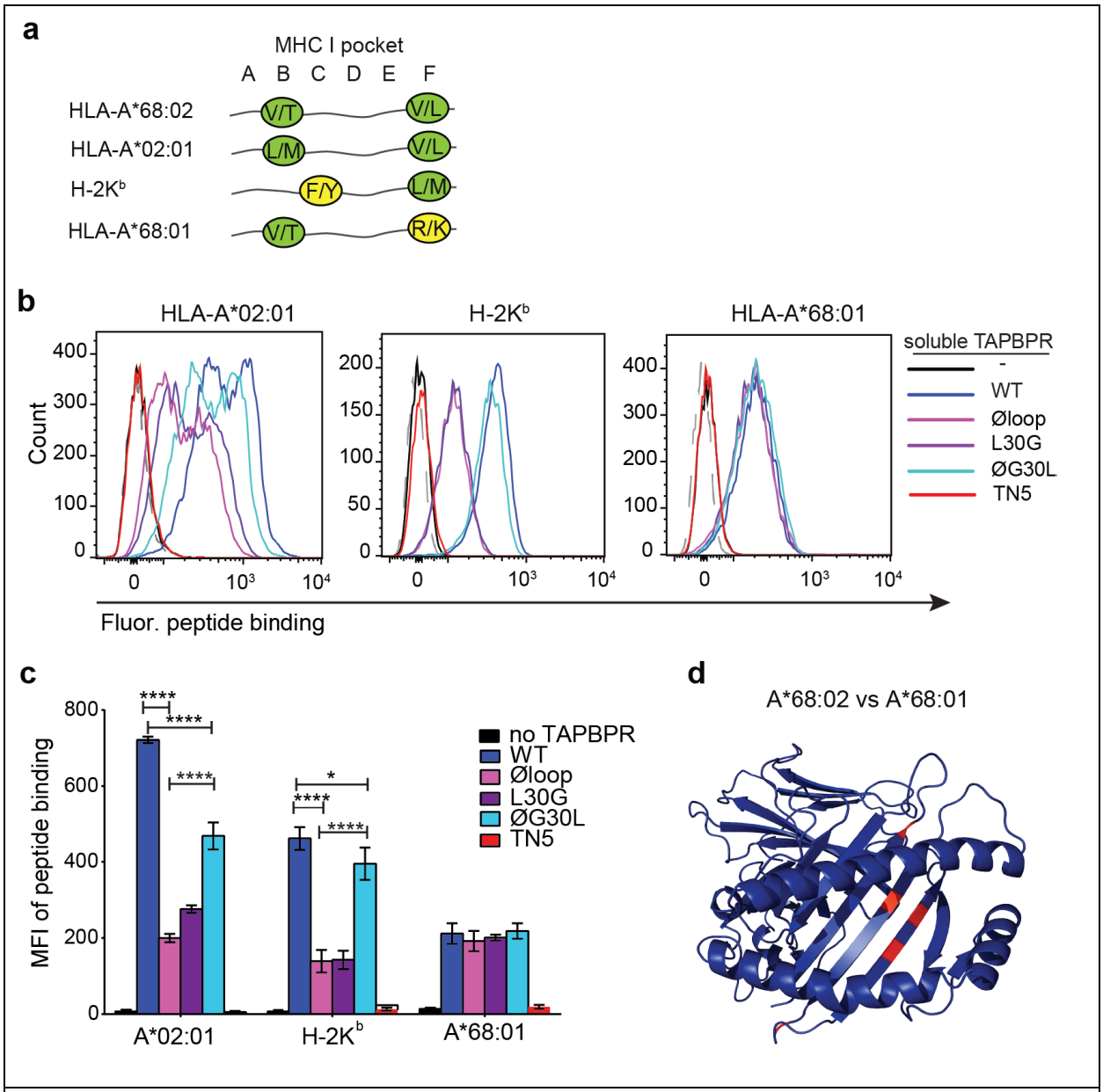

Figure 30: TAPBPR edits peptides in a loop-dependent manner only on MHC class I molecules with F pocket specificities for hydrophobic peptide residues. (**a**) Comparison of the A-F pocket specificities among the peptide binding grooves of HLA-A*68:02, HLA-A*02:01, H-2K^b and HLA-A*68:01. (**b**) Binding of the appropriate fluorescent peptide to IFNγ-treated HeLaM-HLA-ABC^{KO} transduced either with HLA-A*02:01 or with HLA-A*68:01 or to mouse EL4 cells (which express H-2K^b), in the presence or absence of 1 µM soluble TAPBPR variant for 15 min at 37°C, followed by incubation with 10 nM NLVPK*VATV (for HLA-A*02:01) for 60 min, 1 nM SIINFEK*L (for H-2K^b) for 30 min or 100 nM KTGGPIYK*R (for HLA-A*68:01) for 60 min at 37°C. (**c**) Bar graph summarising the peptide loading levels mediated by the soluble TAPBPR variants, as described in **b**). Error bars represent MFI -/+ SD based on four independent experiments. ****p ≤ 0.0001, ***p ≤ 0.001, *p ≤ 0.05, using unpaired two-tailed t-tests. (**d**) Structure of MHC class I seen from above the binding groove (PDB ID 4HWZ) and the different amino acids between HLA-A*68:02 and –A*68:01 highlighted in red. Taken from Ilca et al. (Ilca et al., 2018a).

We observed a similar trend in the ability of the TAPBPR mutants to load another HLA-A2-specific peptide, YLLEK*LWRL, as well as when testing peptide binding to HLA-A2 expressed on a different cell line, namely MCF-7 (**Figure 31**). Similarly, when assessing the binding of the H-

2K^{b}-specific peptide SIINFEK*L to EL4 cells, the ØG30L, Øloop and L30G variants exhibited ~ 85%, 30% and 31% of the catalytic activity of TAPBPR^{WT}, respectively (**Figure 30b and 30c**). Together, these results clearly highlight the crucial role of the L30 residue of TAPBPR in mediating efficient peptide exchange on HLA-A2 and on H-2K^{b}, despite TAPBPR still being able to exchange peptide on these MHC class I molecules to some degree. Remarkably, TAPBPR shows a similar functional dependency on L30 across HLA-A*68:02, HLA-A*02:01 and H-2K^{b}, despite the low degree of similarity between murine and human MHC class I molecules, both in their amino acid sequences and in their peptide binding motifs. However, the key shared feature between all three MHC class I molecules tested is their F pocket specificity for hydrophobic residues.

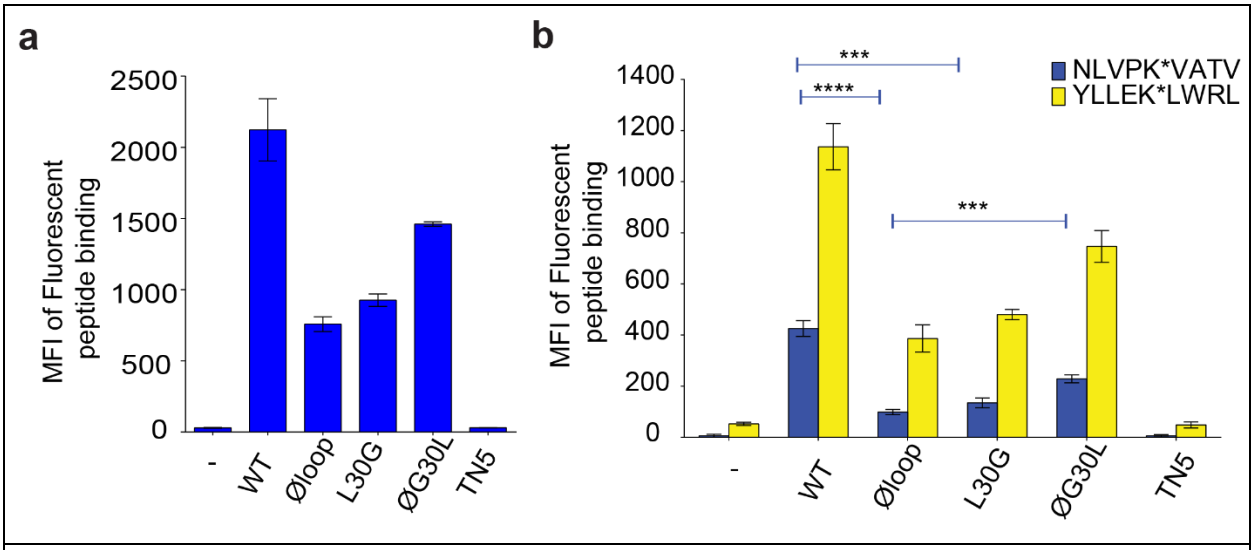

Figure 31: Soluble TAPBPR-mediated peptide loading onto HLA-A*02:01 molecules. (**a**) Bar graphs displaying binding of fluorescent peptide to IFNγ-stimulated HeLaM-HLA-ABC^{KO} reconstituted with HLA-A2, upon incubation with or without 1 µM of each soluble TAPBPR variant for 15 min at 37°C, followed by incubation with 10 nM YLLEK*LWRL (HLA-A2 specific peptide) for 60 min at 37°C. (**b**) Bar graphs showing fluorescent peptide binding to IFNγ-treated MCF-7 cells incubated with or without 1 µM of each soluble TAPBPR variant for 15 min at 37°C, followed by addition of 10 nM of either NLVPK*VATV (blue) or YLLEK*LWRL (yellow) for 60 min at 37°C. Error bars represent MFI -/+SD from four independent experiments. ****p≤0.0001, ***p≤0.001 using unpaired two-tailed t-tests. Taken from Ilca et al. (Ilca et al., 2018a).

4.2.8. TAPBPR cannot use the L30 residue to mediate efficient peptide exchange on MHC class I molecules that accommodate charged residues in their F pocket

To provide further support to my hypothesis that TAPBPR can use its L30 residue to efficiently mediate peptide exchange only on MHC class I molecules with F pocket specificities for hydrophobic amino acids, I tested the ability of the loop mutants to edit peptides on a human MHC class I molecule that accommodates a charged residue in its F pocket. To only explore the contribution of the F pocket specificity, with minimal other differences, I chose HLA-A*68:01. Although HLA-A*68:01 differs from HLA-A*68:02 in only 5 amino acids, most of those dictate the specificity of the F pocket (**Figure 30d**)(Niu et al., 2013). As a result, while the two molecules accommodate similar residues in their B pocket, the F pocket of A*68:02 binds aliphatic residues, whereas the F pocket of A*68:01 binds basic residues (**Figure 30a**). Thus, despite the high degree of similarity between A*68:01 and A*68:02, I predicted A*68:01 would not undergo loop-dependent TAPBPR-mediated peptide exchange, strictly due to it not being able to bind hydrophobic residues in its F pocket.

Remarkably, as expected, in contrast to all three MHC class I molecules tested previously, all of which accommodate hydrophobic residues in their F pocket, TAPBPR showed a clearly impaired ability to load the HLA-A*68:01-specific florescent peptide KTGGPIYK*R onto HeLaM-HLA-ABC^{KO} cells transduced with HLA-A*68:01 (**Figure 30b and 30c**). Moreover, I observed no significant differences in the ability of TAPBPR to mediate peptide exchange on HLA-A*68:01 upon mutation of the loop, all loop mutants displaying an equal ability to exchange peptides as TAPBPR^{WT} (**Figure 30b and 30c**). Thus, in contrast to HLA-A*68:02, on which TAPBPR promotes highly efficient peptide exchange in a L30-dependent manner, HLA-A*68:01 is significantly less responsive to the TAPBPR-mediated peptide exchange, which only occurs independently of the loop. Strikingly, the difference in only five amino acids between the two MHC class I molecules, three of which resulting in different F pocket specificities, strongly influences the ability of TAPBPR to use its K22-D35 loop to facilitate efficient peptide exchange on them. Taken together, these findings support the concept that TAPBPR is capable of inserting its L30 residue into the F pocket of MHC class I, in order to promote effective dissociation of the bound peptide in a competitive manner.

4.2.9. Mutation of residue 116 in the MHC class I F pocket alters TAPBPR binding

Following on from the idea that the L30 residue of TAPBPR is capable of binding into the F pocket of MHC class I molecules, I was curious to whether by artificially changing the F pocket specificity of MHC class I molecules, I could alter the binding of TAPBPR to those molecules. Given the extreme differences in F pocket specificities between HLA-A*68:02 and -A*68:01, which seemed to be influenced by differences in only three amino acids, namely the ones on positions 97, 114 and 116 (Niu et al., 2013), I hypothesised that swapping one or more of these residues between the two MHC class I molecules could result in swapping their F pocket specificities as well. Out of these three F pocket residues that differ between A*68:01 and A*68:02 and were previously reported to influence the F pocket specificity of MHC class I (Guo et al., 1992, Madden et al., 1992, Saper et al., 1991, Sidney et al., 2008), residue 116 appeared to be the one having the highest impact on the interaction of the F pocket with the C-terminal anchor residue of the peptide. Namely, HLA-A*68:02 contains a tyrosine on position 116, whereas HLA-A*68:01 contains an aspartic acid (**Figure 32a**). As it can be observed in the crystal structure, D116 of HLA-A*68:01 forms strong dipole interactions with both residue R114 of the peptide binding groove and with residue K9 of the peptide, determining a strong preference of the HLA-A*68:01 F pocket for basic anchor residues. In contrast, residue Y116 of HLA-A*68:02 points away from H114 residue, keeping the hydrophobic patches of the F pocket in an open conformation, allowing it to accommodate hydrophobic peptide residues (**Figure 32a**). I believe that this is the reason why the L30 residue of the TAPBPR loop has access to the F pocket of HLA-A*68:02, but not to the one of HLA-A*68:01.

To investigate whether altering the F pocket interactions with the anchor residue of the peptide impacts the ability of TAPBPR to bind to MHC class I, I swapped residues on position 116 between HLA-A*68:01 and -A*68:02, resulting in the A*68:01^{D116Y} and A*68:02^{Y116D} mutants. I hypothesized that swapping their residues on positions 116 would more likely lead to a disruption in the architecture of the F pocket than swapping their residues on position 114, which are both basic.

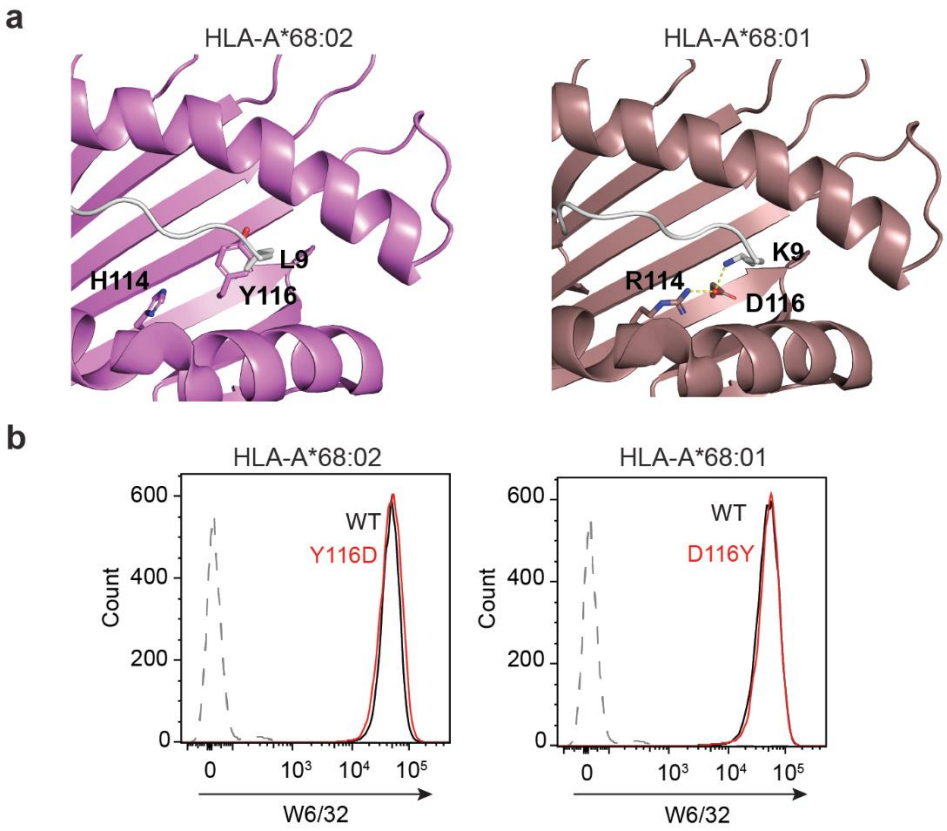

Figure 32: Swapping residue 116 between HLA-A*68:01 and HLA-A*68:02 does not impair their surface expression. (**a**) PyMOL images depicting the binding grooves of HLA-A*68:02 (PDB ID 4HX1) and of HLA-A*68:01 (PDB ID 4HWZ), with residues at position 114 and 116 of MHC class I, as well as the C-terminal residue of the bound peptide, highlighted. (**b**) Histograms showing the expression levels of HLA-A*68:02^{WT}, -A*68:02^{Y116D}, -A*68:01^{WT} and -A*68:01^{D116Y} at the cell surface, detected using W6/32, when transduced into HeLaM-HLA-ABC^{KO} cells. Data is representative of three independent experiments. Taken from Ilca et al. (Ilca et al., 2018a).

The surface expression levels of the chimeric HLA mutants were similar to the ones of their corresponding wild type counterparts, upon transduction into HeLaM-HLA-ABC^{KO} cells, indicating that mutation of residue 116 did not significantly alter the ability of HLA-A*68:01 and -A*68:02 to load and present peptides (**Figure 32b**). When assessing the ability of TAPBPR to bind to these HLA class I mutants present at the cell surface, strikingly, I observed that A*68:02^{Y116D} showed almost no binding to TAPBPR, compared to the high binding observed for A*68:02^{WT} (**Figure 33a and 33b**). Correspondingly, A*68:01^{D116Y} showed a strong enhancement in TAPBPR binding, compared to the extremely low levels of TAPBPR bound to A*68:01^{WT}. I further validated the effect of altering the F pocket on TAPBPR binding on another MHC class I molecules, namely A*02:01 (**Figure 33c**). Similarly to A*68:02, while TAPBPR showed strong binding to A*02:01^{WT}, it displayed a severely impaired ability to associate with A*02:01^{Y116D}. These results demonstrate that the ability of TAPBPR to bind MHC class I molecules is directly influenced by the architecture of the MHC class I F pocket.

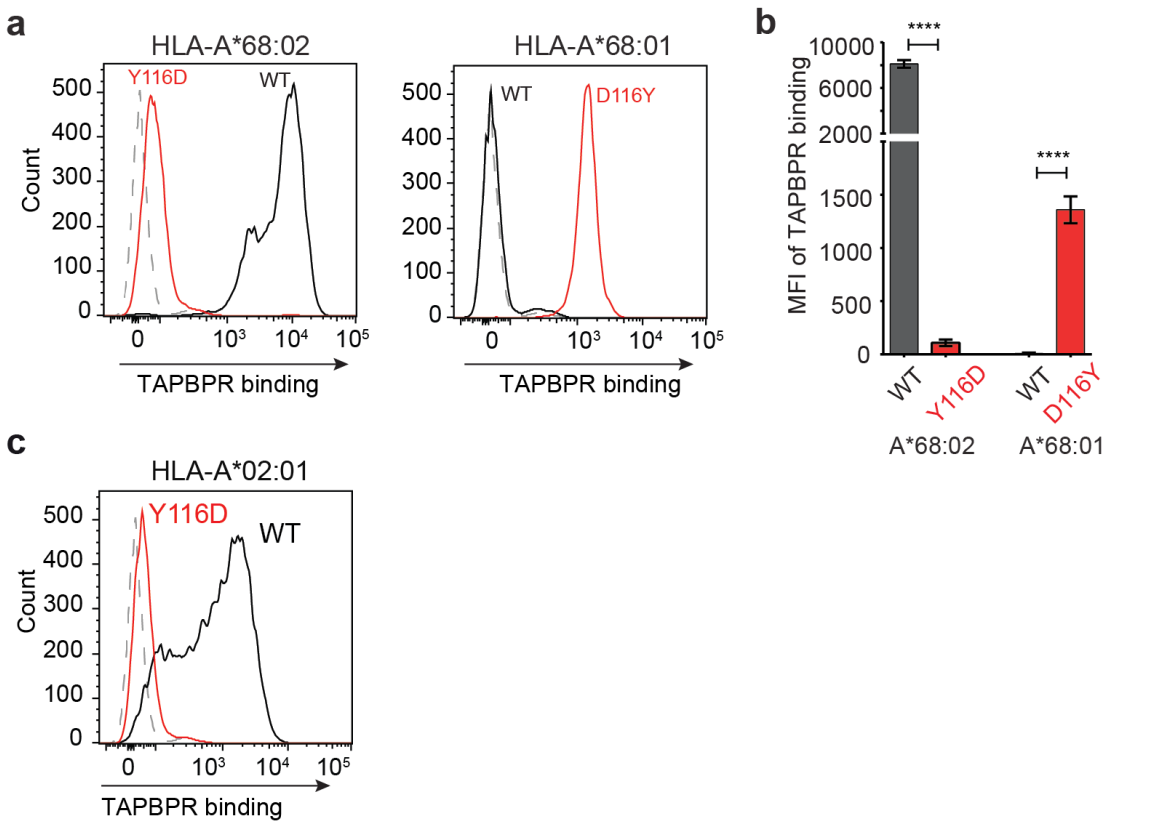

Figure 33: Mutation of the MHC class I F pocket significantly alters TAPBPR binding. HeLaM-HLA-ABC^{KO} cells expressing the panel of HLA-A*68 molecules listed in **Figure 32** were incubated with 1 µM of soluble TAPBPR for 30 min at 37°C, followed by detection of surface bound TAPBPR using PeTe4. (**a** and **c**) Histograms show the level of bound soluble TAPBPR to the surface of **a**) the cell lines expressing each HLA-A68 molecule from **Figure 32** and of **c**) cells expressing either HLA-A*02:01^{WT} or HLA-A*02:01^{Y116D}. Staining with an isotype control antibody was included as a negative control (grey dashed line). (**b**) Bar graphs summarise the MFI of TAPBPR binding depicted in panel **a**), based on three independent experiment ± SD. ****p ≤ 0.0001. Taken from Ilca et al. (Ilca et al., 2018a).

4.2.10. Modifying the F pocket specificity of MHC class I alters TAPBPR-mediated peptide editing

I next tested the ability of TAPBPR to exchange peptides on the chimeric HLA class I mutants. Given that both HLA-A*68:01 and -A*68:02 contain a basic residue on position 114 (**Figure 32a**), I expected that swapping the residues on position 116 between the two molecules may consequently lead to swapping their F pocket specificities for anchor residues. I thus assessed the ability of the chimeric MHC class I mutants to bind both the A*68:02-specific peptide ETVSK*QSNV and the A*68:01-specific peptide KTGGPIYK*R and tested whether the presence of soluble TAPBPR enhanced the loading of either peptide (**Figure 34**). As previously observed, TAPBPR efficiently mediated the loading of ETVSK*QSNV (black line, **Figure 34a and 34b**), but

not of KTGGPIYK*R on A*68:02^{WT} (black line, **Figure 34c and 34d**), while on A*68:01^{WT}, TAPBPR facilitated, to a considerably lower extent, the loading of KTGGPIYK*R (black line, **Figure 34c and 34d**), but did not show any loading of ETVSK*QSNV (black line, **Figure 34a and 34b**). Strikingly however, the corresponding chimeric HLA class I mutants showed complete opposite peptide specificities. Namely, in the presence of TAPBPR, A*68:02^{Y116D} did not promote any binding of ETVSK*QSNV (red line, **Figure 34a and 34b**), however markedly enhanced the loading of KTGGPIYK*R (red line, **Figure 34c and 34d**). Correspondingly, on A*68:01^{D116Y}, TAPBPR was not able to load KTGGPIYK*R (red line, **Figure 34c and 34d**), however led to a strong enhancement in the binding of ETVSK*QSNV (red line, **Figure 34a and 34b**), to comparable levels as observed on A*68:02^{WT}. These results are in keeping with the fact that swapping residues on position 116 between A*68:01 and A*68:02 resulted in switching their peptide specificities, as it can be observed from the peptide binding experiments performed in the absence of TAPBPR (**Figure 34b and 34d**, right panels). Subsequently, altering the F pocket specificities of these MHC class I molecules altered the efficiency of TAPBPR-mediated peptide exchange. Nonetheless, despite the significantly lower levels of TAPBPR bound to both A*68:01^{WT} and A*68:02^{Y116D} compared to their Y116-containing counterparts (**Figure 33a and 33b**), TAPBPR was still capable of mediating peptide exchange on these molecules and, thus, of loading the correct peptide based on the F pocket specificity of MHC class I.

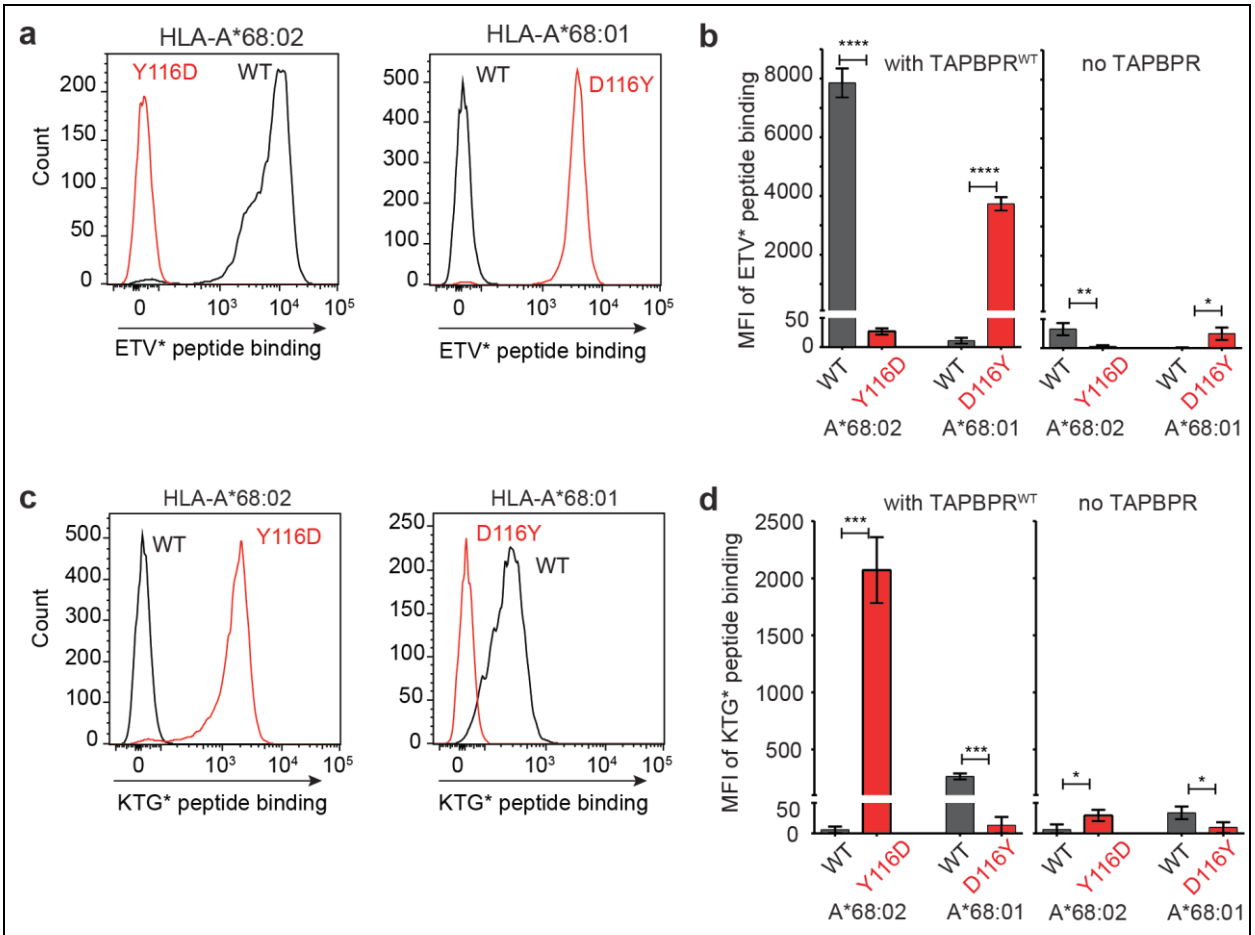

Figure 34: Residue 116 of MHC class I is crucial for the peptide editing ability of TAPBPR. (**a** and **c**) Histograms showing the level of fluorescent peptide binding to IFNγ-treated HeLaM-HLA-ABC^{KO} cells expressing the panel of HLA-A*68 molecules listed in **Figure 32**, upon incubation with 1 µM of soluble TAPBPR for 15 min at 37°C, followed by treatment with either (**a**) 10 nM ETVSK*QSNV (ETV*) or (**c**) 100 nM KTGGPIYK*R (KTG*) peptide for 15 min and 60 min, respectively. (**b** and **d**) Bar graphs summarise the MFI of the fluorescent peptide binding depicted in **a**) and **c**) respectively, in the presence and absence of TAPBPR, based on three independent experiment ± SD. ****p ≤ 0.0001, ***p ≤ 0.001, **p ≤ 0.01, *p ≤ 0.05. Taken from Ilca et al. (Ilca et al., 2018a).

4.3. Discussion

Given the ambiguity concerning the localization of the TAPBPR loop in relationship to the MHC class I binding groove (**Chapter 3, Figure 6**) in recently captured structures and the lack of functional evidence to support any involvement of the loop in peptide exchange on MHC class I molecules (Jiang et al., 2017, Thomas and Tampe, 2017), it was essential to experimentally test this involvement. In this chapter, using the novel cellular assay which I developed for measuring TAPBPR-mediated peptide exchange on MHC class I molecules (see **Chapter 3**), together with immunopeptidomics analysis, I have demonstrated an essential role for the K22-D35 loop of TAPBPR in its peptide editing function. I showed that the loop is required for TAPBPR to efficiently catalyse peptide dissociation from MHC class I molecules and hence promote the binding of an incoming high affinity peptide. Moreover, I have identified residue L30 of the loop to be both necessary and sufficient for the ability of TAPBPR to facilitate peptide exchange on both human and mouse MHC class I molecules that typically accommodate hydrophobic amino acid residues in their F pocket. It is important to mention that our findings prove that mutating the loop only impairs the catalytic function of TAPBPR and does not alter its folding, stability or intrinsic ability to interact with MHC class I molecules.

The findings highlighting the impact of the loop, and particularly of residue L30, on the ability of TAPBPR to mediate peptide editing were similar when either the full-length (**Figure 23**) or the soluble versions of TAPBPR (**Figure 25**) were tested. Moreover, the crucial impact of the loop, and of residue L30 in particular, on the ability of TAPBPR to efficiently promote peptide exchange on MHC class I was further confirmed in cells, by immuno-peptidomics analysis (**Figure 28**). Namely, mutation of the TAPBPR loop led to a significant difference in the pool of peptides presented on MHC class I and, moreover, to a larger pool of peptides presented specifically on HLA-A*68:02. This further supports the role of TAPBPR in peptide selection on MHC class I and that the 22-35 loop of TAPBPR is a catalytic region essential for peptide editing. These findings together, as speculated in the previous chapter, suggests that using the luminal domain of TAPBPR alone to interrogate the peptide editing function of the chaperone on MHC class I molecules represents a reliable assay.

5. Chapter 5: Exploring the allelic susceptibility of HLA class I to peptide editing by TAPBPR

5.1. Background

In **Chapter 4**, I found that TAPBPR functioned more efficiently on some MHC class I molecules (e.g. HLA-A*68:02) compared to others (e.g. HLA-A*68:01) and demonstrated that this was based on specific molecular properties of MHC class I. Given the extreme difference observed in the ability of TAPBPR to function as a peptide editing catalyst on a limited number of different HLA class I molecules, I was interested in exploring the HLA class I allele-preference of TAPBPR. To test this, I sought to assess the ability of TAPBPR to bind a wide range of HLA class I allotypes and to subsequently test its ability to edit peptides on a selected panel of HLA class I allotypes. Finally, I planned to explore the molecular basis behind any preference observed. Extensive exploration of this would allow us to better understand how tightly peptide editing is controlled across different HLA class I molecules and whether the observed differences could have any impact in the pathogenesis of HLA-associated diseases.

5.2. Results

5.2.1. TAPBPR shows binding preference for HLA-A over -B and -C molecules

Thus far, I have only assessed the ability of TAPBPR to bind and exchange peptides on a few HLA class I molecules, namely HLA-A*02:01, -A*68:01 and -A*68:02 (**Figure 30**). I have shown that the catalytic activity of TAPBPR is reflected by the ability of TAPBPR to associate with MHC class I. Thus, to perform the first comprehensive study on the allele-based preference of TAPBPR for HLA class I, I compared the ability of TAPBPR to bind to 97 different HLA class I allotypes, using Labscreen® single antigen HLA class I beads (SABs) (Pei et al., 2003). The same set of beads has been previously used for interrogating HLA class I interactions with various immune receptors, such as leukocyte Ig-like receptors (LILRs) (Jones et al., 2011) or for characterising allotype specificity of anti-HLA antibodies used to assess HLA class I expression levels in primary trophoblast cells (Apps et al., 2009). In addition, similar sets of SABs have

extensively been used clinically, in assessing the pre-transplant risks of host-versus-graft rejection by measuring the levels of anti-HLA antibodies from patients' sera (Wittenbrink et al., 2018). The HLA class I molecules coupled to these beads were produced and purified from a mammalian expression system (Pei et al., 2003) and should therefore be representative of the pool of MHC class I molecules found in cells, loaded with a broad range of peptides. In my experimental set up, in order to quantify the level of TAPBPR binding to individual HLA class I allotypes comprised in the SAB library, the SABs were treated with 1 µM soluble TAPBPR, followed by staining with the TAPBPR specific mAb PeTe4. The level of bound TAPBPR to each of the bead sets was determined by flow cytometry (**Figure 35a**).

The screen revealed a strong preference of TAPBPR for HLA-A over -B and -C molecules. Out of the 97 different HLA molecules screened, the 11 strongest TAPBPR binders were all members of the HLA-A group (**Figure 35b**). Moreover, the strongest HLA-B and -C binders, namely B*73:01 and C*01:02 respectively (**Figure 35b and 36**), showed >10-fold lower level of bound TAPBPR compared to the strongest HLA-A binder, namely A*68:02 (**Figure 35b**). Overall, 14 out of 31 HLA-A molecules showed at least intermediate levels (>500 MFI) of TAPBPR binding (**Figure 37**), while only 4 out of the 50 HLA-B and 1 out of the 16 HLA-C molecules tested presented intermediate abilities to bind TAPBPR (**Figure 36**). The staining of the beads with W6/32, a pan-HLA class I antibody that recognizes peptide-loaded conformations of HLA-A, -B and -C molecules, revealed similar levels of peptide-loaded MHC class I molecules across the entire SAB library (**Table 7**). This suggests that the TAPBPR binding hierarchy obtained was indeed due to the intrinsic ability of TAPBPR to interact with the HLA class I molecules and not due to different MHC class I availability. To ensure that the observed binding of $TAPBPR^{WT}$ occurred strictly in an MHC class I-dependent manner, the binding of the recombinant $TAPBPR^{TN5}$, which is unable to associate with MHC class I, was tested to the beads. No significant binding of $TAPBPR^{TN5}$ was observed to any of the HLA class I allotypes coupled to beads (**Figure 35c**), confirming that TAPBPR does not associate non-specifically to the beads.

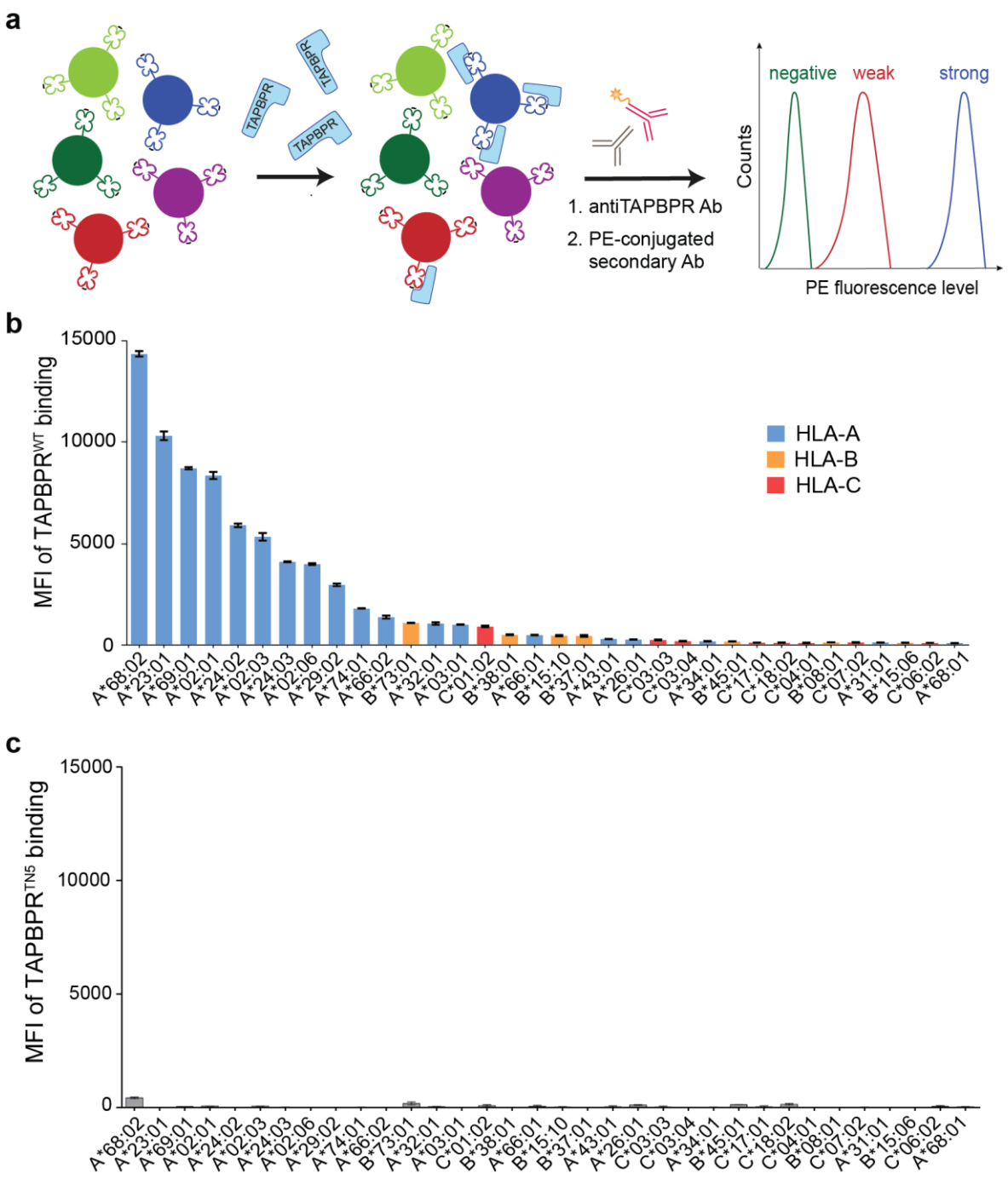

Figure 35: HLA-A molecules exhibit stronger interactions to TAPBPR compared to HLA-B and -C molecules. (**a**) Schematic depiction of the LABScreen® single antigen HLA bead (SAB) assay used to determine soluble TAPBPR binding to individual HLA class I alloytpes. The SABs were incubated with 1 µM TAPBPR for 1 h, at 22°C with rotation and then stained for TAPBPR using the PeTe4 antibody. (**b**) Bar graphs showing the levels of $TAPBPR^{WT}$ binding to the top 34 binders from the library of 97 different bead-coupled HLA class I allotypes, with HLA-A molecules in blue bars, HLA-B molecules in orange bars and HLA-C molecules in red bars. The comprehensive data for all HLA-A, -B and -C molecules can be found in **Figure 37** and **Figure 36**, respectively. (**c**) Bar graphs showing the binding levels of the soluble $TAPBPR^{TN5}$, which is unable to bind MHC class I, to the same HLA class I allotypes shown in panel **b**), when 1 µM soluble $TAPBPR^{TN5}$ was added to cells for 1 h at 22°C. Error bars show mean fluorescence intensity (MFI) -/+ SD from triplicates within one experiment. This experiment is a representative example of three independent experiments.

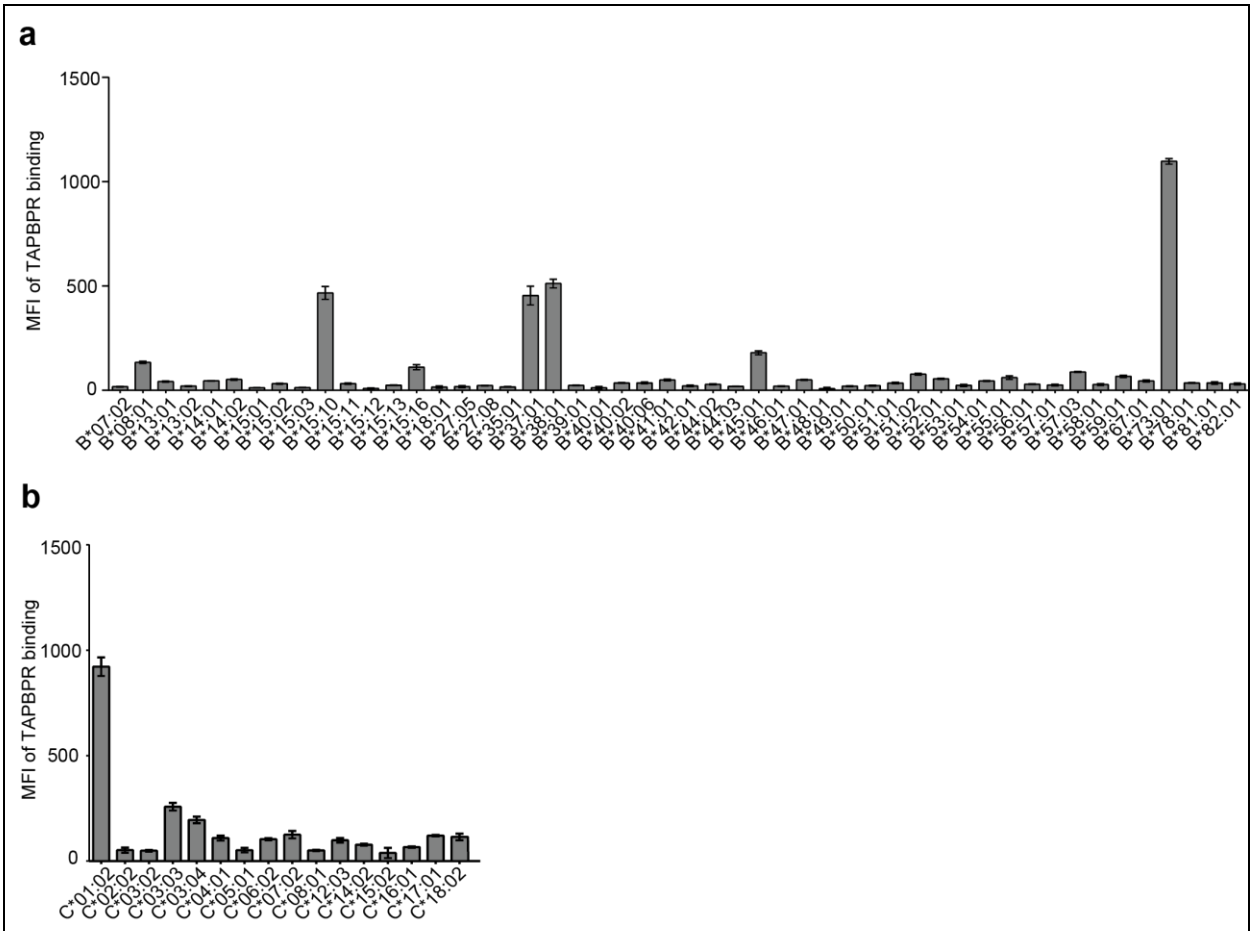

Figure 36: TAPBPR binding to HLA-B and -C molecules on the single HLA beads. Bar graphs showing soluble TAPBPR^{WT} binding to the (**a**) HLA-B and the (**b**) HLA-C molecules of the SAB library, upon treatment with 1 µM TAPBPR$^{WT.}$ at 22°C with rotation. The data including error bars was generated based on triplicates within one experiment. This is a representative example of three independent experiments. Results from equivalent experiments for HLA-A molecules can be found in **Figure 37**.

Table 7: MHC class I levels on single antigen HLA beads detected using W6/32

HLA allele	Bead #	MHC class I levels [MFI]
A*01:01	3	18527
A*02:01	4	19739
A*02:03	5	18974
A*02:06	6	18702
A*03:01	7	19116
A*11:01	8	18910
A*11:02	9	19415
A*23:01	10	19552
A*24:02	11	19068
A*24:03	12	17692
A*25:01	13	19499
A*26:01	14	18366
A*29:01	15	19014
A*29:02	17	18142
A*30:01	18	17818
A*30:02	19	17921
A*31:01	20	18716
A*32:01	21	19548
A*33:01	22	18132
A*33:03	100	18062
A*34:01	23	19320
A*34:02	24	19845
A*36:01	25	17031
A*43:01	26	18328
A*66:01	27	18555
A*66:02	28	19088
A*68:01	29	19016
A*68:02	30	17506
A*69:01	31	18749
A*74:01	32	19216
A*80:01	33	18535
B*07:02	34	20419
B*08:01	35	20346
B*13:01	97	18064
B*13:02	36	19727
B*14:01	37	19502
B*14:02	38	17233
B*15:01	40	19608
B*15:02	41	19350
B*15:03	42	19668
B*15:10	43	20197
B*15:11	98	17639
B*15:12	44	19294
B*15:13	45	19296
B*15:16	46	18461
B*18:01	47	19915
B*27:05	16	19969
B*27:08	48	19129
B*35:01	49	19066
B*37:01	50	18551
B*38:01	51	18845
B*39:01	52	20136
B*40:01	53	19119
B*40:02	54	19336
B*40:06	99	18638
B*41:01	55	20023
B*42:01	56	20116
B*44:02	57	17659
B*44:03	58	18984
B*45:01	59	19214
B*46:01	63	19173
B*47:01	61	17077
B*48:01	62	19200
B*49:01	60	19506
B*50:01	64	19141
B*51:01	65	19516
B*51:02	66	18795
B*52:01	67	17497
B*53:01	68	18690
B*54:01	69	19465
B*55:01	70	19803
B*56:01	71	19119
B*57:01	72	18956
B*57:03	73	19594
B*58:01	74	18524
B*59:01	75	18090
B*67:01	76	19989
B*73:01	77	19542
B*78:01	78	17716
B*81:01	79	18679
B*82:01	80	17708
C*01:02	81	18988
C*02:02	82	16840
C*03:02	83	18982
C*03:03	84	19000
C*03:04	85	18943
C*04:01	86	12491
C*05:01	87	19122
C*06:02	88	16573
C*07:02	89	18133
C*08:01	90	19692
C*12:03	91	20447
C*14:02	92	17786
C*15:02	93	21276
C*16:01	94	14783
C*17:01	95	14369
C*18:02	96	18683

* The SABs were stained with the W6/32 mAb and the amount of antibody bound to each bead set was quantified by flow cytometry and expressed in mean fluorescence intensity (MFI) units

5.2.2. The strongest TAPBPR binders are members of the HLA-A2 and A24 superfamilies

Despite numerous members of the HLA-A group showing considerably stronger ability to bind TAPBPR compared to most -B and -C allotypes, there were numerous HLA-A molecules that showed very week binding to TAPBPR, such as A*01:01, A*11:01, A*26:01, A*33:01, A*36:01, A*68:01, etc (**Figure 35b**). Interestingly, all weak binders are exclusively members of the A1 and A3 superfamilies, whereas the top eight strongest TAPBPR binders, namely A*68:02, A*23:01, A*69:01, A*02:01, A*24:02, A*02:03, A*24:03 and A*02:06, are all members of the HLA-A2 and -A24 superfamilies (**Figure 37**), according to previous classifications (Sidney et al., 2008). HLA class I molecules were classified into supertypes based on overlapping peptide repertoires, chemical specificity of both B and F pockets and on the amino acid sequence similarity around across the regions making up the two pockets.

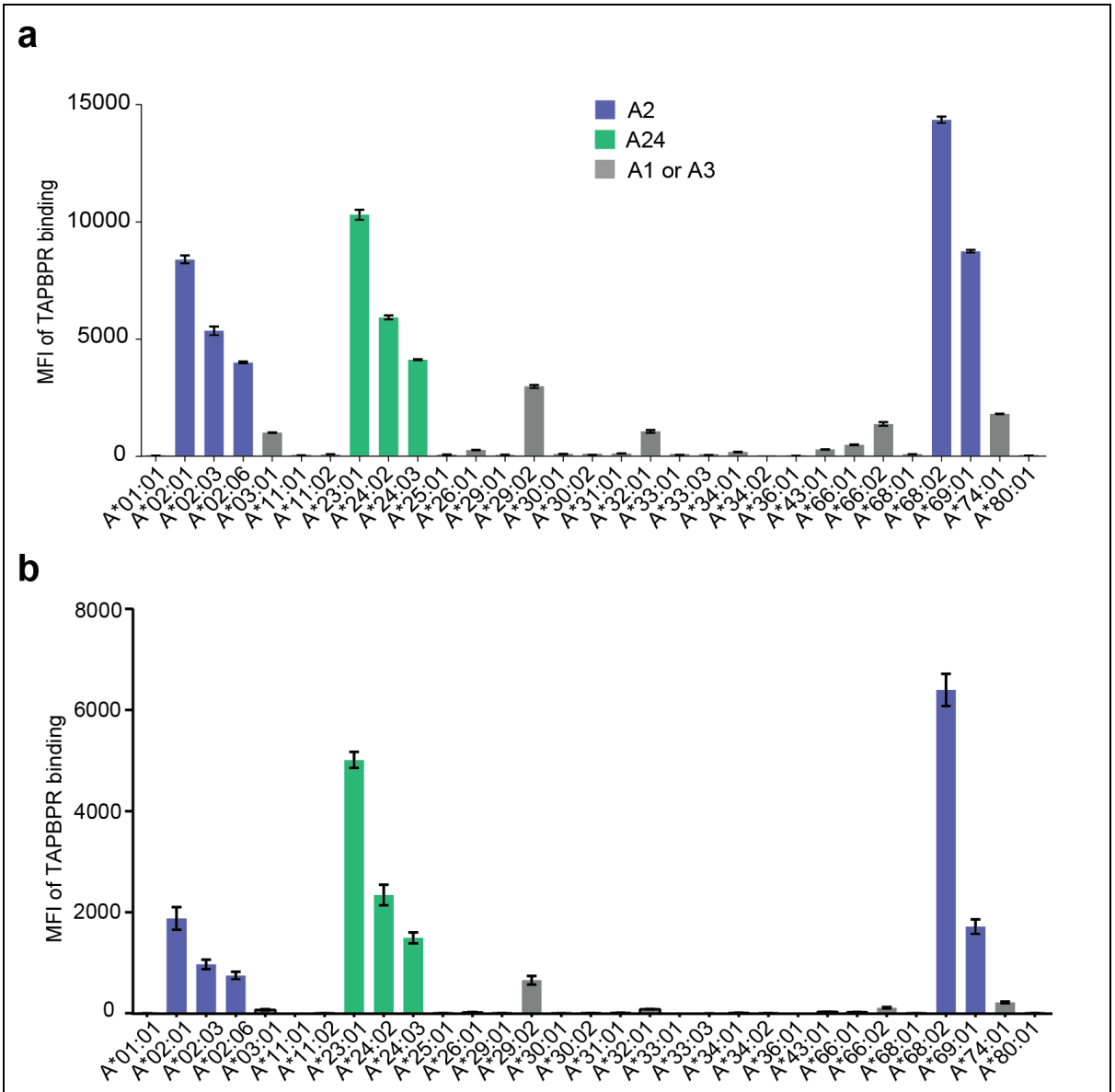

Figure 37: Among HLA-A molecules, TAPBPR shows clear binding preference for members of the A2 and A24 superfamilies. (**a** and **b**) Bar charts showing the level of TAPBPR binding to all HLA-A molecules from the SAB library, grouped based on numerical order, with members of the HLA-A2 (blue) and -A24 (green) superfamilies highlighted. The same TAPBPR binding hierarchy to HLA-A molecules was observed when either (**a**) 1 µM or (**b**) 100 nM soluble TAPBPR was added to the beads for 1 h at 22°C. Error bars show mean fluorescence intensity (MFI) -/+ SD from triplicates within one experiment. This experiment is a representative example of three independent experiments.

5.2.3. TAPBPR shows the same HLA binding hierarchy in a cellular system

Although the HLA class I molecules used for generating the SAB library were expressed and purified from a mammalian system (Pei et al., 2003), thus likely resembling the conformations of HLA class I molecules present on the cell surface, there was still limited information regarding the overall composition of the beads. Therefore, it was important to verify the

findings obtained from the LABscreen® HLA class I SABs using alternative systems. One such alternative involved using our novel cellular assay to determine the binding of TAPBPR to cell surface MHC class I molecules (see **Chapter 3**).

To this end, I reconstituted the MHC class I-deficient HeLaM-HLA-ABC^{KO} cells (Neerincx and Boyle, 2018) with a panel of 27 individual HLA class I molecules (**Figure 38**). This selection contained members representative of all HLA class I superfamilies described up to date and spanned the entire TAPBPR binding hierarchy obtained using the SAB library. Staining with W6/32 revealed similar surface expression levels for all 27 different HLA class I allotypes, upon stable over-expression in the HeLaM-HLA-ABC^{KO} cells, except for HLA-C*02:02, which was expressed at lower levels (**Figure 38**). Additionally, each HLA class I-expressing cell line showed a highly homogenous population in terms of the relative levels of MHC class I present at the cell surface (**Figure 38a**).

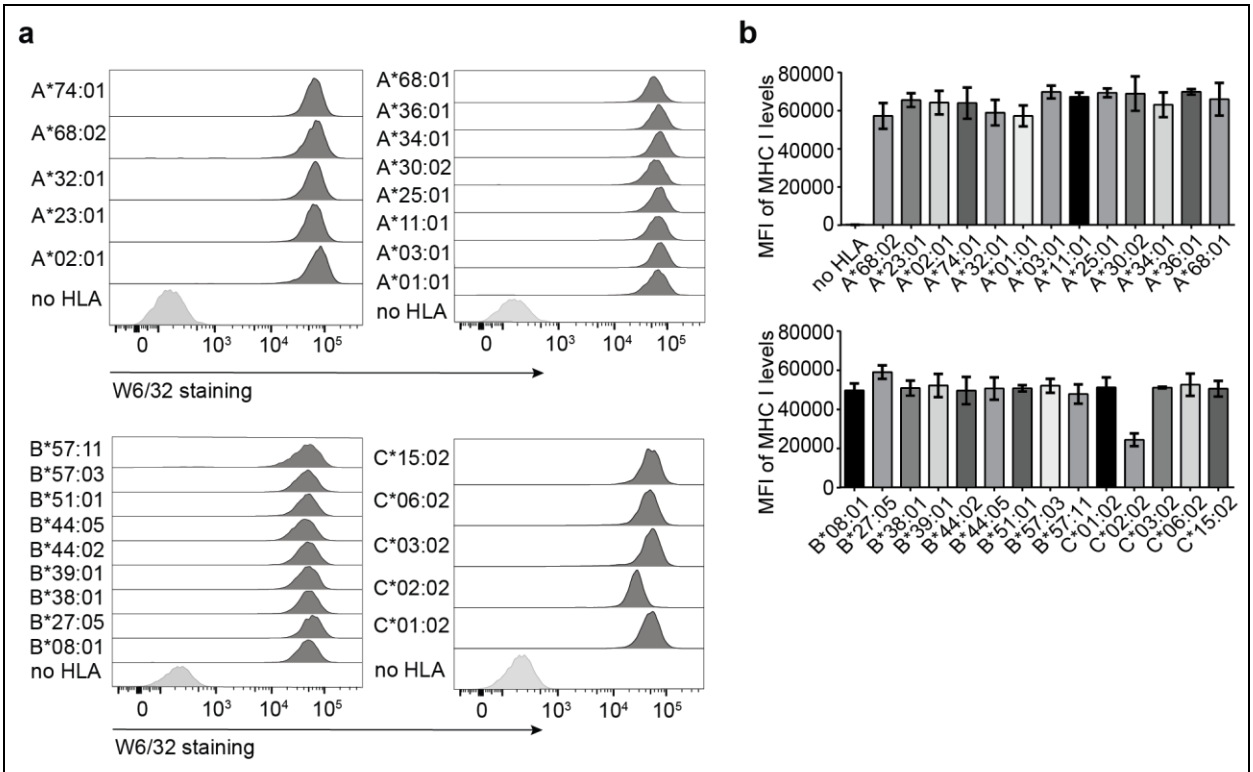

Figure 38: Different HLA class I allotypes show stable and similar surface expression levels.
(**a**) Histograms measuring MHC class I levels at the cell surface, measured by staining with W6/32 antibody, upon transduction of a wide panel of HLA class I allotypes in HeLaM-HLA-ABC^{KO} cells. (**b**) Bar graphs summarising the MFI values in panel **a**) based on three independent experiments. Error bars show mean fluorescence intensity (MFI) -/+ SD.

Upon testing the binding of soluble TAPBPR to the surface of each HLA-expressing cell line, I observed a highly similar TAPBPR binding hierarchy (**Figure 39**) as the one obtained using the SABs (**Figures 35, 36 and 37**). More specifically, all members of the HLA-A2 and -A24

superfamilies present in my panel, namely A*68:02, A*23:01 and A*02:01 showed the highest level of TAPBPR bound when present at the cell surface, while all members of the HLA-A3 and -A1 superfamilies showed either weak or no TAPBPR binding (**Figure 39a and 39b**). Among HLA-B molecules, B*38:01 was the only one which stably associated with TAPBPR, while none of the HLA-C molecules seemed to bind TAPBPR. As expected, I observed a lack of TAPBPR binding to HeLaM-HLA-ABC^{KO} cells (**Figure 39a**), as previously shown (**Figure 18b**). My cellular-based assays thus confirmed the clear binding preference of TAPBPR for members of the HLA-A2 and -A24 superfamilies over other HLA class I subgroups. Taken together, my results exploring HLA class I dependency on TAPBPR in a cellular system, where HLA class I molecules are loaded with a variety of peptides and present the naturally-occurring post-translational modifications, correlate well with my findings obtained using the SABs.

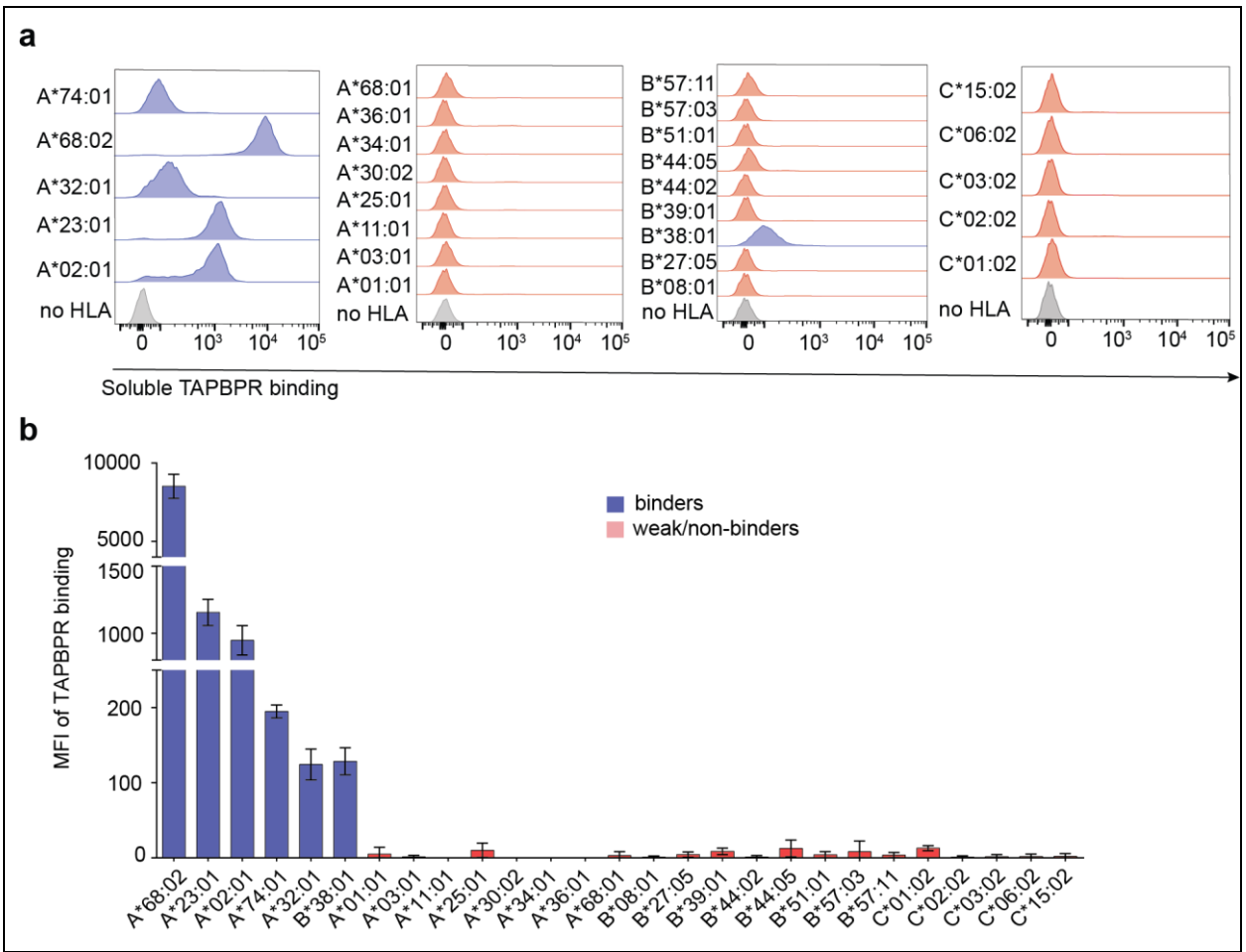

Figure 39: HLA class I allotypes show a similar TAPBPR binding hierarchy in a cellular system as the one observed with the SABs. (**a**) Histograms show levels of soluble TAPBPR binding to each individual HLA class I allotypes from the panel in **Figure 38**, present at the cell surface, upon treating the cells with 1 µM soluble TAPBPR for 30 min at 37°C; blue histograms indicate significant TAPBPR binding, red histograms indicate non-significant TAPBPR binding and grey histograms indicate TAPBPR binding to HeLaM-HLA-ABC^{KO} cells. (**b**) Bar graphs summarising the levels of TAPBPR binding to surface-expressed HLA class I molecules shown in panel **b**). Error bars show mean fluorescence intensity (MFI) -/+ SD from three independent experiments.

5.2.4. TAPBPR shows enhanced binding ability to intracellular species of HLA class I molecules

Up to this point, I have only tested the ability of TAPBPR to interact with various HLA class I molecules when present at the cell surface or when coupled to beads, in peptide loaded conformations. However, TAPBPR naturally resides intracellularly and would thus have access to a wider variety of HLA class I conformations present at different stages of the antigen presentation pathway (Boyle et al., 2013). I therefore wanted to verify the ability of TAPBPR to bind to different HLA class I molecules from the whole cell lysates and compare this relative binding to the one observed at the cell surface. To this end, I performed a fishing experiment using recombinant soluble TAPBPR as bait to pull down MHC class I molecules from the whole cell lysates of the panel of HeLaM-HLA-ABC^{KO} cell lines expressing each of the selected 27 HLA class I allotypes (**Figure 40**). When assessing the relative expression levels of the 27 different HLA class I allotypes, I observed that several of them, namely HLA-A*01:01, -A*23:01, -A*32:01, -B*57:03 and -B*57:11, were not detected by any of our HLA heavy chain-specific antibodies, such as HCA2 or HC10 (**Figure 40a and 40b**). I therefore used the level of β_2m pulled down on TAPBPR as a surrogate read-out for TAPBPR-MHC class I interaction. As expected, I did not observe any β_2m pulled down on TAPBPR in HeLaM-HLA-ABC^{KO} cells, indicating the lack of unspecific β_2m association to TAPBPR in the absence of classical MHC class I heavy chains. Using the pull-down system, I observed a similar trend in the relative ability of the HLA class I allotypes from the panel of 27 to bind TAPBPR, with A*68:02, A*23:01 and A*02:01 showing, by far, the highest level of TAPBPR binding (**Figure 40a**). However, when assessing the interaction of TAPBPR with the total cellular pool of MHC class I, I now observed significant interactions with TAPBPR for several HLA class I molecules of the A1 and A3 superfamilies (such as A*03:01, A*25:01, A*34:01, A*68:01) (**Figure 40a**), that did not appear to bind TAPBPR when present strictly at the cell surface (**Figure 39**). Nonetheless, these HLA class I molecules appeared to bind to TAPBPR very weakly compared to the A*68:02 and A*23:01. In fact, due to the extremely high levels of A*68:02 and A*23:01 pulled down on TAPBPR, the samples containing these allotypes needed to be diluted 10-fold to allow detection of the weak TAPBPR binders. Among the HLA-C molecules tested, HLA-C*01:02 appeared to be the only one able to bind TAPBPR, while B*08:01, B*38:01 and B*44:05 were the only HLA-B molecules found bound to TAPBPR (**Figure 40b**).

I believe that the reason for observing interactions between TAPBPR and a wider panel of HLA class I molecules when taken from the whole cell lysate is the difference in conformations between cell surface and intracellular MHC class I molecules. In contrast to the surface pool of MHC class I, comprising molecules that have undergone peptide selection and are thus loaded with high-affinity peptides, intracellularly, MHC class I molecules occur under various conformations, including peptide-receptive forms. The lack of peptides should make these intracellular HLA class I conformations more accessible by TAPBPR, given that, according to my work here and to previous studies, binding of TAPBPR and peptide to MHC class I molecules occurs in a mutually exclusive manner (Hermann et al., 2015b, McShan et al., 2018, Morozov et al., 2016). In other words, TAPBPR can form a stable interaction with a peptide-bound MHC class I molecules once it manages to dissociate the bound peptide. Thus, the ability of TAPBPR to associate with MHC class I is inversely proportional to the affinity of the loaded peptide.

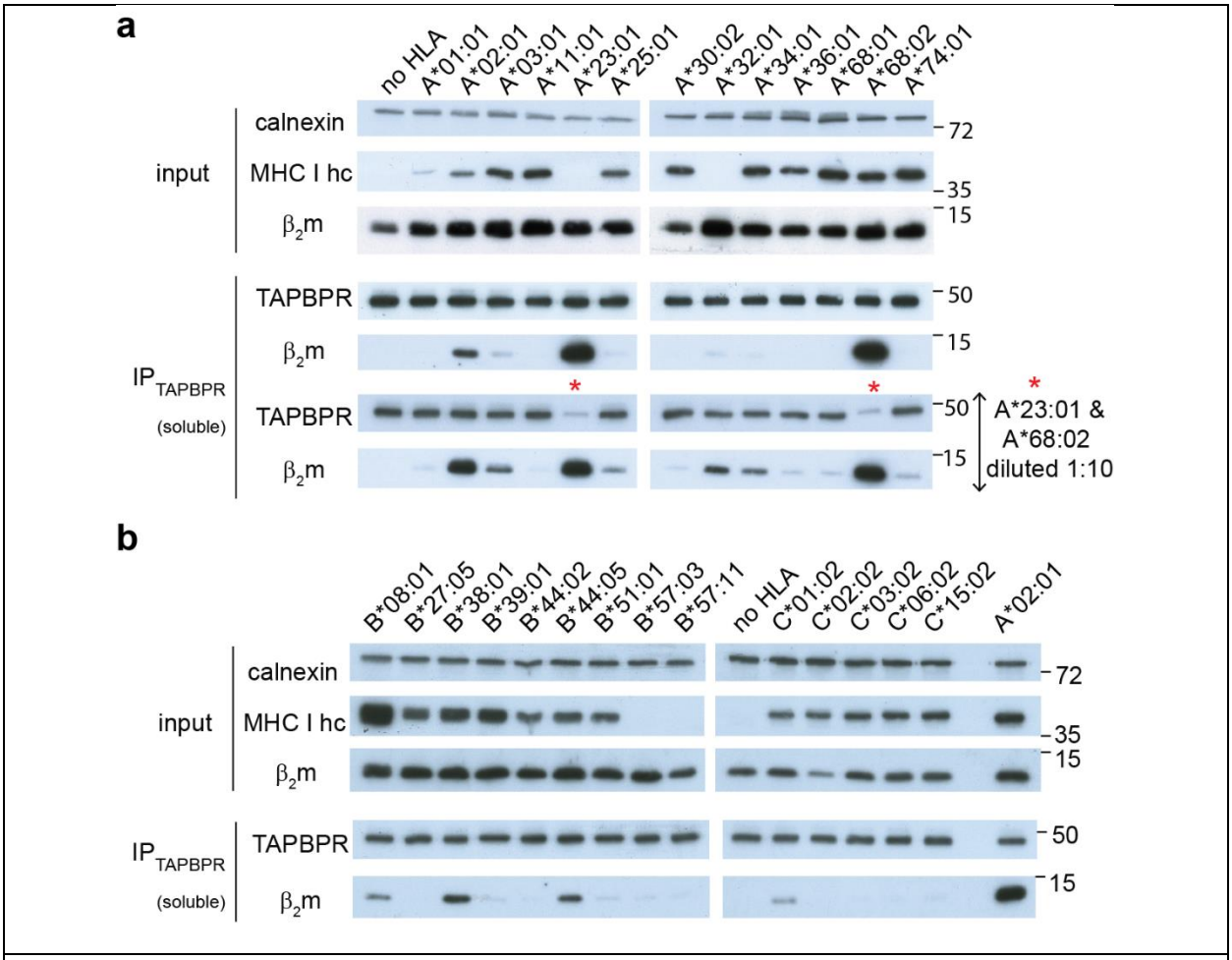

Figure 40: Intracellular species of HLA class I molecules reveal broader reactivity to TAPBPR, while confirming the TAPBPR binding hierarchy. Western blot analysis on recombinant soluble TAPBPR immunoprecipitates from the lysates of each HLA class I-reconstituted HeLaM-HLA-ABC^{KO} cell line, divided into (**a**) HLA-A and (**b**) HLA-B and -C molecules. The detergent used to lyse the cells was triton X-100. The membranes were probed for MHC class I heavy chain (using the HC10 and HCA2 antibodies), TAPBPR, β_2m and calnexin, as indicated. Data is representative of three independent experiments.

Next, it was important to verify that this observed binding of TAPBPR to HLA class I molecules was not an artefact of using soluble TAPBPR. To this end, I performed a similar immuno-precipitation experiment in which endogenous, full length TAPBPR was pulled down from the whole cell lysates of several cells expressing individual HLA class I molecules (**Figure 41**). The results were highly similar to the ones obtained using soluble TAPBPR (**Figure 40**), namely TAPBPR showed the highest binding level to A*68:02 among the different HLA class I molecules tested, while A*68:01 was one of the weakest TAPBPR binders (**Figure 41**). Again, consistent with the systems used so far, B*38:01 showed a considerably higher ability to bind TAPBPR compared to all other HLA-B molecules tested. Interestingly however, when pulled down on endogenous TAPBPR, there was no obvious difference between the levels of HLA-B*44:05 and -B*44:02 bound to TAPBPR. This observed discrepancy was presumably due to the low availability of endogenous TAPBPR in cells, resulting in the interaction between TAPBPR and HLA-B*44:05 being below the detection limit.

Together, these findings suggest that HLA class I molecules exhibit a wide range of affinities for TAPBPR and that subtle polymorphisms naturally-occurring in HLA class I severely influence their ability to interact with TAPBPR.

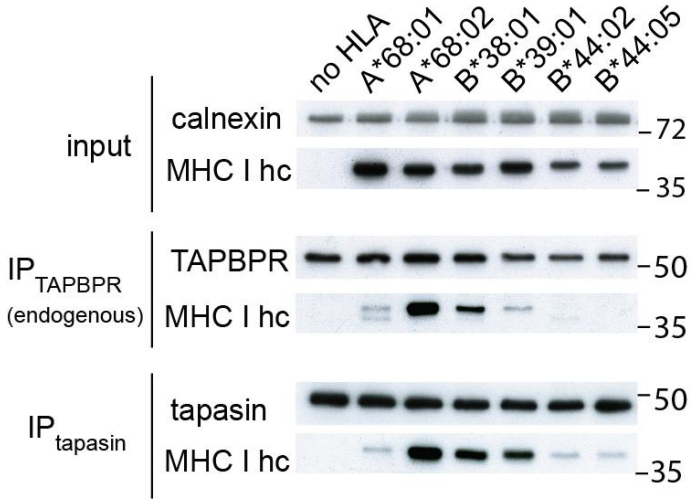

Figure 41: HLA class I molecules show a similar tapasin binding hierarchy as the one observed for TAPBPR. Western blot analysis on endogenous TAPBPR and tapasin pull-downs from HeLaM-HLA-ABC^{KO} cells reconstituted with the listed HLA class I allotypes. The detergent used to lyse the cells was digitonin. The membranes were probed for MHC class I heavy chain (using the HC10 antibody), TAPBPR, tapasin, β_2m and calnexin, as indicated. Data is representative of three independent experiments.

5.2.5. HLA class I molecules that bind strongly to TAPBPR are also strong tapasin binders

It is still poorly understood whether the two peptide editors on the MHC class I pathway, tapasin and TAPBPR, work in synergy to shape the peptide repertoire presented on MHC class I, or whether they perform similar functions while working independently from each other. To provide insight into this, I explored whether there was any correlation between the ability of HLA class I molecules to bind TAPBPR and their ability to bind tapasin. Immunoprecipiation of tapasin from the same panel of HeLaM-HLA cell lines used for TAPBPR pull-down showed that the HLA class I molecules which were strong TAPBPR binders, appeared to interact more strongly with tapasin as well (**Figure 41**). For instance, HLA-A*68:02 was also the strongest binder to tapasin, among the small panel of HLA class I molecules tested, while HLA-A*68:01 was one of the weakest binders. Both B*44:02 and B*44:05 appeared to interact weakly with tapasin, similarly as observed for TAPBPR. Interestingly, the similar binding levels observed for these two HLA-B44 molecules to tapasin correlates well with the findings observed by Park and colleagues (Park et al., 2003), however contrasts with the considerable difference in their relative dependencies on tapasin (Williams et al., 2002, Howarth et al., 2004, Rizvi et al., 2014). In contrast to the data obtained for TAPBPR, there did not seem to be a significant difference in tapasin binding between HLA-B*38:01 and -B*39:01 (**Figure 41**). Nonetheless, the strong interaction of HLA-A*68:02 with both TAPBPR and tapasin and the very weak interaction of HLA-A*68:01 with the two chaperones, relative to the other HLA class I molecules tested, support our recycling model of MHC class I from TAPBPR back to tapasin, potentially via reglucosylation by UGT1 (Neerincx and Boyle, 2017, Hermann et al., 2015b, Neerincx et al., 2017).

5.2.6. Peptide exchange catalysed by TAPBPR is proportional to its ability to associate with HLA class I

My work on a limited number of HLA class I molecules suggests that the ability of TAPBPR to stably associate to HLA class I, when present at the cell surface, determines the efficiency of its peptide exchange function (**Chapter 4**). Thus, I was interested in assessing whether the observed binding preference exhibited by TAPBPR across the HLA class I panel tested (**Figure 39**) reflects its relative ability to function as a peptide edi ting catalyst on them. To this end, I

tested the ability of TAPBPR to mediate peptide exchange on a broad panel of HLA class I molecules, present at the cell surface, using the novel cell-based peptide exchange assays which I developed (**Figure 42**). The HLA class I molecules selected for this experiment included 7 HLA-A, 2 HLA-B and 2 HLA-C allotypes, comprising strong TAPBPR binders (HLA-A*68:02, -A*23:01, -A*02:01), intermediate/weak TAPBPR binders (HLA-A*32:01, -B*38:01, -A*03:01, -A*11:01, -C*01:02) and non-binders (HLA-B*27:05, -C*02:02). I designed fluorescently-labelled peptide specific for each HLA class I allotype and measured their binding to the surface of HeLaM-HLA-ABC^{KO} cells reconstituted with the corresponding HLA class I allotype by flow cytometry, in the presence or absence of recombinant TAPBPR.

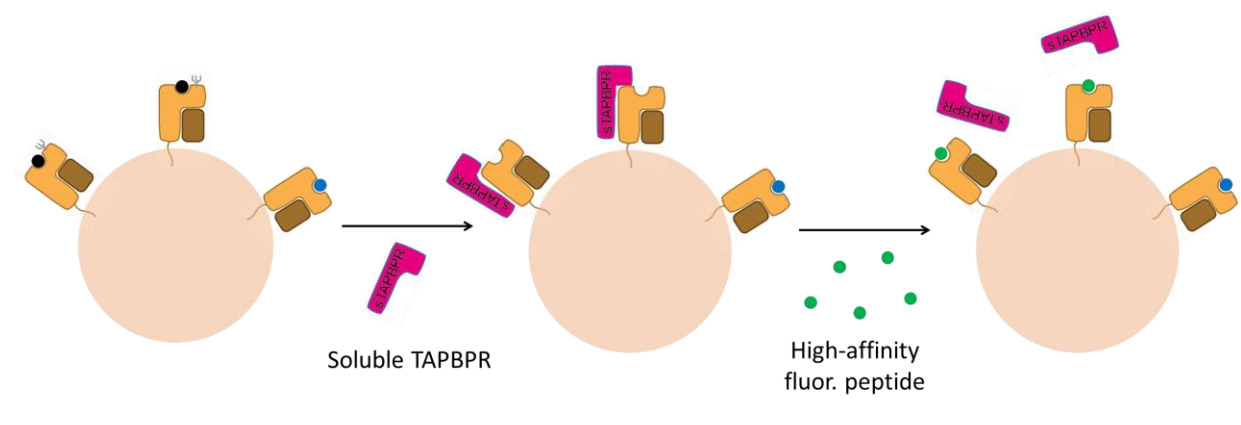

Figure 42: Schematic representation of the peptide exchange assay used to determine TAPBPR-mediated peptide exchange across a panel of HLA class I allotypes.

Due to the low peptide concentration used (10 - 100 nM), very low levels of peptide binding were observed in the absence of TAPBPR, across all HLA class I allomorphs tested (black lines, **Figure 43a** and black bars, **Figure 43b**). The presence of TAPBPR however resulted in a massive enhancement in the peptide binding to HLA class I allotypes classified as strong binders, namely A*68:02, A*02:01 and A*23:01 (blue line, **Figure 43a** and blue bar, **Figure 43b**). The intermediate/weak TAPBPR binders, namely B*38:01, A*03:01, A*11:01 and C*01:02 still showed a significant increase in peptide binding in the presence of TAPBPR, however this observed enhancement was considerably lower compared to the one observed for the strong binders (**Figure 43a and 43b**). As expected, peptide binding to the non-binders, namely B*27:05 and C*01:02, was not affected by TAPBPR (**Figure 43**). None of the peptides tested showed any binding to HeLaM-HLA-ABC^{KO} cells (**Figure 44**), confirming that the observed peptide binding to cells expressing HLA class I occurred exclusively in an MHC class I-dependent manner.

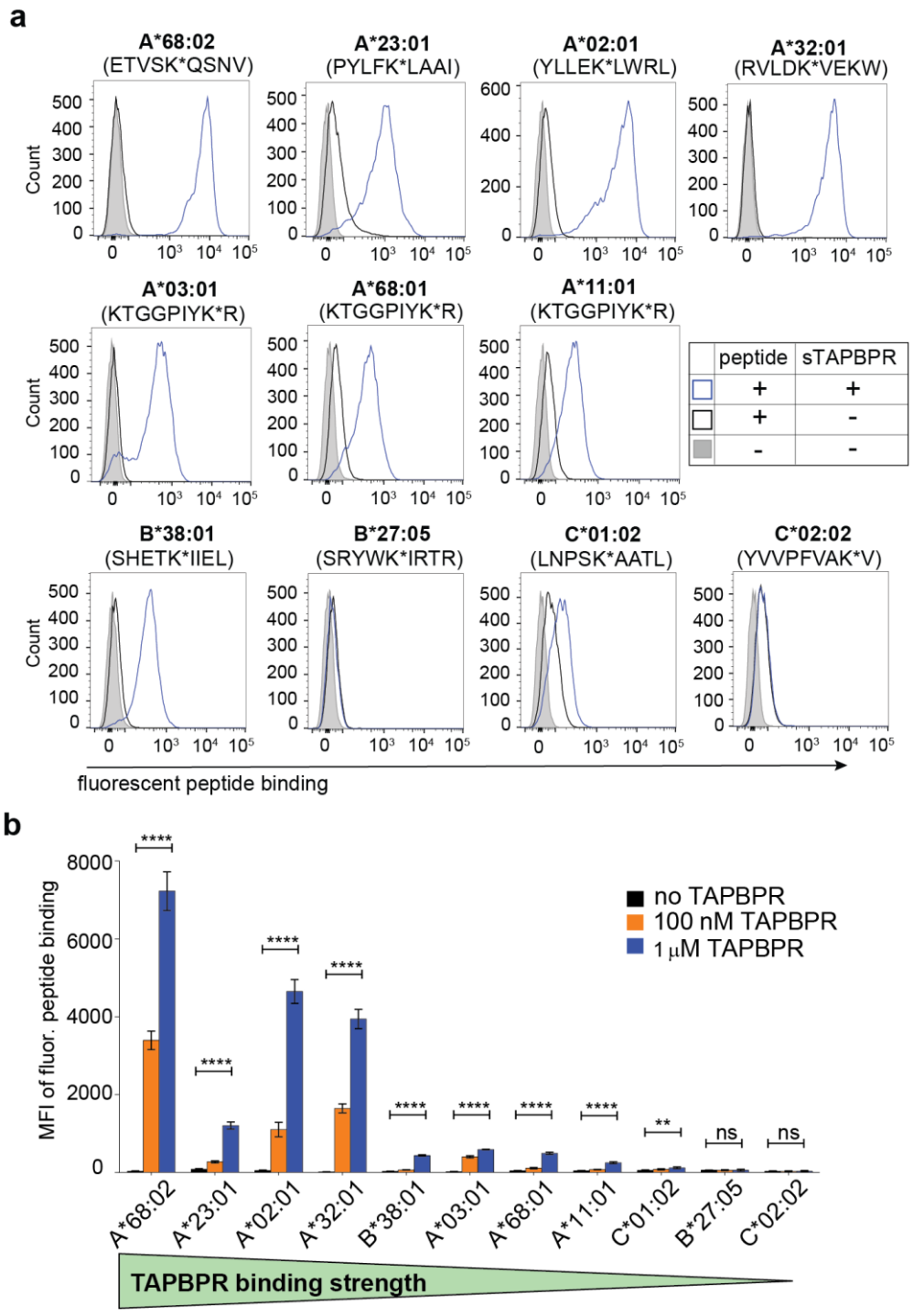

Figure 43: Peptide exchange exerted by TAPBPR is proportional to its ability to bind HLA class I. IFNγ-stimulated HeLaM-HLA-ABC^{KO} cells expressing individual HLA class I allotypes were incubated with 1 μM TAPBPR for 15 min at 37°C and subsequently with a fluorescently-labelled peptide specific for each corresponding HLA class I allotype (peptide sequence shown in brackets), added over an allotype-dependent time and peptide concentration (details described in **materials and methods**). (**a**) Histograms showing the level of fluorescent peptide bound to individual HLA class I-expressing cells, either untreated (filled grey line), treated with peptide alone (black line) or with peptide and TAPBPR (blue line). (**b**) Bar graphs summarising the levels of fluorescent peptide binding in the presence of either no TAPBPR (black bars), 100 nM TAPBPR (orange bars) or 1 μM TAPBPR (blue bars). Error bars show mean fluorescence intensity (MFI) -/+ SD from three independent experiments. n/s not significant, **P≤0.01, ****P≤0.0001, using unpaired two-tailed t-test. The samples in panel **b**) were ordered hierarchically, based on their relative ability to associate with TAPBPR, from strongest to weakest.

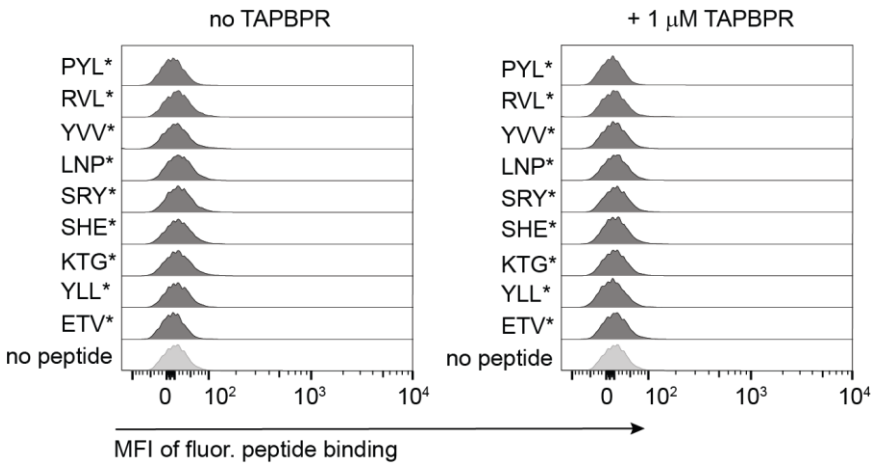

Figure 44: Fluorescent peptides do not bind non-specifically to the surface of cells. (**a**) Histograms showing binding levels of the fluorescent peptides used in **Figure 43** to HeLaM-HLA-ABC^{KO} cells, in the presence (right) or absence (left) of 1 μM TAPBPR. Cells were treated with or without TAPBPR for 15 min at 37°C, and then with peptide for 1 h at 37°C, as described in **Figure 44**. The peptides tested were: ETVSK*QSNV (ETV*), YLLEK*LWRL (YLL*), KTGGPIYK*R (KTG*), SHETK*IIEL (SHE*), SRYWK*IRTR (SRY*), LNPSK*AATL (LNP*), YVVPFVAK*V (YVV*), RVLDK*VEKW (RVL*) and PYLFK*LAAI (PYL*). The levels of bound fluorescent peptides were determined by flow cytometry. Data is representative of three independent experiments.

To better illustrate the difference in the relative peptide editing efficiency of TAPBPR across different HLA class I allotypes, I selected a set of HLA class I allotypes, comprising both strong TAPBPR binders (A*68:02 and A*02:01) and weak binders (B*38:01 and A*68:01) and measured the TAPBPR-mediated enhancement in peptide exchange at the cell surface, when TAPBPR was present at different concentrations (**Figure 45**). Strikingly, the efficiency of TAPBPR in catalysing peptide exchange on A*68:02 was considerably superior to its ability to exchange peptides on the other HLA class I allotypes tested, including A*02:01. Namely, already at 100 nM, TAPBPR was ~4 times more efficient at catalysing peptide exchange on A*68:02 than on A*02:01 and over 40 times more efficient than on A*68:01 and B*38:01 (**Figure 45**). Moreover, despite A*68:02 and A*02:01 reaching almost comparable levels of TAPBPR-mediated peptide exchange in the presence of 2 μM TAPBPR, the EC50 of TAPBPR for peptide exchange on A*68:02 was ~40 nM, while on A*02:01, the EC50 was ~500 nM. Compared to the strong binders A*68:02 and A*02:01, both weak TAPBPR binders, namely B*38:01 and A*68:01, underwent poor levels of TAPBPR-mediated peptide editing (**Figure 45**).

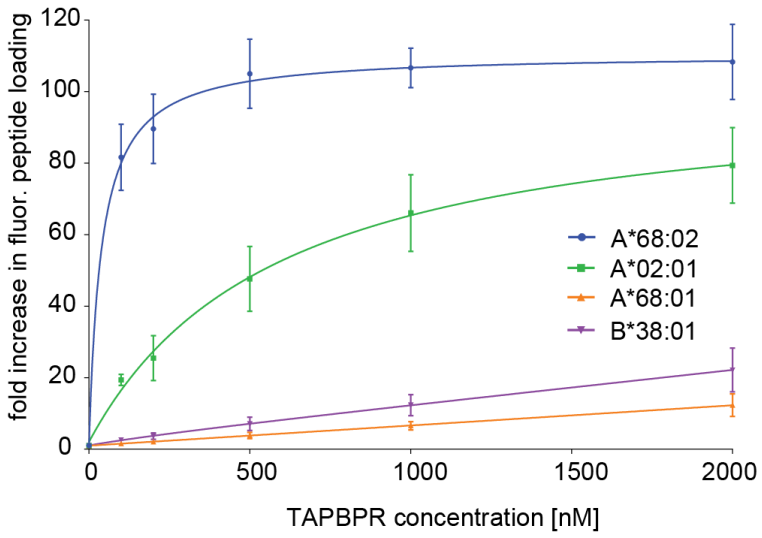

Figure 45: Dose-dependent peptide loading by soluble TAPBPR onto surface-expressed HLA class I molecules. Line graphs depict difference by fold increase in peptide binding to HLA-A*68:02, -A*02:01, -B*38:01 and -A*68:01, in the presence of different TAPBPR concentrations, compared to when peptide alone was added to cells. Error bars show mean fluorescence intensity (MFI) -/+ SD from three independent experiments.

Consistent with my previous observations using only a few different HLA class I allotypes, my results here show that the efficiency of TAPBPR-mediated peptide exchange across different HLA class I allotypes present at the cell surface is proportional to the relative levels of HLA class I bound to TAPBPR in the pull-down experiments (**Figure 40**). One exception however was HLA-A*32:01, a member of the A1 superfamily (Sidney et al., 2008), which showed very similar levels of TAPBPR-meditated peptide exchange as members of the A2 and A24 superfamilies (**Figure 45**), despite showing a considerably lower ability to bind TAPBPR than those molecules (**Figure 39**).

Taken together, these finding suggests that the peptide editing efficiency of TAPBPR strongly depends on its intrinsic ability to associate stably with HLA class I molecules. The presence of outliers, such as H:A-A*32:01, can be attributed to specific intrinsic properties of particular HLA class I molecules that would allow TAPBPR to disrupt their binding groove, thus promoting peptide dissociation, without the need to bind tightly to the MHC class I molecule itself.

5.2.7. The relative susceptibility of HLA class I molecules to undergo peptide editing by TAPBPR does not directly correlate with their relative stability at the cell surface

Given that each HLA class I allotype presents a distinct peptide repertoire at the cell surface, the stability of pMHC class I complexes present at the cell surface can differ significantly among different HLA class I allotypes. Thus, I next tested whether the observed increased susceptibility of the A2 and A24 superfamily members over the rest of the HLA class I molecules tested was due to their intrinsic ability to form stable interactions with TAPBPR or if it was due to their relatively lower stability at the cell surface, which would then lower the energy required by TAPBPR to dissociate the bound peptides. To address this question, I selected several HLA class I candidates spanning the entire TAPBPR binding hierarchy (**Figure 35b**) and assessed their relative stability at the cell surface. This was done by measuring the decay rates of pMHC class I complexes from the cell surface upon treating the cells with brefeldin A (BFA), molecule which inhibits protein trafficking to the cell surface (Fujiwara et al., 1988). The results showed that A*68:02, which is the strongest HLA class I binder to TAPBPR from our panel, also displayed the highest decay rate from the cell surface and hence the lowest stability among the 6 HLA allotypes tested (**Figure 46**). In contrast, B*44:05 and B*27:05, which are among the weakest TAPBPR binders, showed the highest relative stability among the molecules tested, decaying by less than 10% after 16 hours of BFA treatment (**Figure 46**). Based on this comparison alone, the ability of TAPBPR to stably bind to MHC class I would appear to correlate with the molecular stability of MHC class I complexes. However, highly similar decay rates were observed for A*02:01 and for A*68:01, despite A*02:01 being one of the strongest TAPBPR binders and A*68:01 being one of the weakest among HLA-A molecules. Moreover, HLA-B*38:01 showed a significantly lower stability compared to A*02:01 (**Figure 46**), despite its much weaker propensity to undergo peptide editing by TAPBPR (**Figures 43 b and 45**). Overall, while that the molecular stability of HLA class I molecules may affect their propensity to undergo peptide editing by TAPBPR marginally, this process seems to be driven mainly by the intrinsic ability of HLA class I molecules to associate with TAPBPR.

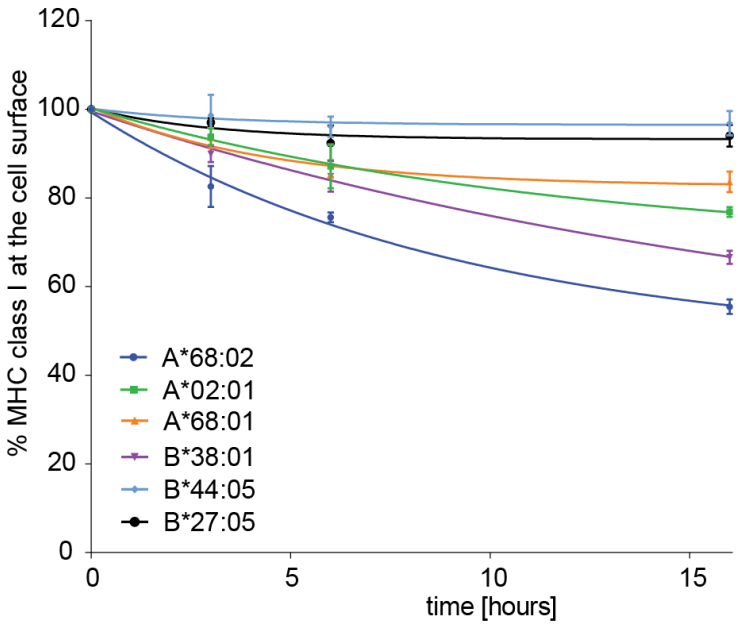

Figure 46: Stability of HLA class I molecules at the cell surface does not correlate with their relative susceptibility to TAPBPR-mediated peptide editing. Decay rates of the W6/32-reactive A*68:02, A*02:01, A*68:01, B*38:01, B*27:05 and B*44:05 from the cell surface upon treatment with 10 µg/mL Brefeldin A for different time periods. Error bars show mean fluorescence intensity (MFI) -/+ SD from triplicate samples. This is a representative example of two independent experiments.

5.2.8. Molecular properties of the F pocket of HLA class I correlate well with TAPBPR binding ability

I have previously proposed that F pocket specificity of HLA class I molecules for hydrophobic peptide residues is crucial for efficient TAPBPR-mediated peptide exchange, by allowing the binding of the L30 residue of TAPBPR, which was shown to promote peptide dissociation (**Chapter 4**). Given the observed preference of TAPBPR for HLA class I members of the A2 and A24 supertypes, I wanted to explore the molecular basis of this preference, focusing mainly on the F pocket region. By comparing the amino acid specificities across a wide range of HLA-A molecules, spanning the entire TAPBPR binding hierarchy, I observed that all members of the A2 and A24 superfamilies naturally accommodate aliphatic (and hence hydrophobic) amino acid residues (**Table 8**)(Sidney et al., 2008, Robinson et al., 2015). In contrast, all members of the A3 superfamily, which exhibit weak interactions with TAPBPR, accommodate basic residues in their F pocket (**Table 8**). The most eloquent example here is the one mentioned previously and namely the comparison between HLA-A*68:02 and HLA-A*68:01. Despite these two molecules differing in only 5 amino acid residues, HLA-A*68:02 is a member of the A2 superfamily and shows the highest level of TAPBPR binding among the allomorphs tested,

whereas HLA-A*68:01 is a member of the A3 supefamily and was shown to bind TAPBPR very weakly. These findings together highlight a strong correlation between F pocket specificity for hydrophobic residues of HLA class I molecules and their ability to bind TAPBPR.

Table 8: Characterization of HLA-A allotypes subjected to TAPBPR binding

HLA class I allotype	Supertype	F pocket specificity	Residue 114	Residue 116
A*68:02	**A2**	**Hydrophobic**	**H**	**Y**
A*23:01	**A24**	**Hydrophobic**	**H**	**Y**
A*69:01	**A2**	**Hydrophobic**	**H**	**Y**
A*02:01	**A2**	**Hydrophobic**	**H**	**Y**
A*24:02	**A24**	**Hydrophobic**	**H**	**Y**
A*02:06	**A2**	**Hydrophobic**	**H**	**Y**
A*03:01	A3	Basic	R	D
A*01:01	A1	Aromatic	R	D
A*26:01	A1	Aromatic	Q	D
A*30:01	A3	Basic / Aromatic	E	H
A*30:02	A1	Aromatic	E	H
A*33:01	A3	Basic	Q	D
A*36:01	A3	Basic	R	D
A*66:01	A3	Basic	Q	D
A*68:01	A3	Basic	R	D

5.2.9. Residues H114 and Y116 are conserved across all members of A2 and A24 superfamily and are not present in any other known HLA class I allotypes

To explore whether the actual architecture of HLA class I F pocket correlates with TAPBPR binding ability, I next compared the amino acid sequences across the same panel of HLA-A molecules, spanning residues 72-120, given the involvement of this HLA class I region in the binding of the C-terminal region of the peptide (**Figure 47**). Among the residues proposed to be particularly important in determining specificity of the F pocket for peptide residues (Sidney et al., 2008), I found residues H114 and Y116 to be conserved among all currently known members of the HLA-A2 and -A24 supertypes. Moreover, none of the A1 and A3 supertype members, nor any other HLA class I allotypes currently known contains this combination of residues at the specified positions (Robinson et al., 2015). These observations are in line with our previous finding that presence of residue Y116 in HLA class I promotes TAPBPR binding (**Figure 33**). Together, this striking correlation, based on a wide panel of HLA class I allotypes

tested, suggest that the susceptibility of HLA class I to TAPBPR-mediated peptide editing may be strongly influenced by the molecular architecture of the MHC class I F pocket.

a

```
         1         12  72                               105      114 116 120
A*68:02  GSHSMRYFYTSMSRP  QTDRVDLGTLRGYYNQSEAGSHTIQRMYGCDVGPDGRFLRGYHQYAYDG
A*69:01  -----------V---  -----------------------V---------S-W-------------
A*02:01  --------F--V---  --H--------------------V---------S-W-------------
A*02:06  -----------V---  --H--------------------V---------S-W-------------
A*23:01  --------S--V---  ----EN-RIALR-----------L-M-F-----S---------------
A*24:02  --------S--V---  ----EN-RIALR-----------L-M-F-----S---------------

A*01:01  --------F--V---  ----AN------------D------I----------------R-D----
A*03:01  --------F--V---  -------------------------I-------S--------R-D----
A*11:01  -----------V---  ------------------D------I----------------R-D----
A*25:01  -----------V---  ----ES-RIALR------D-----------------------Q-D----
A*26:01  -----------V---  ----AN------------D-----------------------Q-D----
A*30:01  --------S--V---  -------------------------I-------S--------E-H----
A*30:02  --------S--V---  ----EN-------------------I-------S--------E-H----
A*33:01  --------T--V---  -I-----------------------M-------S--------Q-D----
A*36:01  --------F--V---  ----AN------------D------I----------------R-D----
A*68:01  -----------V---  -------------------------M-------S--------R-D----
```

b

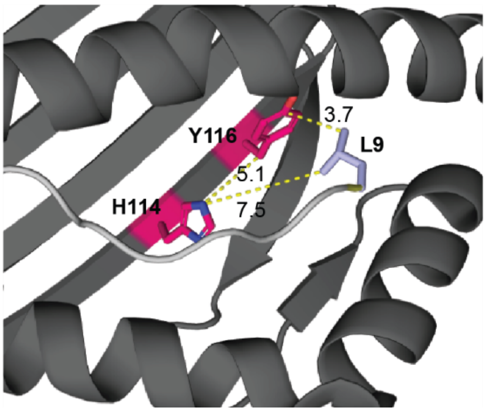

Figure 47: H114/Y116 residues are conserved exclusively across all HLA class I members of the A2 and A24 supertypes. (**a**) Amino acid multiple sequence alignment across different members of all HLA-A supertypes, consisting of residues 1-12 and 72-120; residues 114 and 116 are highlighted in red, while residues 12 and 105 are highlighted in blue. (**b**) PyMOL figure of the HLA-A*68:02 structure folded with peptide SVYDFFVWL (PDB ID 4HX1); residues H114 and Y116 are highlighted in red, the C-terminal L9 residue of the peptide in light blue and the peptide backbone in grey. The MHC class I structure is displayed in black. Dotted yellow lines indicate the shortest distances between the connected amino acid residues, measured in Å.

5.2.10. The F pocket architecture governs the ability of HLA class I molecules to associate with TAPBPR

To assess whether the H114/Y116 residue combination influences the interactions of HLA class I with TAPBPR, I artificially reconstituted these residues in some of the weak TAPBPR binders, belonging to HLA-A, -B and -C molecules. Again, none of the weak TAPBPR binders, including all

HLA-B and HLA-C molecules, contain both H114 and Y116 residues (Robinson et al., 2015), however, there are several HLA-B allotypes that contain one of the two, for instance HLA-B*27:05, with H114 but D116 instead of Y116, or HLA-B*44:05, with Y116, but D114 instead of H114 (**Figure 48a**). I therefore replaced D114 with a histidine in HLA-B*44:05 and replaced D116 with a tyrosine in B*27:05 and assessed the effects of these mutations on the ability of the two HLA-B molecules to bind TAPBPR. Upon reconstitution into HeLaM-HLA-ABC^{KO} cells, both HLA-B*44:05^{D114H} and -B*27:05^{D116Y} showed very similar surface expression levels compared to their corresponding wild type counterparts (**Figure 48b**).

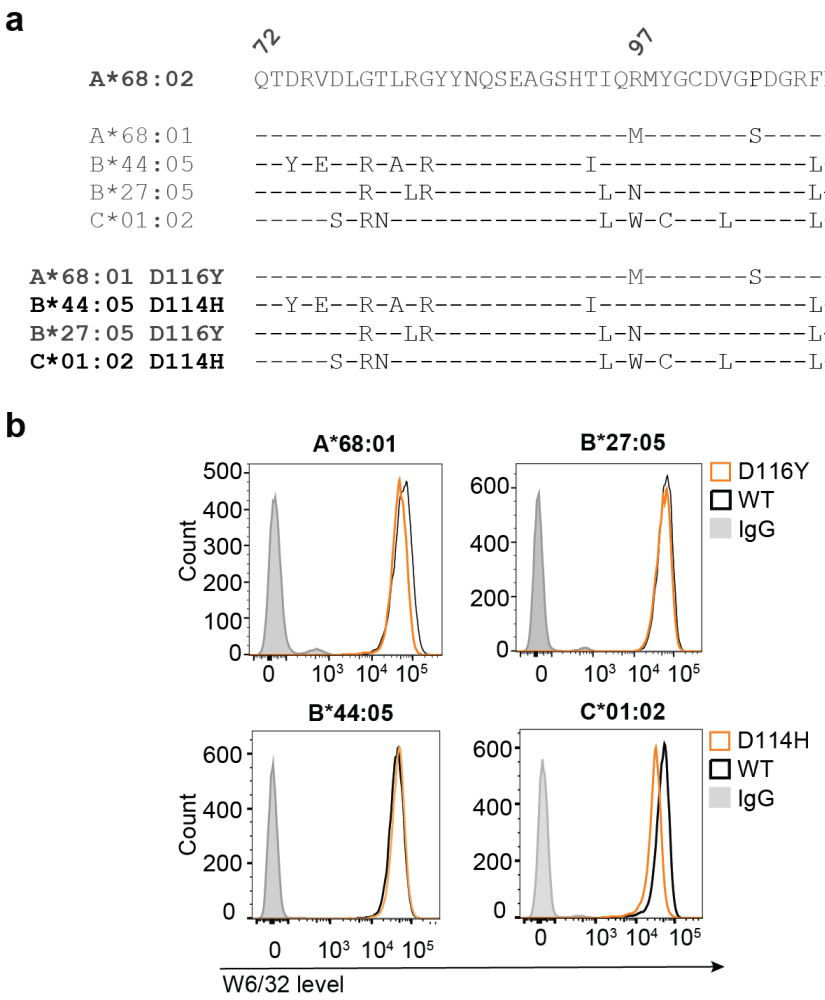

Figure 48: Designing F pocket mutants of HLA-A, -B and -C molecules and assessing their surface expression levels. (**a**) Amino acid sequence alignment of residues 72-120 between A*68:02 and A*68:01, B*44:05 or C*01:02, as well as their corresponding F pocket mutants; residues 114 and 116 are highlighted in red. (**b**) Histograms showing surface expression levels of the individual HLA class I F pocket mutants (orange lines) listed in **a**), without A*68:02, assessed by staining with W6/32, compared to their corresponding wild type counterparts (black lines). Samples stained with an isotype control antibody were chosen as negative controls (filled grey lines). Data is representative of three independent experiments.

As shown previously, neither B*27:05^{WT} nor B*44:05^{WT} was able to stably interact with TAPBPR at the cell surface (black lines – **Figure 49a** and blue bars - **Figure 49b**). Strikingly however, both B*27:05^{D116Y}- and B*44:05^{D114H}-expressing cells showed high levels of surface TAPBPR binding (orange lines – **Figure 49a** and red bars - **Figure 49b**). In fact, reconstitution of an "A*68:02-like F pocket" in both B*27:05^{WT} and B*44:05^{WT}, resulted in a similar increase in their ability to bind TAPBPR as the one recorded for another weak TAPBPR binder, namely A*68:01, upon introducing the D116Y mutation, as previously shown (**Figure 33**). Moreover, altering the F pocket of the strong TAPBPR binder A*68:02, by mutating Y116→D, triggered a severe decrease in TAPBPR binding (**Figure 49b**), as previously observed (**Figure 33**). Here, the A*68:02^{Y116D} chimeric mutant served as an additional control to further confirm the impact of residues H114 and Y116 on the ability of HLA class I molecules to interact with TAPBPR.

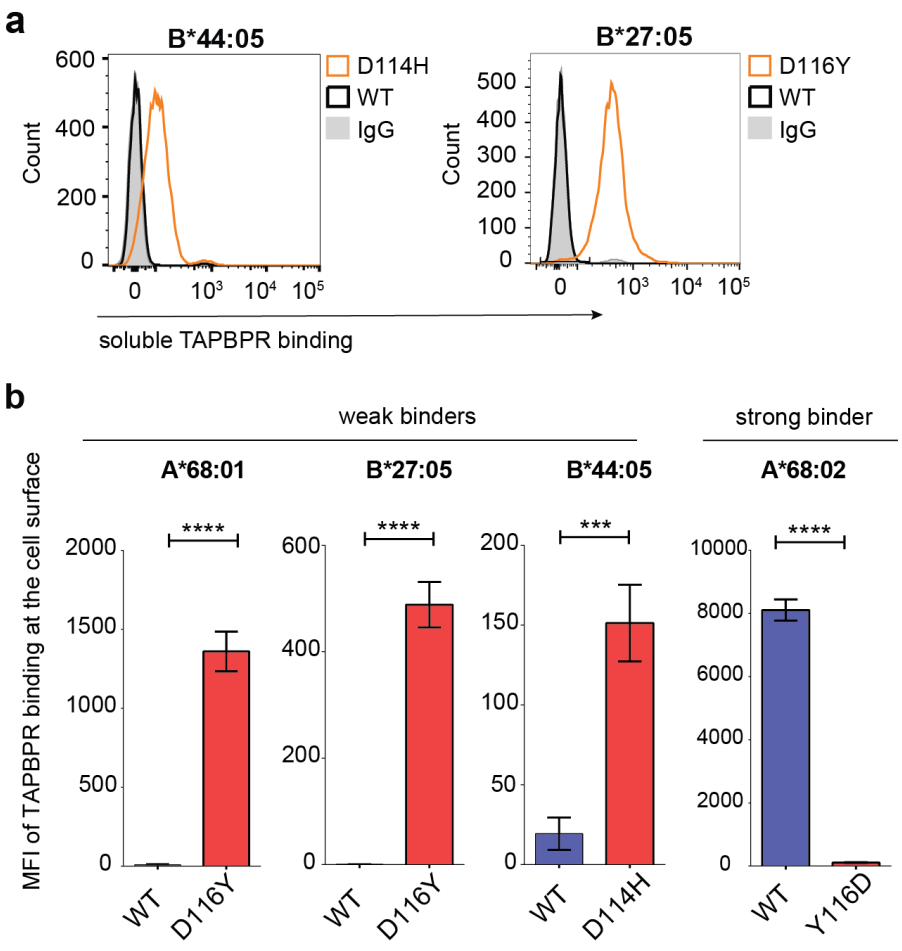

Figure 49: The H114/Y116 residue combination promotes the interaction of HLA-A, -B and -C molecules to TAPBPR. (**a**) Histograms depicting soluble TAPBPR binding to cell surface B*27:05 and B*44:05 (black lines), as well as to their corresponding F pocket mutants (orange lines), upon incubating the cells with 1 μM soluble TAPBPR^{WT}. (**b**) Bar graphs showing the level of TAPBPR binding to cells expressing A*68:01, B*27:05, B*44:05 or A*68:02 (blue) and to their corresponding F pocket mutants (red), from three independent experiments. Error bars show mean fluorescence intensity (MFI) -/+ SD from three independent experiments. n/s not significant, ***P ≤ 0.001, ****P≤0.0001 using unpaired two-tailed t-test.

I next assessed the effects mutating the F pocket on the interaction of TAPBPR with HLA class I molecules present intracellularly, by pull down experiments using recombinant TAPBPR protein. The results revealed that introduction of the H114/Y116 combination into HLA-B*44:05 resulted in a marked increase in TAPBPR binding (**Figure 50a**). These pulldown experiments also confirmed the increased ability of HLA-A*68:01 to bind to TAPBPR upon introduction of Y116 into this HLA class I, as previously shown when examining TAPBPR binding to HLA class I expressed on the cell surface (**Figure 33**). Furthermore, a similar increase in TAPBPR binding was also observed when introducing the H114/Y116 combination in an HLA-C molecule, namely HLA-C*01:02 (**Figure 50a**). The increased binding of HLA-A*68:01, -B*44:05 and -C*01:02 to TAPBPR, upon reconstitution of the "A*68:02-like F pocket", was also confirmed via endogenous TAPBPR pull downs (**Figure 50a**). Correspondingly, altering the F pocket of the strong TAPBPR binders HLA-A*68:02 and HLA-A*02:01, by mutating Y116→D, dramatically impaired their ability to bind TAPBPR (**Figure 50b**).

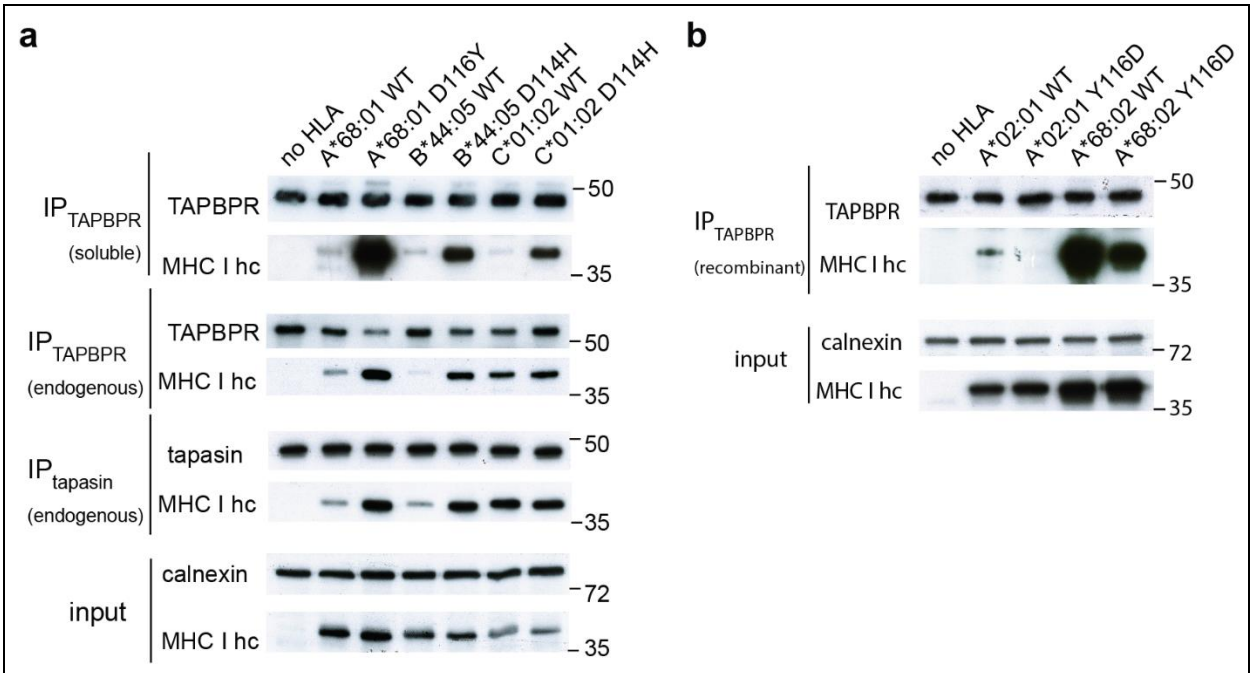

Figure 50: Mutating the F pocket impairs HLA class I binding to TAPBPR. (**a**) Western blot analysis on recombinant TAPBPR pull-downs (top) and on endogenous TAPBPR and tapasin immunoprecipitates (bottom), from cells expressing A*68:01^{WT}, A*68:01^{D116Y}, B*44:05^{WT}, B*44:05^{D114H}, C*01:02^{WT} or C*01:02^{D114H}. (**b**) Western blot analysis on recombinant TAPBPR pull-downs on cells expressing A*02:01, A*68:02, as well as their corresponding Y116D mutants. Membranes were probed for MHC class I heavy chain, TAPBPR, tapasin, and calnexin, as indicated. Data is representative of three independent experiments.

Finally, I wanted to understand to what extent these artificial mutations of the F pocket altered the molecular stability of the HLA class I molecules tested and whether that could have influenced their observed increased ability to bind TAPBPR. To this end, I measured their relative stability of the HLA class I F pocket mutants in comparison to their corresponding wild type counterparts, by performing BFA decay assays (**Figure 51**). While A*68:01^{D116Y} and B*44:05^{D114H} (dashed lines – **Figure 51**) indeed displayed significantly lower stability at the cell surface compared to the wild type molecules (solid lines – **Figure 51**), B*27:05^{D116Y} was surprisingly more stable than B*27:05^{WT} (black lines – **Figure 51**). Moreover, the Y116D mutation in A*68:02, which impaired its ability to bind TAPBPR (**Figure 49b**), also reduced its molecular stability (**Figure 51**). In conclusion, consistent with my observations across wild type HLA class I molecules (**Figure 46**), there does not seem to be any correlation between the change in pMHC class I stability caused by mutating the HLA class I F pocket and the effect of these mutations on TAPBPR binding.

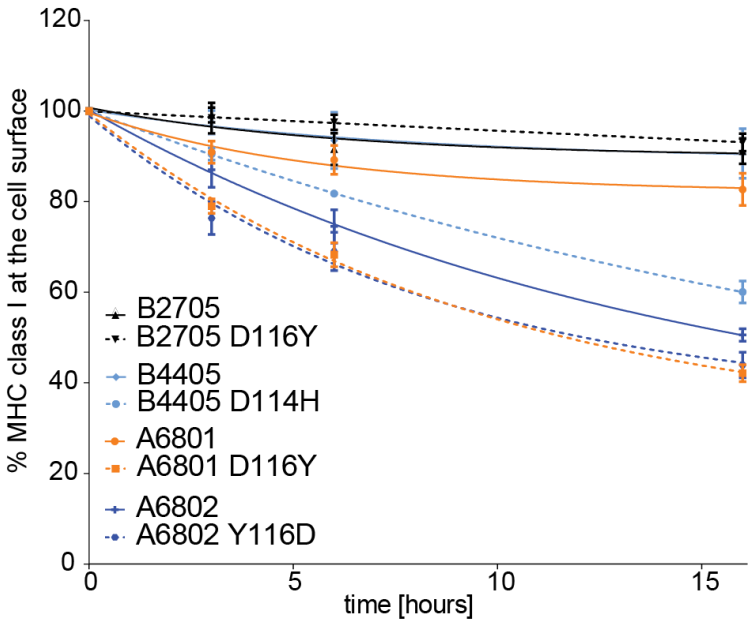

Figure 51: Mutating the F pocket of HLA class I molecules does not necessarily alter their stability at the cell surface. Line graphs depict the decay rates of the W6/32-reactive B*27:05, B*44:05, A*68:01 and A*68:02 from the cell surface, as well as of their corresponding F pocket mutants, upon treatment with 10 µg/mL brefeldin A, for different time periods. Error bars show mean fluorescence intensity (MFI) -/+ SD based on triplicates from one experiment. Data is representative of two independent experiments.

Together, these findings indicate that the residues found at position 114 and 116 strongly influence the intrinsic ability of HLA to interact with TAPBPR. Interestingly, I observed a similar increase in the binding of A*68:01^{D116Y} and B*44:05^{D114H} to tapasin compared to their wild type counterparts (**Figure 50a**). This suggests there may be a correlation between the interaction of

HLA class I molecules with TAPBPR and their net binding to tapasin, similar to the one observed for the panel of wild type HLA molecules tested previously (**Figure 41**), potentially supporting the recycling model of HLA class I molecules from TAPBPR back to the PLC (Boyle et al., 2013, Neerincx et al., 2017).

5.2.11. The F pocket architecture strongly influences the susceptibility of MHC class I molecules to undergo peptide editing by TAPBPR

I next explored whether the alterations made to the F pocket of HLA-B*44:05 and -B*27:05 increased their susceptibility to TAPBPR-mediated peptide exchange (**Figure 52**). Upon addition of exogenous fluorescent peptide, I found that in the presence of TAPBPR, peptide loading was only slightly increased on HLA-B*44:05^{WT} molecules and was not affected at all on HLA-B*27:05 (**Figure 52a and 52b**). Strikingly, however, introducing an "A*68:02-like F pocket" in both HLA-B*44:05 and -B*27:05 triggered a ~100-fold increase in TAPBPR-mediated peptide loading (**Figure 52b**). In fact, restoration of the H114/Y116 motif into two relatively non-responsive HLA-B molecules resulted in them undergoing TAPBPR-mediated peptide editing to the same magnitude as observed for HLA-A*02:01 and -A*68:02 molecules (**Figure 43b**). My findings strongly implicate that residues H114 and Y116, in combination, represent a key molecular signature responsible for the high susceptibility to TAPBPR observed for the HLA class I members of the A2 and A24 supertypes.

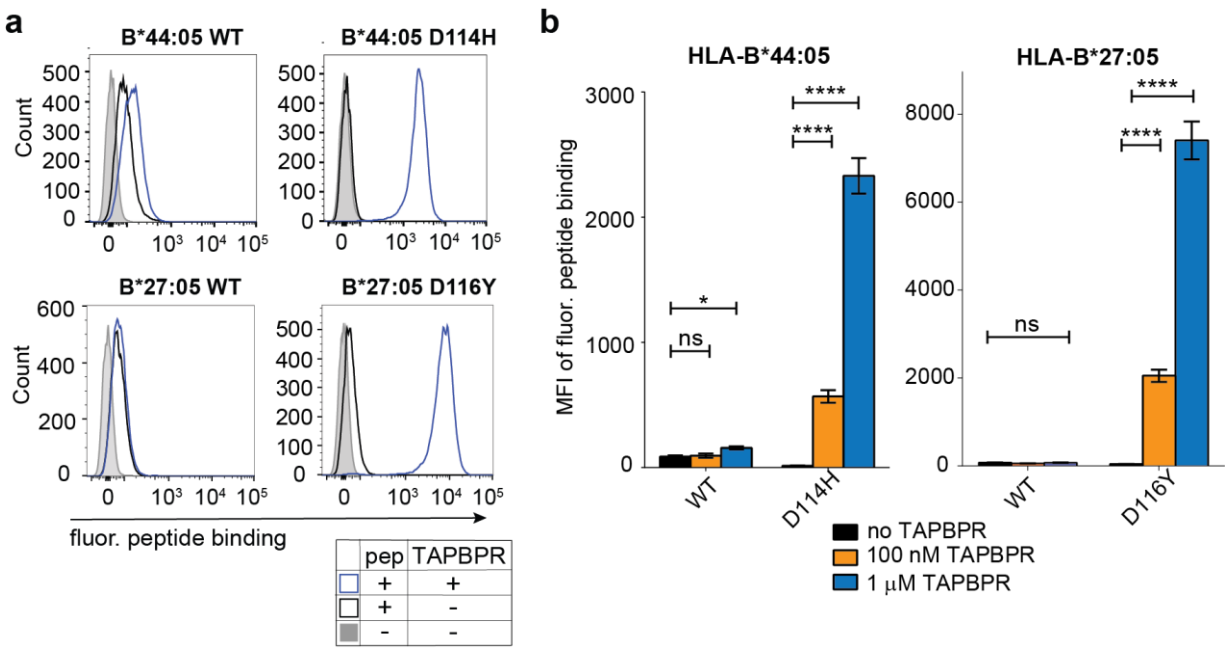

Figure 52: Residues H114 and Y116 promote the susceptibility of MHC class I molecules to peptide editing by TAPBPR. (**a**) Histograms showing the level of bound fluorescent peptide EEFGK*AFSF to cells expressing either B*44:05^{WT} or B*44:05^{D114H} (top) and of SRYWK*IRTR to cells expressing either B*27:05^{WT} or B*27:05^{D116Y} (bottom), upon incubation of the cells with 100 nM peptide and either no TAPBPR (black), 100 nM TAPBPR (orange) or without peptide (filled grey line), as a negative control. (**b**) Bar graphs summarising the level of fluorescent peptide binding in panel **a**), when cells were treated with 100 nM peptide and either no TAPBPR (black), 100 nM TAPBPR (orange) or 1 μM TAPBPR (blue). Error bars show mean fluorescence intensity (MFI) -/+ SD from three independent experiments. n/s not significant, *P≤0.05, ****P≤0.0001 using unpaired two-tailed t-test.

5.2.12. Disease-associated HLA class I allotypes that naturally differ in residue 116 alone show different propensities to undergo TAPBPR-mediated peptide editing

I have thus far shown that artificially mutating residues 114 and 116 considerably alters the susceptibility of HLA class I molecules to peptide editing by TAPBPR (**Figures 34 and 52**). Following on from this finding, I then asked whether naturally-occurring polymorphisms in HLA class I molecules, at one of these two positions alone, has any impact on the propensity of HLA class I to undergo TAPBPR-mediated peptide editing. To address this, I first compared the effect of TAPBPR on peptide editing between HLA-B*27:05 and -B*27:09, which only differ in residue 116 (D→H) (**Figure 53a**). This question was of particular interest also given the implication that this subtle polymorphism in HLA-B27 has on the susceptibility to the autoinflammatory condition ankylosing spondylitis. While HLA-B*27:05 is associated with this condition, HLA-B*27:09 was suggested to be not associated with the disease (Brown, 2010, Fiorillo et al., 2003, Taurog, 2007). I additionally wanted to compare another interesting pair of HLA class I

allotypes, namely HLA-B*35:01 and -B*35:03, also differs in residue 116 alone (S→F) (**Figure 53a**), however, rather interestingly, enable different progression levels of HIV (Gao et al., 2001).

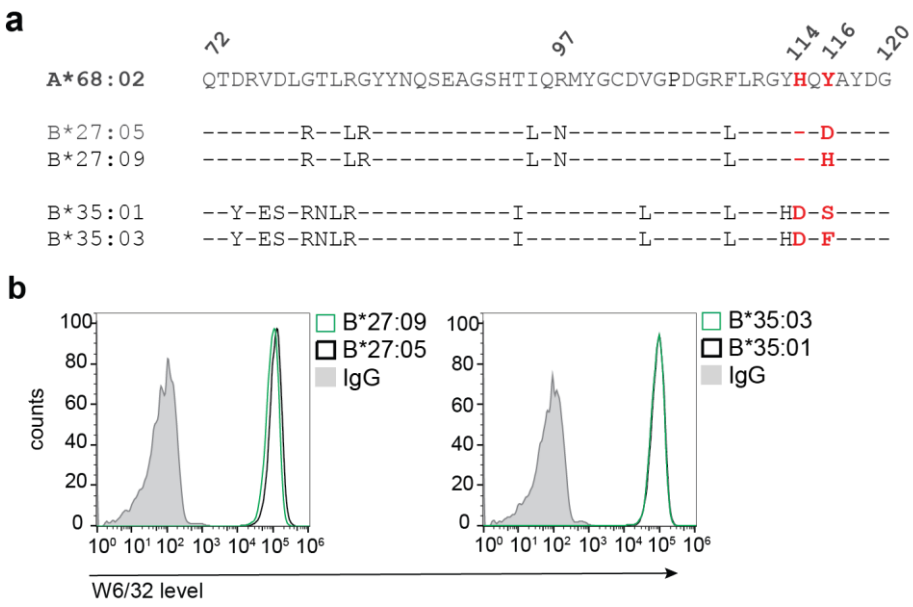

Figure 53: Wild type HLA-B molecules that differ in residue 116 alone are similarly expressed at the cell surface. a) Amino acid sequence alignment across residues 72-120 of A*68:02 with the HLA class I pairs B*27:05 - B*27:09 and B*35:01 - B*35:03; residues 114 and 116 are highlighted in red. (**b**) Histograms depict the levels of MHC class I, measured by staining with W6/32 antibody, on the surface of HeLaM-HLA-ABC^{KO} cells reconstituting with each of the HLA class I allotypes in panel **a**). These histograms are representative examples of three independent experiments.

Since the two HLA-B27 molecules, as well as the two HLA-B35 molecules, were reported to bind similar peptides respectively, I used the peptide SRYWK*IRTR for both B*27:05 and B*27:09 (Nurzia et al., 2012) and SPAIK*QSSM for both B*35:01 and B*35:03 (www.hiv.lanl.gov). Upon reconstitution into HeLaM-HLA-ABC^{KO} cells, all four HLA-B molecules showed similar expression levels, both at the cell surface and intracellularly (**Figure 53b and Figure 54**). When measuring the relative binding of these HLA class I molecules to recombinant TAPBPR by pull-down experiments, none of them showed a stable interaction with TAPBPR (**Figure 54**).

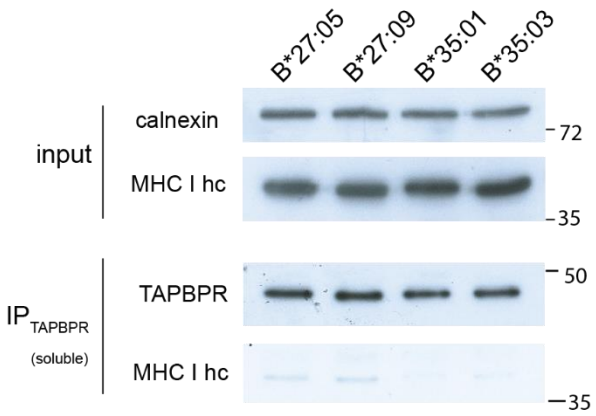

Figure 54: Natural differences in residue 116 across HLA-B allotypes do not significantly influence interaction with TAPBPR. Western blot analysis of recombinant TAPBPR immunoprecipitation experiments on cells expressing each of the HLA class I allotypes shown in **Figure 53**. The membranes were probed for MHC class I heavy chain (using the HC10 antibody), TAPBPR and calnexin, as indicated. Data is representative of three independent repeats.

Upon testing their susceptibility to peptide editing by TAPBPR however, while TAPBPR showed no significant effect on peptide binding to HLA-B*27:05, it facilitated an increase of over 100% in the level of peptide exchange on HLA-B*27:09 (**Figure 55a and 55b**). Regarding the HLA-B35 molecules, peptide exchange on B*35:01 was unaffected by TAPBPR, while B*35:03 exhibited a slight yet significant increase, of almost 20%, in the presence of TAPBPR (**Figure 55a and 55b**). As expected, given that none of these HLA-B molecules contain the H114/Y116 motif, the ability of TAPBPR to mediate peptide exchange on them was significantly lower compared to HLA-A2 and -A24 superfamily members (**Figure 43**). However, the one amino acid difference, at the key position 116, between the B27 allotypes as well as between the B35 allotypes, appears to be enough to cause a difference in the propensity of those molecules to undergo chaperone-mediated peptide editing.

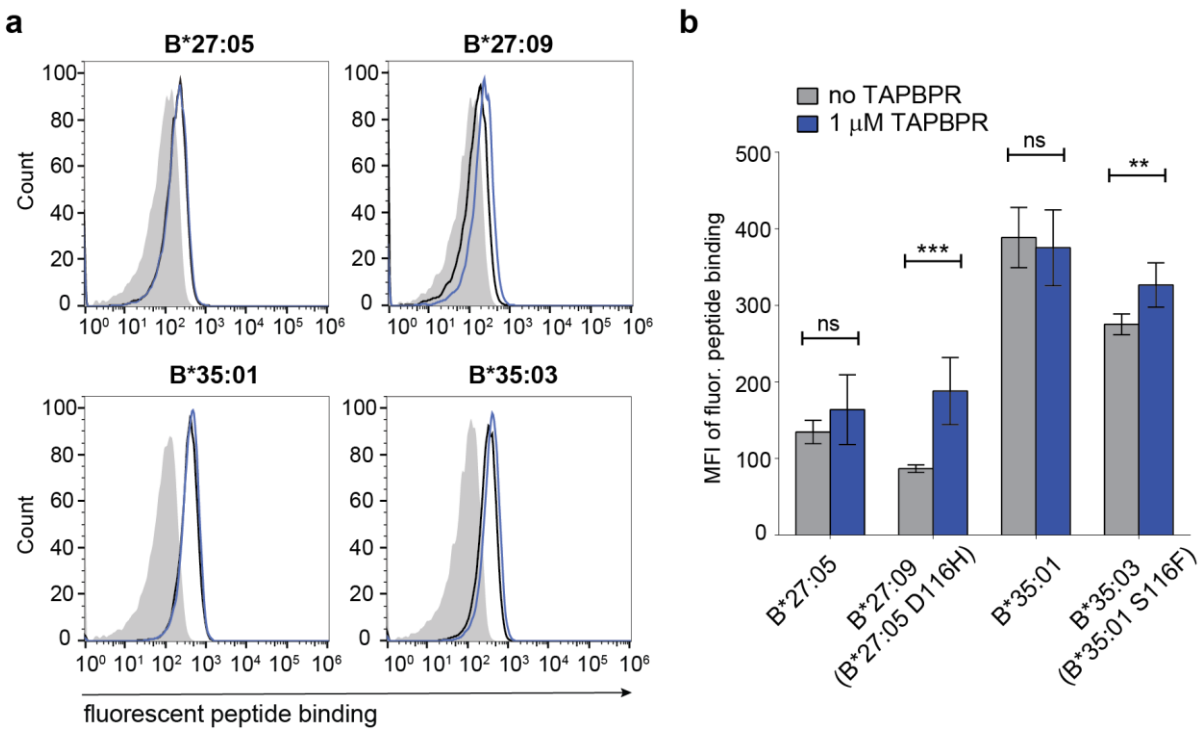

Figure 55: Naturally occurring differences in residue 116 alone across disease-associated HLA-B allotypes influence their susceptibility to peptide editing by TAPBPR. (**a**) Histograms depicting the level of fluorescent peptide binding to cells expressing B*27:05, B*27:09, B*35:01 or B*35:03, when cells were treated either with peptide alone (black lines) or with peptide and 1 µM TAPBPR (blue lines). The peptide SRYWK*IRTR was used for B*27:05 and B*27:09, while SPAIK*QSSM was used for, B*35:01 and B*35:03. Samples treated without peptide were used as negative controls (filled grey lines). (**b**) Bar graphs summarising the peptide binding MFI levels from panel **a**). Error bars show mean fluorescence intensity (MFI) -/+ SD from three independent experiments. n/s not significant, **P≤0.01, ***P ≤ 0.001, using unpaired two-tailed t-test.

5.2.13. Residue M12 of HLA-A*68:02 is responsible for its distinct ability to interact with TAPBPR

My TAPBPR binding data to HLA class I using the SABs (**Figure 35b**) and the cellular systems (**Figure 39 and 40**) all indicate that, while all members of the A2 and A24 supertypes interact strongly with TAPBPR, HLA-A*68:02 shows a much stronger association to TAPBPR than the rest. That implies that residues uniquely present in HLA-A*68:02 among all members of the A2 and A24 superfamilies, not necessarily involved in the F pocket architecture, are responsible for its enhanced ability to bind TAPBPR. Comparison of HLA-A*68:02 with the highly similar HLA-A*68:01 revealed, in addition residues involved in determining F pocket specificity, they differ in two other amino acids, at positions 12 and 105 (**Figure 47a**). Interestingly, despite various differences between HLA-A*68:02 and other members of the A2 and A24 superfamilies, the only residues that were only present in HLA-A*68:02 were the ones at positions 12 and 105

(**Figure 47a**). More specifically, while A*68:02 contains a methionine at position 12 and a proline at position 105, all other members of the A2 and A24 supertypes contain a valine at position 12 and a serine at position 105. For instance, HLA-A*69:01 shows a considerably reduced ability to bind TAPBPR compared to HLA-A*68:02 (**Figures 35b and 37**), despite differing in only five amino acids, two of which are the already mentioned ones, at positions 12 and 105 (**Figure 56a**). Interestingly, HLA-A*02:01, that differs from HLA-A*68:02 in several more amino acids as compared to HLA-A*69:01 (**Figure 56a**), including however residues 12 and 105, showed a similar level of TAPBPR binding to HLA-A*69:01 (**Figures 35b and 37**). Based on these observations, I hypothesized that residues M12 and/or P105 are responsible for this increased ability of HLA-A*68:02 to interact with TAPBPR. I therefore swapped either residue 12 or 105 between A*68:02 and A*02:01, generating the following chimeric HLA class I mutants: A*68:02^{M12V}, A*68:02^{P105S}, A*02:01^{V12M} and A*02:01^{S105P}. All chimeric mutants showed similar surface expression levels as their corresponding wild type counterparts upon stable reconstitution in HeLaM-HLA-ABC^{KO} cells (**Figure 56b**).

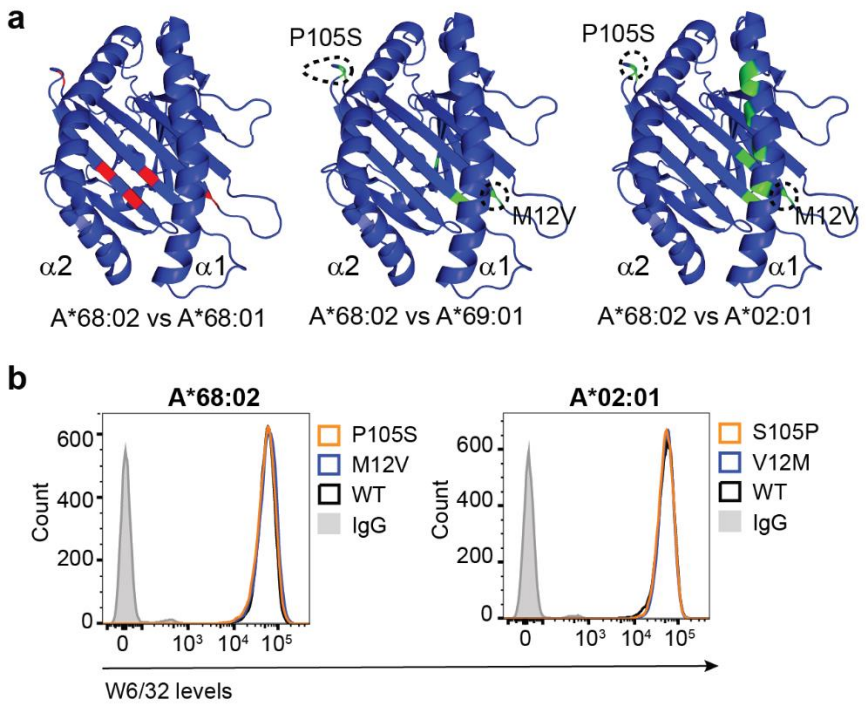

Figure 56: Design of HLA-A*68:02 and HLA-A*02:01 chimeric mutants, by targeting residues M12 and P105. (**a**) PyMOL images of the MHC class I binding groove, as seen from the top, emphasizing the amino acid differences between A*68:02 and A*68:01 (left), A*69:01 (centre) or A*02:01 (right), respectively (PDB ID 4HWZ was used as template for all three comparisons); conserved residues are coloured in blue, while amino acid differences between a strong binder (A*68:02) and the weak binder (A*68:01) are highlighted in red and differences between the strongest TAPBR binder (A*68:02) and other good binders in green. (**b**) Histograms depicting surface expression levels of A*68:02^{WT}, A*68:02^{M12V}, A*68:02^{P105S}, A*02:01^{WT}, A*02:01^{V12M} and A*02:01^{S105P} using the MHC class I specific mAb W6/32. Samples stained with an isotype control antibody were chosen as negative controls (filled grey line). Data is representative of three independent experiments.

When assessing their ability to bind TAPBPR at the cell surface, I found that mutation of residue 105 in either HLA-A*68:02 or HLA-A*02:01 had little or no effect on TAPBPR binding (**Figure 57**). Strikingly however, mutation of residue M12 in HLA-A*68:02 severely decreased its ability to bind TAPBPR (**Figure 57**). Namely, a 10-fold higher TAPBPR concentration was needed to achieve a similar level of binding to HLA-A*68:02^{M12V}, compared to HLA-A*68:02^{WT} (**Figure 57b**). Correspondingly, mutation of V12→M in HLA-A*02:01 led to a >10-fold increase in its ability to bind TAPBPR (**Figure 57**). Remarkably, although A*02:01 differs significantly from A*68:02 in its amino acid sequence, reconstitution of residue M12 alone on A*02:01 enhanced its ability to associate with TAPBPR to levels almost identical to the ones observed for HLA-A*68:02^{WT} (**Figure 57b**). These findings suggest that residue M12, found uniquely in A*68:02 among all HLA-A molecules tested, is mainly responsible for its distinct ability to interact with TAPBPR.

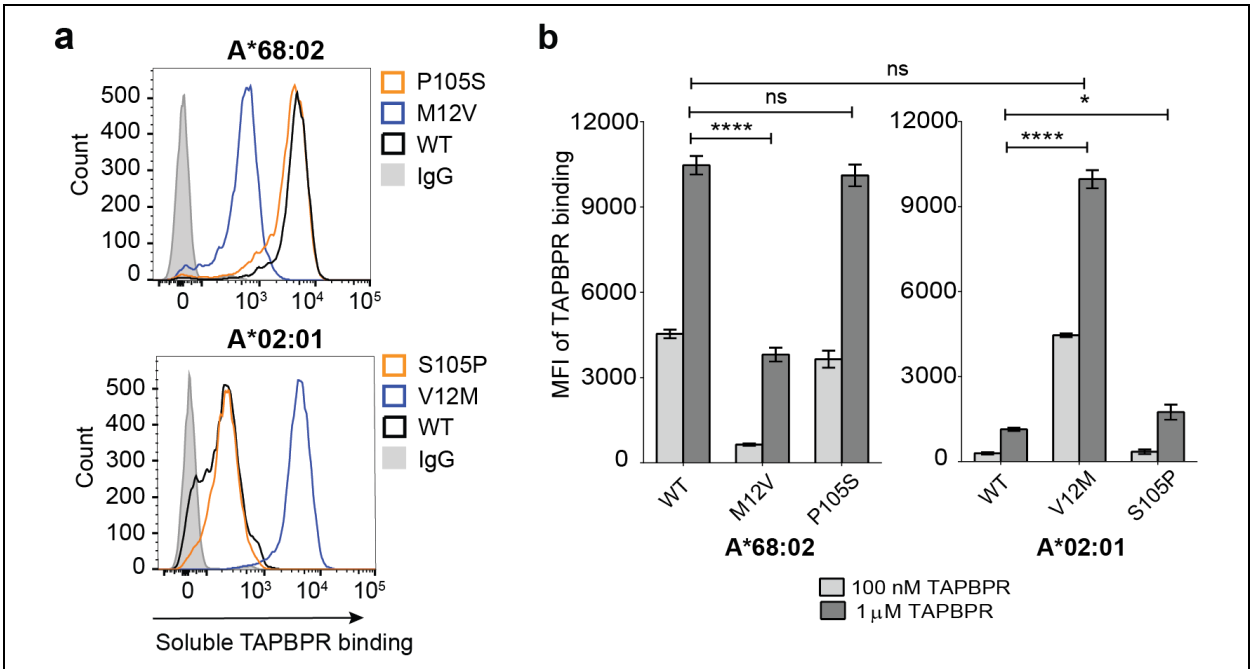

Figure 57: Residue M12 of HLA-A*68:02 promotes its high accessibility to TAPBPR. (**a**) Histograms displaying bound levels of soluble TAPBPR to the MHC class I variants in **Figure 56**, after cells were treated with 100 nM soluble TAPBPR for 30 min at 37°C. (**b**) Bar graphs summarising the levels of TAPBPR bound to each HLA class I allotype tested in panel **a**), upon treatment with either 100 nM (light grey) or 1 μM TAPBPR (dark grey). Bars show mean fluorescence intensity (MFI) -/+ SD from three independent experiments. n/s not significant, *P≤0.05, ****P≤0.0001 using unpaired two-tailed t-test.

This result was rather unexpected, as M12V seems a much more subtle mutation compared to P105S, especially given the position of the two residues in the binding groove. Whereas residue 12 sits at the end of β4 strand, pointing away from the α1 helix (**Figures 56a and 58**), residue 105 is located on the loop between β5 and β6 strands (**Figure 56a**). Therefore, mutating a

proline at position 105 should theoretically provide a higher degree of flexibility of the β5/β6 loop, potentially affecting the entire molecular plasticity of the peptide binding groove. I expected that the P105S change should in any case have a higher impact than M12V on the ability of HLA class I to interact with TAPBPR, mainly as TAPBPR relies on peptide-MHC class I kinetics to associate with MHC class I.

Next, I overlaid HLA-A*68:02 on top of H-2D^{b}, which was crystallised in complex with TAPBPR (Thomas and Tampe, 2017), to understand whether residue M12 of HLA-A*68:02 could potentially influence the contact points between MHC class I and TAPBPR (**Figure 58**). However, this alignment showed considerable distances, of at least 15 Å between residue M12 and the nearest TAPBPR regions, making it unlikely for this residue to be involved in the direct interactions of HLA-A*68:02 with TAPBPR.

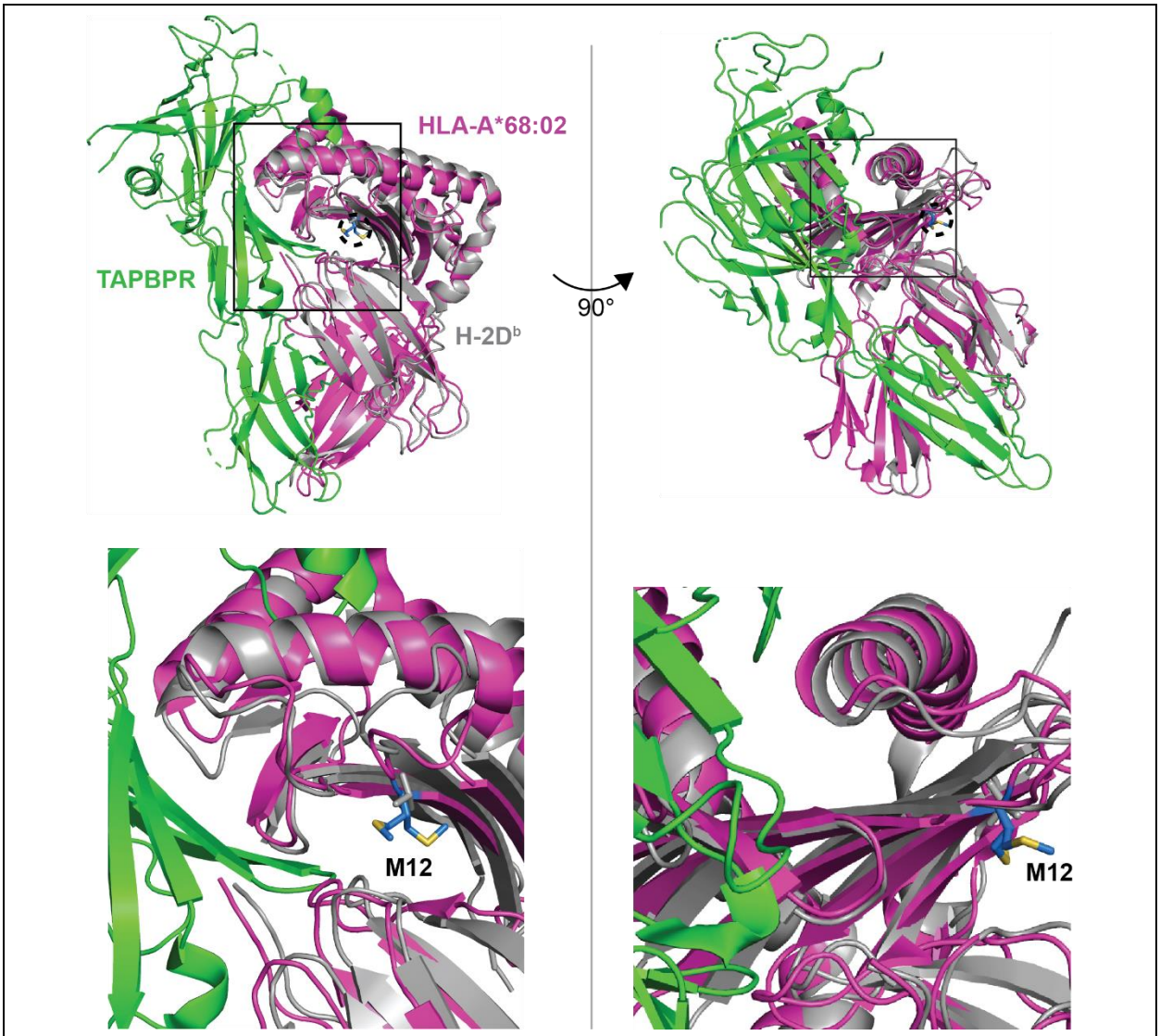

Figure 58: M12 residue of HLA-A*68:02 does not seem to contribute to the direct interaction with TAPBPR. PyMOL image of the structure of HLA-A*68:02 folded with peptide SVYDFFVWL (pink) (PDB ID 4HX1) overlaid onto the structure of the H-2D^b:TAPBPR complex (grey and green respectively) (PDB ID 5OPI), viewed from different angles. Residue M12 of HLA-A*68:02 is highlighted in blue and emphasized in a dotted circle. Magnified views of the selected areas are depicted below the full structures. Residue M12 was captured in two different orientations in the crystal structure of HLA-A*68:02.

Given the observations mentioned above, I believe that residues such as M12 could affect the ability of HLA class I molecules to interact with TAPBPR by affecting the molecular plasticity of the MHC class I peptide binding groove. This would in turn affect the stability of the peptide-MHC complex and hence the ability of TAPBPR to dissociate the peptide (McShan et al., 2018), step required for TAPBPR to form a stable interaction with the MHC class I molecules.

5.3. Discussion

This chapter follows on from my previous observations that TAPBPR facilitates peptide exchange in a loop-dependent manner preferentially on MHC class I molecules that naturally accommodate hydrophobic peptide residues in their F pocket (**Figure 30**). Here, I explored the relative susceptibility of a wide panel of HLA class I allotypes, representative to most HLA class I supertypes currently described, to peptide editing by TAPBPR. The results of this study show a clear preference of TAPBPR for HLA-A, and particularly for HLA-A2 and -A24 supertypes, over HLA-B and -C molecules (**Figures 35 and 37**). Moreover, in exploring the molecular basis of this observed preference, I demonstrate that certain molecular features of the F pocket, in particular residues 114 and 116, strongly influence the propensity of HLA class I to undergo TAPBPR-mediated peptide editing. These findings highlight an additional layer of complexity in the MHC class I allele-dependent peptide selection in cells and provide valuable insight into better understanding the mechanisms of peptide editing on MHC class I.

I speculate that the higher efficiency of TAPBPR in promoting peptide dissociation from some HLA class I allotypes over others is dependent on the compatibility between the 22-35 loop of TAPBPR and the F pocket of the HLA class I molecules. However, I have not tested the ability of the TAPBPR loop mutants to mediate peptide exchange on all of the HLA class I molecules mentioned in the study, but only on a few representative examples, as described in the previous chapter (**Figure 30**). It is entirely possible that other regions of TAPBPR, such as the jack hairpin (Thomas and Tampe, 2017), in a similar manner to the loop, could have a stronger impact on peptide exchange on some HLA class I allotypes than on others.

Finally, it is important to consider that, in this study, I only explored the relative susceptibility of different HLA class I allotypes to TAPBPR-mediated peptide editing, by assessing this process at the cell surface, which is an atypical cellular localization of TAPBPR (Boyle et al., 2013). To address the question of relative dependency of HLA class I molecules to TAPBPR function, one would need to compare the ability of a panel of HLA class I allotypes to load and present peptides, as well as the consequent differences in peptide repertoires for each allotype, in the presence of absence of endogenously-expressed TAPBPR in cells.

6. Chapter 6: Investigating the therapeutic potential of using soluble TAPBPR as a peptide loading catalyst on cell surface MHC class I molecules

6.1. Background

Thus far, I have used the cellular peptide exchange assays described in **Chapter 3** to address a series of fundamental questions regarding the molecular mechanisms governing TAPBPR-mediated peptide editing on MHC class I (**Chapter 4**) and the compatibility between TAPBPR and MHC class I (**Chapter 5**). However, my findings that TAPBPR can function as an efficient peptide loading catalyst onto MHC class I molecules present at the surface of cells have also raised an interesting translational question regarding the potential use of TAPBPR as an immuno-modulator. More specifically, we were interested in whether by facilitating the loading of highly immunogenic peptides of choice directly onto MHC class I molecules present on the surface of cells, we could use TAPBPR to enhance the recognition of tumour cells by $CD8^+$ T cells.

6.2. Results

6.2.1. TAPBPR can be used to load immunogenic peptides onto human tumour cells

To this end, I first tested whether soluble TAPBPR could promote the loading of immunogenic peptides, of tumour origin, onto MCF-7 cells, a breast cancer cell line expressing HLA-A*02:01 (**Figure 59**). I designed fluorescent derivatives of the tumour-derived antigens specific to HLA-A*02:01 IMDQVPFSV (derived from gp100)(Salgaller et al., 1996), ELAGIGILTV (derived from MART-1)(Romero et al., 1997), LLGRNSFEV (derived from p53)(Theobald et al., 1998) and RLLQETELV (derived from Her-2)(Rongcun et al., 1999) and measured their binding to MCF-7 cells in the presence or absence of soluble TAPBPR. While in the absence of soluble TAPBPR, none of the peptides showed efficient loading onto the surface of cells, presence of TAPBPR triggered a strong enhancement in the binding of each peptide tested (**Figure 59**), in a similar

manner as previously observed for the viral peptides YLLEMLWRL (from EBV) and NLVPMVATV (from HCMV) (**Figure 31b**).

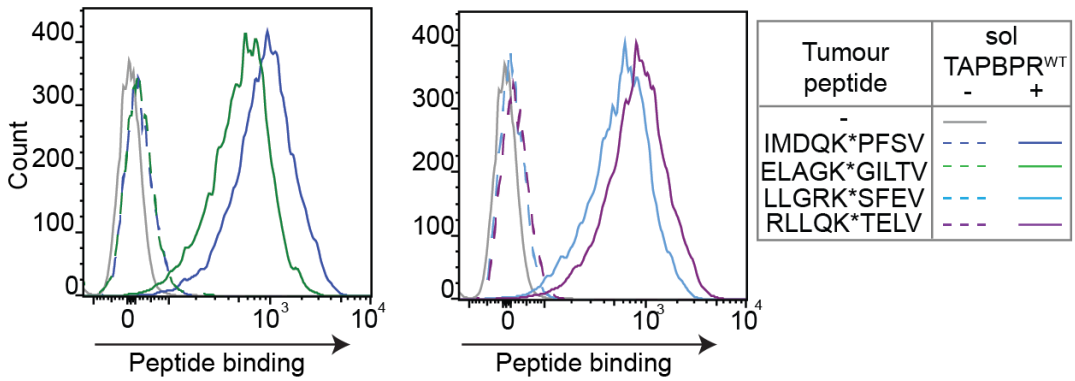

Figure 59: Soluble TAPBPR mediates loading of immunogenic peptides onto MHC class I molecules on the surface of tumour cell lines. MCF-7 cells were incubated with (solid lines) or without (dashed lines) 1 µM soluble TAPBPR for 15 min at 37 °C, followed by treatment with 10 nM of (left) IMDQK*PFSV (dark blue), ELAGK*GILTV (green), or with (right) LLGRK*SFEV (light blue), or RLLQK*TELV (purple) for another 60 min at 37 °C. Bound levels of each fluorescent peptide was measured by flow cytometry. Data is representative of three independent experiments. Taken from Ilca et al. (Ilca et al., 2018b).

6.2.2. Peptides loaded by TAPBPR onto cell surface MHC class I are available for TCR recognition

I subsequently tested whether the abundantly-loaded peptides by TAPBPR on surface-expressed HLA-A*02:01 were available for TCR recognition (**Figure 60**). My previous observation that soluble TAPBPR bound to cell surface MHC class I molecules dissociates upon mediating loading of exogenously-added high affinity peptides (**Figure 18**) raised the possibility that peptides loaded by TAPBPR, in complex with the HLA-A*02:01 molecules, could be accessible for detection by the TCR. To address this question, I first treated MCF-7 cells with the non-labelled peptide YLLEMLWRL (derived from EBV LMP1) in the presence or absence of TAPBPR, having already shown that the fluorescent version of this peptide binds strongly to HLA-A*02:01 (**Figure 19 and Figure 31**). I subsequently assessed the TCR detection of the HLA-A*02:01 molecules loaded specifically with the YLLEMLWRL peptide by staining the cells with a TCR-like mAb specific for this pMHC class I complex (L1) (**Figure 60a and 60b**). The binding of TCR-like mAb to MCF-7 cells (**Figure 60a and 60b**) was proportional to the binding of the actual peptide to the cells (**Figure 31b**). Namely, treatment with the YLLEMLWRL peptide in the absence of TAPBPR resulted in a low binding level of the TCR-like mAb. On the other hand,

when the peptide was added to the cells in the presence of TAPBPR^{WT}, but not of TAPBPR^{TN5}, a strong enhancement in the recognition of MCF-7 cells by the TCR-like mAb was observed (**Figure 60a and 60b**). Moreover, TCR-like mAb binding was strictly peptide-dependent, as treatment of the cells with TAPBPR^{WT} alone did not promote any TCR-like mAb recognition.

A similar TAPBPR-mediated enhancement in the binding of the TCR-like mAb was observed for HeLaM-HLA-ABC^{KO} cells reconstituted with HLA-A*02:01 (HeLa-A2 cells) (**Figure 60c and 60d**), confirming that binding of the TCR-like mAb was also HLA-A*02:01-specific. These results together indicate that the exogenous peptides loaded onto surface-expressed MHC class I by TAPBPR are available for TCR recognition.

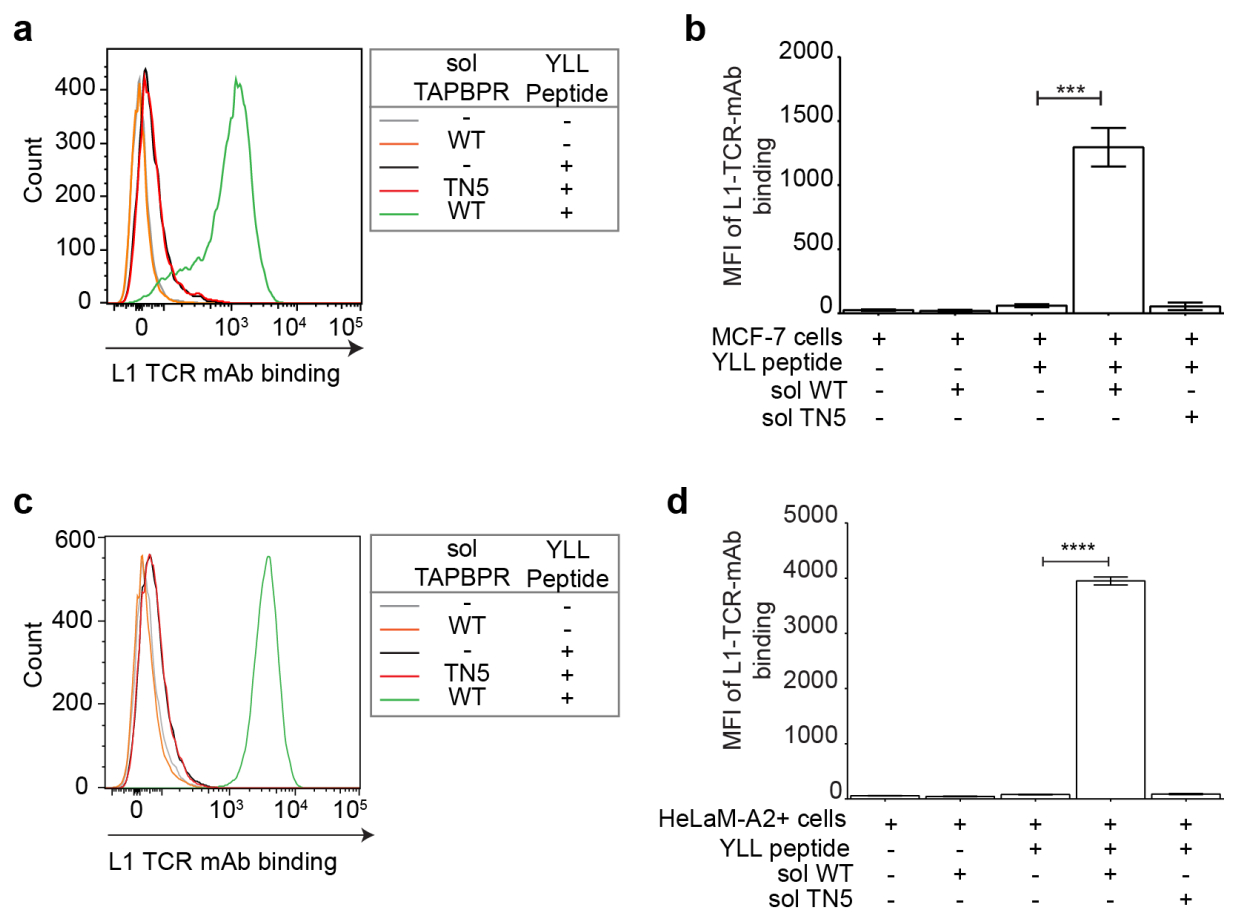

Figure 60: Antigenic peptides loaded onto tumour cells by soluble TAPBPR are available for TCR recognition. (**a** and **c**) Histograms showing bound levels of the TCR-like mAb L1, specific for YLLEMLWRL/HLA-A2 complexes, to either (**a**) MCF-7 or (**c**) HeLa-A2 cells, after cells were treated with 10 nM YLLEMLWRL (YLL), in the presence or absence of 1 µM TAPBPR^{WT} or TAPBPR^{TN5}. (**b** and **d**) Bar graphs summarising the levels of L1 binding to either (**b**) MCF-7 or (**d**) HeLa-A2 cells, as performed in **a**) and **c**) respectively. Bars show mean fluorescence intensity (MFI) -/+ SD from three independent experiments. n/s not significant, ***P ≤ 0.001, ****P≤0.0001 using unpaired two-tailed t-test. Taken from Ilca et al. (Ilca et al., 2018b).

6.2.3. TAPBPR-mediated loading of immunogenic peptides on MHC class I enhances recognition of tumour cells by $CD8^+$ T cells

Having shown that peptides loaded by TAPBPR onto surface MHC class I molecules are accessible by soluble recombinant TCRs, in solution, I next asked whether these resulting pMHC class I complexes are also available for recognition by TCRs expressed on actual $CD8^+$ T cells. In collaboration with Dr. Mark Wills (Department of Medicine, University of Cambridge), I set up an assay to interrogate whether we can induce $CD8^+$ T cell-mediated recognition of tumour cells by using TAPBPR to load the tumour cells with immunogenic peptides. To this end, I first treated target MCF-7 cells with the NLVPMVATV peptide, comprising residues 495-503 of the HCMV protein pp65 ($pp65_{495–503}$), in the presence of absence of TAPBPR. I have already shown that the fluorescent version of the NLVPMVATV peptide is efficiently loaded by TAPBPR onto surface-expressed HLA-A*02:01 (**Figure 19 and Figure 31**). Moreover, this peptide has been shown to induce strong $CD8^+$ T cell responses (Gillespie et al., 2000). Upon washing the target cells to remove the excess peptide, I then co-cultured them with primary $CD8^+$ T cells that were harvested from HLA-A*02:01-positive patients suffering from HCMV infection and selected for their recognition of the NLVPMVATV bound to HLA-A*02:01. The activation level of the $CD8^+$ T cells by target MCF-7 cells was measured using a FluoroSpot assay, which allowed for the quantification of fluorescent signal equivalent to the IFN release by the T cells.

Due to my lack of knowledge regarding the abundance of pMHC class I complexes at the cell surface required to induce T cell activation, I treated the MCF-7 cells with a range of peptide concentrations (10 pM – 10 nM), in the presence or absence of a fixed concentration of soluble TAPBPR (1 μM), and measured their ability to induce T cell activation. Moreover, I subsequently cultured each target cell sample with T cells, at an effector to target (E:T) cell ratio of either 1:6 or 1:12 (**Figure 61**). Satisfyingly, no activation of the T cells was observed upon simply co-culturing them with non-treated MCF-7 cells (**Figure 61**). Second, I observed that at lower peptide concentrations, (either 10 pM or 100 pM), cells treated with peptide alone induced a low level of T cell activation and that presence of TAPBPR induced a strong enhancement in the activation of T cells. However, upon increasing the peptide concentration above 100 pM, cells treated with peptide alone started inducing T cell activation similarly to the ones treated with peptide in the presence TAPBPR. In fact, the level of T cell activation in the presence of TAPBPR seemed to saturate already at ~100 pM peptide, whereas in the absence of TAPBPR, ~10 nM peptide was needed to achieve saturation in T cell activation. Despite only testing a few

different peptide concentrations in this experiment, these results clearly indicated that TAPBPR can indeed promote T cell recognition of tumour cells.

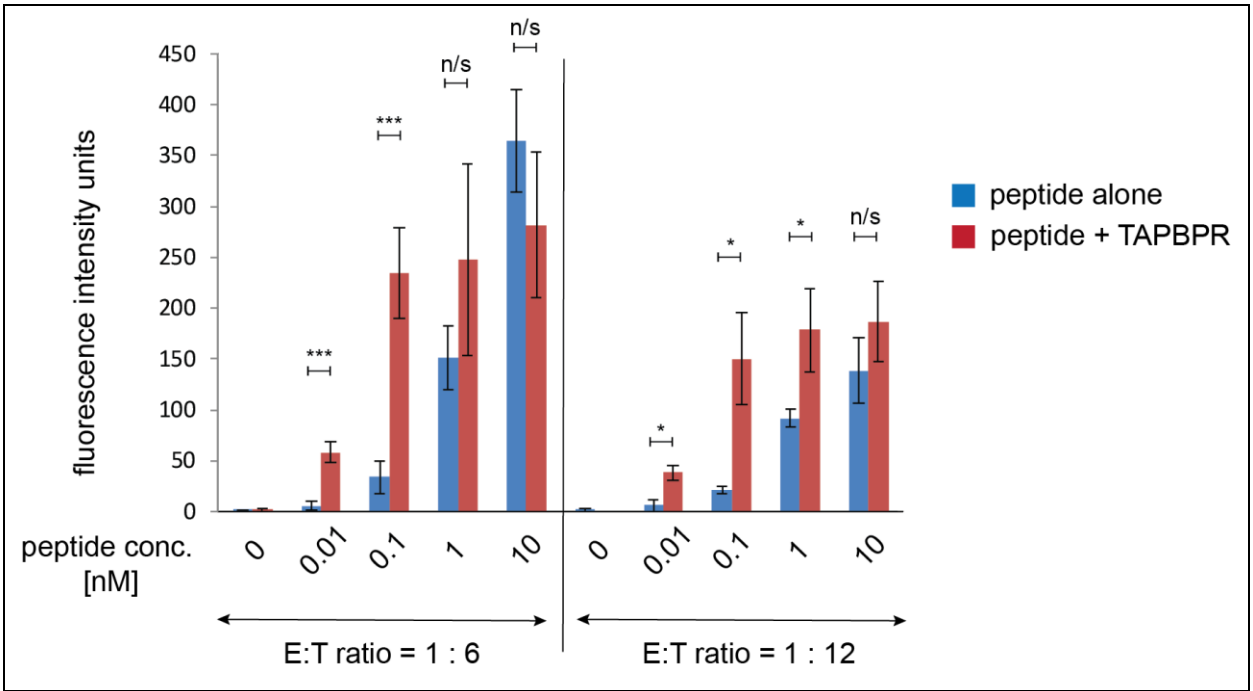

Figure 61: TAPBPR induces T cell recognition of tumour cells at low peptide concentrations. MCF-7 target cells were treated with or without different concentrations of NLVPMVATV peptide for 60 min in the presence (red bars) or absence (blue bars) of 1 µM soluble TAPBPR^{WT}. Target cells were then washed thoroughly and then incubated with NLVPMVATV-restricted CD8$^+$ T cells, at an E:T cell ratio of either 1:6 (left) or 1:12 (right). The activity of T cells, measured by IFN-γ secretion, was quantified using a fluorospot assay. Results are from triplicate wells representative of two independent experiments. Error bars ± SD.*$P \leq 0.05$, ***$P \leq 0.001$ using unpaired two-tailed *t* test.

To ensure the reproducibility of these findings, I performed a similar T cell activation experiment using a different batch of primary CD8$^+$ T cells. This time, I tested the effect of TAPBPR on the T cell-mediated recognition of an additional cell line expressing HLA-A*02:01, namely HeLaM-A2 cells, to ensure that the results were not restricted to the MCF-7 cells (**Figure 62**). Finally, I included two additional controls, namely treatment of the target cells with TAPBPR^{WT} alone or with peptide in the presence of TAPBPR^{TN5}, to test whether presence of TAPBPR alone triggered any T cell activation. The peptide concentration used in this experiment was 100 pM, as it offered the clearest enhancement in the T cell-mediated recognition of target cells by TAPBPR (**Figure 61**).

Consistent with the observations from the previous experiment, very little T cell activation was observed to either MCF-7 cells (**Figure 62a**) or to HeLaM-A2 cells (**Figure 62b**) treated with peptide alone, while addition of TAPBPR resulted in a high increase, of almost 10-fold, in the activation of T cells for both target cell lines. As expected, treatment with peptide in the

presence of TAPBPR^{TN5} did not show any enhancement in T cell activation compared to when the target cells were treated with peptide alone. Moreover, treatment of either target cell line with TAPBPR^{WT} alone did not promote T cell activation (**Figure 62a and 62b**), confirming that the activation of T cells was strictly as a result of recognition of the NLVPMVATV peptide loaded on HLA-A*02:01. Together, these findings demonstrate that TAPBPR can induce CD8$^+$ T cell-mediated recognition of tumour cells, by efficiently mediating their loading with immunogenic peptides added exogenously.

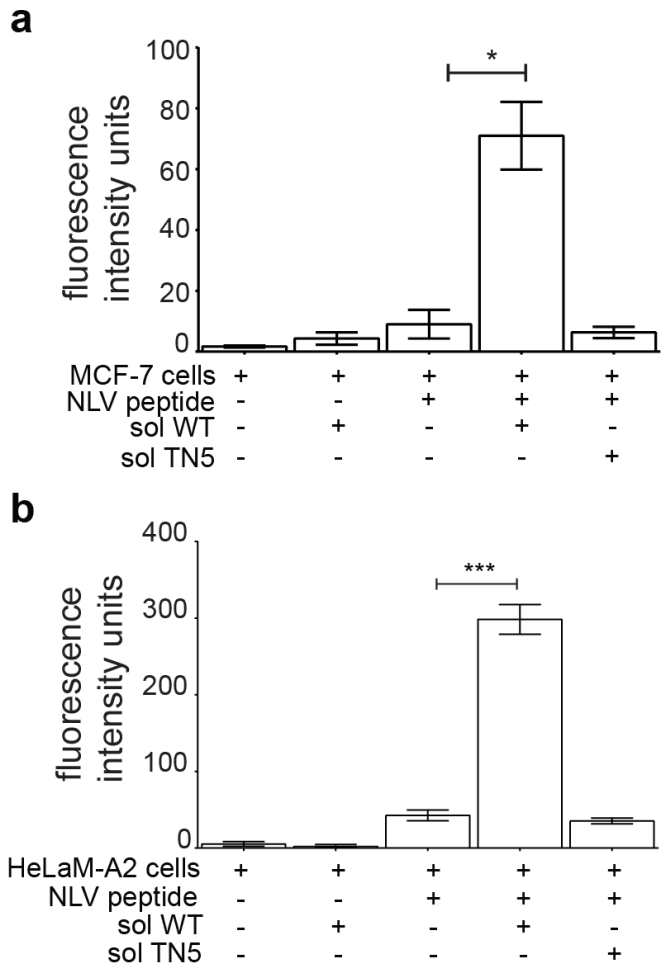

Figure 62: TAPBPR-mediated antigenic peptide binding to tumour cells induces their recognition by T cells. (**a**) MCF-7 or (**b**) HeLa-A2 target cells were treated with or without 100 pM NLVPMVATV peptide for 60 min in the presence or absence of 1 µM soluble TAPBPR^{WT} or TAPBPR^{TN5}. Target cells were then washed thoroughly and then incubated with NLVPMVATV-restricted CD8$^+$ T cells. The activity of T cells, measured by IFN-γ secretion, was quantified using a FluoroSpot assay. Results are from triplicate wells representative of two independent experiments. Error bars ± SD.*$P \leq 0.05$, ***$P \leq 0.001$ using unpaired two-tailed *t* test. Taken from Ilca et al. (Ilca et al., 2018b).

6.2.4. Using TAPBPR to induce T cell-mediated killing of tumour cells

The next step was to show that the observed induction of T cell recognition of tumour cells by TAPBPR (**Figure 62**) results in a corresponding enhancement in the actual killing of the target cells by $CD8^+$ T cells. To address this question, in collaboration with Dr. Maike de la Roche (CRUK, University of Cambridge), we decided to use a murine system. Namely, I assessed the effect of TAPBPR-mediated peptide loading on the killing of EL4 cells (a murine lymphoma cell line)(Gorer, 1950) by OT-1 T cells, which are primary $CD8^+$ T cells that recognize the ovalbumin-derived peptide SIINFEKL (SL8) loaded on H-$2K^b$ (Carbone et al., 1992). There were a few reasons for switching to a murine system for this particular experiment. First, I have previously shown that the soluble version of human TAPBPR facilitates efficient peptide loading (and specifically of the SIINFEKL peptide) on H-$2K^b$ expressed on EL4 cells (**Figure 30b and 30c**). Second, measuring OT-1 T cell-mediated killing of EL4 target cells has been a well-established and perfected assay (Jenkins et al., 2009, de la Roche et al., 2013), requiring less preparation and probably significantly less troubleshooting as well in comparison to a killing assay using human primary T cells. For instance, primary T cells required harvesting from patients' blood, selection for the particular T cell clone reactive to the pMHC class I complex of interest and subsequent clonal expansion in culture (Weekes et al., 1999), which would ultimately yield significantly different T cell batches compared to one another (personal communication). In contrast, the primary OT-1 T cells are generated in a transgenic mouse line, in which all $CD8^+$ T cells express the TCR specific for the ovalbumin-derived peptide SIINFEKL (Carbone et al., 1992). Therefore, there was no need to select and expand a specific set/clone of T cells from the lymphocytes harvested from the spleens of OT-1 mice. Instead, the OT-1 T cells were readily available for assaying a few days after their harvest. This system also enabled high consistency across different T cell batches.

Prior to attempting to measure the effect on T cell killing of the TAPBPR-mediated peptide loading on EL4 cells, I again wanted to test first whether the SIINFEKL peptide loaded by TAPBPR onto H-$2K^b$ molecules could be accessible for recognition by TCRs. To this end, I stained EL4 cells treated with SIINFEKL, in the presence or absence of $TAPBPR^{WT}$, with the mAb 25D-1.16, specific for SIINFEKL in complex with H-$2K^b$ (Porgador et al., 1997) (**Figure 63a and 63b**). This antibody is therefore similar to a recombinant TCR-like mAb. Satisfyingly, the results were similar to the ones recorded using the human TCR-like mAb on MCF-7 cells (**Figure 60**). Namely, a low level of 25D-1.16 binding was observed to cells treated with peptide alone, while

treatment with peptide in the presence of TAPBPR^{WT}, but not of TAPBPR^{TN5}, resulted in a considerable increase in the recognition of the cells by 25D-1.16 (**Figure 63a and 63b**). Again, treatment of cells with TAPBPR^{WT} alone did not promote any 25D-1.16 binding, confirming that 25D-1.16 did not associate with TAPBPR, or with H-2K^{b} in the absence of SIINFEKL.

Having clearly shown that peptides loaded using TAPBPR onto surface expressed H-2K^{b} molecules are accessible by soluble TCR-like mAb, I proceeded by measuring the effect of TAPBPR-mediated peptide loading on the killing of EL4 cells by CD8^{+} T cells (**Figure 63c**). To this end, EL4 cells were first treated with low concentrations of SIINFEKL, in the presence or absence of TAPBPR. Upon washing off the excess peptide, EL4 cells were incubated with OT-1 cells and the level of target cell death was measured by the amount of LDH release (**Figure 63c**). I observed a significant enhancement, of roughly 2.5-fold, in the level of T cell killing of target cells in the presence of TAPBPR^{WT}, but not of TAPBPR^{TN5}, compared to when peptide was added alone to cells. This increase in TAPBPR-mediated T cell killing of EL4 cells was highly consistent across a wide range of E:T cell ratios (**Figure 63c**). However, the enhancement in T cell killing of murine tumour cells by TAPBPR was not nearly as high as the increase in T cell recognition of human cells (**Figure 62**). I believe that the main reason for this is, consistent with previous literature, that murine MHC class I molecules have a considerably higher molecular plasticity compared to human MHC class I molecules (Saini et al., 2013). This would make mouse MHC class I more receptive to TAPBPR-independent peptide binding than human MHC class I, which translates into a lower fold increase in peptide loading by TAPBPR. Nonetheless, our findings clearly demonstrate that TAPBPR can be utilised to enhance the killing of tumour cells by CD8^{+} T cells, in a peptide-specific manner.

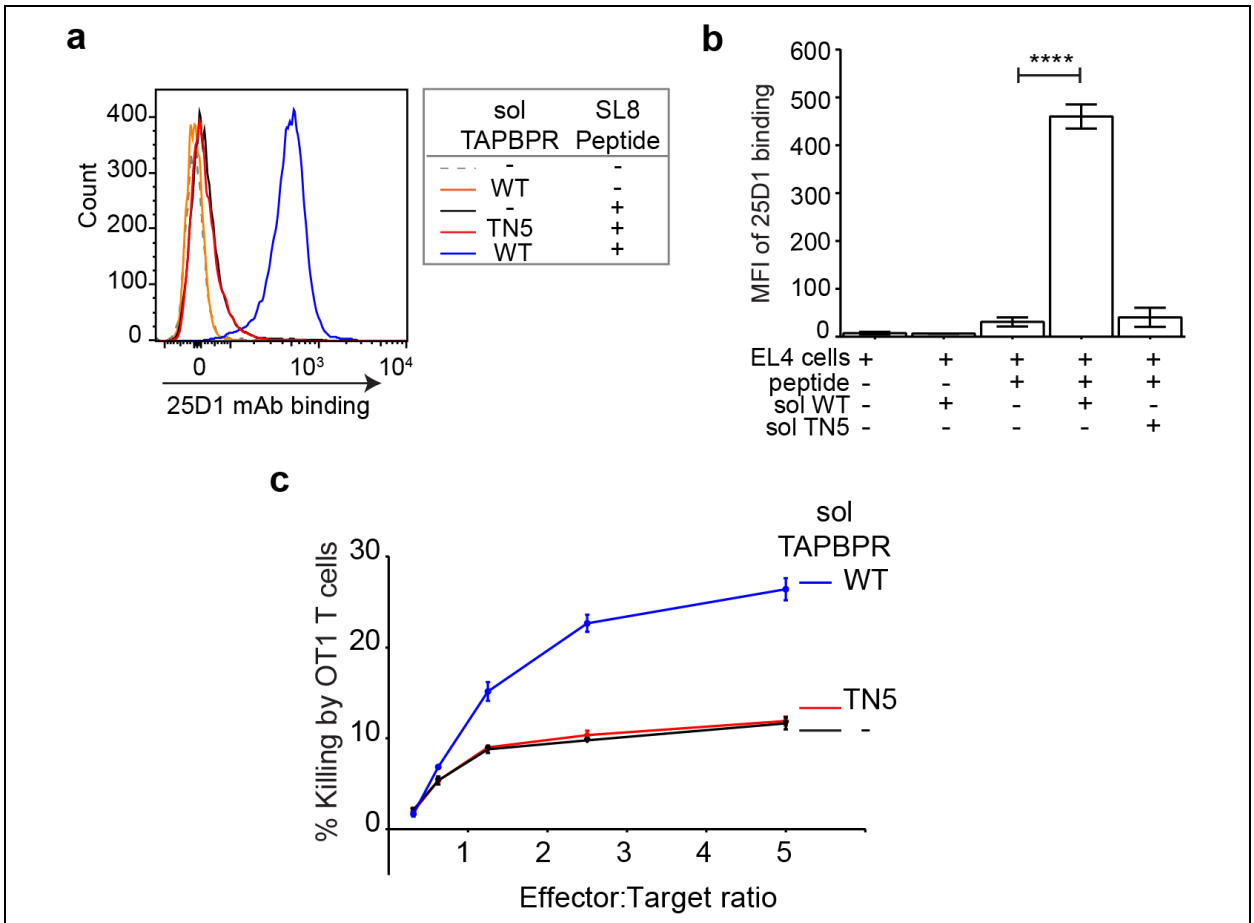

Figure 63: Soluble TAPBPR-mediated peptide loading enhances T cell killing of tumour cells. EL4 cells were incubated with or without 1 µM soluble TAPBPR^{WT} or TAPBPR^{TN5} and subsequently treated with or without 1 nM SIINFEKL peptide for 30 min. (**a** and **b**) Cells were then stained with the 25-D1.16 mAb, which recognizes SIINFEKL/H-2K^{b} complexes. (**a**) Histograms show levels of 25-D1.16 mAb binding and are representative of three independent experiments. (**b**) Bar graphs summarize the MFI of 25-D1.16 binding ± SD from three independent experiments. (**c**) % EL4 target cell killing by OT1 cells, at different cellular ratios, when target cells were treated as stated above. Error bars ± SEM from triplicate wells. Data are representative of three independent experiments. ****$P \leq 0.0001$ using unpaired two-tailed *t* test. Taken from Ilca et al. (Ilca et al., 2018b).

6.3. Discussion

Here, I showed that using soluble TAPBPR as a loading catalyst of immunogenic peptides onto MHC class I molecules expressed on the surface of tumour cells, of either human or mouse origin, induces their recognition and killing by $CD8^+$ T cells. This finding provides the foundation for exploring potential therapeutic applications of using TAPBPR for increasing the immunogenicity of tumours.

The initial observation that enabled us to explore the therapeutic potential of TAPBPR was the artefactual presence of TAPBPR at the surface of cells upon over-expression (Boyle et al., 2013). This finding enabled me to make the surprising discovery that TAPBPR present at the cell surface could function as an efficient peptide exchange catalyst on surface-expressed MHC class I molecules (**Chapter 3**). We then realized that we could exploit this property of TAPBPR to override the internal peptide editing and selection machinery, that naturally dictates which peptides are presented on MHC class I, by facilitating the loading of the desired peptides directly on surface MHC class I molecules.

In exploring the translational applications of this finding, one question that immediately followed was whether TAPBPR could be used to modulate $CD8^+$ T cell-mediate immune responses against specific target cell lines, by decorating them with highly immunogenic peptide antigens of choice. Of particular interest was the idea of enhancing the immune recognition of tumour cells. The recognition of immunogenic peptides presented on MHC class I molecules on the surface of tumour cells is crucial for the elimination of cancer by CTLs. While cancer cells do normally present such immunogenic peptides in the form of neoantigens, which arise *de novo* as tumour-specific mutations (Kawakami et al., 2004), for the majority of cancer types, presentation of neoantigens is likely to be low (Yadav et al., 2014, Kalaora et al., 2016). This is one of the reasons behind the low recognition and clearance of cancer cells by the immune system (Andersen et al., 2012). Therefore, increasing the availability of immunogenic peptides, such as neoantigens or viral antigens, on the surface of tumour cells, would represent a fundamental advance in enhancing the immune recognition of cancer. For this reason, using TAPBPR to efficiently promote the loading of highly immunogenic peptides onto cancer cells could represent a significant step forward in the field of tumour immunotherapies.

Here, I showed that using TAPBPR to facilitate the loading of exogenously-added viral peptides, reported to be highly immunogenic, onto different tumour cell lines, promotes their recognition and killing by primary $CD8^+$ T cells. However, despite the clear enhancement in T cell recognition of target cells in the presence of TAPBPR, much work needed to be done in optimising and troubleshooting the T cell assays in order to achieve this effect. One problem encountered while troubleshooting the T cell assays performed on human cells was the high proliferation rates of both HeLaM and MCF-7 cells during the incubation period with the T cells. Consequently, the target cell cultures would overgrow during the incubation period and hamper the fluorescence read-out of the experiment. To overcome this issue, we decided to irradiate the target cells immediately prior to incubating them with the T cells, to stop their proliferation without dramatically altering their overall physiology. This relatively common strategy used in T cell assays allowed for considerably better detection of fluorescent spots corresponding to stimulated T cells. It is worth mentioning that only the target cells where T cell activation was measured were irradiated, and not also the ones where actual killing by T cell was assessed.

Another hurdle arose after switching to mouse system, used for quantifying induction of T cell killing by soluble TAPBPR by measuring LDH release from target cells. Since the EL4 cells were highly sensitive to culturing and treatment conditions, they would often passively die during the incubation period of the experiment, even in the control condition, where no T cells were present. Due to the high level of LDH release from the cells in the negative control groups, it was impossible to quantify the effect of TAPBPR on T cell killing. To minimise passive cell death, I decided to wash and change the media of the target cells the night prior to the experiment and to reduce their exposure to different temperature and CO_2 proportion as much as possible throughout the experiment. This led to almost full survival of the target cells in the absence of T cells during the entire duration of the experiment, allowing for accurately quantifying TAPBPR-mediated T cell killing of EL4 cells.

7. Discussion

7.1. Summary of results

In this dissertation, I revealed that when given access to the cell surface, TAPBPR is capable of functioning on as a peptide exchange catalyst on surface expressed MHC class I molecules. I decided to use this system as a novel cellular assay for measuring the efficiency of TAPBPR-mediated peptide exchange on MHC class I molecules. This technique allowed me to demonstrate that the K22-D35 loop of TAPBPR is essential for its peptide exchange function and subsequently for its effect on peptide selection on specific MHC class I molecules such as HLA-A*68:02 and HLA-A*02:01. In particular, the L30 residue within the loop appears to be both necessary and sufficient for the ability of TAPBPR to efficiently dissociate peptides from MHC class I molecules that typically accommodate hydrophobic peptide residues in their F pocket. TAPBPR cannot mediate effective peptide exchange on MHC class I molecules with F pocket specificities for non-hydrophobic amino acids, due to the incompatibility of these F pockets with the L30 residue of TAPBPR. Following on from this, I investigated whether this compatibility model was generally applicable to a wide panel of HLA class I allomorphs, in determining their susceptibility to TAPBPR-mediated peptide editing. By screening a library of 97 HLA class I allotypes for their ability to interact with TAPBPR, I revealed that TAPBPR shows a strong preference for HLA-A, particularly for supertypes A2 and A24, over HLA-B and -C molecules. Moreover, the propensity of HLA class I molecules to undergo peptide editing by TAPBPR appears to heavily rely on the molecular properties of the MHC class I F pocket, specifically residues 114 and 116. Based on the findings resulted from my work, I proposed a novel catalytic model for the mechanism of TAPBPR-mediated peptide editing on MHC class I molecules. Finally, apart from using this novel cellular assay for addressing key fundamental questions regarding the catalytical mechanism and molecular properties of TAPBPR, I started exploring the potential translational applications enabled by this discovery. Namely, I showed that TAPBPR can be used to load highly immunogenic peptides of choice directly onto MHC class I molecules present on the surface of tumour cells, thus promoting their recognition and killing by CTLs. These findings open an interesting translational avenue of developing TAPBPR into a product with therapeutic potential, that would specifically target tumour and enhance their immunogenicity.

7.2. Developing an improved assay for assessing TAPBPR-mediated peptide editing on MHC class I molecules

Prior to this work, the peptide exchange activity of both tapasin and TAPBPR had been measured exclusively by cell-free assays. Namely, two techniques were developed more than ten years ago two assess the ability of tapasin to mediate peptide exchange on MHC class I molecules. One of them used recombinant tapasin-ERp57 disulfide-conjugated dimers and tested their ability to mediate exchange of iodinated peptides on MHC class I in a cell free system, whereas the other one involved artificially zippering tapasin to recombinant MHC class I refolds and measuring the dissociation of fluorescently-labelled peptides from MHC class I by fluorescence polarization experiments (Chen and Bouvier, 2007). Our lab and others had previously used an approach similar to the one developed by Chen and Bouvier to demonstrate that TAPBPR is also capable of facilitating peptide exchange on recombinant MHC class I refolds (Hermann et al., 2015b, Morozov et al., 2016); however, in contrast to tapasin, the luminal domain of TAPBPR alone, without the need of an artificial zipper, was sufficient for promoting peptide exchange on MHC class I in this system.

Since TAPBPR normally mediates peptide editing on glycosylated MHC class I molecules, in a cellular environment, I was interested in whether a more physiological system could be developed to assess TAPBPR-mediated peptide exchange on MHC class I. Despite the function of TAPBPR being naturally restricted to intracellular compartments, I show that, when artificially given access to the cell surface, TAPBPR can function as a peptide exchange catalyst on surface MHC class I molecules (Ilca et al., 2018b). By exploring a trafficking artefact of TAPBPR over-expression, namely its presence at the cell surface, I was able to design two novel assays for assessing the efficiency of TAPBPR-mediated peptide exchange on MHC class I molecules on a cellular membrane. These assays rely on flow cytometry measurements to quantify the effect of TAPBPR on the level of fluorescently-labelled peptide bound to cell surface MHC class I molecules. This technique thus carries several advantages over the previously established assay, using soluble TAPBPR and recombinant MHC class I refolds expressed in bacteria (Hermann et al., 2015b, Morozov et al., 2016). For instance, unlike the bacterial refolds, the MHC class I molecules present in the cellular system carry the naturally-occurring post-translational modifications, which were recently shown to strongly influence the interactions with TAPBPR (Neerincx and Boyle, 2018). Second, whereas recombinant MHC class I refolds are refolded with individual peptides of choice, the MHC class I molecules present at

the cell surface are loaded with a broad variety of peptides, over a wide affinity spectrum, which again, offers a considerably more accurate representation of the MHC class I pool that is naturally subjected to chaperone function in cells. Another consequence of the availability of a wide peptide pool on MHC class I over the presence of individual peptides of high affinity is the increased sensitivity of assaying the ability of a catalyst to dissociate the peptides. This is well reflected by the very low peptide dissociation rates from bacterial MHC class I refolds in the presence of TAPBPR, the reaction being not near equilibrium even after 6 hours (Hermann et al., 2015b). In contrast, the level of TAPBPR-mediated peptide exchange on cell surface MHC class I appears to saturate after only 15 minutes. Finally, by exploiting the cellular folding and trafficking machinery to express stable peptide-MHC class I complexes, the cellular assays overcome the challenge of manually expressing, refolding and purifying recombinant MHC class I molecules.

7.3. Peptide exchange mechanisms of TAPBPR on MHC class I

Regarding the molecular mechanisms by which TAPBPR catalyzes peptide dissociation from MHC class I molecules, I propose that TAPBPR uses its K22-D35 loop to displace the C-terminus of the peptide from the peptide binding groove of MHC class I (**Chapter 4** – published in (Ilca et al., 2018a)). More specifically, my findings suggest that a leucine residue along this loop, which is the only long hydrophobic residue of this region, is both necessary and sufficient for the ability of TAPBPR to efficiently dissociate peptides from MHC class I molecules that typically accommodate hydrophobic amino acid residues in their F pocket. Interestingly, the same loop does not seem to have a significant effect on the peptide exchange function of TAPBPR on MHC class I molecules with F pocket specificities for non-hydrophobic anchor residues. The differences observed in the loop-dependency of the catalytic function of TAPBPR across multiple MHC class I molecules are remarkable, especially considering the comparison between HLA-A*68:02 and HLA-A*68:01, which only differ in 5 amino acids, but have different F pocket specificities (Niu et al., 2013). Correspondingly, swapping the different residue around the F pocket between these two HLA class I molecules leads to a complete reverse in the ability of TAPBPR to bind and exchange peptides onto them.

While mutation of the loop significantly impairs the efficiency of TAPBPR-mediated peptide editing, TAPBPR seems to be capable, though to a considerably lower extent, of exchanging

peptides on MHC class I, even in the absence of the loop, across MHC class I molecules with different peptide specificities. This indicates that TAPBPR uses alternative catalytic mechanisms, which may rely on other regions of TAPBPR, such as the already-described "jack-hairpin" (Thomas and Tampe, 2017). Nevertheless, the loop-independent ability of TAPBPR to edit peptides seems to occur in a more generic and significantly less efficient manner and may be influenced more by the intrinsic ability of TAPBPR to interact with a particular MHC class I molecule or by the relative molecular plasticity of individual pMHC class I complexes. In other words, one can envisage that TAPBPR can associate, in a loop-independent manner, with MHC class I molecules loaded with peptides that are more prone to dissociation (i.e. sub-optimally loaded peptides).

Our findings suggest that TAPBPR appears to be using the loop, and particularly the L30 residue, to probe the content of the MHC class I groove in a highly dynamic manner. This would explain the ambiguities in the loop localization and conformation observed in the two crystal structures of TAPBPR in complex with MHC class I (Jiang et al., 2017, Thomas and Tampe, 2017). For instance, our data suggesting that the loop seems to facilitate dissociation of the peptide specifically at the F pocket region of the MHC class I groove would be particularly important for the structure where modifications were made to H-2D^{d} to help stabilize the F pocket (Jiang et al., 2017). This artificial stabilization of the MHC class I F pocket could have occluded the ability of the loop to insert into the groove.

Mechanistically, based on all data which I have managed to generate using this novel cellular peptide exchange assay, together with previous mechanistic views, I propose the following model of TAPBPR-mediated peptide editing on MHC class I (**Figure 64**). Whenever MHC class I molecules accessible by TAPBPR enter a state in which the bound peptide partially dissociates ("breathes") at the C-terminus from the F pocket (step 2 – **Figure 64**), TAPBPR binds to MHC class I, inserting its 22–35 loop into the peptide binding groove (step 3 – **Figure 64**). At this point, TAPBPR and MHC class I interact in a transient manner. The loop of TAPBPR samples the MHC class I groove, inserting its leucine 30 residue into the F pocket, if hydrophobic. The binding of the loop into the F pocket subsequently inhibits the reassociation of the C-terminal anchor residue of the peptide, in a competitive manner. The resulting high-free energy intermediate TAPBPR-MHC class I-peptide complex allows TAPBPR to pull the α2–1 region of the peptide binding groove away from the peptide, as captured in the crystal structures, forcing the MHC class I into a conformation to which it can bind more stably (step 4 – **Figure 64**). This

further prevents the reassociation of the C-terminus of the peptide to the MHC class I groove and thus facilitates its complete dissociation (step 5 – **Figure 64**). Due to its stable interaction with peptide-receptive MHC class I molecules, TAPBPR prevents these empty MHC class I molecules from unfolding ("crashing"), as they would normally do immediately after the bound peptide dissociates (Hulsmeyer et al., 2005). I speculate that this consequently facilitates binding of incoming peptides to MHC class I, with affinities above the threshold required to outcompete TAPBPR. This entire mechanism appears to share similar features with the "tug-of-war" model that was previously proposed for tapasin-mediated peptide exchange (Fisette et al., 2016).

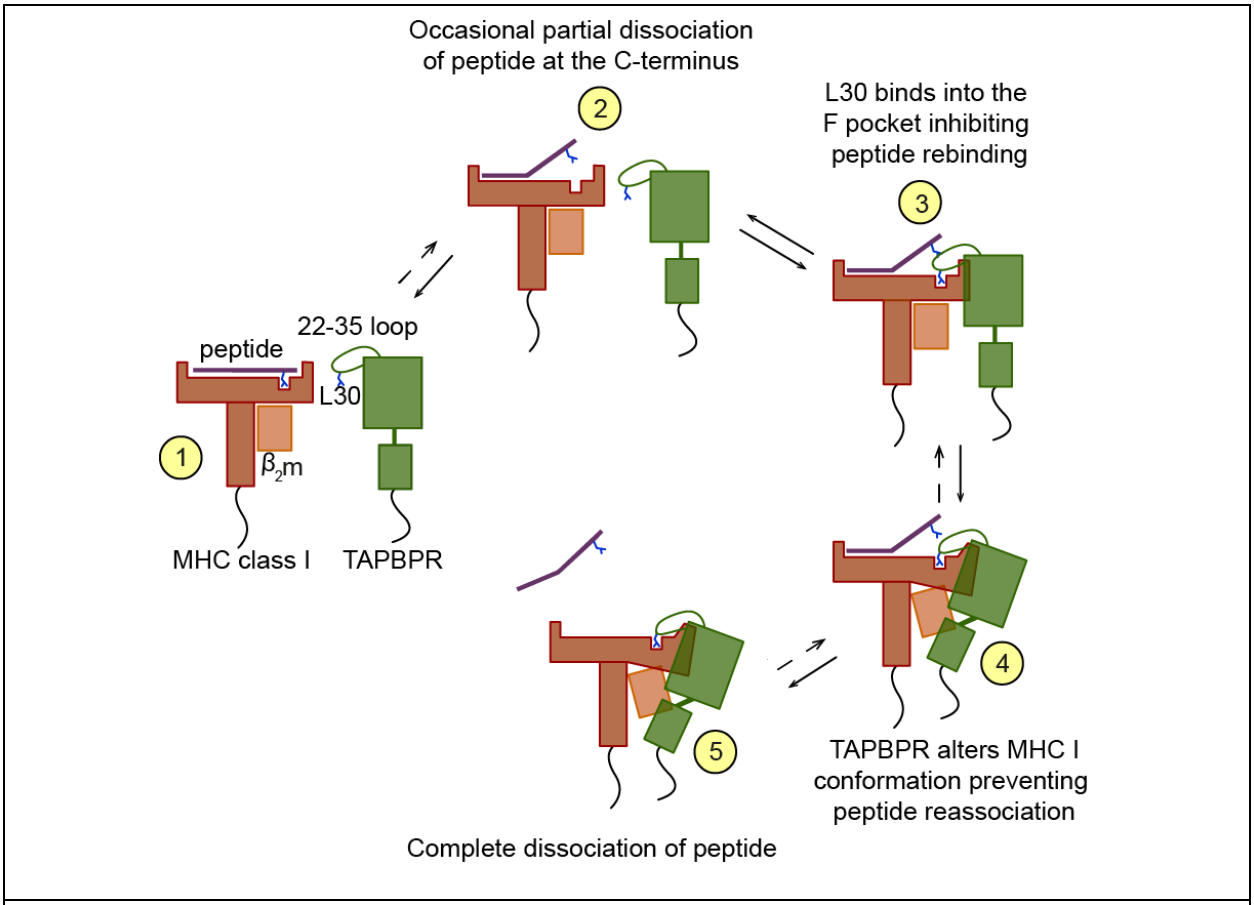

Figure 64: Proposed model of the peptide exchange mechanism on MHC class I molecules, catalyzed by TAPBPR, taken from Ilca et al. (Ilca et al., 2018a).

Based on the data from our lab and others, the molecular mechanisms of peptide editing by TAPBPR and tapasin appear to be relatively similar (Fisette et al., 2016, Ilca et al., 2018a, Jiang et al., 2017, McShan et al., 2018, Thomas and Tampe, 2017). First, both chaperones seem to display similar orientations when bound to MHC class I molecules and share similar MHC class I binding sites (Hermann et al., 2013). Second, in the two crystal structures, TAPBPR appears to

be pulling the α2-1 region of MHC class I away from the peptide (Jiang et al., 2017, Thomas and Tampe, 2017), property which was also predicted for tapasin based on molecular dynamics simulations (Fisette et al., 2016). Finally, recent work suggests that tapasin also relies on a homologous loop to the one of TAPBPR in performing efficient peptide editing on MHC class I molecules (Hafstrand et al., 2019) and, furthermore, this effect seems to also be facilitated by a leucine residue on the loop. However, in contrast to tapasin, my data suggests that the TAPBPR loop enables TAPBPR to facilitate the dissociation of peptides with relatively high affinity for MHC class I molecules (Ilca et al., 2018b, Ilca et al., 2018a). This data is consistent with our model that TAPBPR can mediate peptide editing on MHC class I molecules after tapasin (Neerincx and Boyle, 2017, Neerincx et al., 2017). Based on work presented in this dissertation and from other studies, I believe that while tapasin is essential for the efficient loading of MHC class I molecules with stably-bound peptides (Williams et al., 2002, Howarth et al., 2004), TAPBPR is considerably more efficient at dissociating stably-bound peptides from MHC class I molecules which have already passed through tapasin-mediated peptide loading (**Chapter 3** – published in (Ilca et al., 2018b))(Hermann et al., 2015b) but do not meet certain criteria for presentation at the cell surface.

7.4. Criteria used by TAPBPR in selecting peptides

Regardless of the exact cellular compartment(s) where TAPBPR facilitates peptide exchange on MHC class I molecules, currently, the precise selection criteria used by TAPBPR in selecting peptides on MHC class I for presentation remain largely enigmatic. In the case of tapasin, it has been rather well established that it promotes peptides exchange strictly based on affinity (Fisette et al., 2016, Howarth et al., 2004, Williams et al., 2002). Namely, tapasin was suggested to repeatedly mediate the dissociation of sub-optimally loaded peptides that get loaded onto peptide-receptive MHC class I molecules, until these MHC class I molecules acquire peptides of high enough affinity, which exceed the binding energy that tapasin needs to overcome in order to open the groove (Fisette et al., 2016). Moreover, once MHC class I molecules get loaded with high-affinity peptides, the PLC was shown to dissociate and, additionally, tapasin was shown to no longer be capable of accessing the resulting pMHC class I complex.

Unlike tapasin however, based on the work presented in this dissertation, TAPBPR seems to be capable of binding even to MHC class I molecules loaded with high-affinity peptides, such as the

ones present at the surface of cells, upon interferon stimulation (**Figures 18, 26 and 27**). Moreover, when given access to this pool of stable pMHC class I complexes, TAPBPR dissociates the bound high-affinity peptides in a highly rapid and efficient manner (**Figure 18**). Efficient dissociation by TAPBPR has also been directly observed for fluorescent derivatives of high-affinity neoantigens or self-peptides (**Figure 13**) that were naturally shown to be presented on MHC class I at the cell surface.

There is little indication of how the observed ability of TAPBPR to dissociate peptides from MHC class I molecules at the cell surface, or in solution for that matter, would relate to its catalytic function performed intracellularly. In order to gain deeper understanding in the biochemical and biophysical characteristics that make a specific peptide, loaded on MHC class I, prone to dissociation by TAPBPR, one would need to more thoroughly compare the immuno-peptidomes presented on individual MHC class I allotypes, in the presence or absence of TAPBPR. The caveat of this approach however is that knocking out TAPBPR would potentially also alter UGT1-mediated quality control of MHC class I molecules, or, on the opposite, the effect of knocking out TAPBPR on the peptide repertoire could be partially compensated by UGT1 (Neerincx et al., 2017, Zhang et al., 2011). An alternative approach to this question, although less physiologically-relevant, would be assess the effect of adding soluble TAPBPR directly onto the cell surface on the peptide repertoire presented on MHC class I. This would inform on the specific MHC class I-loaded peptides which TAPBPR alone is capable of dissociating, without any interference caused by other components of the pathway.

7.5. Allelic preference of TAPBPR for MHC class I molecules

7.5.1. Molecular basis

Consistent with our mechanistic model of TAPBPR-mediated peptide exchange on MHC class I molecules is the striking preference of TAPBPR for HLA class I allotypes that naturally accommodate hydrophobic residues in their F pocket. Interestingly however, although many HLA class I allotypes, particularly belonging to the HLA-B and -C groups, appear to interact weakly with TAPBPR and do not undergo TAPBPR-mediated peptide editing in an efficient manner. Therefore, while the overall specificity of the F pocket seems to be necessary for the

susceptibility of class I molecules to peptide editing by TAPBPR, it appears to be too vague to represent the sole selection criteria of TAPBPR for HLA class I.

According to our study, it is not only the specificity of the F pocket that drives HLA class I susceptibility to peptide editing by TAPBPR, but also the molecular architecture of this region. Namely, there is a perfect correlation between presence of the HxY motif at positions 114-116 in the F pocket region and the efficient interactions of HLA class I with TAPBPR. Interestingly, this motif is conserved across all known members of the HLA-A2 and -A24 superfamilies (Robinson et al., 2015), molecules which display high susceptibility to TAPBPR function. Moreover, these residues are not present in any other HLA-A allotype, nor in any HLA-B and -C molecules, all of which form very weak interactions with TAPBPR. This motif is also absent in all non-classical HLA class I molecules (Robinson et al., 2015). Further supporting the impact of the HxY motif at positions 114-116 is that reconstitution of these residues in HLA class I molecules which interact weakly with TAPBPR considerably enhances their ability to associate with, and undergo peptide editing by TAPBPR.

Regarding our understanding of the molecular basis of HLA class I susceptibility to TAPBPR function, my findings thus far support the idea that compatibility between the 22-35 loop, and particularly of residue L30, of TAPBPR and the F pocket of HLA class I drives efficient TAPBPR-peptide editing. Therefore, I believe that TAPBPR facilitates peptide dissociation from MHC class I molecules in a “lock-and-key” model and consequently speculate that the intracellular effect of TAPBPR on shaping the peptide repertoire presented by MHC class I molecules occurs in a highly allele-specific manner.

7.5.2. Comparison to tapasin

Interestingly, studies exploring tapasin have suggested the same residues, on positions 114 and 116, to be particularly important for the dependence of different HLA class I molecules on tapasin, in terms of their ability to efficiently present peptides at the cell surface (Park et al., 2003, Williams et al., 2002, Rizvi et al., 2014). However, these findings on tapasin have mainly focused on HLA-B molecules and have not yet identified a conserved motif or architecture of the F pocket region of MHC class I as a general driving feature for tapasin dependency. It is also important to point out that the studies investigating MHC class I dependency on tapasin have thus far only relied on indirect approaches, such as measuring the effect of knocking-out

tapasin on the surface expression levels of MHC class I molecules. However, it is widely accepted that absence of tapasin also destabilizes TAP (Lehner et al., 1998) and thus alters the peptide pool available for loading on MHC class I molecules, potentially to a different degrees across different HLA class I allotypes.

Furthermore, there does not seem to be any specific group or category of HLA class I molecules showing a clearly increased tapasin dependency compared to the rest. Namely, tapasin does not seem to differentiate among HLA class I allotypes based on criteria such as peptide binding specificity or molecular signatures along the peptide binding groove. Instead, Springer and colleagues have proposed that tapasin functions preferentially on MHC class I molecules with a high degree of molecular plasticity, particularly around the F pocket region (Sieker et al., 2007, Sieker et al., 2008).

7.6. Biological explanation for allelic dependency of HLA class I on TAPBPR-mediated peptide editing

7.6.1. Preference of TAPBPR for HLA-A2 and -A24 supertypes

The molecular basis of the observed preference of TAPBPR for this select group of HLA class I allotypes raises the next obvious question regarding the biological explanation for this phenomenon. One potential biological reason for this preference could be that the HLA molecules of the A2 and A24 superfamilies might have access to significantly wider peptide pools, which can fit their individual binding motifs, within the ER lumen. This could be a result of either a wider availability of peptides carrying hydrophobic amino acids at their C-terminus inside the ER or to an increased promiscuity in the peptide binding grooves of HLA-A2 and -A24 superfamily members, allowing these specific HLA molecules to naturally accommodate a broader variety of peptides. Thus, these HLA class I allotypes could in principle require an additional peptide selection checkpoint, potentially represented by TAPBPR, in order to further refine their peptide repertoire presented for recognition.

Another possible explanation for this observed preference of TAPBPR could be that this particular group of HLA-A molecules that interacts more strongly with TAPBPR might potentially also be the one that is relatively less dependent on tapasin-mediated peptide editing. Although

allelic-dependency of HLA class I on tapasin remains to be thoroughly investigated, this scenario would support the compensatory relationship between TAPBPR and tapasin on MHC class I rather than their successive, synergistic effect on peptide selection.

The lower propensity of HLA-B and HLA-C molecules to undergo peptide editing by TAPBPR could also be due to the fact that they may naturally require less peptide editing compared to HLA-A molecules. This could be a consequence of their stronger recognition by KIRs (**Figure 65**), which has been proposed to occur in a much less antigen-specific manner than recognition by TCRs (Natarajan et al., 2002). However, this scenario would mainly be applicable for HLA-C molecules, as they are primarily involved in recognition by KIRs, while their involvement in T cell-mediated immune responses in still poorly defined (Blais et al., 2011). HLA-B molecules on the other hand, despite their broader recognition by KIRs compared to HLA-A molecules (Colonna and Samaridis, 1995), are also heavily involved in generating $CD8^+$ T cell-based immune responses and hence in the recognition by TCRs. This would argue against chaperone-mediated peptide editing and selection being less important for HLA-B than for HLA-A molecules.

Overall, while the biological explanation for the observed preference of TAPBPR for HLA-A molecules, particularly the ones belonging to the A2 and A24 supertypes, over HLA-B and -C molecules remains largely enigmatic, it appears that these findings have introduced an additional layer of complexity in HLA class I biology.

7.6.2. Impact of TAPBPR on susceptibility to HLA-associated diseases

Interestingly, subtle polymorphisms occurring in specific HLA class I molecules associated with disease susceptibility impact their propensity to undergo peptide exchange by TAPBPR. Across the multitude of HLA-B27 subtypes, HLA-B*27:05 and -B*27:04 display a strong association with ankylosing spondylitis, while HLA-B*27:06 and HLA-B*27:09, are either not associated at all or only weakly associated with ankylosing spondylitis (Fiorillo et al., 2003, Brown, 2010). Through my work here, I reveal that HLA-B*27:05 and -B*27:09, molecules that differ in residue 116 alone, appear to be differently susceptible to undergoing peptide editing by TAPBPR. In other words, natural variations in residue 116 among HLA-B27 molecules, which seems to correlate with disease association (Fiorillo et al., 2003, Brown, 2010), appear to also influence their level of peptide editing by TAPBPR. Moreover, I reveal that a similar subtle polymorphism

in residue 116 alone between two HLA class I allotypes that were shown to enable different progression rates of HIV, namely HLA-B*35:01 and -B*35:03 (Gao et al., 2001), also impacts their propensity to undergo peptide editing by TAPBPR.

It is important to consider that the assays which I used to address these questions measure the capacity of TAPBPR to catalyse peptide exchange on HLA class I molecules expressed on the surface of cells, molecules which have already been selected intracellularly by quality control checkpoints. Therefore, the observed differences in the magnitude of TAPBPR-mediated peptide editing between these HLA class I allotypes is likely to be considerably greater when assessed in its natural intracellular setting. Since the level of peptide selection on these HLA class I molecules most likely contributes to their association with both ankylosing spondylitis and HIV progression, my findings could provide new insight regarding the mechanism by which apparently subtle variations in HLA I may play a significant role in disease susceptibility.

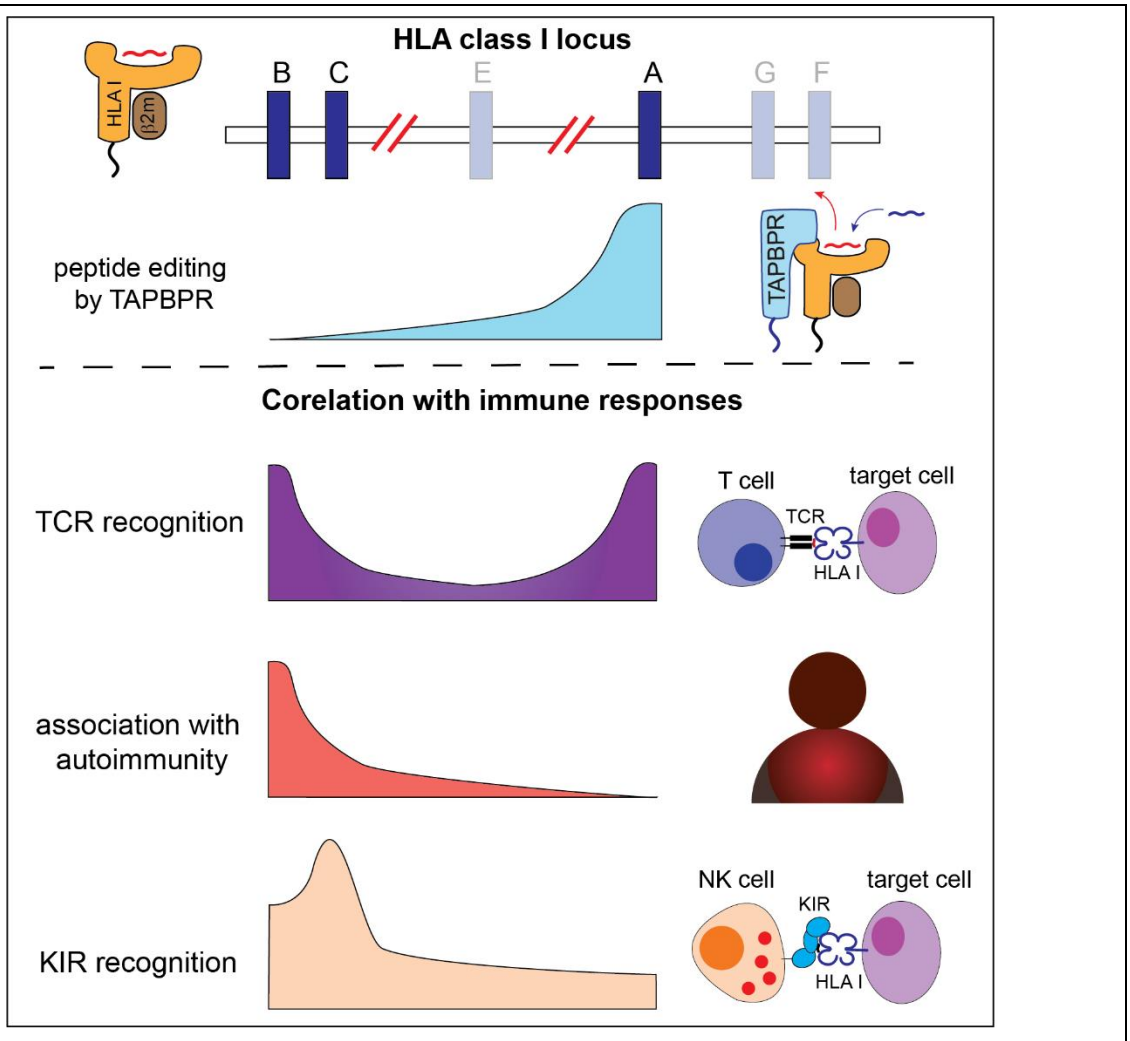

Figure 65: Varying susceptibility of classical HLA class I molecules to peptide editing by TAPBPR and its correlation with differences in immune responses.

7.7. Potential role of TAPBPR in the MHC class I pathway

7.7.1. Function of TAPBPR inside the ER

Despite TAPBPR appearing to be an efficient peptide editor on MHC class I, outside of the PLC (Hermann et al., 2015b, Morozov et al., 2016), TAPBPR cannot compensate for the absence of tapasin, with respect to the efficient loading of MHC class I molecules with high affinity peptides (Boyle et al., 2013). However, this might be an effect of the destabilization of TAP in the absence of tapasin, which would impair the abundance of peptides available for loading, potentially by TAPBPR, onto peptide-receptive MHC class I molecules. On the other hand, TAPBPR was suggested to localize in different sub-compartments of the ER compared to tapasin and TAP, and thus away from the peptide points of peptide influx into the ER (Hermann et al., 2015a, Neerincx et al., 2017). This favors the idea that the role of TAPBPR is more in dissociating peptides from MHC class I molecules already loaded with peptide by the PLC, functioning as a proof-reader instead of as a peptide-loader.

The role of TAPBPR in peptide selection on MHC class I molecules following their peptide loading by the PLC is further supported by the observed interaction of TAPBPR with UGT1 (Neerincx et al., 2017), enzyme which has been previously shown to proof-read MHC class I molecules prior to their export from the ER (Zhang et al., 2011, Wearsch et al., 2011). Finally, consistent with this recycling model of MHC class I molecules from TAPBPR, via UGT1, back to the PLC, absence of TAPBPR has been shown to reduce the interaction of MHC class I molecules with the PLC as well as to increase export rate of MHC class I molecule from the ER (Boyle et al., 2013).

7.7.2. Function of TAPBPR outside the ER

Despite being mainly present inside the ER, TAPBPR has been also shown to interact with MHC class I outside of the ER (Boyle et al., 2013). Moreover, I have shown in this dissertation that, upon over-expression, TAPBPR interacts with MHC class I molecules present at the cell surface. The ability of TAPBPR to interact with MHC class I in different sub-cellular compartments, independently of additional factors, suggest that TAPBPR might be affecting/regulating the trafficking on MHC class I molecules through the export pathway. This idea would be further supported by data from my work and from previous studies, according to which over-

expression of TAPBPR downregulates surface expression of MHC class I molecules (**Figure 5**) (Boyle et al., 2013). This work raises a few interesting questions regarding the interdependence of MHC class I and TAPBPR in their anterograde trafficking.

In future studies, it would be useful to better understand the biological reason behind this phenomenon. I currently speculate that, given its ability to traffic in complex with MHC class I and to edit peptides at different cellular locations, TAPBPR might facilitate peptide exchange on MHC class I in endosomal compartments, for the biological purpose of cross-presentation via the vacuolar pathway (**Figure 66**). I base my speculation on a number of factors which seem in accordance with one-another. First, we have shown that TAPBPR traffics in complex with MHC class I through the medial Golgi (Boyle et al., 2013), however presence of TAPBPR has never been detected at the cell surface. Thus, the most obvious trafficking route of TAPBPR in complex with MHC class I would be through endosomal compartments. Second, the capacity of TAPBPR to edit peptide on MHC class I molecules in a cell, but outside of the ER, would allow TAPBPR to catalyze the exchange of endogenous peptide bound to MHC class I for exogenously-derived peptides internalized by pinocytosis. In fact, one of the few sub-cellular compartments where TAPBPR-bound MHC class I molecules would have access to an abundance of peptides outside of the ER would be the endosomes rich in peptides of exogenous origin. If TAPBPR will be indeed proven in the future to be the directly involved in MHC class I molecules acquiring exogenous peptides for cross-presentation, it would imply that TAPBPR fulfils a similar role on MHC class I as the one of HLA-DM on MHC class II molecules.

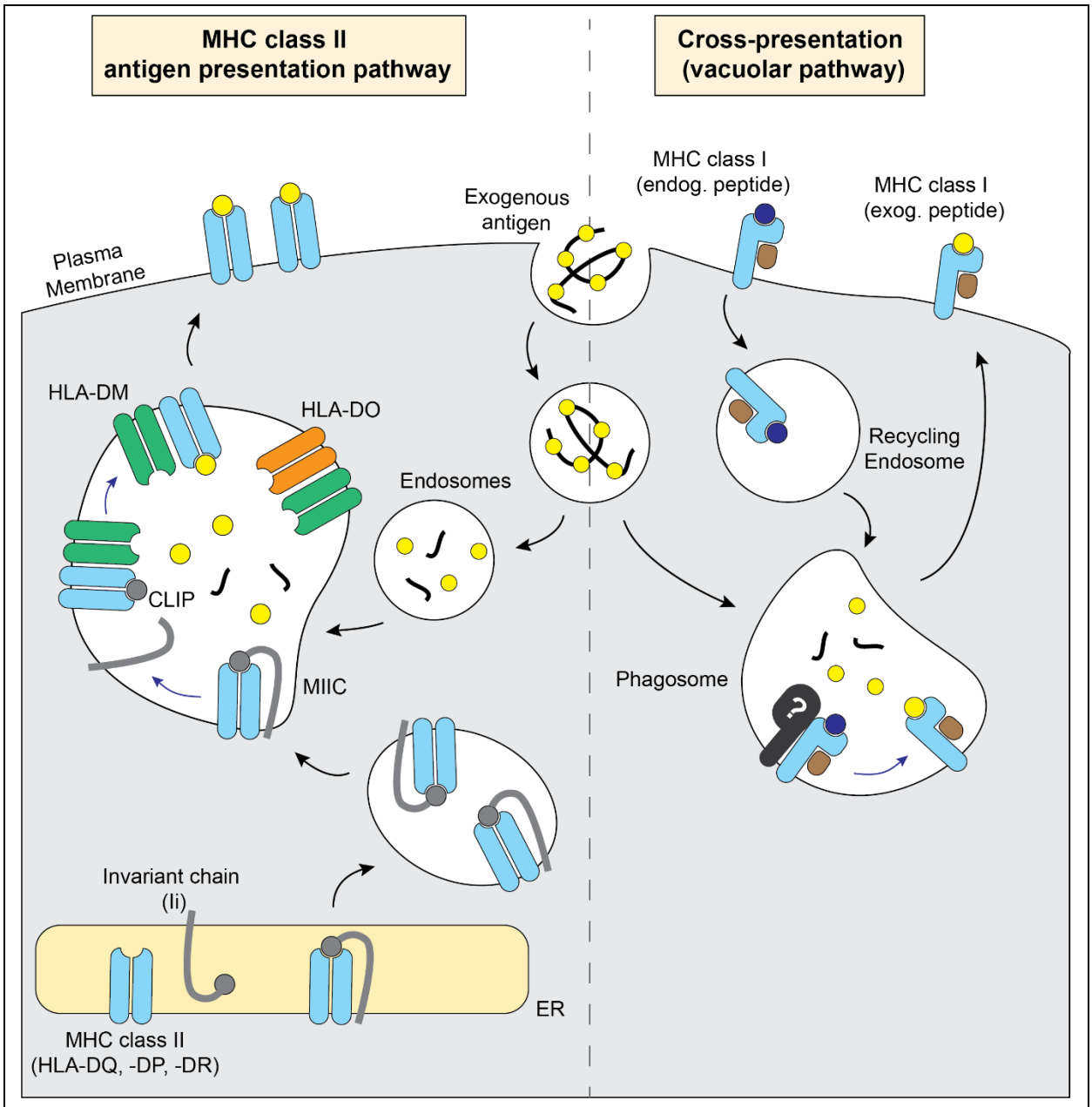

Figure 66: Similarities between the role of HLA-DM in the MHC class II pathway and the potential involvement of TAPBPR in the vacuolar pathway of cross-presentation.

7.8. Potential therapeutic application of TAPBPR against cancer

Apart from the contribution of the findings described here thus far towards the fundamental understanding of the biological role of TAPBPR in the MHC class I antigen presentation pathway and hence in the generation of adaptive immune responses, perhaps the most fascinating implication of my work is the translational potential of using TAPBPR to load immunogenic peptides onto the surface of tumour cells, in order to target them for recognition by CTLs. Recent advances in the development of tumour immunotherapies have highlighted the

potential of exploiting CTL-mediated immune responses in eliminating cancer. Crucial for developing efficient CTL-mediated elimination of cancer is the recognition of immunogenic peptides presented on MHC class I molecules at the surface of tumour cells. Neoantigens, which are mutated versions of self-derived peptides, arisen *de novo* from tumour-specific mutations (Kawakami et al., 2004), are considered optimal targets for recognition by CTLs, as they are only present in cancer cells and therefore avoid central tolerance. However, their presentation on MHC class I is generally low and they are only present in cancer types with high mutational burden (Yadav et al., 2014, Kalaora et al., 2016). Therefore, a fundamental step forward in overcoming the low immunogenicity observed in tumour cells would to increase the expression levels of such neoantigens or to induce presentation of foreign antigens that are highly immunogenic, such as ones derived from viruses. Conclusively, the observed ability of TAPBPR to load immunogenic peptides, either viral or neoantigens, onto the surface of different cancer cell lines highlights a potential therapeutic application of using TAPBPR to increase tumour immunogenicity. Provided that one could achieve efficient targeting of TAPBPR specifically to tumour cells (e.g. in a similar manner as designing chimeric antigen receptors (CARs) for the engineering of CAR-T cells), this may represent a significant advance in the field of cancer immunotherapies, with the potential of improving treatment outcomes in patients with cancer types resistant to currently-existing therapies.

8. References

ANDERSEN, R. S., THRUE, C. A., JUNKER, N., LYNGAA, R., DONIA, M., ELLEBAEK, E., SVANE, I. M., SCHUMACHER, T. N., THOR STRATEN, P. & HADRUP, S. R. 2012. Dissection of T-cell antigen specificity in human melanoma. *Cancer Res,* 72**,** 1642-50.

APPS, R., MURPHY, S. P., FERNANDO, R., GARDNER, L., AHAD, T. & MOFFETT, A. 2009. Human leucocyte antigen (HLA) expression of primary trophoblast cells and placental cell lines, determined using single antigen beads to characterize allotype specificities of anti-HLA antibodies. *Immunology,* 127**,** 26-39.

BAKKE, O. & DOBBERSTEIN, B. 1990. MHC class II-associated invariant chain contains a sorting signal for endosomal compartments. *Cell,* 63**,** 707-16.

BARNSTABLE, C. J., BODMER, W. F., BROWN, G., GALFRE, G., MILSTEIN, C., WILLIAMS, A. F. & ZIEGLER, A. 1978. Production of monoclonal antibodies to group A erythrocytes, HLA and other human cell surface antigens-new tools for genetic analysis. *Cell,* 14**,** 9-20.

BEISSBARTH, T., SUN, J., KAVATHAS, P. B. & ORTMANN, B. 2000. Increased efficiency of folding and peptide loading of mutant MHC class I molecules. *Eur J Immunol,* 30**,** 1203-13.

BEVAN, M. J. 1976a. Cross-priming for a secondary cytotoxic response to minor H antigens with H-2 congenic cells which do not cross-react in the cytotoxic assay. *J Exp Med,* 143**,** 1283-8.

BEVAN, M. J. 1976b. Minor H antigens introduced on H-2 different stimulating cells cross-react at the cytotoxic T cell level during in vivo priming. *J Immunol,* 117**,** 2233-8.

BJORKMAN, P. J., SAPER, M. A., SAMRAOUI, B., BENNETT, W. S., STROMINGER, J. L. & WILEY, D. C. 1987. Structure of the human class I histocompatibility antigen, HLA-A2. *Nature,* 329**,** 506-12.

BLAIS, M. E., DONG, T. & ROWLAND-JONES, S. 2011. HLA-C as a mediator of natural killer and T-cell activation: spectator or key player? *Immunology,* 133**,** 1-7.

BLANCHARD, N., GONZALEZ, F., SCHAEFFER, M., JONCKER, N. T., CHENG, T., SHASTRI, A. J., ROBEY, E. A. & SHASTRI, N. 2008. Immunodominant, protective response to the parasite Toxoplasma gondii requires antigen processing in the endoplasmic reticulum. *Nat Immunol,* 9**,** 937-44.

BLEES, A., JANULIENE, D., HOFMANN, T., KOLLER, N., SCHMIDT, C., TROWITZSCH, S., MOELLER, A. & TAMPE, R. 2017. Structure of the human MHC-I peptide-loading complex. *Nature,* 551**,** 525-528.

BLUM, J. S., WEARSCH, P. A. & CRESSWELL, P. 2013. Pathways of antigen processing. *Annu Rev Immunol,* 31**,** 443-73.

BODMER, W. F. 1987. The HLA system: structure and function. *J Clin Pathol,* 40**,** 948-58.

BOYLE, L. H., HERMANN, C., BONAME, J. M., PORTER, K. M., PATEL, P. A., BURR, M. L., DUNCAN, L. M., HARBOUR, M. E., RHODES, D. A., SKJODT, K., LEHNER, P. J. & TROWSDALE, J. 2013. Tapasin-related protein TAPBPR is an additional component of the MHC class I presentation pathway. *Proc Natl Acad Sci U S A,* 110**,** 3465-70.

BREUER, W., EPSZTEJN, S. & CABANTCHIK, Z. I. 1995. Iron acquired from transferrin by K562 cells is delivered into a cytoplasmic pool of chelatable iron(II). *J Biol Chem,* 270**,** 24209-15.

BROWN, M. A. 2010. Genetics of ankylosing spondylitis. *Curr Opin Rheumatol,* 22**,** 126-32.

BROWN, M. G., DRISCOLL, J. & MONACO, J. J. 1991. Structural and serological similarity of MHC-linked LMP and proteasome (multicatalytic proteinase) complexes. *Nature,* 353**,** 355-7.

CAMPBELL, R. D. & TROWSDALE, J. 1993. Map of the human MHC. *Immunol Today,* 14**,** 349-52.

CARBONE, F. R., STERRY, S. J., BUTLER, J., RODDA, S. & MOORE, M. W. 1992. T cell receptor alpha-chain pairing determines the specificity of residue 262 within the Kb-restricted, ovalbumin257-264 determinant. *Int Immunol,* 4**,** 861-7.

CELLA, M., DOHRING, C., SAMARIDIS, J., DESSING, M., BROCKHAUS, M., LANZAVECCHIA, A. & COLONNA, M. 1997. A novel inhibitory receptor (ILT3) expressed on monocytes, macrophages, and dendritic cells involved in antigen processing. *J Exp Med,* 185**,** 1743-51.

CHANG, S. C., MOMBURG, F., BHUTANI, N. & GOLDBERG, A. L. 2005. The ER aminopeptidase, ERAP1, trims precursors to lengths of MHC class I peptides by a "molecular ruler" mechanism. *Proc Natl Acad Sci U S A,* 102**,** 17107-12.

CHAPMAN, D. C. & WILLIAMS, D. B. 2010. ER quality control in the biogenesis of MHC class I molecules. *Semin Cell Dev Biol,* 21**,** 512-9.

CHEN, M. & BOUVIER, M. 2007. Analysis of interactions in a tapasin/class I complex provides a mechanism for peptide selection. *EMBO J,* 26**,** 1681-90.

CHO, S. G., ATTAYA, M. & MONACO, J. J. 1991. New class II-like genes in the murine MHC. *Nature,* 353**,** 573-6.

COLONNA, M., NAVARRO, F., BELLON, T., LLANO, M., GARCIA, P., SAMARIDIS, J., ANGMAN, L., CELLA, M. & LOPEZ-BOTET, M. 1997. A common inhibitory receptor for major histocompatibility complex class I molecules on human lymphoid and myelomonocytic cells. *J Exp Med,* 186**,** 1809-18.

COLONNA, M. & SAMARIDIS, J. 1995. Cloning of immunoglobulin-superfamily members associated with HLA-C and HLA-B recognition by human natural killer cells. *Science,* 268**,** 405-8.

COSMAN, D., FANGER, N., BORGES, L., KUBIN, M., CHIN, W., PETERSON, L. & HSU, M. L. 1997. A novel immunoglobulin superfamily receptor for cellular and viral MHC class I molecules. *Immunity,* 7**,** 273-82.

CRESSWELL, P., BLUM, J. S., KELNER, D. N. & MARKS, M. S. 1987. Biosynthesis and processing of class II histocompatibility antigens. *Crit Rev Immunol,* 7**,** 31-53.

DE LA ROCHE, M., RITTER, A. T., ANGUS, K. L., DINSMORE, C., EARNSHAW, C. H., REITER, J. F. & GRIFFITHS, G. M. 2013. Hedgehog signaling controls T cell killing at the immunological synapse. *Science,* 342**,** 1247-50.

DE LA SALLE, H., SAULQUIN, X., MANSOUR, I., KLAYME, S., FRICKER, D., ZIMMER, J., CAZENAVE, J. P., HANAU, D., BONNEVILLE, M., HOUSSAINT, E., LEFRANC, G. & NAMAN, R. 2002. Asymptomatic deficiency in the peptide transporter associated to antigen processing (TAP). *Clin Exp Immunol,* 128**,** 525-31.

DENZIN, L. K. & CRESSWELL, P. 1995. HLA-DM induces CLIP dissociation from MHC class II alpha beta dimers and facilitates peptide loading. *Cell,* 82**,** 155-65.

DENZIN, L. K., SANT'ANGELO, D. B., HAMMOND, C., SURMAN, M. J. & CRESSWELL, P. 1997. Negative regulation by HLA-DO of MHC class II-restricted antigen processing. *Science,* 278**,** 106-9.

DEVERSON, E. V., GOW, I. R., COADWELL, W. J., MONACO, J. J., BUTCHER, G. W. & HOWARD, J. C. 1990. MHC class II region encoding proteins related to the multidrug resistance family of transmembrane transporters. *Nature,* 348**,** 738-41.

DICK, T. P., BANGIA, N., PEAPER, D. R. & CRESSWELL, P. 2002. Disulfide bond isomerization and the assembly of MHC class I-peptide complexes. *Immunity,* 16**,** 87-98.

DONG, G., WEARSCH, P. A., PEAPER, D. R., CRESSWELL, P. & REINISCH, K. M. 2009. Insights into MHC class I peptide loading from the structure of the tapasin-ERp57 thiol oxidoreductase heterodimer. *Immunity,* 30**,** 21-32.

DRISCOLL, J., BROWN, M. G., FINLEY, D. & MONACO, J. J. 1993. MHC-linked LMP gene products specifically alter peptidase activities of the proteasome. *Nature,* 365**,** 262-4.

DU PASQUIER, L. 2000. The phylogenetic origin of antigen-specific receptors. *Curr Top Microbiol Immunol,* 248**,** 160-85.

EISENLOHR, L. C., HUANG, L. & GOLOVINA, T. N. 2007. Rethinking peptide supply to MHC class I molecules. *Nat Rev Immunol,* 7**,** 403-10.

ELLIOTT, T. 1997. How does TAP associate with MHC class I molecules? *Immunol Today,* 18**,** 375-9.

ELLIOTT, T. & WILLIAMS, A. 2005. The optimization of peptide cargo bound to MHC class I molecules by the peptide-loading complex. *Immunol Rev,* 207**,** 89-99.

EMMRICH, F., STRITTMATTER, U. & EICHMANN, K. 1986. Synergism in the activation of human CD8 T cells by cross-linking the T-cell receptor complex with the CD8 differentiation antigen. *Proc Natl Acad Sci U S A,* 83**,** 8298-302.

ENG, J. K., MCCORMACK, A. L. & YATES, J. R. 1994. An approach to correlate tandem mass spectral data of peptides with amino acid sequences in a protein database. *J Am Soc Mass Spectrom,* 5**,** 976-89.

EVANS, D. M., SPENCER, C. C., POINTON, J. J., SU, Z., HARVEY, D., KOCHAN, G., OPPERMANN, U., DILTHEY, A., PIRINEN, M., STONE, M. A., APPLETON, L., MOUTSIANAS, L., LESLIE, S., WORDSWORTH, T., KENNA, T. J., KARADERI, T., THOMAS, G. P., WARD, M. M., WEISMAN, M. H., FARRAR, C., BRADBURY, L. A., DANOY, P., INMAN, R. D., MAKSYMOWYCH, W., GLADMAN, D., RAHMAN, P., SPONDYLOARTHRITIS RESEARCH CONSORTIUM OF, C., MORGAN, A., MARZO-ORTEGA, H., BOWNESS, P., GAFFNEY, K., GASTON, J. S., SMITH, M., BRUGES-ARMAS, J., COUTO, A. R., SORRENTINO, R., PALADINI, F., FERREIRA, M. A., XU, H., LIU, Y., JIANG, L., LOPEZ-LARREA, C., DIAZ-PENA, R., LOPEZ-VAZQUEZ, A., ZAYATS, T., BAND, G., BELLENGUEZ, C., BLACKBURN, H., BLACKWELL, J. M., BRAMON, E., BUMPSTEAD, S. J., CASAS, J. P., CORVIN, A., CRADDOCK, N., DELOUKAS, P., DRONOV, S., DUNCANSON, A., EDKINS, S., FREEMAN, C., GILLMAN, M., GRAY, E., GWILLIAM, R., HAMMOND, N., HUNT, S. E., JANKOWSKI, J., JAYAKUMAR, A., LANGFORD, C., LIDDLE, J., MARKUS, H. S., MATHEW, C. G., MCCANN, O. T., MCCARTHY, M. I., PALMER, C. N., PELTONEN, L., PLOMIN, R., POTTER, S. C., RAUTANEN, A., RAVINDRARAJAH, R., RICKETTS, M., SAMANI, N., SAWCER, S. J., STRANGE, A., TREMBATH, R. C., VISWANATHAN, A. C., WALLER, M., WESTON, P., WHITTAKER, P., WIDAA, S., WOOD, N. W., MCVEAN, G., REVEILLE, J. D., WORDSWORTH, B. P., BROWN, M. A., DONNELLY, P., AUSTRALO-ANGLO-AMERICAN SPONDYLOARTHRITIS, C. & WELLCOME TRUST CASE CONTROL, C. 2011. Interaction between ERAP1 and HLA-B27 in ankylosing spondylitis implicates peptide handling in the mechanism for HLA-B27 in disease susceptibility. *Nat Genet,* 43**,** 761-7.

FALK, K., ROTZSCHKE, O., STEVANOVIC, S., JUNG, G. & RAMMENSEE, H. G. 1991. Allele-specific motifs revealed by sequencing of self-peptides eluted from MHC molecules. *Nature,* 351**,** 290-6.

FIORILLO, M. T., CAULI, A., CARCASSI, C., BITTI, P. P., VACCA, A., PASSIU, G., BETTOSINI, F., MATHIEU, A. & SORRENTINO, R. 2003. Two distinctive HLA haplotypes harbor the B27 alleles negatively or positively associated with ankylosing spondylitis in Sardinia: implications for disease pathogenesis. *Arthritis Rheum,* 48**,** 1385-9.

FIORILLO, M. T., GRECO, G., MARAGNO, M., POTOLICCHIO, I., MONIZIO, A., DUPUIS, M. L. & SORRENTINO, R. 1998. The naturally occurring polymorphism Asp116-->His116, differentiating the ankylosing spondylitis-associated HLA-B*2705 from the non-associated HLA-B*2709 subtype, influences peptide-specific CD8 T cell recognition. *Eur J Immunol,* 28**,** 2508-16.

FISETTE, O., WINGBERMUHLE, S., TAMPE, R. & SCHAFER, L. V. 2016. Molecular mechanism of peptide editing in the tapasin-MHC I complex. *Sci Rep,* 6**,** 19085.

FORBES, S. A. & TROWSDALE, J. 1999. The MHC quarterly report. *Immunogenetics,* 50**,** 152-9.

FREMONT, D. H., MATSUMURA, M., STURA, E. A., PETERSON, P. A. & WILSON, I. A. 1992. Crystal structures of two viral peptides in complex with murine MHC class I H-2Kb. *Science,* 257**,** 919-27.

FRICKEL, E. M., RIEK, R., JELESAROV, I., HELENIUS, A., WUTHRICH, K. & ELLGAARD, L. 2002. TROSY-NMR reveals interaction between ERp57 and the tip of the calreticulin P-domain. *Proc Natl Acad Sci U S A,* 99**,** 1954-9.

FUJIWARA, T., ODA, K., YOKOTA, S., TAKATSUKI, A. & IKEHARA, Y. 1988. Brefeldin A causes disassembly of the Golgi complex and accumulation of secretory proteins in the endoplasmic reticulum. *J Biol Chem,* 263**,** 18545-52.

GACZYNSKA, M., ROCK, K. L., SPIES, T. & GOLDBERG, A. L. 1994. Peptidase activities of proteasomes are differentially regulated by the major histocompatibility complex-encoded genes for LMP2 and LMP7. *Proc Natl Acad Sci U S A,* 91**,** 9213-7.

GADOLA, S. D., MOINS-TEISSERENC, H. T., TROWSDALE, J., GROSS, W. L. & CERUNDOLO, V. 2000. TAP deficiency syndrome. *Clin Exp Immunol,* 121**,** 173-8.

GAO, B., ADHIKARI, R., HOWARTH, M., NAKAMURA, K., GOLD, M. C., HILL, A. B., KNEE, R., MICHALAK, M. & ELLIOTT, T. 2002. Assembly and antigen-presenting function of MHC class I molecules in cells lacking the ER chaperone calreticulin. *Immunity,* 16**,** 99-109.

GAO, G. F., TORMO, J., GERTH, U. C., WYER, J. R., MCMICHAEL, A. J., STUART, D. I., BELL, J. I., JONES, E. Y. & JAKOBSEN, B. K. 1997. Crystal structure of the complex between human CD8alpha(alpha) and HLA-A2. *Nature,* 387**,** 630-4.

GAO, X., NELSON, G. W., KARACKI, P., MARTIN, M. P., PHAIR, J., KASLOW, R., GOEDERT, J. J., BUCHBINDER, S., HOOTS, K., VLAHOV, D., O'BRIEN, S. J. & CARRINGTON, M. 2001. Effect of a single amino acid change in MHC class I molecules on the rate of progression to AIDS. *N Engl J Med,* 344**,** 1668-75.

GARBI, N., TAN, P., DIEHL, A. D., CHAMBERS, B. J., LJUNGGREN, H. G., MOMBURG, F. & HAMMERLING, G. J. 2000. Impaired immune responses and altered peptide repertoire in tapasin-deficient mice. *Nat Immunol,* 1**,** 234-8.

GARRETT, T. P., SAPER, M. A., BJORKMAN, P. J., STROMINGER, J. L. & WILEY, D. C. 1989. Specificity pockets for the side chains of peptide antigens in HLA-Aw68. *Nature,* 342**,** 692-6.

GARSTKA, M. A., FRITZSCHE, S., LENART, I., HEIN, Z., JANKEVICIUS, G., BOYLE, L. H., ELLIOTT, T., TROWSDALE, J., ANTONIOU, A. N., ZACHARIAS, M. & SPRINGER, S. 2011. Tapasin dependence of major histocompatibility complex class I molecules correlates with their conformational flexibility. *FASEB J,* 25**,** 3989-98.

GENETIC ANALYSIS OF PSORIASIS, C., THE WELLCOME TRUST CASE CONTROL, C., STRANGE, A., CAPON, F., SPENCER, C. C., KNIGHT, J., WEALE, M. E., ALLEN, M. H., BARTON, A., BAND, G., BELLENGUEZ, C., BERGBOER, J. G., BLACKWELL, J. M., BRAMON, E., BUMPSTEAD, S. J., CASAS, J. P., CORK, M. J., CORVIN, A., DELOUKAS, P., DILTHEY, A., DUNCANSON, A., EDKINS, S., ESTIVILL, X., FITZGERALD, O., FREEMAN, C., GIARDINA, E., GRAY, E., HOFER, A., HUFFMEIER, U., HUNT, S. E., IRVINE, A. D., JANKOWSKI, J., KIRBY, B., LANGFORD, C., LASCORZ, J., LEMAN, J., LESLIE, S., MALLBRIS, L., MARKUS, H. S., MATHEW, C. G., MCLEAN, W. H., MCMANUS, R., MOSSNER, R., MOUTSIANAS, L., NALUAI, A. T., NESTLE, F. O., NOVELLI, G., ONOUFRIADIS, A., PALMER, C. N., PERRICONE, C., PIRINEN, M., PLOMIN, R., POTTER, S. C., PUJOL, R. M., RAUTANEN, A., RIVEIRA-MUNOZ, E., RYAN, A. W., SALMHOFER, W., SAMUELSSON, L., SAWCER, S. J., SCHALKWIJK, J., SMITH, C. H., STAHLE, M., SU, Z., TAZI-AHNINI, R., TRAUPE, H., VISWANATHAN, A. C., WARREN, R. B., WEGER, W., WOLK, K., WOOD, N., WORTHINGTON, J., YOUNG, H. S., ZEEUWEN, P. L., HAYDAY, A., BURDEN, A. D., GRIFFITHS, C. E., KERE, J., REIS, A., MCVEAN, G., EVANS, D. M., BROWN, M. A., BARKER, J. N., PELTONEN, L., DONNELLY, P. & TREMBATH, R. C. 2010. A genome-wide association study identifies new psoriasis susceptibility loci and an interaction between HLA-C and ERAP1. *Nat Genet,* 42**,** 985-90.

GILLESPIE, G. M., WILLS, M. R., APPAY, V., O'CALLAGHAN, C., MURPHY, M., SMITH, N., SISSONS, P., ROWLAND-JONES, S., BELL, J. I. & MOSS, P. A. 2000. Functional heterogeneity and high

frequencies of cytomegalovirus-specific CD8(+) T lymphocytes in healthy seropositive donors. *J Virol,* 74**,** 8140-50.

GLYNNE, R., POWIS, S. H., BECK, S., KELLY, A., KERR, L. A. & TROWSDALE, J. 1991. A proteasome-related gene between the two ABC transporter loci in the class II region of the human MHC. *Nature,* 353**,** 357-60.

GORER, P. A. 1950. Studies in antibody response of mice to tumour inoculation. *Br J Cancer,* 4**,** 372-9.

GORER, P. A. & SCHUTZE, H. 1938. Genetical studies on immunity in mice: II. Correlation between antibody formation and resistance. *J Hyg (Lond),* 38**,** 647-62.

GRANDEA, A. G., 3RD, GOLOVINA, T. N., HAMILTON, S. E., SRIRAM, V., SPIES, T., BRUTKIEWICZ, R. R., HARTY, J. T., EISENLOHR, L. C. & VAN KAER, L. 2000. Impaired assembly yet normal trafficking of MHC class I molecules in Tapasin mutant mice. *Immunity,* 13**,** 213-22.

GREENWOOD, R., SHIMIZU, Y., SEKHON, G. S. & DEMARS, R. 1994. Novel allele-specific, post-translational reduction in HLA class I surface expression in a mutant human B cell line. *J Immunol,* 153**,** 5525-36.

GROETTRUP, M., KRAFT, R., KOSTKA, S., STANDERA, S., STOHWASSER, R. & KLOETZEL, P. M. 1996. A third interferon-gamma-induced subunit exchange in the 20S proteasome. *Eur J Immunol,* 26**,** 863-9.

GROMME, M., UYTDEHAAG, F. G., JANSSEN, H., CALAFAT, J., VAN BINNENDIJK, R. S., KENTER, M. J., TULP, A., VERWOERD, D. & NEEFJES, J. 1999. Recycling MHC class I molecules and endosomal peptide loading. *Proc Natl Acad Sci U S A,* 96**,** 10326-31.

GROS, M. & AMIGORENA, S. 2019. Regulation of Antigen Export to the Cytosol During Cross-Presentation. *Front Immunol,* 10**,** 41.

GUERMONPREZ, P., SAVEANU, L., KLEIJMEER, M., DAVOUST, J., VAN ENDERT, P. & AMIGORENA, S. 2003. ER-phagosome fusion defines an MHC class I cross-presentation compartment in dendritic cells. *Nature,* 425**,** 397-402.

GUO, H. C., JARDETZKY, T. S., GARRETT, T. P., LANE, W. S., STROMINGER, J. L. & WILEY, D. C. 1992. Different length peptides bind to HLA-Aw68 similarly at their ends but bulge out in the middle. *Nature,* 360**,** 364-6.

HAFSTRAND, I., SAYITOGLU, E. C., APAVALOAEI, A., JOSEY, B. J., SUN, R., HAN, X., PELLEGRINO, S., OZKAZANC, D., POTENS, R., JANSSEN, L., NILVEBRANT, J., NYGREN, P. A., SANDALOVA, T., SPRINGER, S., GEORGOUDAKI, A. M., DURU, A. D. & ACHOUR, A. 2019. Successive crystal structure snapshots suggest the basis for MHC class I peptide loading and editing by tapasin. *Proc Natl Acad Sci U S A,* 116**,** 5055-5060.

HAMMOND, C., BRAAKMAN, I. & HELENIUS, A. 1994. Role of N-linked oligosaccharide recognition, glucose trimming, and calnexin in glycoprotein folding and quality control. *Proc Natl Acad Sci U S A,* 91**,** 913-7.

HEBERT, D. N., FOELLMER, B. & HELENIUS, A. 1995. Glucose trimming and reglucosylation determine glycoprotein association with calnexin in the endoplasmic reticulum. *Cell,* 81**,** 425-33.

HENDERSON, R. A., COX, A. L., SAKAGUCHI, K., APPELLA, E., SHABANOWITZ, J., HUNT, D. F. & ENGELHARD, V. H. 1993. Direct identification of an endogenous peptide recognized by multiple HLA-A2.1-specific cytotoxic T cells. *Proc Natl Acad Sci U S A,* 90**,** 10275-9.

HENDERSON, R. A., MICHEL, H., SAKAGUCHI, K., SHABANOWITZ, J., APPELLA, E., HUNT, D. F. & ENGELHARD, V. H. 1992. HLA-A2.1-associated peptides from a mutant cell line: a second pathway of antigen presentation. *Science,* 255**,** 1264-6.

HERMANN, C., STRITTMATTER, L. M., DEANE, J. E. & BOYLE, L. H. 2013. The binding of TAPBPR and Tapasin to MHC class I is mutually exclusive. *J Immunol,* 191**,** 5743-50.

HERMANN, C., TROWSDALE, J. & BOYLE, L. H. 2015a. TAPBPR: a new player in the MHC class I presentation pathway. *Tissue Antigens,* 85**,** 155-66.

HERMANN, C., VAN HATEREN, A., TRAUTWEIN, N., NEERINCX, A., DURIEZ, P. J., STEVANOVIC, S., TROWSDALE, J., DEANE, J. E., ELLIOTT, T. & BOYLE, L. H. 2015b. TAPBPR alters MHC class I peptide presentation by functioning as a peptide exchange catalyst. *Elife,* 4.

HOGAN, K. T., EISINGER, D. P., CUPP, S. B., 3RD, LEKSTROM, K. J., DEACON, D. D., SHABANOWITZ, J., HUNT, D. F., ENGELHARD, V. H., SLINGLUFF, C. L., JR. & ROSS, M. M. 1998. The peptide recognized by HLA-A68.2-restricted, squamous cell carcinoma of the lung-specific cytotoxic T lymphocytes is derived from a mutated elongation factor 2 gene. *Cancer Res,* 58**,** 5144-50.

HOUDE, M., BERTHOLET, S., GAGNON, E., BRUNET, S., GOYETTE, G., LAPLANTE, A., PRINCIOTTA, M. F., THIBAULT, P., SACKS, D. & DESJARDINS, M. 2003. Phagosomes are competent organelles for antigen cross-presentation. *Nature,* 425**,** 402-6.

HOWARTH, M., WILLIAMS, A., TOLSTRUP, A. B. & ELLIOTT, T. 2004. Tapasin enhances MHC class I peptide presentation according to peptide half-life. *Proc Natl Acad Sci U S A,* 101**,** 11737-42.

HUCZKO, E. L., BODNAR, W. M., BENJAMIN, D., SAKAGUCHI, K., ZHU, N. Z., SHABANOWITZ, J., HENDERSON, R. A., APPELLA, E., HUNT, D. F. & ENGELHARD, V. H. 1993. Characteristics of endogenous peptides eluted from the class I MHC molecule HLA-B7 determined by mass spectrometry and computer modeling. *J Immunol,* 151**,** 2572-87.

HULPKE, S. & TAMPE, R. 2013. The MHC I loading complex: a multitasking machinery in adaptive immunity. *Trends Biochem Sci,* 38**,** 412-20.

HULSMEYER, M., WELFLE, K., POHLMANN, T., MISSELWITZ, R., ALEXIEV, U., WELFLE, H., SAENGER, W., UCHANSKA-ZIEGLER, B. & ZIEGLER, A. 2005. Thermodynamic and structural equivalence of two HLA-B27 subtypes complexed with a self-peptide. *J Mol Biol,* 346**,** 1367-79.

ILCA, F. T., NEERINCX, A., HERMANN, C., MARCU, A., STEVANOVIC, S., DEANE, J. E. & BOYLE, L. H. 2018a. TAPBPR mediates peptide dissociation from MHC class I using a leucine lever. *Elife,* 7.

ILCA, F. T., NEERINCX, A., WILLS, M. R., DE LA ROCHE, M. & BOYLE, L. H. 2018b. Utilizing TAPBPR to promote exogenous peptide loading onto cell surface MHC I molecules. *Proc Natl Acad Sci U S A,* 115**,** E9353-E9361.

ILLING, P. T., VIVIAN, J. P., DUDEK, N. L., KOSTENKO, L., CHEN, Z., BHARADWAJ, M., MILES, J. J., KJER-NIELSEN, L., GRAS, S., WILLIAMSON, N. A., BURROWS, S. R., PURCELL, A. W., ROSSJOHN, J. & MCCLUSKEY, J. 2012. Immune self-reactivity triggered by drug-modified HLA-peptide repertoire. *Nature,* 486**,** 554-8.

JACKSON, M. R., NILSSON, T. & PETERSON, P. A. 1990. Identification of a consensus motif for retention of transmembrane proteins in the endoplasmic reticulum. *EMBO J,* 9**,** 3153-62.

JANEWAY, C. A., JR., CARDING, S., JONES, B., MURRAY, J., PORTOLES, P., RASMUSSEN, R., ROJO, J., SAIZAWA, K., WEST, J. & BOTTOMLY, K. 1988. CD4+ T cells: specificity and function. *Immunol Rev,* 101**,** 39-80.

JENKINS, M. R., TSUN, A., STINCHCOMBE, J. C. & GRIFFITHS, G. M. 2009. The strength of T cell receptor signal controls the polarization of cytotoxic machinery to the immunological synapse. *Immunity,* 31**,** 621-31.

JIANG, J., NATARAJAN, K., BOYD, L. F., MOROZOV, G. I., MAGE, M. G. & MARGULIES, D. H. 2017. Crystal structure of a TAPBPR-MHC I complex reveals the mechanism of peptide editing in antigen presentation. *Science,* 358**,** 1064-1068.

JONES, D. C., KOSMOLIAPTSIS, V., APPS, R., LAPAQUE, N., SMITH, I., KONO, A., CHANG, C., BOYLE, L. H., TAYLOR, C. J., TROWSDALE, J. & ALLEN, R. L. 2011. HLA class I allelic sequence and conformation regulate leukocyte Ig-like receptor binding. *J Immunol,* 186**,** 2990-7.

KALAORA, S., BARNEA, E., MERHAVI-SHOHAM, E., QUTOB, N., TEER, J. K., SHIMONY, N., SCHACHTER, J., ROSENBERG, S. A., BESSER, M. J., ADMON, A. & SAMUELS, Y. 2016. Use of HLA peptidomics and whole exome sequencing to identify human immunogenic neo-antigens. *Oncotarget,* 7**,** 5110-7.

KALL, L., CANTERBURY, J. D., WESTON, J., NOBLE, W. S. & MACCOSS, M. J. 2007. Semi-supervised learning for peptide identification from shotgun proteomics datasets. *Nat Methods,* 4**,** 923-5.

KAMHI-NESHER, S., SHENKMAN, M., TOLCHINSKY, S., FROMM, S. V., EHRLICH, R. & LEDERKREMER, G. Z. 2001. A novel quality control compartment derived from the endoplasmic reticulum. *Mol Biol Cell,* 12**,** 1711-23.

KARRE, K., LJUNGGREN, H. G., PIONTEK, G. & KIESSLING, R. 1986. Selective rejection of H-2-deficient lymphoma variants suggests alternative immune defence strategy. *Nature,* 319**,** 675-8.

KATZ, D. H., HAMAOKA, T. & BENACERRAF, B. 1973a. Cell interactions between histoincompatible T and B lymphocytes. II. Failure of physiologic cooperative interactions between T and B lymphocytes from allogeneic donor strains in humoral response to hapten-protein conjugates. *J Exp Med,* 137**,** 1405-18.

KATZ, D. H., HAMAOKA, T., DORF, M. E. & BENACERRAF, B. 1973b. Cell interactions between histoincompatible T and B lymphocytes. The H-2 gene complex determines successful physiologic lymphocyte interactions. *Proc Natl Acad Sci U S A,* 70**,** 2624-8.

KAUFMAN, J., MILNE, S., GOBEL, T. W., WALKER, B. A., JACOB, J. P., AUFFRAY, C., ZOOROB, R. & BECK, S. 1999. The chicken B locus is a minimal essential major histocompatibility complex. *Nature,* 401**,** 923-5.

KAUFMAN, J., VOLK, H. & WALLNY, H. J. 1995. A "minimal essential Mhc" and an "unrecognized Mhc": two extremes in selection for polymorphism. *Immunol Rev,* 143**,** 63-88.

KAUFMAN, J. & WALLNY, H. J. 1996. Chicken MHC molecules, disease resistance and the evolutionary origin of birds. *Curr Top Microbiol Immunol,* 212**,** 129-41.

KAWAKAMI, Y., FUJITA, T., MATSUZAKI, Y., SAKURAI, T., TSUKAMOTO, M., TODA, M. & SUMIMOTO, H. 2004. Identification of human tumor antigens and its implications for diagnosis and treatment of cancer. *Cancer Sci,* 95**,** 784-91.

KELLY, A., POWIS, S. H., GLYNNE, R., RADLEY, E., BECK, S. & TROWSDALE, J. 1991a. Second proteasome-related gene in the human MHC class II region. *Nature,* 353**,** 667-8.

KELLY, A. P., MONACO, J. J., CHO, S. G. & TROWSDALE, J. 1991b. A new human HLA class II-related locus, DM. *Nature,* 353**,** 571-3.

KLAUSNER, R. D., VAN RENSWOUDE, J., ASHWELL, G., KEMPF, C., SCHECHTER, A. N., DEAN, A. & BRIDGES, K. R. 1983. Receptor-mediated endocytosis of transferrin in K562 cells. *J Biol Chem,* 258**,** 4715-24.

KLOVERPRIS, H. N., HARNDAHL, M., LESLIE, A. J., CARLSON, J. M., ISMAIL, N., VAN DER STOK, M., HUANG, K. H., CHEN, F., RIDDELL, L., STEYN, D., GOEDHALS, D., VAN VUUREN, C., FRATER, J., WALKER, B. D., CARRINGTON, M., NDUNG'U, T., BUUS, S. & GOULDER, P. 2012a. HIV control through a single nucleotide on the HLA-B locus. *J Virol,* 86**,** 11493-500.

KLOVERPRIS, H. N., STRYHN, A., HARNDAHL, M., VAN DER STOK, M., PAYNE, R. P., MATTHEWS, P. C., CHEN, F., RIDDELL, L., WALKER, B. D., NDUNG'U, T., BUUS, S. & GOULDER, P. 2012b. HLA-B*57 Micropolymorphism shapes HLA allele-specific epitope immunogenicity, selection pressure, and HIV immune control. *J Virol,* 86**,** 919-29.

KOVACSOVICS-BANKOWSKI, M. & ROCK, K. L. 1995. A phagosome-to-cytosol pathway for exogenous antigens presented on MHC class I molecules. *Science,* 267**,** 243-6.

KOWALEWSKI, D. J. & STEVANOVIC, S. 2013. Biochemical large-scale identification of MHC class I ligands. *Methods Mol Biol,* 960**,** 145-157.

KROPSHOFER, H., VOGT, A. B., MOLDENHAUER, G., HAMMER, J., BLUM, J. S. & HAMMERLING, G. J. 1996. Editing of the HLA-DR-peptide repertoire by HLA-DM. *EMBO J,* 15**,** 6144-54.

KROPSHOFER, H., VOGT, A. B., THERY, C., ARMANDOLA, E. A., LI, B. C., MOLDENHAUER, G., AMIGORENA, S. & HAMMERLING, G. J. 1998. A role for HLA-DO as a co-chaperone of HLA-DM in peptide loading of MHC class II molecules. *EMBO J,* 17**,** 2971-81.

KVIST, S., WIMAN, K., CLAESSON, L., PETERSON, P. A. & DOBBERSTEIN, B. 1982. Membrane insertion and oligomeric assembly of HLA-DR histocompatibility antigens. *Cell,* 29**,** 61-9.

LANDIS, E. D., PALTI, Y., DEKONING, J., DREW, R., PHILLIPS, R. B. & HANSEN, J. D. 2006. Identification and regulatory analysis of rainbow trout tapasin and tapasin-related genes. *Immunogenetics,* 58**,** 56-69.

LAUTSCHAM, G., MAYRHOFER, S., TAYLOR, G., HAIGH, T., LEESE, A., RICKINSON, A. & BLAKE, N. 2001. Processing of a multiple membrane spanning Epstein-Barr virus protein for CD8(+) T cell recognition reveals a proteasome-dependent, transporter associated with antigen processing-independent pathway. *J Exp Med,* 194**,** 1053-68.

LEDERBERG, J. 1999. J. B. S. Haldane (1949) on infectious disease and evolution. *Genetics,* 153**,** 1-3.

LEHNER, P. J., SURMAN, M. J. & CRESSWELL, P. 1998. Soluble tapasin restores MHC class I expression and function in the tapasin-negative cell line .220. *Immunity,* 8**,** 221-31.

LEHOANG, P., OZDEMIR, N., BENHAMOU, A., TABARY, T., EDELSON, C., BETUEL, H., SEMIGLIA, R. & COHEN, J. H. 1992. HLA-A29.2 subtype associated with birdshot retinochoroidopathy. *Am J Ophthalmol,* 113**,** 33-5.

LEWIS, J. W., NEISIG, A., NEEFJES, J. & ELLIOTT, T. 1996. Point mutations in the alpha 2 domain of HLA-A2.1 define a functionally relevant interaction with TAP. *Curr Biol,* 6**,** 873-83.

LI, S., SJOGREN, H. O., HELLMAN, U., PETTERSSON, R. F. & WANG, P. 1997. Cloning and functional characterization of a subunit of the transporter associated with antigen processing. *Proc Natl Acad Sci U S A,* 94**,** 8708-13.

LILJEDAHL, M., KUWANA, T., FUNG-LEUNG, W. P., JACKSON, M. R., PETERSON, P. A. & KARLSSON, L. 1996. HLA-DO is a lysosomal resident which requires association with HLA-DM for efficient intracellular transport. *EMBO J,* 15**,** 4817-24.

LITTLE, C. C. & TYZZER, E. E. 1916. Further experimental studies on the inheritance of susceptibility to a Transplantable tumor, Carcinoma (J. W. A.) of the Japanese waltzing Mouse. *J Med Res,* 33**,** 393-453.

LJUNGGREN, H. G. & KARRE, K. 1990. In search of the 'missing self': MHC molecules and NK cell recognition. *Immunol Today,* 11**,** 237-44.

LOTTEAU, V., TEYTON, L., PELERAUX, A., NILSSON, T., KARLSSON, L., SCHMID, S. L., QUARANTA, V. & PETERSON, P. A. 1990. Intracellular transport of class II MHC molecules directed by invariant chain. *Nature,* 348**,** 600-5.

MACHAMER, C. E. & CRESSWELL, P. 1982. Biosynthesis and glycosylation of the invariant chain associated with HLA-DR antigens. *J Immunol,* 129**,** 2564-9.

MACIA, E., EHRLICH, M., MASSOL, R., BOUCROT, E., BRUNNER, C. & KIRCHHAUSEN, T. 2006. Dynasore, a cell-permeable inhibitor of dynamin. *Dev Cell,* 10**,** 839-50.

MADDEN, D. R., GORGA, J. C., STROMINGER, J. L. & WILEY, D. C. 1991. The structure of HLA-B27 reveals nonamer self-peptides bound in an extended conformation. *Nature,* 353**,** 321-5.

MADDEN, D. R., GORGA, J. C., STROMINGER, J. L. & WILEY, D. C. 1992. The three-dimensional structure of HLA-B27 at 2.1 A resolution suggests a general mechanism for tight peptide binding to MHC. *Cell,* 70**,** 1035-48.

MATSUMURA, M., FREMONT, D. H., PETERSON, P. A. & WILSON, I. A. 1992. Emerging principles for the recognition of peptide antigens by MHC class I molecules. *Science,* 257**,** 927-34.

MCSHAN, A. C., NATARAJAN, K., KUMIROV, V. K., FLORES-SOLIS, D., JIANG, J., BADSTUBNER, M., TOOR, J. S., BAGSHAW, C. R., KOVRIGIN, E. L., MARGULIES, D. H. & SGOURAKIS, N. G. 2018. Peptide exchange on MHC-I by TAPBPR is driven by a negative allostery release cycle. *Nat Chem Biol,* 14**,** 811-820.

MORETTA, A., SIVORI, S., VITALE, M., PENDE, D., MORELLI, L., AUGUGLIARO, R., BOTTINO, C. & MORETTA, L. 1995. Existence of both inhibitory (p58) and activatory (p50) receptors for HLA-C molecules in human natural killer cells. *J Exp Med,* 182**,** 875-84.

MOROZOV, G. I., ZHAO, H., MAGE, M. G., BOYD, L. F., JIANG, J., DOLAN, M. A., VENNA, R., NORCROSS, M. A., MCMURTREY, C. P., HILDEBRAND, W., SCHUCK, P., NATARAJAN, K. & MARGULIES, D. H. 2016. Interaction of TAPBPR, a tapasin homolog, with MHC-I molecules promotes peptide editing. *Proc Natl Acad Sci U S A,* 113**,** E1006-15.

MORRIS, P., SHAMAN, J., ATTAYA, M., AMAYA, M., GOODMAN, S., BERGMAN, C., MONACO, J. J. & MELLINS, E. 1994. An essential role for HLA-DM in antigen presentation by class II major histocompatibility molecules. *Nature,* 368**,** 551-4.

NANDI, D., JIANG, H. & MONACO, J. J. 1996. Identification of MECL-1 (LMP-10) as the third IFN-gamma-inducible proteasome subunit. *J Immunol,* 156**,** 2361-4.

NARANBHAI, V. & CARRINGTON, M. 2017. Host genetic variation and HIV disease: from mapping to mechanism. *Immunogenetics,* 69**,** 489-498.

NATARAJAN, K., DIMASI, N., WANG, J., MARIUZZA, R. A. & MARGULIES, D. H. 2002. Structure and function of natural killer cell receptors: multiple molecular solutions to self, nonself discrimination. *Annu Rev Immunol,* 20**,** 853-85.

NEERINCX, A. & BOYLE, L. H. 2017. Properties of the tapasin homologue TAPBPR. *Curr Opin Immunol,* 46**,** 97-102.

NEERINCX, A. & BOYLE, L. H. 2018. Preferential interaction of MHC class I with TAPBPR in the absence of glycosylation. *Mol Immunol*.

NEERINCX, A., HERMANN, C., ANTROBUS, R., VAN HATEREN, A., CAO, H., TRAUTWEIN, N., STEVANOVIC, S., ELLIOTT, T., DEANE, J. E. & BOYLE, L. H. 2017. TAPBPR bridges UDP-glucose:glycoprotein glucosyltransferase 1 onto MHC class I to provide quality control in the antigen presentation pathway. *Elife,* 6.

NELDE, A., KOWALEWSKI, D. J., BACKERT, L., SCHUSTER, H., WERNER, J. O., KLEIN, R., KOHLBACHER, O., KANZ, L., SALIH, H. R., RAMMENSEE, H. G., STEVANOVIC, S. & WALZ, J. S. 2018. HLA ligandome analysis of primary chronic lymphocytic leukemia (CLL) cells under lenalidomide treatment confirms the suitability of lenalidomide for combination with T-cell-based immunotherapy. *Oncoimmunology,* 7**,** e1316438.

NEWCOMB, J. R. & CRESSWELL, P. 1993. Characterization of endogenous peptides bound to purified HLA-DR molecules and their absence from invariant chain-associated alpha beta dimers. *J Immunol,* 150**,** 499-507.

NGUYEN, T. T., CHANG, S. C., EVNOUCHIDOU, I., YORK, I. A., ZIKOS, C., ROCK, K. L., GOLDBERG, A. L., STRATIKOS, E. & STERN, L. J. 2011. Structural basis for antigenic peptide precursor processing by the endoplasmic reticulum aminopeptidase ERAP1. *Nat Struct Mol Biol,* 18**,** 604-13.

NILSSON, T., JACKSON, M. & PETERSON, P. A. 1989. Short cytoplasmic sequences serve as retention signals for transmembrane proteins in the endoplasmic reticulum. *Cell,* 58**,** 707-18.

NIU, L., CHENG, H., ZHANG, S., TAN, S., ZHANG, Y., QI, J., LIU, J. & GAO, G. F. 2013. Structural basis for the differential classification of HLA-A*6802 and HLA-A*6801 into the A2 and A3 supertypes. *Mol Immunol,* 55**,** 381-92.

NURZIA, E., NARZI, D., CAULI, A., MATHIEU, A., TEDESCHI, V., CARISTI, S., SORRENTINO, R., BOCKMANN, R. A. & FIORILLO, M. T. 2012. Interaction pattern of Arg 62 in the A-pocket of differentially disease-associated HLA-B27 subtypes suggests distinct TCR binding modes. *PLoS One,* 7**,** e32865.

OLIVEIRA, C. C. & VAN HALL, T. 2013. Importance of TAP-independent processing pathways. *Mol Immunol,* 55**,** 113-6.

ORTIZ-NAVARRETE, V., SEELIG, A., GERNOLD, M., FRENTZEL, S., KLOETZEL, P. M. & HAMMERLING, G. J. 1991. Subunit of the '20S' proteasome (multicatalytic proteinase) encoded by the major histocompatibility complex. *Nature,* 353**,** 662-4.

ORTMANN, B., COPEMAN, J., LEHNER, P. J., SADASIVAN, B., HERBERG, J. A., GRANDEA, A. G., RIDDELL, S. R., TAMPE, R., SPIES, T., TROWSDALE, J. & CRESSWELL, P. 1997. A critical role for tapasin in the assembly and function of multimeric MHC class I-TAP complexes. *Science,* 277**,** 1306-9.

PAQUET, M. E. & WILLIAMS, D. B. 2002. Mutant MHC class I molecules define interactions between components of the peptide-loading complex. *Int Immunol,* 14**,** 347-58.

PARHAM, P., ALPERT, B. N., ORR, H. T. & STROMINGER, J. L. 1977. Carbohydrate moiety of HLA antigens. Antigenic properties and amino acid sequences around the site of glycosylation. *J Biol Chem,* 252**,** 7555-67.

PARK, B., LEE, S., KIM, E. & AHN, K. 2003. A single polymorphic residue within the peptide-binding cleft of MHC class I molecules determines spectrum of tapasin dependence. *J Immunol,* 170**,** 961-8.

PAZAR, B., SAFRANY, E., GERGELY, P., SZANTO, S., SZEKANECZ, Z. & POOR, G. 2010. Association of ARTS1 gene polymorphisms with ankylosing spondylitis in the Hungarian population: the rs27044 variant is associated with HLA-B*2705 subtype in Hungarian patients with ankylosing spondylitis. *J Rheumatol,* 37**,** 379-84.

PEACE-BREWER, A. L., TUSSEY, L. G., MATSUI, M., LI, G., QUINN, D. G. & FRELINGER, J. A. 1996. A point mutation in HLA-A*0201 results in failure to bind the TAP complex and to present virus-derived peptides to CTL. *Immunity,* 4**,** 505-14.

PEH, C. A., BURROWS, S. R., BARNDEN, M., KHANNA, R., CRESSWELL, P., MOSS, D. J. & MCCLUSKEY, J. 1998. HLA-B27-restricted antigen presentation in the absence of tapasin reveals polymorphism in mechanisms of HLA class I peptide loading. *Immunity,* 8**,** 531-42.

PEI, R., LEE, J. H., SHIH, N. J., CHEN, M. & TERASAKI, P. I. 2003. Single human leukocyte antigen flow cytometry beads for accurate identification of human leukocyte antigen antibody specificities. *Transplantation,* 75**,** 43-9.

PETERSON, J. R., ORA, A., VAN, P. N. & HELENIUS, A. 1995. Transient, lectin-like association of calreticulin with folding intermediates of cellular and viral glycoproteins. *Mol Biol Cell,* 6**,** 1173-84.

PFEIFER, J. D., WICK, M. J., ROBERTS, R. L., FINDLAY, K., NORMARK, S. J. & HARDING, C. V. 1993. Phagocytic processing of bacterial antigens for class I MHC presentation to T cells. *Nature,* 361**,** 359-62.

PORGADOR, A., YEWDELL, J. W., DENG, Y., BENNINK, J. R. & GERMAIN, R. N. 1997. Localization, quantitation, and in situ detection of specific peptide-MHC class I complexes using a monoclonal antibody. *Immunity,* 6**,** 715-26.

POS, W., SETHI, D. K., CALL, M. J., SCHULZE, M. S., ANDERS, A. K., PYRDOL, J. & WUCHERPFENNIG, K. W. 2012. Crystal structure of the HLA-DM-HLA-DR1 complex defines mechanisms for rapid peptide selection. *Cell,* 151**,** 1557-68.

PRAVEEN, P. V., YANEVA, R., KALBACHER, H. & SPRINGER, S. 2010. Tapasin edits peptides on MHC class I molecules by accelerating peptide exchange. *Eur J Immunol,* 40**,** 214-24.

PURCELL, A. W., GORMAN, J. J., GARCIA-PEYDRO, M., PARADELA, A., BURROWS, S. R., TALBO, G. H., LAHAM, N., PEH, C. A., REYNOLDS, E. C., LOPEZ DE CASTRO, J. A. & MCCLUSKEY, J. 2001. Quantitative and qualitative influences of tapasin on the class I peptide repertoire. *J Immunol,* 166**,** 1016-27.

RAMMENSEE, H., BACHMANN, J., EMMERICH, N. P., BACHOR, O. A. & STEVANOVIC, S. 1999. SYFPEITHI: database for MHC ligands and peptide motifs. *Immunogenetics,* 50**,** 213-9.

RAMSBOTTOM, K. A., CARR, D. F., JONES, A. R. & RIGDEN, D. J. 2018. Critical assessment of approaches for molecular docking to elucidate associations of HLA alleles with adverse drug reactions. *Mol Immunol,* 101**,** 488-499.

REYES, V. E., LU, S. & HUMPHREYS, R. E. 1991. Cathepsin B cleavage of Ii from class II MHC alpha- and beta-chains. *J Immunol,* 146**,** 3877-80.

RIZVI, S. M., DEL CID, N., LYBARGER, L. & RAGHAVAN, M. 2011. Distinct functions for the glycans of tapasin and heavy chains in the assembly of MHC class I molecules. *J Immunol,* 186**,** 2309-20.

RIZVI, S. M., SALAM, N., GENG, J., QI, Y., BREAM, J. H., DUGGAL, P., HUSSAIN, S. K., MARTINSON, J., WOLINSKY, S. M., CARRINGTON, M. & RAGHAVAN, M. 2014. Distinct assembly profiles of HLA-B molecules. *J Immunol,* 192**,** 4967-76.

ROBINSON, J., HALLIWELL, J. A., HAYHURST, J. D., FLICEK, P., PARHAM, P. & MARSH, S. G. 2015. The IPD and IMGT/HLA database: allele variant databases. *Nucleic Acids Res,* 43**,** D423-31.

ROCHE, P. A. & CRESSWELL, P. 1990. Invariant chain association with HLA-DR molecules inhibits immunogenic peptide binding. *Nature,* 345**,** 615-8.

ROCHE, P. A. & CRESSWELL, P. 1991. Proteolysis of the class II-associated invariant chain generates a peptide binding site in intracellular HLA-DR molecules. *Proc Natl Acad Sci U S A,* 88**,** 3150-4.

ROCHE, P. A. & FURUTA, K. 2015. The ins and outs of MHC class II-mediated antigen processing and presentation. *Nat Rev Immunol,* 15**,** 203-16.

ROCK, K. L., FARFAN-ARRIBAS, D. J., COLBERT, J. D. & GOLDBERG, A. L. 2014. Re-examining class-I presentation and the DRiP hypothesis. *Trends Immunol,* 35**,** 144-52.

ROCK, K. L. & GOLDBERG, A. L. 1999. Degradation of cell proteins and the generation of MHC class I-presented peptides. *Annu Rev Immunol,* 17**,** 739-79.

ROCK, K. L. & SHEN, L. 2005. Cross-presentation: underlying mechanisms and role in immune surveillance. *Immunol Rev,* 207**,** 166-83.

ROMERO, P., GERVOIS, N., SCHNEIDER, J., ESCOBAR, P., VALMORI, D., PANNETIER, C., STEINLE, A., WOLFEL, T., LIENARD, D., BRICHARD, V., VAN PEL, A., JOTEREAU, F. & CEROTTINI, J. C. 1997. Cytolytic T lymphocyte recognition of the immunodominant HLA-A*0201-restricted Melan-A/MART-1 antigenic peptide in melanoma. *J Immunol,* 159**,** 2366-74.

RONGCUN, Y., SALAZAR-ONFRAY, F., CHARO, J., MALMBERG, K. J., EVRIN, K., MAES, H., KONO, K., HISING, C., PETERSSON, M., LARSSON, O., LAN, L., APPELLA, E., SETTE, A., CELIS, E. & KIESSLING, R. 1999. Identification of new HER2/neu-derived peptide epitopes that can elicit specific CTL against autologous and allogeneic carcinomas and melanomas. *J Immunol,* 163**,** 1037-44.

ROSENTHAL, A. S. & SHEVACH, E. M. 1973. Function of macrophages in antigen recognition by guinea pig T lymphocytes. I. Requirement for histocompatible macrophages and lymphocytes. *J Exp Med,* 138**,** 1194-212.

SADASIVAN, B., LEHNER, P. J., ORTMANN, B., SPIES, T. & CRESSWELL, P. 1996. Roles for calreticulin and a novel glycoprotein, tapasin, in the interaction of MHC class I molecules with TAP. *Immunity,* 5**,** 103-14.

SAINI, S. K., OSTERMEIR, K., RAMNARAYAN, V. R., SCHUSTER, H., ZACHARIAS, M. & SPRINGER, S. 2013. Dipeptides promote folding and peptide binding of MHC class I molecules. *Proc Natl Acad Sci U S A,* 110**,** 15383-8.

SAINI, S. K., SCHUSTER, H., RAMNARAYAN, V. R., RAMMENSEE, H. G., STEVANOVIC, S. & SPRINGER, S. 2015. Dipeptides catalyze rapid peptide exchange on MHC class I molecules. *Proc Natl Acad Sci U S A,* 112**,** 202-7.

SALGALLER, M. L., MARINCOLA, F. M., CORMIER, J. N. & ROSENBERG, S. A. 1996. Immunization against epitopes in the human melanoma antigen gp100 following patient immunization with synthetic peptides. *Cancer Res,* 56**,** 4749-57.

SALTER, R. D., BENJAMIN, R. J., WESLEY, P. K., BUXTON, S. E., GARRETT, T. P., CLAYBERGER, C., KRENSKY, A. M., NORMENT, A. M., LITTMAN, D. R. & PARHAM, P. 1990. A binding site for the T-cell co-receptor CD8 on the alpha 3 domain of HLA-A2. *Nature,* 345**,** 41-6.

SALTER, R. D. & CRESSWELL, P. 1986. Impaired assembly and transport of HLA-A and -B antigens in a mutant TxB cell hybrid. *EMBO J,* 5**,** 943-9.

SALTER, R. D., HOWELL, D. N. & CRESSWELL, P. 1985. Genes regulating HLA class I antigen expression in T-B lymphoblast hybrids. *Immunogenetics,* 21**,** 235-46.

SAPER, M. A., BJORKMAN, P. J. & WILEY, D. C. 1991. Refined structure of the human histocompatibility antigen HLA-A2 at 2.6 A resolution. *J Mol Biol,* 219**,** 277-319.

SARIC, T., CHANG, S. C., HATTORI, A., YORK, I. A., MARKANT, S., ROCK, K. L., TSUJIMOTO, M. & GOLDBERG, A. L. 2002. An IFN-gamma-induced aminopeptidase in the ER, ERAP1, trims precursors to MHC class I-presented peptides. *Nat Immunol,* 3**,** 1169-76.

SCHIRMBECK, R., MELBER, K. & REIMANN, J. 1995. Hepatitis B virus small surface antigen particles are processed in a novel endosomal pathway for major histocompatibility complex class I-restricted epitope presentation. *Eur J Immunol,* 25**,** 1063-70.

SCHMID, S. L. & CARTER, L. L. 1990. ATP is required for receptor-mediated endocytosis in intact cells. *J Cell Biol,* 111**,** 2307-18.

SCHUMACHER, T. N., HEEMELS, M. T., NEEFJES, J. J., KAST, W. M., MELIEF, C. J. & PLOEGH, H. L. 1990. Direct binding of peptide to empty MHC class I molecules on intact cells and in vitro. *Cell,* 62**,** 563-7.

SERWOLD, T., GONZALEZ, F., KIM, J., JACOB, R. & SHASTRI, N. 2002. ERAAP customizes peptides for MHC class I molecules in the endoplasmic reticulum. *Nature,* 419**,** 480-3.

SHEN, L., SIGAL, L. J., BOES, M. & ROCK, K. L. 2004. Important role of cathepsin S in generating peptides for TAP-independent MHC class I crosspresentation in vivo. *Immunity,* 21**,** 155-65.

SHEVACH, E. M. & ROSENTHAL, A. S. 1973. Function of macrophages in antigen recognition by guinea pig T lymphocytes. II. Role of the macrophage in the regulation of genetic control of the immune response. *J Exp Med,* 138**,** 1213-29.

SIDNEY, J., PETERS, B., FRAHM, N., BRANDER, C. & SETTE, A. 2008. HLA class I supertypes: a revised and updated classification. *BMC Immunol,* 9**,** 1.

SIEKER, F., SPRINGER, S. & ZACHARIAS, M. 2007. Comparative molecular dynamics analysis of tapasin-dependent and -independent MHC class I alleles. *Protein Sci,* 16**,** 299-308.

SIEKER, F., STRAATSMA, T. P., SPRINGER, S. & ZACHARIAS, M. 2008. Differential tapasin dependence of MHC class I molecules correlates with conformational changes upon peptide dissociation: a molecular dynamics simulation study. *Mol Immunol,* 45**,** 3714-22.

SIM, A. C., TOO, C. T., OO, M. Z., LAI, J., EIO, M. Y., SONG, Z., SRINIVASAN, N., TAN, D. A., PANG, S. W., GAN, S. U., LEE, K. O., LOH, T. K., CHEN, J., CHAN, S. H. & MACARY, P. A. 2013. Defining the

expression hierarchy of latent T-cell epitopes in Epstein-Barr virus infection with TCR-like antibodies. *Sci Rep,* 3**,** 3232.

SLOAN, V. S., CAMERON, P., PORTER, G., GAMMON, M., AMAYA, M., MELLINS, E. & ZALLER, D. M. 1995. Mediation by HLA-DM of dissociation of peptides from HLA-DR. *Nature,* 375**,** 802-6.

SNELL, G. D. 1948. Methods for the study of histocompatibility genes. *J Genet,* 49**,** 87-108.

SONG, R. & HARDING, C. V. 1996. Roles of proteasomes, transporter for antigen presentation (TAP), and beta 2-microglobulin in the processing of bacterial or particulate antigens via an alternate class I MHC processing pathway. *J Immunol,* 156**,** 4182-90.

SOUSA, M. C., FERRERO-GARCIA, M. A. & PARODI, A. J. 1992. Recognition of the oligosaccharide and protein moieties of glycoproteins by the UDP-Glc:glycoprotein glucosyltransferase. *Biochemistry,* 31**,** 97-105.

SPIES, T., BRESNAHAN, M., BAHRAM, S., ARNOLD, D., BLANCK, G., MELLINS, E., PIOUS, D. & DEMARS, R. 1990. A gene in the human major histocompatibility complex class II region controlling the class I antigen presentation pathway. *Nature,* 348**,** 744-7.

SPIES, T., CERUNDOLO, V., COLONNA, M., CRESSWELL, P., TOWNSEND, A. & DEMARS, R. 1992. Presentation of viral antigen by MHC class I molecules is dependent on a putative peptide transporter heterodimer. *Nature,* 355**,** 644-6.

SPIES, T. & DEMARS, R. 1991. Restored expression of major histocompatibility class I molecules by gene transfer of a putative peptide transporter. *Nature,* 351**,** 323-4.

SPILIOTIS, E. T., MANLEY, H., OSORIO, M., ZUNIGA, M. C. & EDIDIN, M. 2000. Selective export of MHC class I molecules from the ER after their dissociation from TAP. *Immunity,* 13**,** 841-51.

STAM, N. J., SPITS, H. & PLOEGH, H. L. 1986. Monoclonal antibodies raised against denatured HLA-B locus heavy chains permit biochemical characterization of certain HLA-C locus products. *J Immunol,* 137**,** 2299-306.

STAM, N. J., VROOM, T. M., PETERS, P. J., PASTOORS, E. B. & PLOEGH, H. L. 1990. HLA-A- and HLA-B-specific monoclonal antibodies reactive with free heavy chains in western blots, in formalin-fixed, paraffin-embedded tissue sections and in cryo-immuno-electron microscopy. *Int Immunol,* 2**,** 113-25.

STEWART, C. A., LAUGIER-ANFOSSI, F., VELY, F., SAULQUIN, X., RIEDMULLER, J., TISSERANT, A., GAUTHIER, L., ROMAGNE, F., FERRACCI, G., AROSA, F. A., MORETTA, A., SUN, P. D., UGOLINI, S. & VIVIER, E. 2005. Recognition of peptide-MHC class I complexes by activating killer immunoglobulin-like receptors. *Proc Natl Acad Sci U S A,* 102**,** 13224-9.

STRYHN, A., PEDERSEN, L. O., ROMME, T., OLSEN, A. C., NISSEN, M. H., THORPE, C. J. & BUUS, S. 1996. pH dependence of MHC class I-restricted peptide presentation. *J Immunol,* 156**,** 4191-7.

SUH, W. K., DERBY, M. A., COHEN-DOYLE, M. F., SCHOENHALS, G. J., FRUH, K., BERZOFSKY, J. A. & WILLIAMS, D. B. 1999. Interaction of murine MHC class I molecules with tapasin and TAP enhances peptide loading and involves the heavy chain alpha3 domain. *J Immunol,* 162**,** 1530-40.

SUN, L. D., CHENG, H., WANG, Z. X., ZHANG, A. P., WANG, P. G., XU, J. H., ZHU, Q. X., ZHOU, H. S., ELLINGHAUS, E., ZHANG, F. R., PU, X. M., YANG, X. Q., ZHANG, J. Z., XU, A. E., WU, R. N., XU, L. M., PENG, L., HELMS, C. A., REN, Y. Q., ZHANG, C., ZHANG, S. M., NAIR, R. P., WANG, H. Y., LIN, G. S., STUART, P. E., FAN, X., CHEN, G., TEJASVI, T., LI, P., ZHU, J., LI, Z. M., GE, H. M., WEICHENTHAL, M., YE, W. Z., ZHANG, C., SHEN, S. K., YANG, B. Q., SUN, Y. Y., LI, S. S., LIN, Y., JIANG, J. H., LI, C. T., CHEN, R. X., CHENG, J., JIANG, X., ZHANG, P., SONG, W. M., TANG, J., ZHANG, H. Q., SUN, L., CUI, J., ZHANG, L. J., TANG, B., HUANG, F., QIN, Q., PEI, X. P., ZHOU, A. M., SHAO, L. M., LIU, J. L., ZHANG, F. Y., DU, W. D., FRANKE, A., BOWCOCK, A. M., ELDER, J. T., LIU, J.

J., YANG, S. & ZHANG, X. J. 2010. Association analyses identify six new psoriasis susceptibility loci in the Chinese population. *Nat Genet,* 42**,** 1005-9.

SUNG, E. & JONES, P. P. 1981. The invariant chain of murine Ia antigens: its glycosylation, abundance and subcellular localization. *Mol Immunol,* 18**,** 899-913.

SWAIN, S. L. 1983. T cell subsets and the recognition of MHC class. *Immunol Rev,* 74**,** 129-42.

TAUROG, J. D. 2007. The mystery of HLA-B27: if it isn't one thing, it's another. *Arthritis Rheum,* 56**,** 2478-81.

TENG, M. S., STEPHENS, R., DU PASQUIER, L., FREEMAN, T., LINDQUIST, J. A. & TROWSDALE, J. 2002. A human TAPBP (TAPASIN)-related gene, TAPBP-R. *Eur J Immunol,* 32**,** 1059-68.

THEOBALD, M., RUPPERT, T., KUCKELKORN, U., HERNANDEZ, J., HAUSSLER, A., FERREIRA, E. A., LIEWER, U., BIGGS, J., LEVINE, A. J., HUBER, C., KOSZINOWSKI, U. H., KLOETZEL, P. M. & SHERMAN, L. A. 1998. The sequence alteration associated with a mutational hotspot in p53 protects cells from lysis by cytotoxic T lymphocytes specific for a flanking peptide epitope. *J Exp Med,* 188**,** 1017-28.

THOMAS, C. & TAMPE, R. 2017. Structure of the TAPBPR-MHC I complex defines the mechanism of peptide loading and editing. *Science,* 358**,** 1060-1064.

TOURET, N., PAROUTIS, P., TEREBIZNIK, M., HARRISON, R. E., TROMBETTA, S., PYPAERT, M., CHOW, A., JIANG, A., SHAW, J., YIP, C., MOORE, H. P., VAN DER WEL, N., HOUBEN, D., PETERS, P. J., DE CHASTELLIER, C., MELLMAN, I. & GRINSTEIN, S. 2005. Quantitative and dynamic assessment of the contribution of the ER to phagosome formation. *Cell,* 123**,** 157-70.

TROMBETTA, S. E., BOSCH, M. & PARODI, A. J. 1989. Glucosylation of glycoproteins by mammalian, plant, fungal, and trypanosomatid protozoa microsomal membranes. *Biochemistry,* 28**,** 8108-16.

TROWSDALE, J., HANSON, I., MOCKRIDGE, I., BECK, S., TOWNSEND, A. & KELLY, A. 1990. Sequences encoded in the class II region of the MHC related to the 'ABC' superfamily of transporters. *Nature,* 348**,** 741-4.

TROWSDALE, J. & KNIGHT, J. C. 2013. Major histocompatibility complex genomics and human disease. *Annu Rev Genomics Hum Genet,* 14**,** 301-23.

TURNQUIST, H. R., VARGAS, S. E., REBER, A. J., MCILHANEY, M. M., LI, S., WANG, P., SANDERSON, S. D., GUBLER, B., VAN ENDERT, P. & SOLHEIM, J. C. 2001. A region of tapasin that affects L(d) binding and assembly. *J Immunol,* 167**,** 4443-9.

TURNQUIST, H. R., VARGAS, S. E., SCHENK, E. L., MCILHANEY, M. M., REBER, A. J. & SOLHEIM, J. C. 2002. The interface between tapasin and MHC class I: identification of amino acid residues in both proteins that influence their interaction. *Immunol Res,* 25**,** 261-9.

VAN HATEREN, A., BAILEY, A., WERNER, J. M. & ELLIOTT, T. 2015. Plasticity of empty major histocompatibility complex class I molecules determines peptide-selector function. *Mol Immunol,* 68**,** 98-101.

VAN HATEREN, A., JAMES, E., BAILEY, A., PHILLIPS, A., DALCHAU, N. & ELLIOTT, T. 2010. The cell biology of major histocompatibility complex class I assembly: towards a molecular understanding. *Tissue Antigens,* 76**,** 259-75.

VAN KAER, L., ASHTON-RICKARDT, P. G., PLOEGH, H. L. & TONEGAWA, S. 1992. TAP1 mutant mice are deficient in antigen presentation, surface class I molecules, and CD4-8+ T cells. *Cell,* 71**,** 1205-14.

VASSILAKOS, A., COHEN-DOYLE, M. F., PETERSON, P. A., JACKSON, M. R. & WILLIAMS, D. B. 1996. The molecular chaperone calnexin facilitates folding and assembly of class I histocompatibility molecules. *EMBO J,* 15**,** 1495-506.

VOGT, A. B., KROPSHOFER, H., MOLDENHAUER, G. & HAMMERLING, G. J. 1996. Kinetic analysis of peptide loading onto HLA-DR molecules mediated by HLA-DM. *Proc Natl Acad Sci U S A,* 93**,** 9724-9.

VYAS, J. M., VAN DER VEEN, A. G. & PLOEGH, H. L. 2008. The known unknowns of antigen processing and presentation. *Nat Rev Immunol,* 8**,** 607-18.

WEARSCH, P. A. & CRESSWELL, P. 2007. Selective loading of high-affinity peptides onto major histocompatibility complex class I molecules by the tapasin-ERp57 heterodimer. *Nat Immunol,* 8**,** 873-81.

WEARSCH, P. A., PEAPER, D. R. & CRESSWELL, P. 2011. Essential glycan-dependent interactions optimize MHC class I peptide loading. *Proc Natl Acad Sci U S A,* 108**,** 4950-5.

WEEKES, M. P., WILLS, M. R., MYNARD, K., CARMICHAEL, A. J. & SISSONS, J. G. 1999. The memory cytotoxic T-lymphocyte (CTL) response to human cytomegalovirus infection contains individual peptide-specific CTL clones that have undergone extensive expansion in vivo. *J Virol,* 73**,** 2099-108.

WEI, M. L. & CRESSWELL, P. 1992. HLA-A2 molecules in an antigen-processing mutant cell contain signal sequence-derived peptides. *Nature,* 356**,** 443-6.

WELLCOME TRUST CASE CONTROL, C., AUSTRALO-ANGLO-AMERICAN SPONDYLITIS, C., BURTON, P. R., CLAYTON, D. G., CARDON, L. R., CRADDOCK, N., DELOUKAS, P., DUNCANSON, A., KWIATKOWSKI, D. P., MCCARTHY, M. I., OUWEHAND, W. H., SAMANI, N. J., TODD, J. A., DONNELLY, P., BARRETT, J. C., DAVISON, D., EASTON, D., EVANS, D. M., LEUNG, H. T., MARCHINI, J. L., MORRIS, A. P., SPENCER, C. C., TOBIN, M. D., ATTWOOD, A. P., BOORMAN, J. P., CANT, B., EVERSON, U., HUSSEY, J. M., JOLLEY, J. D., KNIGHT, A. S., KOCH, K., MEECH, E., NUTLAND, S., PROWSE, C. V., STEVENS, H. E., TAYLOR, N. C., WALTERS, G. R., WALKER, N. M., WATKINS, N. A., WINZER, T., JONES, R. W., MCARDLE, W. L., RING, S. M., STRACHAN, D. P., PEMBREY, M., BREEN, G., ST CLAIR, D., CAESAR, S., GORDON-SMITH, K., JONES, L., FRASER, C., GREEN, E. K., GROZEVA, D., HAMSHERE, M. L., HOLMANS, P. A., JONES, I. R., KIROV, G., MOSKIVINA, V., NIKOLOV, I., O'DONOVAN, M. C., OWEN, M. J., COLLIER, D. A., ELKIN, A., FARMER, A., WILLIAMSON, R., MCGUFFIN, P., YOUNG, A. H., FERRIER, I. N., BALL, S. G., BALMFORTH, A. J., BARRETT, J. H., BISHOP, T. D., ILES, M. M., MAQBOOL, A., YULDASHEVA, N., HALL, A. S., BRAUND, P. S., DIXON, R. J., MANGINO, M., STEVENS, S., THOMPSON, J. R., BREDIN, F., TREMELLING, M., PARKES, M., DRUMMOND, H., LEES, C. W., NIMMO, E. R., SATSANGI, J., FISHER, S. A., FORBES, A., LEWIS, C. M., ONNIE, C. M., PRESCOTT, N. J., SANDERSON, J., MATTHEW, C. G., BARBOUR, J., MOHIUDDIN, M. K., TODHUNTER, C. E., MANSFIELD, J. C., AHMAD, T., et al. 2007. Association scan of 14,500 nonsynonymous SNPs in four diseases identifies autoimmunity variants. *Nat Genet,* 39**,** 1329-37.

WILLIAMS, A. P., PEH, C. A., PURCELL, A. W., MCCLUSKEY, J. & ELLIOTT, T. 2002. Optimization of the MHC class I peptide cargo is dependent on tapasin. *Immunity,* 16**,** 509-20.

WILLS, M. R., CARMICHAEL, A. J., MYNARD, K., JIN, X., WEEKES, M. P., PLACHTER, B. & SISSONS, J. G. 1996. The human cytotoxic T-lymphocyte (CTL) response to cytomegalovirus is dominated by structural protein pp65: frequency, specificity, and T-cell receptor usage of pp65-specific CTL. *J Virol,* 70**,** 7569-79.

WITTENBRINK, N., HERRMANN, S., BLAZQUEZ-NAVARRO, A., BAUER, C., LINDBERG, E., REINKE, P., SAWITZKI, B., THOMUSCH, O., HUGO, C., BABEL, N., SEITZ, H. & OR-GUIL, M. 2018. A novel approach reveals that HLA class 1 single antigen bead-signatures provide a means of high-accuracy pre-transplant risk assessment of acute cellular rejection. 433318.

WRIGHT, C. A., KOZIK, P., ZACHARIAS, M. & SPRINGER, S. 2004. Tapasin and other chaperones: models of the MHC class I loading complex. *Biol Chem,* 385**,** 763-78.

YADAV, M., JHUNJHUNWALA, S., PHUNG, Q. T., LUPARDUS, P., TANGUAY, J., BUMBACA, S., FRANCI, C., CHEUNG, T. K., FRITSCHE, J., WEINSCHENK, T., MODRUSAN, Z., MELLMAN, I., LILL, J. R. & DELAMARRE, L. 2014. Predicting immunogenic tumour mutations by combining mass spectrometry and exome sequencing. *Nature,* 515**,** 572-6.

YEWDELL, J. W., ANTON, L. C. & BENNINK, J. R. 1996. Defective ribosomal products (DRiPs): a major source of antigenic peptides for MHC class I molecules? *J Immunol,* 157**,** 1823-6.

YORK, I. A., BREHM, M. A., ZENDZIAN, S., TOWNE, C. F. & ROCK, K. L. 2006. Endoplasmic reticulum aminopeptidase 1 (ERAP1) trims MHC class I-presented peptides in vivo and plays an important role in immunodominance. *Proc Natl Acad Sci U S A,* 103**,** 9202-7.

YU, Y. Y., TURNQUIST, H. R., MYERS, N. B., BALENDIRAN, G. K., HANSEN, T. H. & SOLHEIM, J. C. 1999. An extensive region of an MHC class I alpha 2 domain loop influences interaction with the assembly complex. *J Immunol,* 163**,** 4427-33.

ZACHARIAS, M. & SPRINGER, S. 2004. Conformational flexibility of the MHC class I alpha1-alpha2 domain in peptide bound and free states: a molecular dynamics simulation study. *Biophys J,* 87**,** 2203-14.

ZEHN, D., COHEN, C. J., REITER, Y. & WALDEN, P. 2006. Efficiency of peptide presentation by dendritic cells compared with other cell types: implications for cross-priming. *Int Immunol,* 18**,** 1647-54.

ZHANG, W., WEARSCH, P. A., ZHU, Y., LEONHARDT, R. M. & CRESSWELL, P. 2011. A role for UDP-glucose glycoprotein glucosyltransferase in expression and quality control of MHC class I molecules. *Proc Natl Acad Sci U S A,* 108**,** 4956-61.

ZHANG, W., YOUNG, A. C., IMARAI, M., NATHENSON, S. G. & SACCHETTINI, J. C. 1992. Crystal structure of the major histocompatibility complex class I H-2Kb molecule containing a single viral peptide: implications for peptide binding and T-cell receptor recognition. *Proc Natl Acad Sci U S A,* 89**,** 8403-7.

ZHANG, Y., BAIG, E. & WILLIAMS, D. B. 2006. Functions of ERp57 in the folding and assembly of major histocompatibility complex class I molecules. *J Biol Chem,* 281**,** 14622-31.

ZINKERNAGEL, R. M. & DOHERTY, P. C. 1974. Restriction of in vitro T cell-mediated cytotoxicity in lymphocytic choriomeningitis within a syngeneic or semiallogeneic system. *Nature,* 248**,** 701-2.

ZINKERNAGEL, R. M. & DOHERTY, P. C. 1979. MHC-restricted cytotoxic T cells: studies on the biological role of polymorphic major transplantation antigens determining T-cell restriction-specificity, function, and responsiveness. *Adv Immunol,* 27**,** 51-177.